frontiers | Research Topics

Update on diagnostic and prognostic biomarkers for women's cancers

Edited by
Ming Yi, Ying Luo and Yujiao Deng

Published in
Frontiers in Oncology
Frontiers in Medicine

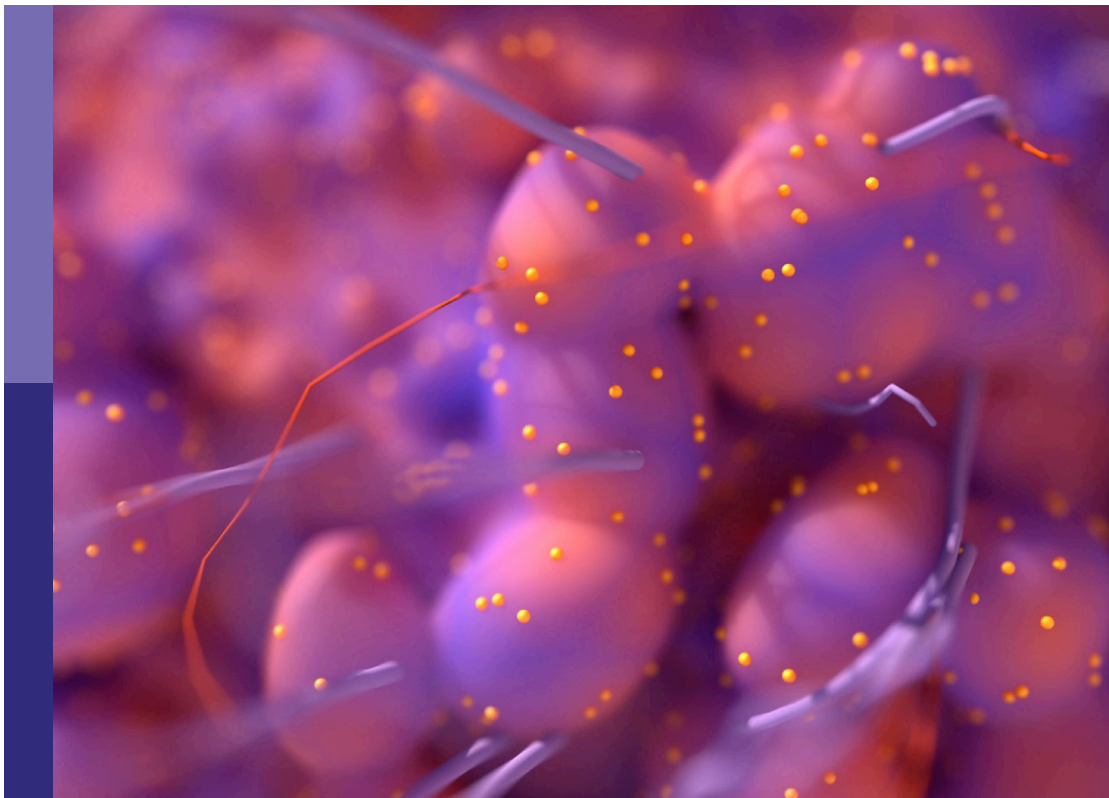

ISSN 1664-8714
ISBN 978-2-8325-2856-3
DOI 10.3389/978-2-8325-2856-3

About Frontiers

Frontiers is more than just an open access publisher of scholarly articles: it is a pioneering approach to the world of academia, radically improving the way scholarly research is managed. The grand vision of Frontiers is a world where all people have an equal opportunity to seek, share and generate knowledge. Frontiers provides immediate and permanent online open access to all its publications, but this alone is not enough to realize our grand goals.

Frontiers journal series

The Frontiers journal series is a multi-tier and interdisciplinary set of open-access, online journals, promising a paradigm shift from the current review, selection and dissemination processes in academic publishing. All Frontiers journals are driven by researchers for researchers; therefore, they constitute a service to the scholarly community. At the same time, the *Frontiers journal series* operates on a revolutionary invention, the tiered publishing system, initially addressing specific communities of scholars, and gradually climbing up to broader public understanding, thus serving the interests of the lay society, too.

Dedication to quality

Each Frontiers article is a landmark of the highest quality, thanks to genuinely collaborative interactions between authors and review editors, who include some of the world's best academicians. Research must be certified by peers before entering a stream of knowledge that may eventually reach the public - and shape society; therefore, Frontiers only applies the most rigorous and unbiased reviews. Frontiers revolutionizes research publishing by freely delivering the most outstanding research, evaluated with no bias from both the academic and social point of view. By applying the most advanced information technologies, Frontiers is catapulting scholarly publishing into a new generation.

What are Frontiers Research Topics?

Frontiers Research Topics are very popular trademarks of the *Frontiers journals series*: they are collections of at least ten articles, all centered on a particular subject. With their unique mix of varied contributions from Original Research to Review Articles, Frontiers Research Topics unify the most influential researchers, the latest key findings and historical advances in a hot research area.

Find out more on how to host your own Frontiers Research Topic or contribute to one as an author by contacting the Frontiers editorial office: frontiersin.org/about/contact

Update on diagnostic and prognostic biomarkers for women's cancers

Topic editors

Ming Yi — Zhejiang University, China

Ying Luo — Department of Immunology, UT Southwestern Medical Center, United States

Yujiao Deng — The Second Affiliated Hospital of Xi'an Jiaotong University, China

Citation

Yi, M., Luo, Y., Deng, Y., eds. (2023). *Update on diagnostic and prognostic biomarkers for women's cancers*. Lausanne: Frontiers Media SA.

doi: 10.3389/978-2-8325-2856-3

Table of contents

04 Editorial: Update on diagnostic and prognostic biomarkers for women's cancers
Yunxia Zhu and Ming Yi

08 Methylation-mediated silencing of *EDN3* promotes cervical cancer proliferation, migration and invasion
Peng Zhu, Xiang Li, Yujie Liu, Jing Xiong, Ding Yuan, Yan Chen, Lili Luo, Ju Huang, Binbin Wang, Quanfang Nie, Shuli Wang, Liying Dang, Shu Li, Yan Shu, Wei Zhang, Honghao Zhou, Lan Fan and Qing Li

19 Evaluation of Lee–Carter model to breast cancer mortality prediction in China and Pakistan
Sumaira Mubarik, Fang Wang, Lisha Luo, Kamal Hezam and Chuanhua Yu

30 Clinical and non-clinical determinants of cervical cancer mortality: A retrospective cohort study in Lagos, Nigeria
Idris Olasunmbo Ola, Adeyemi Adebola Okunowo, Muhammad Yaqub Habeebu and Junmei Miao Jonasson

40 Correlation between human papillomavirus viral load and cervical lesions classification: A review of current research
Yilu Zhou, Xiaoyu Shi, Jiaxin Liu and Lina Zhang

46 The temporal trend of women's cancer in Changle, China and a migrant epidemiological study
Yu Chen, Mengjie Song, Yanyu Zhang, Xingxing Yu, Shuqing Zou, Pingxiu Zhu, Yulin Zhou and Haomin Yang

54 EREG is a risk factor for the prognosis of patients with cervical cancer
Tianye Li, Ruijing Feng, Bingxin Chen and Jianwei Zhou

69 Circulating tumor cells in peripheral blood as a diagnostic biomarker of breast cancer: A meta-analysis
Tao Jin, Yao Chen, Qing-Yan Chen, Yang Xiong and Ji-Qiao Yang

77 Comprehensive analysis of the expression and prognosis for RAI2: A promising biomarker in breast cancer
Ying Jiao, Shiyu Li, Juejun Gong, Kun Zheng and Ya Xie

91 An autophagy-related diagnostic biomarker for uterine fibroids: FOS
Lei Cai, Jie Li, Rui Long, Zhiqi Liao, Juejun Gong, Bowen Zheng and Hanwang Zhang

101 Therapeutic prospect on umbilical cord mesenchymal stem cells in animal model with primary ovarian insufficiency: a meta-analysis
Xinrun Wang, Tianye Li, Xuechai Bai, Yun Zhu, Meiliang Zhang and Liang Wang

117 Case Report: Exploration of changes in serum immunoinflammation-related protein complexes of patients with metastatic breast cancer
Chang Chen, Yali Xu, Zhizhen Lai, Zhili Li and Qiang Sun

frontiers | Frontiers in Medicine

TYPE Editorial
PUBLISHED 14 June 2023
DOI 10.3389/fmed.2023.1225982

OPEN ACCESS

EDITED AND REVIEWED BY
Simcha Yagel,
Hadassah Medical Center, Israel

*CORRESPONDENCE
Ming Yi
✉ mingyi_onco@outlook.com

RECEIVED 20 May 2023
ACCEPTED 06 June 2023
PUBLISHED 14 June 2023

CITATION
Zhu Y and Yi M (2023) Editorial: Update on diagnostic and prognostic biomarkers for women's cancers. *Front. Med.* 10:1225982. doi: 10.3389/fmed.2023.1225982

Editorial: Update on diagnostic and prognostic biomarkers for women's cancers

Yunxia Zhu[1] and Ming Yi[2]*

[1]Department of Obstetrics and Gynecology, Haiyan People's Hospital, Jiaxing, China, [2]The First Affiliated Hospital, College of Medicine, Zhejiang University, Hangzhou, China

KEYWORDS

predictive biomarker, cervical cancer, ovarian cancer, uterine cancer, breast cancer, women's cancer

Editorial on the Research Topic
Update on diagnostic and prognostic biomarkers for women's cancers

Women's cancers, including breast, cervical, ovarian, and uterine cancers, have a significant impact on global health, resulting in numerous fatalities and imposing substantial economic burdens on women and their families. As the world population continues to age, there is an urgent need for international efforts to reduce the incidence and mortality rates of women's cancers and improve overall women's health (Figure 1) (1, 2). The identification of novel biomarkers linked to molecular subtypes, aggressive characteristics, and prognosis is indeed crucial for the development of targeted therapies, disease monitoring, and precise treatment of women's cancers (3, 4). Advancements in imaging techniques and the utilization of biochemical biomarkers, such as proteins, DNA, mRNA, and microRNA, hold great promise as diagnostic and therapeutic tools for these types of cancers (5–8). A collection of 10 manuscripts focused on diagnostic and prognostic biomarkers for women's cancers would provide valuable insights into various aspects of these diseases. By bringing together expertise from multiple disciplines, researchers can explore different angles and approaches to advance our understanding of biomarkers in women's cancers.

In the context of breast cancer, several biomarkers have been extensively studied for their potential as prognostic indicators (9–13). Hormone receptors, HER2, Ki-67, TP53, and BRCA1/BRCA2 are among the biomarkers that have been widely adopted for breast cancer prognosis (14, 15). These biomarkers, when combined with other clinical factors, provide a comprehensive assessment of prognosis and guide treatment decisions. However, the field of biomarker research in breast cancer continues to evolve, with ongoing exploration of novel markers and their prognostic value. The findings of Jin et al. demonstrated that circulating tumor cells (CTCs) have emerged as a valuable component in non-invasive methods for diagnosing breast cancer. Studies have shown their potential as diagnostic biomarkers, but it's important to consider the limitations and variations in the included studies when interpreting these findings. Further research and validation are necessary to establish the clinical utility of CTCs in breast cancer diagnosis. Besides, Jiao et al. found that RAI2 may play a crucial role in inhibiting the initiation and development of breast cancer. This research contributes to a better understanding of the molecular mechanisms involving RAI2 and provides potential biomarkers for predicting the prognosis of patients with breast cancer.

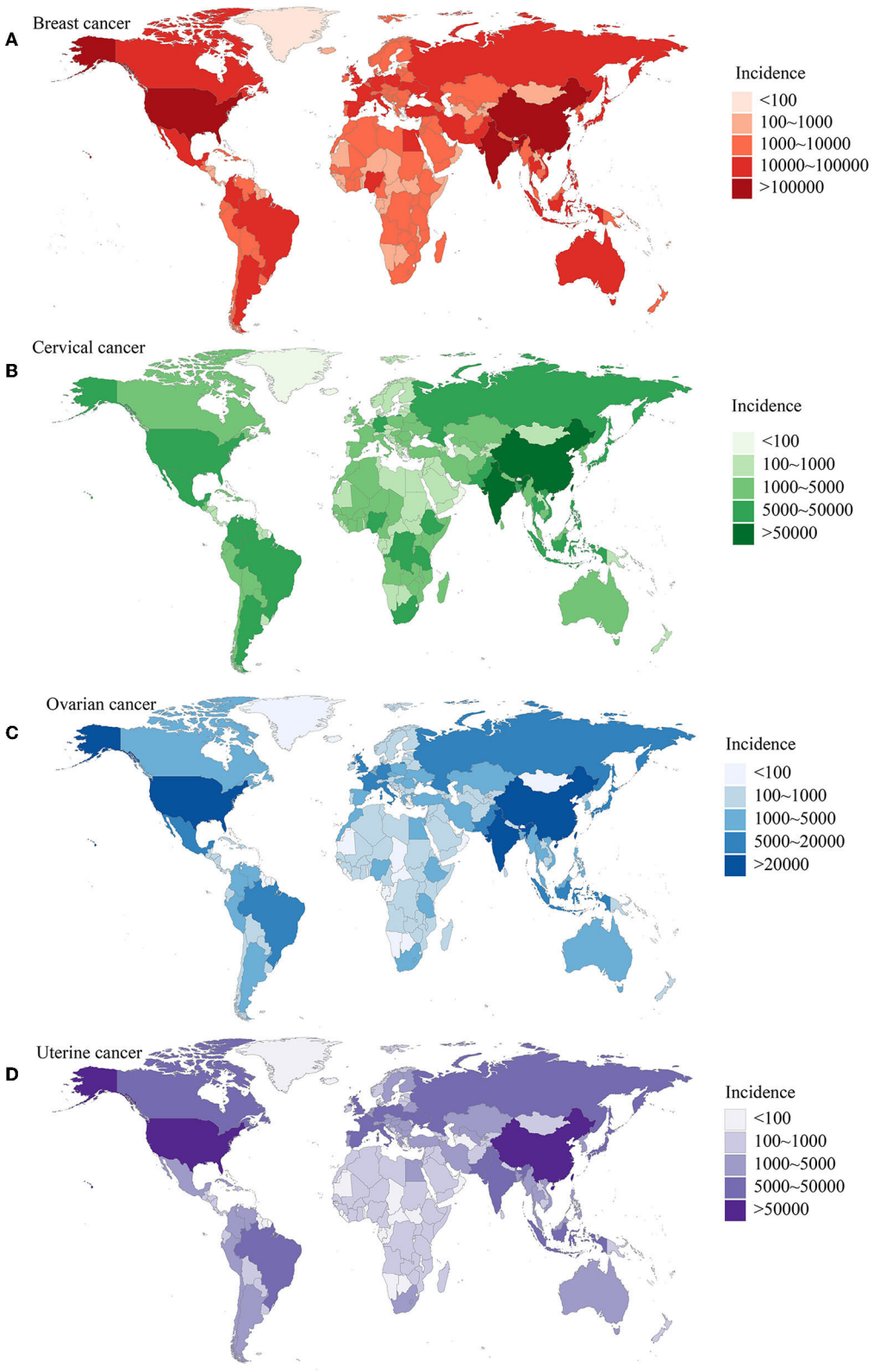

FIGURE 1
The burden of women's cancers worldwide based on the GBD 2019 database. **(A)** The incidence of breast cancer; **(B)** the incidence of cervical cancer; **(C)** the incidence of ovarian cancer; **(D)** the incidence of uterine cancer. Adapted from Yi et al. (1).

In the field of gynecological oncology, identifying key genes or signaling pathways has significant implications for risk stratification, early detection, personalized medicine, drug development, and understanding tumor biology (16–18). For instance, EDN3 and EREG have been identified as potential biomarkers and therapeutic targets in cervical cancer. The downregulation and hypermethylation of EDN3 suggest its involvement in cervical cancer progression, while the upregulation of EREG is associated with advanced stages of cervical cancer. Zhu et al. found EDN3 silence in cervical cancer is caused by methylation. This methylation-mediated silencing can be reversed by 5-Aza treatment in cervical cancer cells. Furthermore, EDN3 overexpression has the ability to suppress the proliferation, clone formation, and movement of cervical cancer cells. Li et al. revealed a significant association between high EREG expression and poor survival outcomes in patients with cervical cancer. Specifically, EREG expression was found to be elevated in advanced tumor stages. Enrichment analysis further demonstrated that EREG was closely associated with several important oncogenic signaling pathways. *In vitro* experiments demonstrated that knocking down EREG expression limited cell proliferation, promoted cell apoptosis, and alleviated cisplatin resistance in cervical cancer cells. Based on these findings, it can be concluded that EREG functions as a driving factor in cervical cancer progression and contributes to chemotherapy resistance. These findings provide insights into potential prognostic biomarkers and avenues for targeted therapy.

Moreover, Zhou et al. demonstrated that the impact of different HPV genotypes, multiple infections, and viral load on cervical precancerous lesions is crucial for guiding early interventions and preventing the development of cervical cancer. By considering specific genotypes, assessing multiple infections, and evaluating viral load, risk stratification can be improved, leading to appropriate management strategies for individuals with cervical precancerous lesions. In cervical cancer screening, the measurement of HPV viral load alone is not sufficient, and it should be combined with other methods to achieve maximum sensitivity and specificity. The integration of multiple detection techniques in early cervical cancer screening is essential. Therefore, further research is needed to explore the various factors that may influence the development and progression of cervical lesions. The comprehensive approach involving HPV vaccination, combined with advanced screening methods, will significantly enhance the chances of eradicating cervical cancer worldwide (19).

Apart from malignancies, this special issue also includes studies on benign gynecological tumors, such as uterine fibroids (UFs) (20). UFs are the most prevalent non-cancerous tumors that affect women of reproductive age. Traditionally, UF diagnosis has relied on transvaginal ultrasonography and pathological examination. However, in recent years, molecular biomarkers have emerged as promising tools for understanding the origin and progression of UFs. Cai et al. investigated the potential of DNA-methylated autophagy as a biomarker for UFs. Through the identification of key genes and investigation of their functional implications, they provide clinicians with a comprehensive assessment tool for UFs. The down-regulation of FOS, validated at both the transcriptional and protein levels, suggests its potential as a diagnostic biomarker for UFs. Their findings contribute to the understanding of UF pathogenesis and may guide future research efforts and clinical management strategies for this common gynecologic condition.

However, it is notable that the clinical implementation and validation of biomarkers require rigorous testing in large patient cohorts. Biomarker discovery is an ongoing process, and advancements in technologies and research will continue to contribute to the development of robust prognostic biomarkers for women's cancers.

Collectively, this Research Topic encompasses the use of biochemical biomarkers, gene expression profiling, and liquid biopsy sampling to enhance the diagnosis, treatment decision-making, and personalized therapy in breast, cervical, ovarian, and uterine cancers. By monitoring these biomarkers over time, clinicians can make informed decisions about adjusting and optimizing individualized treatment plans. These advancements hold the potential to improve patient outcomes, minimize unnecessary treatments, and facilitate long-term monitoring for these cancers.

Author contributions

YZ and MY performed the selection of literature, drafted the manuscript, and prepared the figures. YZ collected the related references and participated in discussion. MY designed and revised the manuscript. All authors contributed to this manuscript, read, and approved the final manuscript.

Funding

This work was supported by China Postdoctoral Science Foundation (No. 2022M722766).

Conflict of interest

The authors declare that the research was conducted in the absence of any commercial or financial relationships that could be construed as a potential conflict of interest.

Publisher's note

References

1. Yi M, Li T, Niu M, Luo S, Chu Q, Wu K. Epidemiological trends of women's cancers from 1990 to 2019 at the global, regional, and national levels: a population-based study. *Biomark Res.* (2021) 9:55. doi: 10.1186/s40364-021-00310-y

2. Siegel RL, Miller KD, Fuchs HE, Jemal A. Cancer statistics, 2022. *CA Cancer J Clin.* (2022) 72:7–33. doi: 10.3322/caac.21708

3. Yi M, Wu Y, Niu M, Zhu S, Zhang J, Yan Y, et al. Anti-TGF-β/PD-L1 bispecific antibody promotes T cell infiltration and exhibits enhanced antitumor activity in triple-negative breast cancer. *J Immunother Cancer.* (2022) 10:553. doi: 10.1136/jitc-2022-005543

4. Li T, Wang X, Qin S, Chen B, Yi M, Zhou J. Targeting PARP for the optimal immunotherapy efficiency in gynecologic malignancies. *Biomed Pharmacother.* (2023) 162:114712. doi: 10.1016/j.biopha.2023.114712

5. Hong M, Tao S, Zhang L, Diao LT, Huang X, Huang S, et al. RNA sequencing: new technologies and applications in cancer research. *J Hematol Oncol.* (2020) 13:166. doi: 10.1186/s13045-020-01005-x

6. Zhu L, Li J, Gong Y, Wu Q, Tan S, Sun D, et al. Exosomal tRNA-derived small RNA as a promising biomarker for cancer diagnosis. *Mol Cancer.* (2019) 18:74. doi: 10.1186/s12943-019-1000-8

7. Wu L, Qu X. Cancer biomarker detection: recent achievements and challenges. *Chem Soc Rev.* (2015) 44:2963–97. doi: 10.1039/C4CS00370E

8. Li Y, Zheng Q, Bao C, Li S, Guo W, Zhao J, et al. Circular RNA is enriched and stable in exosomes: a promising biomarker for cancer diagnosis. *Cell Res.* (2015) 25:981–4. doi: 10.1038/cr.2015.82

9. Dong B, Yi M, Luo S, Li A, Wu K. RDGN-based predictive model for the prognosis of breast cancer. *Exp Hematol Oncol.* (2020) 9:13. doi: 10.1186/s40164-020-00169-z

10. Mueller C, Haymond A, Davis JB, Williams A, Espina V. Protein biomarkers for subtyping breast cancer and implications for future research. *Expert Rev Proteomics.* (2018) 15:131–52. doi: 10.1080/14789450.2018.1421071

11. Cocco S, Piezzo M, Calabrese A, Cianniello D, Caputo R, Lauro VD, et al. Biomarkers in triple-negative breast cancer: state-of-the-art and future perspectives. *Int J Mol Sci.* (2020) 21:579. doi: 10.3390/ijms21134579

12. Bertoli G, Cava C, Castiglioni I. MicroRNAs: new biomarkers for diagnosis, prognosis, therapy prediction and therapeutic tools for breast Cancer. *Theranostics.* (2015) 5:1122–43. doi: 10.7150/thno.11543

13. Penault-Llorca F, Radosevic-Robin N. Ki67 assessment in breast cancer: an update. *Pathology.* (2017) 49:166–71. doi: 10.1016/j.pathol.2016.11.006

14. Harbeck N, Gnant M. Breast cancer. *Lancet.* (2017) 389:1134–50. doi: 10.1016/S0140-6736(16)31891-8

15. Yi M, Zhang D, Song B, Zhao B, Niu M, Wu Y, et al. Increased expression of ECT2 predicts the poor prognosis of breast cancer patients. *Exp Hematol Oncol.* (2022) 11:107. doi: 10.1186/s40164-022-00361-3

16. Cohen AC, Roane BM, Leath CA. Novel therapeutics for recurrent cervical cancer: moving toward personalized therapy. *Drugs.* (2020) 80:217–27. doi: 10.1007/s40265-019-01249-z

17. Xiao Y, Bi M, Guo H, Li M. Multi-omics approaches for biomarker discovery in early ovarian cancer diagnosis. *EBioMedicine.* (2022) 79:104001. doi: 10.1016/j.ebiom.2022.104001

18. Zhang M, Cheng S, Jin Y, Zhao Y, Wang Y. Roles of CA125 in diagnosis, prediction, and oncogenesis of ovarian cancer. *Biochim Biophys Acta Rev Cancer.* (2021) 1875:188503. doi: 10.1016/j.bbcan.2021.188503

19. Cohen PA, Jhingran A, Oaknin A, Denny L. Cervical cancer. *Lancet.* (2019) 393:169–82. doi: 10.1016/S0140-6736(18)32470-X

20. Giuliani E, As-Sanie S, Marsh EE. Epidemiology and management of uterine fibroids. *Int J Gynaecol Obstet.* (2020) 149:3–9. doi: 10.1002/ijgo.13102

frontiers | Frontiers in Oncology

TYPE Original Research
PUBLISHED 03 February 2023
DOI 10.3389/fonc.2023.1010132

OPEN ACCESS

EDITED BY
Ming Yi,
Zhejiang University, China

REVIEWED BY
Junhua Mai,
Houston Methodist Research Institute, United States
Lanxiang Wu,
Chongqing Medical University, China

*CORRESPONDENCE
Qing Li
liqing9251026@csu.edu.cn
Jing Xiong
xiongjing79@csu.edu.cn

†These authors have contributed equally to this work

SPECIALTY SECTION
This article was submitted to Gynecological Oncology, a section of the journal Frontiers in Oncology

RECEIVED 13 August 2022
ACCEPTED 25 January 2023
PUBLISHED 03 February 2023

CITATION
Zhu P, Li X, Liu Y, Xiong J, Yuan D, Chen Y, Luo L, Huang J, Wang B, Nie Q, Wang S, Dang L, Li S, Shu Y, Zhang W, Zhou H, Fan L and Li Q (2023) Methylation-mediated silencing of *EDN3* promotes cervical cancer proliferation, migration and invasion. *Front. Oncol.* 13:1010132. doi: 10.3389/fonc.2023.1010132

Methylation-mediated silencing of *EDN3* promotes cervical cancer proliferation, migration and invasion

Peng Zhu[1,2,3†], Xiang Li[4†], Yujie Liu[1,2,3], Jing Xiong[5*], Ding Yuan[6], Yan Chen[1,2,3,7], Lili Luo[8], Ju Huang[8], Binbin Wang[9], Quanfang Nie[9], Shuli Wang[10], Liying Dang[10], Shu Li[7], Yan Shu[1,2,3], Wei Zhang[1,2,3], Honghao Zhou[1,2,3], Lan Fan[1,2,3] and Qing Li[1,2,3*]

[1]Department of Clinical Pharmacology, Xiangya Hospital, Central South University, Changsha, China, [2]Institute of Clinical Pharmacology, Central South University, Hunan Key Laboratory of Pharmacogenetics, Changsha, China, [3]Engineering Research Center of Applied Technology of Pharmacogenomics, Ministry of Education, Changsha, China, [4]Department of Gynaecology, The Third Xiangya Hospital, Central South University, Changsha, China, [5]Department of Gynaecology and Obstetrics, The Second Xiangya Hospital, Central South University, Changsha, China, [6]Health Management Center, Xiangya Hospital, Central South University, Changsha, China, [7]Xiangya Medical Laboratory, Central South University, Changsha, China, [8]Department of Gynaecology, The First Affiliated Hospital of Shantou University Medical College, Shantou, China, [9]Department of Obstetrics and Gynecology, Loudi Central Hospital, Loudi, China, [10]Department of Obstetrics and Gynecology, Zhengzhou Central Hospital Affiliated to Zhengzhou University, Zhengzhou, China

Cervical cancer (CC) remains one of the leading causes of cancer-related deaths worldwide. However, cervical cancer is preceded by the pre-malignant cervical intraepithelial neoplasia (CIN) that can last for up to 20 years before becoming malignant. Therefore, early screening is the key to prevent the progression of cervical lesions into invasive cervical cancer and decrease the incidence. The genes, down-regulated and hypermethylated in cancers, may provide potential drug targets for cervical cancer. In our current study, using the datasets from Gene Expression Omnibus (GEO) and the Cancer Genome Atlas (TCGA) databases, we found that endothelin 3 (*EDN3*) was downregulated and hypermethylated in cervical squamous cell carcinoma (CSCC). The further analysis in GSE63514 (n=128) dataset and in our samples (n=221) found that the expression of *EDN3* was decreased with the degree of cervical lesions. Pyrosequencing was performed to evaluate 4 CpG sites of the *EDN3* promoter region in our samples (n=469). The data indicated that the methylation level of *EDN3* was increased with the degree of cervical lesions. *EDN3* silencing mediated by methylation can be blocked by 5-Azacytidine (5-Aza), a DNA methyltransferase 1 (DNMT1) inhibitor, treatment in cervical cancer cell lines. Ethynyldeoxyuridine (EdU) assay, would-healing assay, clone formation assay and transwell assay were conducted to investigate the biological function of *EDN3* in cervical cancer cell lines. The results of these experiments confirmed that overexpression of *EDN3* could inhibit the proliferation, clone formation, migration and invasion of cervical cancer cells. *EDN3* may provide potential biomarker and therapeutic target for CSCC.

KEYWORDS

EDN3, DNA methylation, cervical cancer, CIN, biomarker

Introduction

Cervical cancer (CC) is the fourth most common cancer in women worldwide (1). Approximately 604,127 new cases of cervical cancer and 341,831 related deaths in 2020 (1). More than 80% of cervical cancer related death occur in developing countries (1). In China, 47,739 deaths and 106,430 new cases of cervical cancer have been recorded, account for 18.7 percent of diagnosis and 15.3 percent of deaths globally (2). The occurrence and development of cervical cancer goes through a long pre-cancerous stage, known as cervical intraepithelial neoplasia (CIN) and graded 1-3 (3). Various risk factors that induce cervical cancer can cause early epigenetic changes and lead to abnormal gene expression, thus providing favorable conditions for the early growth of cervical cancer cells and contributing to the origin of cancer cells. Therefore, the change of epigenetics in the early stage of cervical cancer has been extensively studied (4–7).

DNA methylation is the most extensively studied epigenetic mechanism that occurs by the addition of methyl groups to specific DNA bases, typically the cytosine of CpG dinucleotides (8, 9). The addition of methyl group is catalyzed by a family of enzymes called DNA methyltransferases (DNMTs) (10, 11). DNA can be methylated throughout the genome, not only at promoter and CpG-rich regions but also at intergenic regions (12). The promoter regions of tumor suppression genes (TSG), DNA repair genes or oncogenes were frequently hypermethylated in cancers (12, 13). Abnormal methylation at promoter regions can lead to abnormal gene transcription, while abnormal levels of overall methylation are associated with many cancers (14, 15). An increasing number of studies have demonstrated the DNA methylation of specific genes, such as TSG, is associated with the pathogenesis of cervical cancer (16). Hypermethylation of specific TSG reduces the transcriptional activity of TSG, resulting in a decrease in the mRNA level of the gene's transcriptional product and a significant decrease in the subsequent protein expression level. It indicated that the genes, down-regulated and hypermethylated in cancers, may provide potential drug targets for cervical cancer.

In order to find the novel potential genes, we analyzed all the differentially expressed genes (DEGs) in the GSE7803, GSE9750 and GSE63514 dataset. We found 67 genes were down-regulated in three datasets. Additionally, we found the expression of DNA methyltransferase 1 (DNMT1) was increased in cancer specimens in three datasets. It suggested that the change of DNA methylation must play a critical role in the development of CC. Subsequently, we used DiseaseMeth 2.0 to investigate the methylation levels of 67 down-regulated genes in normal (n=20) and cancer specimens of cervical squamous cell carcinoma (CSCC) (n=261) (17). The results showed that one of the investigated genes, endothelin 3(*EDN3*), is hypermethylated in CSCC specimens.

EDN3 is one of the endothelin (EDN) family members. There are three endothelin peptides in this family, the other two peptides are EDN1 and EDN2 (18). EDN1/2 is highly expressed in a variety of solid tumors, such as ovarian cancer, breast cancer and bladder cancer. By binding with Endothelin Receptor A (EDNRA), they can activate cell proliferation, stimulate angiogenesis, resist cell apoptosis and increase the invasion ability of cancer cells (19, 20). Unlike EDN1 and EDN2, the affinity of EDN3 and EDNRA is very low. Recent studies have demonstrated that EDN3 participate in cell proliferation, differentiation and metastasis by interacting with Endothelin Receptor B (EDNRB) (18). In breast cancer, cervical cancer, colorectal cancer and glioma, the expression of *EDN3* gene is significantly down-regulated, which may be regulated by epigenetics (21–26). *EDN3* methylation levels are high in cervical cancer patients, and *EDN3* methylation may serve as a molecular marker for cervical cancer (22, 23). However, there is no report on the role and specific mechanism of *EDN3* in cervical precancerous lesions.

In current study, we firstly detected the expression and the methylation level of *EDN3* in cervical scrapings and cervical cancer cell lines, including C-33A, SiHa and CaSki cell lines. Secondly, we the measured the expression of *EDN3* after 5-Azacytidine (5-Aza), a DNMT1 inhibitor, treatment in cervical cancer cell lines to investigate the effect of methylation on *EDN3* expression. After that, ethynyldeoxyuridine (EdU) assay, would-healing assay, clone formation assay and transwell assay were conducted to investigate the biological function of *EDN3* in cervical cancer cell lines.

Materials and methods

Differentially expressed genes analysis

A total of three original datasets (GSE7803, GSE9750 and GSE63514) were downloaded from Gene Expression Omnibus database (GEO; http://www.ncbi.nlm.nih.gov/geo/). GSE7803 contains 10 normal squamous cervical epitheilia samples and 21 invasive squamous cell carcinomas of the cervix samples (27). GSE9750 contains 24 normal cervix epithelium samples and 33 cervical cancers samples (28). GSE63514 contains 24 normal cervix epithelium samples, 14 CIN1, 22 CIN2, 40 CIN3 and 28 cervical cancers samples (29). Genes with adjusted $P<0.05$ and $\log_2$ FC < -1 (normal vs cancer) were considered as down-regulated DEGs. The overlapping DEGs were identified using jvenn online tool (http://jvenn.toulouse.inra.fr/app/index.html) (30). We found 67 genes were down-regulated in three datasets.

Methylation analysis

The human disease methylation database (DiseaseMeth 2.0, http://www.bio-bigdata.com/diseasemeth/analyze.html) was used to investigate the methylation levels of 67 down-regulated genes in normal (n=20) and cancer specimens of CSCC (n=261) (17). This database is based on the Cancer Genome Atlas (TCGA) and GEO database. The clinical characters of patients were obtained from cBioPortal (http://www.cbioportal.org). We set the technology experimental platform as 450k (Illumina Infinium HumanMethylation 450 BeadChip), absolute methylation difference as > 0.2 and P value as < 0.05.

Clinical samples

Between Jan 2021 and June 2022, cervical scrapings were collected from Xiangya Hospital of Central South University, the Second Xiangya Hospital of Central South University, the Third Xiangya Hospital of Central South University, the First Affiliated Hospital of Shantou University Medical College, Loudi Central Hospital and Zhengzhou Central Hospital Affiliated to Zhengzhou University. This study was undertaken in accordance with the Declaration of Helsinki, and the protocol was approved by the local ethical committees where applicable. All patients gave written informed consent before participation in this study. Exclusion criteria applied in this study were patients with a history of cervical cancer or existence of other cancer, cervical related-surgery, vaccinated with anti-HPV vaccine or pregnancy.

This study included women who had a normal uterine cervix (n =167), CIN1 (n=49), CIN2 (n=98), CIN3 (n=91) and CSCC (n=64) diagnosed according to the histologic reports. The final diagnosis was made by tissue-proven pathology in the CIN1+ test result group. When the biopsy results revealed CIN3+, the patients underwent cervical conization or major surgery. Methylation detection tests for *EDN3* were carried out by using residual cervical cells from cytological tests. Additionally, quantitative real-time PCR (qPCR) for *EDN3* were conducted. Only 60 normal, 29 CIN1, 37 CIN2, 57 CIN3 and 38 CSCC patients had enough residual cervical cells to isolate high-quality RNA for qPCR.

DNA preparation

The residual cervical scrapings cells were stored in preservation solution (JIANG SU JIANYOU MEDICAL TECHNOLOGY, CHN) at −20°C. The residual cervical cells were centrifuged and washed with phosphate buffer solution (PBS). Genomic DNA (gDNA) was extracted from the cells using the PureLink Genomic DNA Mini Kit (Invitrogen, USA). The concentrations of gDNA in each sample were measured using a BioSpec-nano spectrophotometer (Shimadzu Corporation, JPN).

Pyrosequencing

After determination of the amount of gDNA, up to 500 ng of gDNA was subjected to bisulfite conversion using ZYMO EZ DNA Methylation-Gold Kit (ZYMO RESEARCH, USA). Pyrosequencing was performed to evaluate 4 CpG sites of the *EDN3* promoter region (NC_000020.10:57875929-57875940, CGGGGCGGCGCG). PyroMark Assay Design 2.0. were used to design PCR and pyrosequencing primers. The primers were listed as follows: *EDN3*-F: 5′-GTTTGATTTAGGTTTATGGAGT-3′; *EDN3*-R: 5′- AATC CCCCCCCCTAAATCCTTTT-3′; *EDN3*-S: 5′- GTGATTTTAGT AGTAGGTAAG -3′. All the primers were produced by Shanghai Sangon Biotech Co., Ltd. Bisulfite-treated DNA was then amplified using TaKaRa Ex Taq (TaKaRa, CHN). The reaction mixture including 13.5 μl of nuclease-free water, 2 μL of 10 × Ex Taq Buffer, 2 μL of dNTP, 0.4 μL former primer and reverse primer, 0.2 μL of Ex Taq HS and 1.5 uL of bisulfite-treated DNA. The PCR product act as a template in Pyrosequencing reactions, using the PyroMark Q24 instrument (Qiagen, MD) according to the manufacturer's recommended protocol (31). Raw data were analyzed using the Pyromark Q24 analysis software (Qiagen, MD). Pyrosequencing yields a quantitative result giving the percentage of methylated alleles for each of the 4 investigated CpG sites. The average percentage of methylation across 4 CpG sites were obtained. The average percentage of methylation of each sample was higher than 10% was regarded as methylation-positive.

Quantitative real-time PCR

Total RNA was isolated from the tissues and cells using RNAiso Plus (TaKaRa, CHN). One microgram of total RNA was reverse-transcribed using PrimeScript™ RT reagent Kit (TaKaRa, CHN). The amplification was performed using the SYBR Green Real-Time PCR Kit (TaKaRa, CHN) on LightCycler®480 Instrument (Roche, CH). The primers were listed as follows: *EDN3*, F:5′-GGGACTGTGAAGAGACTGTGG-3′, R:5′-AGACACACTCCTTGTCCTTGTA-3′; β-actin, F:5′-GTGGGGC GCCCCAGGCACCA-3′, R:5′-CTCCTTAATGTCACGCACGATTTC-3′. All the primers were produced by Shanghai Sangon Biotech Co., Ltd, Shanghai, China. The qPCR was performed as described (32). Data were analyzed using the -ΔCt method and the expression of β-actin was used as normalization control.

Cell culture and transfection

C-33A (RRID: CVCL_1094), SiHa (RRID: CVCL_0032) and CaSki (RRID: CVCL_1100) cell lines were obtained from Shanghai Institute of Biochemistry and Cell Biology of the Chinese Academy of Sciences. All cell lines were authenticated by Shanghai Biowing Applied Biotechnology Co. LTD, Shanghai, China. C-33A and SiHa cells were maintained in Minimum Essential Medium (MEM) supplemented with 10% FBS. CaSki cells was maintained in 1640 supplemented with 10% fetal bovine serum (FBS) (Gibco, USA). Cells were cultured in an incubator at 37°C and 5% CO_2. All experiments were performed with mycoplasma-free cells. Full-length human *EDN3* cDNA was synthesized and cloned into pcDNA3.1 vector to construct the EDN3 overexpression vector (OE-*EDN3*) (Genechem, CHN). The empty pcDNA3.1 vector was used as a control. C-33A, SiHa and CaSki cell lines were seeded onto 6-well plate and transfected with OE-*EDN3* and control vector using Lipofectamine 2000 (Invitrogen, USA) according to the manufacturer's instructions. Cells used in the following experiment were transfected with OE-*EDN3* and control vector for 48 hours.

5-Azacytidine treatment

After transfection, C-33A cells were seeded at 2×10^5 cells/well in 6-well plate, while SiHa and CaSki cells were seeded at 1×10^5 cells/well. After 24 hours later, the culture medium was replaced with fresh medium containing 5 or 10 μM 5-Aza (Selleck, CHN) or an equal volume of PBS. The cells were harvested after 24 hours.

Western blot

Collect the cells from the cell flask into a 1.5 mL EP tube and added RIPA lysis buffer (Beyotime, CHN). The protein lysate (30 μg) was subjected to 10% SDS-PAGE and then electrotransferred onto the polyvinylidene difluoride (PVDF) membrane (Millipore IPVH00010, Solarbio, CHN). The main antibodies are as follows: β-actin (ab6276, Abcam, UK), EDN3 (H00001908-M01, Novus Biologicals, USA), the ratios of them to the primary antibody dilution buffer (Beyotime, CHN) are 1:10000 and 1:1000. The bands were washed the next day and the secondary antibodies were incubated for one hour at room temperature. The ratio of β-actin and EDN3's secondary antibody (Proteintech, CHN) to the secondary antibody dilution buffer (Beyotime, CHN) is 1:10000 and 1:5000. The bands were washed and soaked in ECL kit (yeasen, CHN) and analyzed by ChemiDoc XRS + image analyzer (Bio-Rad, USA).

Ethynyldeoxyuridine assay

Transfected C-33A (5000), SiHa (1000) and CaSki (1000) cells were seeded in 96-well plates. After 24 hours later, cells were pulsed with EdU and Hoechst (Cell-Light EdU Apollo567 *In Vitro* Kit, RiboBio, CHN) according to the manufacturer's protocol. Coverslips were mounted on slides and imaged using a Thermofisher EVOS M7000 microscope. Using Image J 1.8.0 (Bethesda, USA) to quantify the positive EdU cancer cells and calculate the proliferation rate of cells.

Wound-healing assay

Transfected cells were seeded in 6-well plate at 2×10^5 cells/well (C-33A) or 1×10^5 cells/well (SiHa and CaSki) for 24 hours and allowed to adhere. The cells were transfected with OE-*EDN3* and control vector as mentioned above. An acellular area was created by a 200 μL pipette tip. Photos were taken with the NIKON ECLIPSE Ts2 Microscope at 0, 48 hours and 96 hours (C-33A, SiHa), at 0, 12 hours and 24 hours (CaSki). The area of the wound was quantified by ImageJ 1.8.0 (Bethesda, USA).

Clone formation assay

For clone formation assay, transfected C-33A cells were plated at 10000 cells per well, SiHa and CaSki cells were plated at 5000 cells per well in 6-well plates and cultured for 7 days. The complete culture medium was changed every 2 days. After 7 days, clones were fixed in 4% paraformaldehyde (Servicebio, CHN) for 30 minutes and stained with 1 mL crystal violet (Beyotime, CHN) for 1 hour. Clones containing > 50 cells were counted by Image J 1.8.0 (Bethesda, USA) for analysis.

Transwell assay

Transwell migration assay was performed using Corning Transwell (Corning, USA). Transfected C-33A (1×10^6), SiHa (3×10^5) and CaSki (1×10^5) cells were seeded in the upper chambers in 200 μL medium without serum. While the lower chambers were filled with 600 μL complete medium. After 48-72 hours later, the cells in the upper chambers were wiped off gently with a cotton swab. The lower cells were incubated with 600 μL 4% paraformaldehyde (Servicebio, CHN) for 30 minutes, stained with 600 μL crystal violet (Beyotime, CHN) for 1 hour and photographed under a microscope, and counted by Image J 1.8.0 (Bethesda, USA).

Transfected C-33A (2×10^6), SiHa (6×10^5) and CaSki (2×10^5) cells were seeded in the upper chambers in 200 μL medium without serum. Invasion assay and analysis were done as mentioned above. The only difference was that the upper chambers of Corning Transwell should be coated with 80 μL ice-dissolved matrigel (Corning, USA) prior to cell invasion assay.

Statistical analysis

All data were expressed as mean ± standard deviation (mean ± SD). Statistical analyses were performed using SPSS 24.0 or GraphPad Prism 8 (GraphPad Software, Inc., La Jolla, CA, USA). Statistical comparisons between two groups were performed using Student's t test. The Benjamini & Hochberg (false discovery rate) method was used to adjust the *P*-value for multiple testing. All the other data were analyzed with one-way ANOVA followed by LSD (equal variances assumed) or Dunnett's-T3 test (equal variances not assumed). χ^2 -testing was used to analyze categorical data. All *P*-values were two-sided, and $P < 0.05$ was considered to indicate statistical significance.

Results

EDN3 is downregulated and hypermethylated in CSCC

A total of three original datasets (GSE7803, GSE9750 and GSE63514) were downloaded from GEO database. Genes with adjusted $P < 0.05$ and $\log_2 FC < -1$ (normal vs cancer) were down-regulated DEGs. Then we used an online tool, jvenn (http://jvenn.toulouse.inra.fr/app/index.html), to find overlapping down-regulated DEGs in at least two of the GEO datasets (30). We found 67 genes were down-regulated in three datasets (Figure 1A; Table S1). Additionally, we found the expression of DNMT1 was increased in cancer specimens in three datasets (Figures 1B–D). It suggested that the change of DNA methylation must play a critical role in the development of CC.

The genes, down-regulated and hypermethylated in cancers, may provide potential drug targets for cervical cancer. Thus, subsequently, we used DiseaseMeth 2.0 to investigate the methylation levels of 67 down-regulated genes in normal (n=20) and cancer specimens of CSCC (n=261) (17). We set the technology experimental platform as 450k (Illumina Infinium HumanMethylation 450 BeadChip), absolute methylation difference as > 0.2 and P value as < 0.05. The results showed only two investigate genes are hypermethylated in CSCC specimens, one of which, named *EDN3*, had more significant difference (Figure 1E).

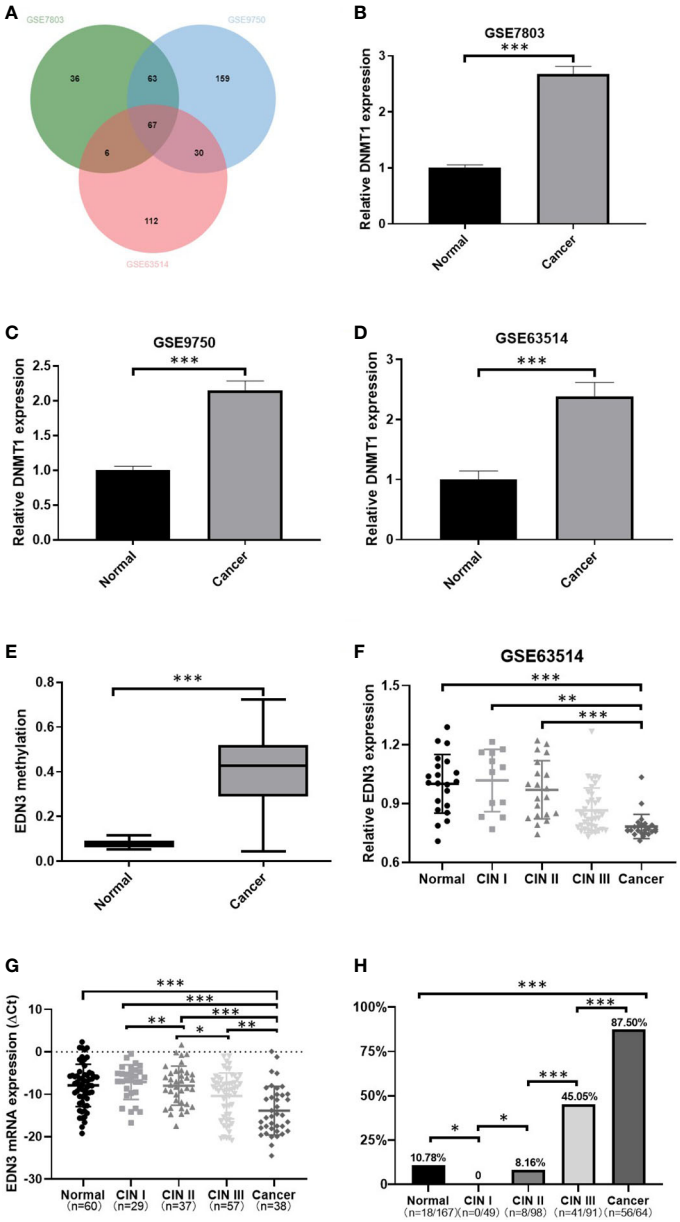

FIGURE 1
The methylation level of *EDN3* was increased and positively correlated with the severity of CIN, however, the mRNA expression level of *EDN3* was decreased and show a negative correlation with the severity of CIN. **(A)** Venn diagram of down-regulated DEGs in GSE7803, GSE9750 and GSE63514. **(B–D)** Comparison of DNMT1 expression between cancer and normal tissues. The results show that the increased expression of DNMT1 in CC tissues compared to normal tissue. **(E)** *EDN3* methylation in CSCC samples compared with that in normal samples was analyzed by the DiseaseMeth version 2.0 database. **(F)** Data from GSE63514 showed that mRNA expression of *EDN3* in CC tissues is lower than in normal and CIN1-2 tissue. **(G)** The mRNA expression of *EDN3* in our collected scrapings from patients with no CIN lesion (normal), CIN1, CIN2, CIN3 and cancer. **(H)** Bar chart showing the positive percent of *EDN3* promoter methylation levels in each histologic category. Values are mean ± SD, *P<0.05; **P<0.01; ***P<0.001.

The expression of *EDN3* was decreased with the degree of cervical lesions, but the methylation level of *EDN3* was increased

To further investigate the expression of *EDN3* in cervical precancerous lesions, we used GSE63514 dataset and analyzed the expression of *EDN3* in different degree of cervical lesions. We found that the expression of *EDN3* was decreased with the degree of cervical lesions (Figure 1F). Then we measured the expression of *EDN3* in our own samples (n=221), including 60 normal, 29 CIN1, 37 CIN2, 57 CIN3 and 38 CSCC. The results are consistent with the idea that the expression of *EDN3* was decreased with the degree of cervical lesions (Figure 1G).

Pyrosequencing was performed to evaluate 4 CpG sites of the *EDN3* promoter region (NC_000020.10:57875929-57875940, CGGGGCGGCGCG) in our samples (n=469). The average percentage of methylation across 4 CpG sites were obtained. The average methylation percentage of each sample was higher than 10% was regarded as methylation-positive. As shown in Figure 1H, the methylation level of *EDN3* was increased significantly with the degree

of cervical lesions, except for the normal group. The positive percent of *EDN3* promoter methylation levels in CIN1, CIN2, CIN3 and CSCC patients were 0 (0/49), 8.16% (8/98), 45.05% (41/91) and 87.50% (56/64).

EDN3 silencing mediated by methylation could be blocked by 5-Aza treatment in cervical cancer cell lines

Firstly, we detected the expression of *EDN3* in C-33A, SiHa and CaSki cell lines. The results revealed that the expression of *EDN3* were at low level in all cervical cancer cells, especially in SiHa and CaSki cells (Figure 2A). Next, to investigate whether there was a correlation between *EDN3* expression and methylation in cervical cancer cell lines, we measured the methylation levels of *EDN3* by pyrosequencing. Results showed that the methylation levels of *EDN3* were at high level in all cervical cancer cells (>10%), especially in SiHa and CaSki cells (Figure 2B). Collectively, these data indicated that methylation might mediate silence of EDN3 in cervical cancer cell lines.

5-Aza is a DNMT1 inhibitor. The cervical cancer cell lines C-33A, SiHa and CaSki were treated with 5 or 10 μM 5-Aza or an equal volume of PBS. The expression of *EDN3* were measured after 24 hours. The results showed that the expression of *EDN3* in three cervical cancer cells was increased after 10 μM 5-Aza treatment and was only increased in SiHa and CaSki cells after 5 μM 5-Aza treatment. There was no significant difference in C-33A cells after 5 μM Aza treatment (Figure 2C). One explanation for this phenomenon was that the methylation level of *EDN3* was relatively low in C-33A cells. The inhibitor treatment at low concentration was not enough to cause the significant change of *EDN3* expression in C-33A. All these results indicated that there was a close correlation between EDN3 expression and methylation in cervical cancer cell lines. Furthermore, *EDN3* silencing mediated by methylation can be blocked by 5-AZA treatment in cervical cancer cell lines.

Overexpression of *EDN3* inhibited the proliferation of C-33A, SiHa and CaSki cells.

To investigate the biological functions of *EDN3* in cervical cancer cell lines, OE-*EDN3* vector was constructed. We detected the expression of *EDN3* in C-33A, SiHa and CaSki cells after transfected OE-*EDN3* or vector to verify the transfection efficiency. As the results shown in Figures 3A, B *EDN3* was successfully overexpressed in all cervical cancer cell lines. Subsequently, EdU and clone formation assays were conducted to assess the influence of *EDN3* on cervical cancer cell proliferation. As shown in Figures 3C, D and Figure 4, the proliferation ability and clone formation ability of cervical cancer cell lines with *EDN3* overexpression were found significantly decreased, compared with the vector, in all three cell lines.

Overexpression of *EDN3* inhibited the migration and invasion of C-33A, SiHa and CaSki cells

Subsequently, we investigated that whether there is an influence of *EDN3* on cervical cancer cells migration. The wound-healing assay indicated that overexpression of *EDN3* inhibited the migration in C-33A (after 4 days), SiHa (after 2 days and 4 days) and CaSki (after 24 hours) cells (Figure 5). Similar results were obtained in a transwell assay (Figures 6A, B). In addition, the number of invasion cells were measured after 48 to 72 hours. All these results verified that the invasion capacities of cervical cancer cells in all three cell lines were significantly inhibited by overexpression of *EDN3* (Figures 6C, D).

Discussion

In this study, using the datasets from GEO and TCGA databases, we found that *EDN3* was downregulated and hypermethylated in CSCC. The further analysis in GSE63514 dataset and in our own

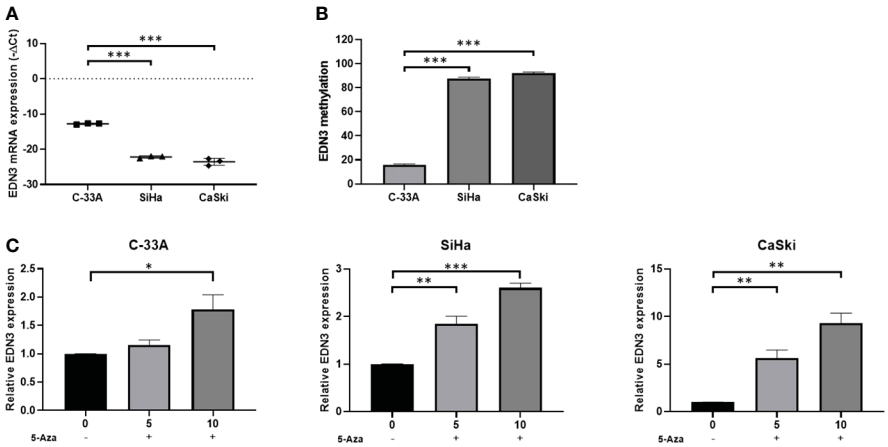

FIGURE 2
EDN3 expression in cervical cancer cells treated with 5-Aza. **(A)** Expression levels of *EDN3* in C-33A, SiHa and CaSki cells. **(B)** Methylation levels (average percentage of methylation across 4 CpG sites) of *EDN3* in C-33A, SiHa and CaSki cells. **(C)** The mRNA expression of *EDN3* in C-33A, SiHa and CaSki cells before and after treatment with 5 and 10 μM 5-Aza. Values are mean ± SD, N = 3; *P<0.05; **P<0.01; ***P<0.001.

10.3389/fonc.2023.1010132

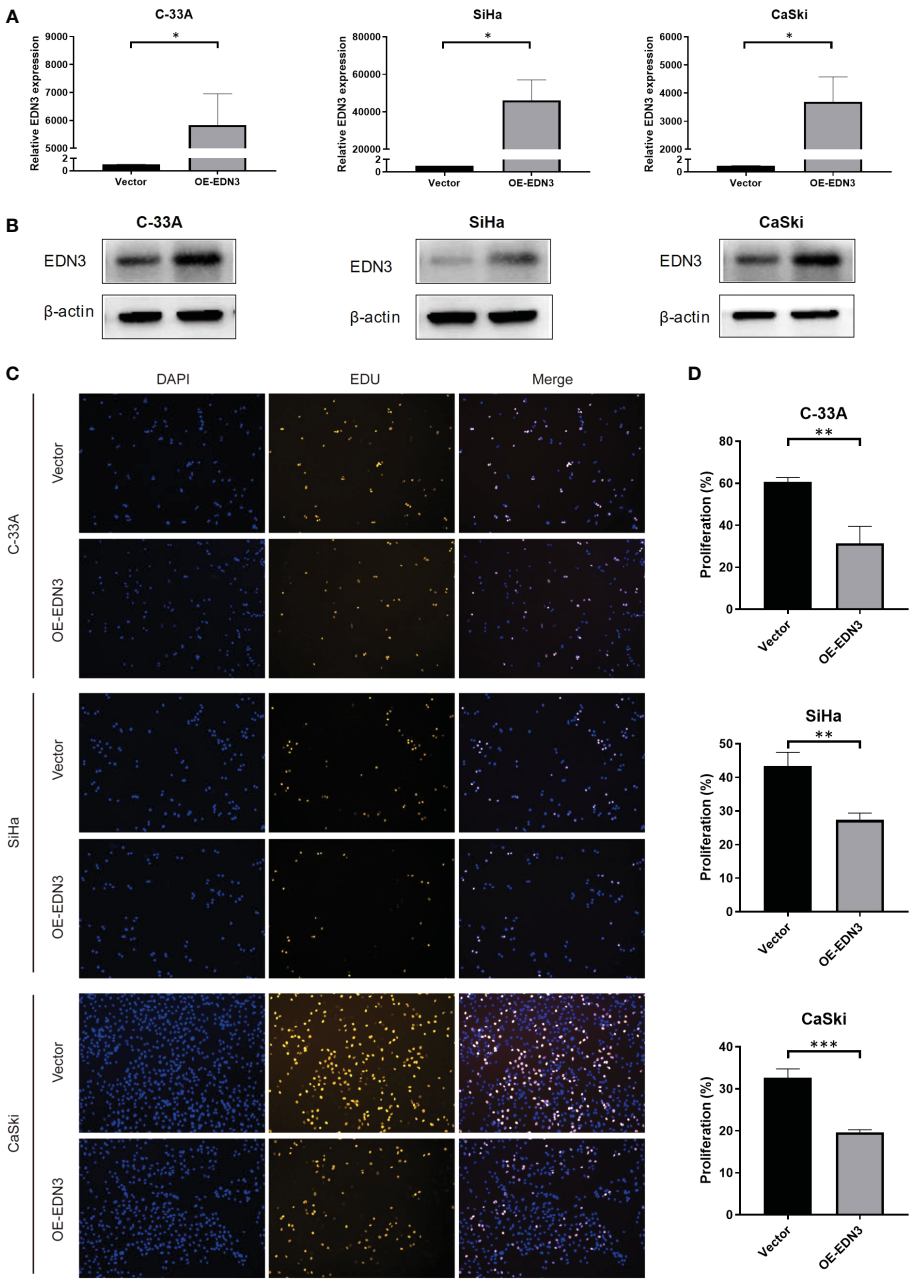

FIGURE 3
Overexpression of *EDN3* inhibited the proliferation of C-33A, SiHa and CaSki cells. **(A)** The mRNA expression of *EDN3* in C-33A, SiHa and CaSki cells transfected with OE-*EDN3* and vector. **(B)** The protein expression of EDN3 in C-33A, SiHa and CaSki cells transfected with OE-*EDN3* and vector. **(C)** Overexpression of *EDN3* inhibited the proliferation of C-33A, SiHa and CaSki cells by EdU assay. **(D)** The proliferation percent after transfection of OE-*EDN3* and vector were measured. Values are mean ± SD, N = 3; *P<0.05; **P<0.01; ***P<0.001.

samples found that the expression of *EDN3* was decreased with the degree of cervical lesions. Pyrosequencing was performed to evaluate 4 CpG sites of the *EDN3* promoter region in our samples, the data indicated that the methylation level of *EDN3* was increased with the degree of cervical lesions. Subsequently, we found that the expression of *EDN3* was decreased, but the methylation of *EDN3* was increased in cervical cancer cell lines. *EDN3* silencing mediated by methylation can be blocked by 5-Aza, a DNMT1 inhibitor, treatment in cervical cancer cell lines. Using EdU assay, would-healing assay, clone formation assay and transwell assay, we confirmed that overexpression of *EDN3* could inhibit the proliferation, clone formation, migration and invasion of cervical cancer cells.

Increasing evidence in the past decade has demonstrated that DNA methylation in certain genes played a critical role in the progression of cervical cancer (16, 33). DNA methylation of TSGs can serve as a mechanism of carcinogenesis (34, 35). Recent studies demonstrated that many genes, such as *ADCYAP1* (36), *ASCL1* (36), *ASTN1* (37, 38), *ATP10* (36), *CADM1* (36), *DCC* (36), *DBC1* (36), *DLX1* (37, 38), *EPB41L3* (39), *FAM19A4* (40), *HS3ST2* (36), *ITGA4* (37, 38), *JAM3* (39), *LHX8* (41), *MAL*, *miR-124* (40), *MOS*, *MYOD1* (36), *PAX1* (41–43), *RXFP3* (37, 38), *SOX1*, *SOX17* (36),

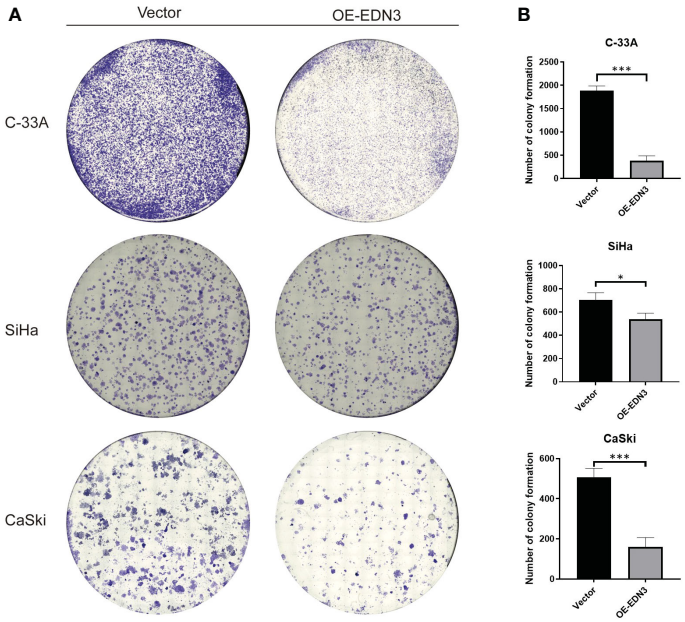

FIGURE 4
Overexpression of *EDN3* inhibited the clone formation of C-33A, SiHa and CaSki cells. **(A)** Representative images of clone formation assay using C-33A, SiHa and CaSki cells transfected with OE-*EDN3* or vector. **(B)** Quantification of clone formation assay is shown. Values are mean ± SD, N = 3; *P<0.05; ***P<0.001.

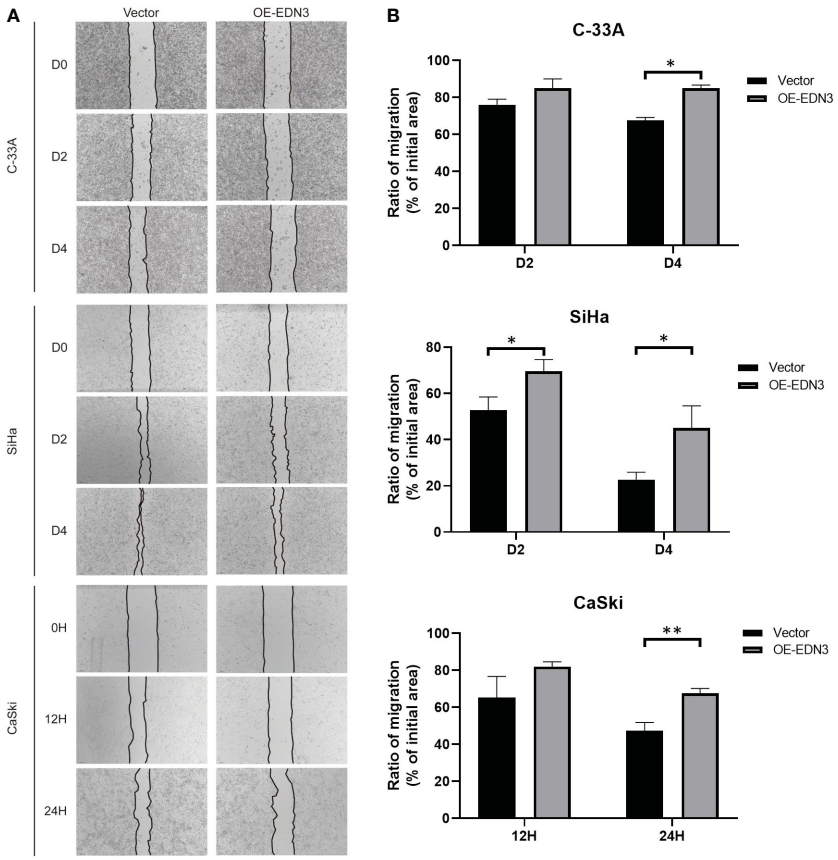

FIGURE 5
Overexpression of *EDN3* inhibited the migration of C-33A, SiHa and CaSki cells by wound healing assay. **(A)** Representative images of wound healing assay using C-33A, SiHa and CaSki cells transfected with OE-*EDN3* or vector. **(B)** Quantification of wound healing assay is shown. Values are mean ± SD, N = 3; *P<0.05; **P<0.01.

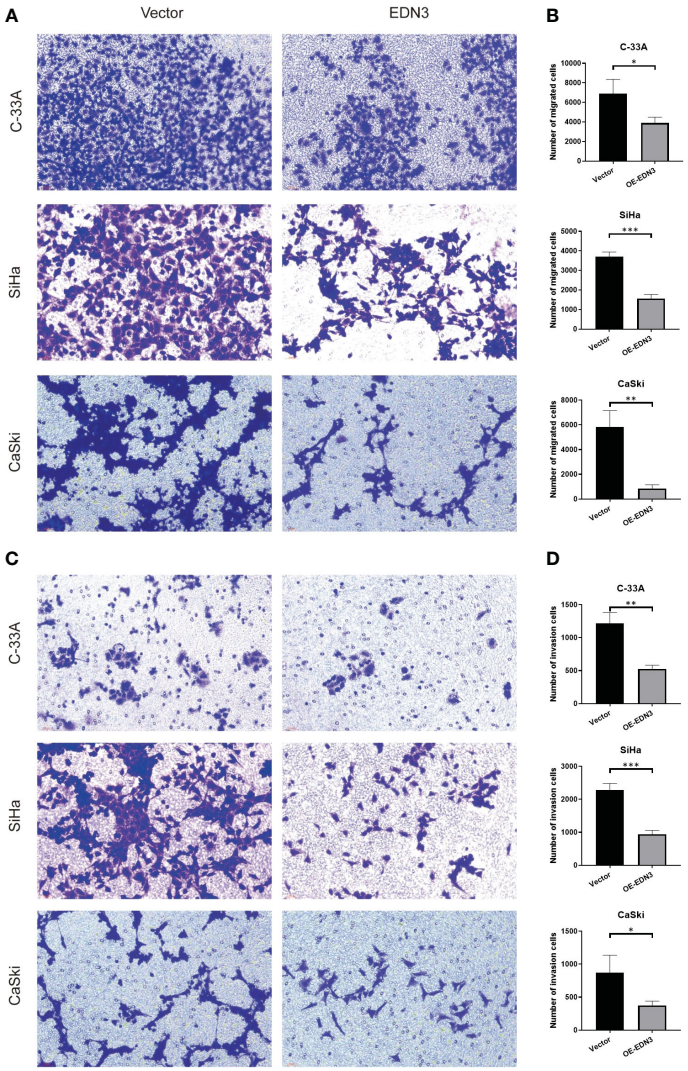

FIGURE 6
Overexpression of *EDN3* inhibited the migration and invasion of C-33A, SiHa and CaSki cells by transwell assay. **(A)** Representative images of cell migration by transwell assay using C-33A, SiHa and CaSki cells transfected with OE-EDN3 or vector. **(B)** Quantification of cell migration by transwell assay is shown. Values are mean ± SD, N = 3; *P<0.05; **P<0.01; ***P<0.001. **(C)** Representative images of cell invasion by transwell assay using C-33A, SiHa and CaSki cells transfected with OE-EDN3 or vector. **(D)** Quantification of cell invasion by transwell assay is shown. Values are mean ± SD, N = 3; *, P<0.05; **, P<0.01; ***, P<0.001.

ST6GALNAC5 (41), *TMEFF2* (36), *ZNF582* (42, 43) and ZNF671 (37, 38) et al, exhibited increased DNA methylation in cervical precancer. However, most of the research has only focused the early diagnosis function of these gene in cervical cancer screening. Researchers have paid little attention to investigate the expression change of most of these genes in different cervical lesions. Whether there is any connection between genes methylation level and expression level is unknow. Additionally, the function of these genes in cancer biology is relatively unexplored and remains largely unknown.

In our current study, detecting the expression and methylation level of *EDN3* both in clinical samples and cervical cancer cell lines, we confirmed the expression of *EDN3* was decreased, but the methylation level of *EDN3* was increased, with the degree of cervical lesions. The results in cervical cancer cell lines treated with 5-Aza further confirmed that methylation mediated silencing of *EDN3* in cervical cancer. The genes, down-regulated and hypermethylated in cancers, may provide potential drug targets for cervical cancer. We used several types of assays in this study to investigate the function of *EDN3* in cancer biology from different aspects. All results together verified that overexpression of *EDN3* could inhibit the proliferation, clone formation, migration and invasion of cervical cancer cells. It suggested that *EDN3* played a tumor suppressive function in cervical cancer. Collectively, *EDN3* is a potential biomarker and therapeutic target for CSCC. However, in this study, we only analysis the expression and methylation level of *EDN3* in CSCC samples. Whether there is any association between *EDN3* and cervical adenocarcinoma is still unknown. We should investigate that in the future research.

Recent studies reported that *EDN3* participated in cell proliferation, differentiation and metastasis in some solid tumors. In breast cancer, cervical cancer, colorectal cancer, glioma and papillary thyroid cancer, the expression of *EDN3* gene is

significantly down-regulated, which may be regulated by epigenetics (21, 23–26, 44, 45). *EDN3* promotes cell apoptosis and inhibits cell invasion and migration in malignant glioma cells (21). *EDN3* is hypermethylated and down-regulated in human primary colon cancer and colon cancer cell lines, and overexpression of *EDN3* can inhibit the invasion and migration of colon cancer cells (26, 46). Abnormal methylation of *EDN3* gene is closely related to breast cancer, and hypermethylation of this gene can reduce or even silence its expression in breast cancer tissue. Patients with high expression of *EDN3* have long overall survival and disease-free survival, and *EDN3* can be used as a biomarkers for early diagnosis and prognosis of breast cancer (24, 47). In addition, reduced *EDN3* expression was associated with the progression of papillary thyroid cancer (45).

In our studies we confirmed that methylation mediated silencing of *EDN3* in cervical cancer. And this silencing mediated by methylation could be blocked by 5-Aza treatment in cervical cancer cell lines. Overexpression of *EDN3* could inhibit the proliferation, clone formation, migration and invasion of cervical cancer cells. *EDN3* played a tumor suppressive function in cervical cancer. Based on our findings, *EDN3* may serve as a potential biomarker and therapeutic target for CSCC. The detail mechanism of *EDN3* suppression of cervical cancer has not been elucidated in this study and will be further investigated in our future work.

Data availability statement

The datasets presented in this study can be found in online repositories. The names of the repository/repositories and accession number(s) can be found in the article/Supplementary Material.

Ethics statement

The studies involving human participants were reviewed and approved by the Medical Ethics Committee of Xiangya Hospital Central South University. The patients/participants provided their written informed consent to participate in this study.

Author contributions

Designed research: QL, JX, LF, HZ, WZ, YS. Performed research: PZ, YL. Analysis data: PZ, XL. Obtained informed consent and acquired patient samples and clinical information: XL, JX, DY, LL, JH, BW, QN, SW, LD. Provided technical support: YC, SL. Wrote manuscript: PZ, XL. Revised manuscript: PZ, QL, JX. All authors contributed to the article and approved the submitted version.

Funding

National Natural Science Foundation (NNSF) of China (81973401, 81773824). Natural Science Foundation of Hunan Province (2020JJ4818).

Conflict of interest

The authors declare that the research was conducted in the absence of any commercial or financial relationships that could be construed as a potential conflict of interest.

Publisher's note

All claims expressed in this article are solely those of the authors and do not necessarily represent those of their affiliated organizations, or those of the publisher, the editors and the reviewers. Any product that may be evaluated in this article, or claim that may be made by its manufacturer, is not guaranteed or endorsed by the publisher.

Supplementary material

The Supplementary Material for this article can be found online at: https://www.frontiersin.org/articles/10.3389/fonc.2023.1010132/full#supplementary-material

References

1. Sung H, Ferlay J, Siegel RL, Laversanne M, Soerjomataram I, Jemal A, et al. Global cancer statistics 2020: GLOBOCAN estimates of incidence and mortality worldwide for 36 cancers in 185 countries. *CA Cancer J Clin* (2021) 71:209–49. doi: 10.3322/caac.21660

2. Bruni L, Albero G, Serrano B, Mena M, Gómez D, Munoz J, et al. ICO/IARC information centre on HPV and cancer (HPV information centre). *Hum Papillomavirus Related Dis Mali. Summary Rep* (2019).

3. Fabrizii M, Moinfar F, Jelinek HF, Karperien A, Ahammer H. Fractal analysis of cervical intraepithelial neoplasia. *PloS One* (2014) 9:e108457. doi: 10.1371/journal.pone.0108457

4. Mazumder Indra D, Singh RK, Mitra S, Dutta S, Chakraborty C, Basu PS, et al. Genetic and epigenetic changes of HPV16 in cervical cancer differentially regulate E6/E7 expression and associate with disease progression. *Gynecologic Oncol* (2011) 123:597–604. doi: 10.1016/j.ygyno.2011.08.004

5. Lee KW, Pausova Z. Cigarette smoking and DNA methylation. *Front Genet* (2013) 4:132. doi: 10.3389/fgene.2013.00132

6. Bishop KS, Ferguson LR. The interaction between epigenetics, nutrition and the development of cancer. *Nutrients* (2015) 7:922–47. doi: 10.3390/nu7020922

7. Güzel C, van Sten-Van't Hoff J, de Kok I, Govorukhina NI, Boychenko A, Luider TM, et al. Molecular markers for cervical cancer screening. *Expert Rev Proteomics* (2021) 18:675–91. doi: 10.1080/14789450.2021.1980387

8. Bird A. DNA Methylation patterns and epigenetic memory. *Genes Dev* (2002) 16:6–21. doi: 10.1101/gad.947102

9. Laird PW. The power and the promise of DNA methylation markers. *Nat Rev Cancer* (2003) 3:253–66. doi: 10.1038/nrc1045

10. Hermann A, Gowher H, Jeltsch A. Biochemistry and biology of mammalian DNA methyltransferases. *Cell Mol Life Sci* (2004) 61:2571–87. doi: 10.1007/s00018-004-4201-1

11. Goyal R, Reinhardt R, Jeltsch A. Accuracy of DNA methylation pattern preservation by the Dnmt1 methyltransferase. *Nucleic Acids Res* (2006) 34:1182–8. doi: 10.1093/nar/gkl002

12. Supic G, Jagodic M, Magic Z. Epigenetics: a new link between nutrition and cancer. *Nutr Cancer* (2013) 65:781–92. doi: 10.1080/01635581.2013.805794

13. Jair KW, Bachman KE, Suzuki H, Ting AH, Rhee I, Yen RW, et al. *De novo* CpG island methylation in human cancer cells. *Cancer Res* (2006) 66:682–92. doi: 10.1158/0008-5472.CAN-05-1980

14. Klutstein M, Nejman D, Greenfield R, Cedar H. DNA Methylation in cancer and aging. *Cancer Res* (2016) 76:3446–50. doi: 10.1158/0008-5472.CAN-15-3278

15. Morgan AE, Davies TJ, Mc Auley MT. The role of DNA methylation in ageing and cancer. *Proc Nutr Soc* (2018) 77:412–22. doi: 10.1017/S0029665118000150

16. Zhu H, Zhu H, Tian M, Wang D, He J, Xu T. DNA Methylation and hydroxymethylation in cervical cancer: Diagnosis, prognosis and treatment. *Front Genet* (2020) 11:347. doi: 10.3389/fgene.2020.00347

17. Xiong Y, Wei Y, Gu Y, Zhang S, Lyu J, Zhang B, et al. DiseaseMeth version 2.0: A major expansion and update of the human disease methylation database. *Nucleic Acids Res* (2017) 45:D888–d895. doi: 10.1093/nar/gkw1123

18. Grimshaw MJ. Endothelins and hypoxia-inducible factor in cancer. *Endocr Relat Cancer* (2007) 14:233–44. doi: 10.1677/ERC-07-0057

19. Levin ER. Endothelins. *New Engl J Med* (1995) 333:356–63. doi: 10.1056/NEJM199508103330607

20. Rosano L, Spinella F, Bagnato A. Endothelin 1 in cancer: biological implications and therapeutic opportunities. *Nat Rev Cancer* (2013) 13:637–51. doi: 10.1038/nrc3546

21. Liu Y, Ye F, Yamada K, Tso JL, Zhang Y, Nguyen DH, et al. Autocrine endothelin-3/endothelin receptor b signaling maintains cellular and molecular properties of glioblastoma stem cells. *Mol Cancer Res* (2011) 9:1668–85. doi: 10.1158/1541-7786.MCR-10-0563

22. Espinosa AM, Alfaro A, Roman-Basaure E, Guardado-Estrada M, Palma Í., Serralde C, et al. Mitosis is a source of potential markers for screening and survival and therapeutic targets in cervical cancer. *PloS One* (2013) 8:e55975. doi: 10.1371/journal.pone.0055975

23. Chen YC, Huang RL, Huang YK, Liao YP, Su PH, Wang HC, et al. Methylomics analysis identifies epigenetically silenced genes and implies an activation of β-catenin signaling in cervical cancer. *Int J Cancer* (2014) 135:117–27. doi: 10.1002/ijc.28658

24. Salhia B, Kiefer J, Ross JT, Metapally R, Martinez RA, Johnson KN, et al. Integrated genomic and epigenomic analysis of breast cancer brain metastasis. *PloS One* (2014) 9: e85448. doi: 10.1371/journal.pone.0085448

25. Lin H, Ma Y, Wei Y, Shang H. Genome-wide analysis of aberrant gene expression and methylation profiles reveals susceptibility genes and underlying mechanism of cervical cancer. *Eur J obstetrics gynecology Reprod Biol* (2016) 207:147–52. doi: 10.1016/j.ejogrb.2016.10.017

26. Olender J, Nowakowska-Zajdel E, Kruszniewska-Rajs C, Orchel J, Mazurek U, Wierzgon A, et al. Epigenetic silencing of endothelin-3 in colorectal cancer. *Int J immunopathol Pharmacol* (2016) 29:333–40. doi: 10.1177/0394632015600371

27. Zhai Y, Kuick R, Nan B, Ota I, Weiss SJ, Trimble CL, et al. Gene expression analysis of preinvasive and invasive cervical squamous cell carcinomas identifies HOXC10 as a key mediator of invasion. *Cancer Res* (2007) 67:10163–72. doi: 10.1158/0008-5472.CAN-07-2056

28. Scotto L, Narayan G, Nandula SV, Arias-Pulido H, Subramaniyam S, Schneider A, et al. Identification of copy number gain and overexpressed genes on chromosome arm 20q by an integrative genomic approach in cervical cancer: potential role in progression. *Genes Chromosomes Cancer* (2008) 47:755–65. doi: 10.1002/gcc.20577

29. den Boon JA, Pyeon D, Wang SS, Horswill M, Schiffman M, Sherman M, et al. Molecular transitions from papillomavirus infection to cervical precancer and cancer: Role of stromal estrogen receptor signaling. *Proc Natl Acad Sci U.S.A.* (2015) 112:E3255–64. doi: 10.1073/pnas.1509322112

30. Bardou P, Mariette J, Escudié F, Djemiel C, Klopp C. Jvenn: an interactive Venn diagram viewer. *BMC Bioinf* (2014) 15:293. doi: 10.1186/1471-2105-15-293

31. Iwagami S, Baba Y, Watanabe M, Shigaki H, Miyake K, Ishimoto T, et al. LINE-1 hypomethylation is associated with a poor prognosis among patients with curatively resected esophageal squamous cell carcinoma. *Ann Surg* (2013) 257:449–55. doi: 10.1097/SLA.0b013e31826d8602

32. Guo J, Zhu P, Ye Z, Wang M, Yang H, Huang S, et al. YRDC mediates the resistance of lenvatinib in hepatocarcinoma cells *via* modulating the translation of KRAS. *Front Pharmacol* (2021) 12:2447. doi: 10.3389/fphar.2021.744578

33. Dueñas-González A, Lizano M, Candelaria M, Cetina L, Arce C, Cervera E. Epigenetics of cervical cancer. an overview and therapeutic perspectives. *Mol Cancer* (2005) 4:38. doi: 10.1186/1476-4598-4-38

34. Baylin SB, Ohm JE. Epigenetic gene silencing in cancer - a mechanism for early oncogenic pathway addiction? *Nat Rev Cancer* (2006) 6:107–16. doi: 10.1038/nrc1799

35. Dawson MA, Kouzarides T. Cancer epigenetics: From mechanism to therapy. *Cell* (2012) 150:12–27. doi: 10.1016/j.cell.2012.06.013

36. Clarke MA, Luhn P, Gage JC, Bodelon C, Dunn ST, Walker J, et al. Discovery and validation of candidate host DNA methylation markers for detection of cervical precancer and cancer. *Int J Cancer* (2017) 141:701–10. doi: 10.1002/ijc.30781

37. Schmitz M, Eichelkraut K, Schmidt D, Zeiser I, Hilal Z, Tettenborn Z, et al. Performance of a DNA methylation marker panel using liquid-based cervical scrapes to detect cervical cancer and its precancerous stages. *BMC Cancer* (2018) 18:1197. doi: 10.1186/s12885-018-5125-8

38. Zhang L, Zhao X, Hu S, Chen S, Zhao S, Dong L, et al. Triage performance and predictive value of the human gene methylation panel among women positive on self-collected HPV test: Results from a prospective cohort study. *Int J Cancer* (2022) 151:878–87. doi: 10.1002/ijc.34041

39. Kong L, Wang L, Wang Z, Xiao X, You Y, Wu H, et al. DNA Methylation for cervical cancer screening: A training set in China. *Clin Epigenet* (2020) 12:91. doi: 10.1186/s13148-020-00885-7

40. Zummeren MV, Kremer WW, Leeman A, Bleeker MCG, Jenkins D, Sandt MV, et al. HPV E4 expression and DNA hypermethylation of CADM1, MAL, and miR124-2 genes in cervical cancer and precursor lesions. *Mod Pathol* (2018) 31:1842–50. doi: 10.1038/s41379-018-0101-z

41. Kremer WW, Van Zummeren M, Novianti PW, Richter KL, Verlaat W, Snijders PJ, et al. Detection of hypermethylated genes as markers for cervical screening in women living with HIV. *J Int AIDS Soc* (2018) 21:e25165. doi: 10.1002/jia2.25165

42. Liou YL, Zhang Y, Liu Y, Cao L, Qin CZ, Zhang TL, et al. Comparison of HPV genotyping and methylated ZNF582 as triage for women with equivocal liquid-based cytology results. *Clin Epigenet* (2015) 7:50. doi: 10.1186/s13148-015-0084-2

43. Liou YL, Zhang TL, Yan T, Yeh CT, Kang YN, Cao L, et al. Combined clinical and genetic testing algorithm for cervical cancer diagnosis. *Clin Epigenet* (2016) 8:66. doi: 10.1186/s13148-016-0232-3

44. Qiu J, Zhang W, Zang C, Liu X, Liu F, Ge R, et al. Identification of key genes and miRNAs markers of papillary thyroid cancer. *Biol Res* (2018) 51:45. doi: 10.1186/s40659-018-0188-1

45. Chen H, Cai B, Liu K, Hua Q. miR–27a–3p regulates the inhibitory influence of endothelin 3 on the tumorigenesis of papillary thyroid cancer cells. *Mol Med Rep* (2021) 23.

46. Wang R, Lohr CV, Fischer K, Dashwood WM, Greenwood JA, Ho E, et al. Epigenetic inactivation of endothelin-2 and endothelin-3 in colon cancer. *Int J Cancer* (2013) 132:1004–12. doi: 10.1002/ijc.27762

47. Wiesmann F, Veeck J, Galm O, Hartmann A, Esteller M, Knüchel R, et al. Frequent loss of endothelin-3 (EDN3) expression due to epigenetic inactivation in human breast cancer. *Breast Cancer Res* (2009) 11:R34. doi: 10.1186/bcr2319

frontiers | Frontiers in Oncology

TYPE Original Research
PUBLISHED 10 February 2023
DOI 10.3389/fonc.2023.1101249

OPEN ACCESS

EDITED BY
Ming Yi,
Zhejiang University, China

REVIEWED BY
Yang Deng,
Shandong First Medical University, China
Wenxi Tang,
China Pharmaceutical University, China

*CORRESPONDENCE
Chuanhua Yu
yuchua@whu.edu.cn

SPECIALTY SECTION
This article was submitted to Cancer Epidemiology and Prevention, a section of the journal Frontiers in Oncology

RECEIVED 25 November 2022
ACCEPTED 27 January 2023
PUBLISHED 10 February 2023

CITATION
Mubarik S, Wang F, Luo L, Hezam K and Yu C (2023) Evaluation of Lee–Carter model to breast cancer mortality prediction in China and Pakistan. *Front. Oncol.* 13:1101249. doi: 10.3389/fonc.2023.1101249

Evaluation of Lee–Carter model to breast cancer mortality prediction in China and Pakistan

Sumaira Mubarik [1], Fang Wang [2], Lisha Luo [3], Kamal Hezam [4] and Chuanhua Yu [1]*

[1]Department of Epidemiology and Biostatistics, School of Public Health, Wuhan University, Wuhan, China, [2]Department of Biostatistics, School of Public Health, Xuzhou Medical University, Xuzhou, Jiangsu, China, [3]Center for Evidence-Based and Translational Medicine, Zhongnan Hospital of Wuhan University, Wuhan, Hubei, China, [4]Nankai University, School of Medicine, Tianjin, China

Background: Precise breast cancer–related mortality forecasts are required for public health program and healthcare service planning. A number of stochastic model–based approaches for predicting mortality have been developed. The trends shown by mortality data from various diseases and countries are critical to the effectiveness of these models. This study illustrates the unconventional statistical method for estimating and predicting the mortality risk between the early-onset and screen-age/late-onset breast cancer population in China and Pakistan using the Lee–Carter model.

Methods: Longitudinal death data for female breast cancer from 1990 to 2019 obtained from the Global Burden of Disease study database were used to compare statistical approach between early-onset (age group, 25–49 years) and screen-age/late-onset (age group, 50–84 years) population. We evaluated the model performance both within (training period, 1990–2010) and outside (test period, 2011–2019) data forecast accuracy using the different error measures and graphical analysis. Finally, using the Lee–Carter model, we predicted the general index for the time period (2011 to 2030) and derived corresponding life expectancy at birth for the female breast cancer population using life tables.

Results: Study findings revealed that the Lee–Carter approach to predict breast cancer mortality rate outperformed in the screen-age/late-onset compared with that in the early-onset population in terms of goodness of fit and within and outside forecast accuracy check. Moreover, the trend in forecast error was decreasing gradually in the screen-age/late-onset compared with that in the early-onset breast cancer population in China and Pakistan. Furthermore, we observed that this approach had provided almost comparable results between the early-onset and screen-age/late-onset population in forecast accuracy for more varying mortality behavior over time like in Pakistan. Both the early-onset and screen-age/late-onset populations in Pakistan were expected to have an increase in breast cancer mortality by 2030. whereas, for China, it was expected to decrease in the early-onset population.

Conclusion: The Lee–Carter model can be used to estimate breast cancer mortality and so to project future life expectancy at birth, especially in the screen-age/late-onset population. As a result, it is suggested that this approach may be useful and convenient for predicting cancer-related mortality even when

epidemiological and demographic disease data sets are limited. According to model predictions for breast cancer mortality, improved health facilities for disease diagnosis, control, and prevention are required to reduce the disease's future burden, particularly in less developed countries.

KEYWORDS

breast cancer, Lee-Carter model, forecast accuracy, life expectancy, MAPE

Introduction

Cancer is one of the leading causes of death and disability worldwide. Breast cancer (BC) is the most common cancer diagnosed in women and is the first leading cause of cancer-related mortality in women (1, 2). It develops from a single cell that divides and multiplies into a lump that can be detected clinically. Its severe form from cancer's prolonged development is the metastasis phase that is the more challenging treated phase (3, 4). The most common clinical manifestations of BC are a tumorous mass in the breast, enlarged lymph nodes in the armpits, and distant metastases. Recent studies have found that chronic inflammation plays a role in the development and progression of BC, in addition to genetics and the environment (5–7). Stage at diagnosis has been confirmed as a key prognostic factor for BC, and the previous study revealed that the advanced (III) and metastatic stage (IV) are highly associated with lower survival rates (8). Consequently, addressing healthcare policies for early diagnosis may reduce the morbidity and mortality of BC.

The burden of BC has been rising faster in low- and middle-income countries (LMICs) compared with high-income countries in last three decades due to the lack of healthcare policies. Drafting public health policy and devising interventions against cancer require accurate data in LMICs. However, because of insufficient and demographic and disease registration data in LMICs, statisticians are unable to evaluate disease consequences. Among the previous studies on BC mortality predictive models, some studies used simple models such as the joinpoint model or single-population model (9), and some have used machine learning algorithms to predict specific mortality for BC based on specific populations (10), but the application of dynamic predictions and models for whole population or age-specific mortality is still lacking. The introduction of stochastic mortality models provides us an opportunity to forecast cancer-specific mortality in LMICs. A number of suitable statistical approaches for mortality prediction have been proposed, and the performance of these models differs in various diseases and countries (11–13).

Several efforts have been directed toward finding an appropriate model for the accurate prediction of age-specific death patterns. In this regard, various parametric curves (14, 15) were considered to predict the mortality rate by year. Following these concepts, different approaches are established to predict mortality rates using stochastic models (16–19). As part of stochastic mortality models, the Lee–Carter (LC) method of mortality forecasting has become one of the most useful tools for forecasting age-specific mortality rates, and it has been previously employed for this purpose in several works (20–22). The model posits that variations in mortality trends over time are governed solely by a single parameter (k_t.)the mortality index. The mortality forecast is created using this index by selecting an appropriate time series model (23). LC-based modeling frameworks are one of the most efficient and transparent methods of modeling and projecting mortality dynamics (13, 16, 20, 24–29). Moreover, this model has also been suggested for predicting cause-specific mortality rate, for instance, BC causes mortality, which follows a smooth curvilinear and rapid change pattern over time (24).

Most Asian countries are facing an increased BC burden and do not have sufficient health-related facilities like proper diagnosis, screening, and treatment. Moreover, because of population aging and increasing life expectancy, the disease burden has been shifting from communicable to non-communicable diseases in these countries. These countries are having similar circumstances related to population expansion and aging (13). Furthermore, because of the shortcomings in these countries' statistical registry systems, researchers are constantly confronted with the challenge of insufficient and unsatisfactory demographic and disease registration data sets to undertake suitable statistical analysis. Given the scarcity of data and its poor quality, advanced statistical approaches may be useful in modeling and predicting the mortality patterns in developing countries, and the LC model is one of the good options (11, 12).

Age-specific BC incidence curves have been shown to superimpose two distinct rate curves, one for early-onset BC with a median age of diagnosis below 50 years and another for late-onset BC with a median age of diagnosis above 70 years, disproving the long-held belief that the inflection point in the overall curve occurs around menopause (30, 31). Therefore, this study investigates the application of the LC model for BC mortality prediction between early-onset and age-screen/late-screen female populations in China and Pakistan. In our study, two age groups of 25–49 years and 50–84 years are stratified to assess the model applicability, and the early-onset population was defined as BC occurring in women under the age of 50, whereas the late-onset population was recognized as BC occurring in women aged 50–84 years. It is proved that early-onset BC has more aggressive clinicopathological characteristic and worse prognosis (32), so more specific studies are needed to compare the disparities

Abbreviations: BC, breast cancer; LC, Lee–Carter; SVD, singular value decomposition; LMICs, low- and middle-income countries; GBD, global burden of diseases; DR, death rates; PV, percentage of variation; ASMR, age-standardized mortality rates; ARIMA, autoregressive integrated moving average; MAPE, mean absolute percent error.

of BC mortality trends between the early-onset and screen-age/late-onset female population. To the best our knowledge, this is the first study using advanced statistical methods in evaluating and predicting the BC-related mortality trends between the early-onset and screen-age/late-onset population for two developing countries.

Data and methods

The annual mortality rates of the two Asian countries due to BC from 1990 to 2019 at the early-onset (age category of 25–49 years) and screen-age/late-onset (age category of 50–84 years) population were selected to run the application of the LC model. The Institute for Health Metrics and Evaluation (http://ghdx.healthdata.org/gbd-results-tool) provided BC mortality data for two Asian countries: China and Pakistan (33, 34). The availability of data and the sources are both included in the "Data and materials availability" declaration at the end of this study. BC mortality rates were calculated using the ratio of "number of deaths" to "exposure to risk", which was grouped in a matrix for the specific age x and time t. We separated the data set into two parts to study the within-sample and out-of-sample model performance: training data set (1990–2010) and test data set (2011–2019). We fitted the) model on the training data set and evaluated the model performance using within and outside forecast accuracy.

The LC model (16) estimates mortality index k_t. utilizing age-specific death rates. This assessment is made for the early-onset and screen-age/late-onset female population for China and Pakistan. The estimated model is evaluated for both goodness of fit and accuracy of forecast ability. Using the mortality index (k_t.)stimation, BC death rates and life expectancy may be predicted.

Statistical analysis

Lee–Carter model

The LC model considers a statistical and demographic model that predicts mortality rates to derive life tables (16). The fundamental assumption of the model is that there is a linear connection between the age-specific death rates on logarithm scale ($m_{x,t}$). age interval x and time t. This relationship is described as follows:

$$m_{x,t} = exp(a_x + b_x k_t + e_{xt}), \qquad t = 1, 2, \ldots, n \quad x = 1, 2, \ldots, \omega \qquad (1)$$

Equation (1) can be expressed by taking natural logarithm on both sides as follows:

$$f_{x,t} = \ln(m_{x,t}) = a_x + b_x k_t + e_{xt}, \qquad t = 1, 2, \ldots, n \quad x = 1, 2, \ldots, \omega \quad (2)$$

In Equation (2), $m_{x,t}$. represents age-specific death rate for the x age interval and year t, a_x. notes the average age-specific mortality, k_t represents the mortality index in the year t, b_x. a mortality deviation caused by changes in the k_t. index, e_{xt} is the random error, and ω. the start of the last age interval (35).

There are various issues with parameter estimation when the bilinear term $b_x k_t$ is present. Lee and Carter used a technique known as the singular value decomposition (SVD) to partially alleviate these issues. This method necessitates the assumption that the random component is homoscedastic. According to research, the sample's variance is not distributed uniformly (36, 37). For instance, when contrasting the variance between the age ranges of 25–50 years and 50 + years, this phenomena is very obvious. The greatest likelihood method is an alternative to the SVD approach. We assume that the number of deaths is a random variable with a Poisson distribution while using this estimation technique.

The earlier research demonstrates that mortality modeling can be done successfully using the LC models. To estimate structural parameters, one can utilize the greatest likelihood technique. However, when simulating the number of deaths, additional distributions in addition to the Poisson distribution should be utilized. Previous studies have demonstrated that using the negative binomial distribution can produce positive outcomes when dealing with heterogeneous populations. In that instance, the LC model offered better results in terms of goodness of fit (36).

To get an estimate for the values of a_x, b_x and k_t, a system of simultaneous equations is needed to be solved, which is called the system's solutions. Therefore, death rates for various age groups (r) observed at different points in time (n) produces a system of equations containing $2r+n$ unknown variables that correspond to the total of the r values of a_x, r values of b_x, n values of k_t, and the total number of equations is $r \times n$. The matrix form of such system of equations can be represented as below:

$$\boldsymbol{D} = \boldsymbol{A} + \boldsymbol{b} \,.\, \boldsymbol{k} \qquad (3)$$

D is an matrix of the order $r \times n$, and an element $D_{i,j}$ represents the age-specific death rate (on natural logarithm scale) in the age group i in year j. A denotes a matrix with of order $r \times n$. For the same year j, the elements that belong to the same categories are identical: $a_{ij}=a_{2j}=\ldots a_{rj}$, while b represents a vector of order $r \times 1$ and k is a vector of order $1 \times n$

A unique solution of equation (3) can be arrived by imposing following two restrictions: $\sum_{x=1}^{\omega} b_x = 1$; $\sum_{t=1}^{n} k_t = 0$.

When such restrictions are applied, the a_x coefficient represents mean mortality rate over time. Therefore, the parameter b_x and k_t are calculated individually. The coefficients of a_x are obtained from the following equation.

$$a_x = \frac{\sum_{t=1}^{n} \ln(m_{x,t})}{n} \qquad (4)$$

When the matrix A is computed, the system (3) may be recast as follows:

$$D^{*} = D - A = b \,.\, k \qquad (5)$$

The aforementioned system offers a unique solution when these restrictions are met. The SVD technique is used to estimate the b and k parameters. This technique is used to get the best fit of least squares. D^{*} can be expressed as the product of two matrices using SVD. The element (i, j) in D^{*} shows the product of the i^{th} row of B and the j^{th} row of K, resulting in the following:

$$m_{i,j} = \sum_{l=1}^{r} B_{i,l} K_{j,l}^{T} \qquad (6)$$

As a result, the decomposition yields r terms that exactly match the D^{*} matrix element. Lee and Carter (16) proposed D^{*} as the product of the b and k vectors. When employing SVD, these were

regarded first-order approximations, i.e., D′ can be represented as follows:

$$D' \approx B_1 K_1^T \tag{7}$$

Finally, B_1=B and K_1=K are computed, implying an initial estimate of the model's parameters in equation (14).

Re-estimation of k_t parameter

In general, the results produced from the model's initial estimates do not offer an acceptable match to the observed data. Lee and Carter (16) and Bell (38) point out that there may be deviations from the predictions. Therefore, a second step is required to estimate the parameters. This step utilizes the a_x and b_x values from the previous step to get a new estimate of k_t reflecting that a total number of deaths for the given year must be observed. The goal is to determine k_t values, which satisfy the following condition:

$$D_t = \sum_{x=0}^{\omega} N_{x,\,t}\, exp(a_x + b_x k_t + e_{x,\,t}) \tag{8}$$

In Equation (8), D_t is the total number of deaths during the calendar year t. The population in the x age interval in the year t is denoted by $N_{x,\,t}$ and ω is the age of the final observed group in mortality tables (16). The model estimation is carried out using the ilc package in R programming language (Development Core Team, 2008).

Age-specific death rate prediction

After obtaining the time series for the k_t index as described in section (2, 3), autoregressive integrated moving average (ARIMA) model may be used to forecast such an index; then, it is possible to obtain the death rates for the anticipated years. In the equation, the predicted values of k_{n+h} e substituted.

$$\hat{m}_{x,\,n+h} = \hat{m}_{x,\,n}\ \ exp\left\{\hat{b}_x(\hat{k}_{n+h} - \hat{k}_n)\right\},\ \ h = 1, 2, \ldots\ \ x = 1, 2, \ldots,\ \ \omega \tag{9}$$

In Equation (9), n represents the most recent year for which data are available, h represents the prediction horizon, and x represents the age group. Equation (9) is used to forecast death rates based on the most recent death rate. To anticipate death rates, the LC model offered an approximate prediction interval (16). The interval is calculated using estimates of b_x pameters and standard errors of the k_t projections.

$$PI: \left\{m_{x,t}\ \ exp(2b_x\ \ se_{kt})\right\};\ \left\{m_{x,t}\ \ exp(-2b_x\ \ se_{kt})\right\} \tag{10}$$

Life expectancy at birth

Age-specific life expectancy estimates the average number of years left in a person's life, assuming that current mortality rates remain unchanged. It is computed by considering age-specific death rates (39). The standard technique of Chiang (40) is used to calculate life expectancy at birth using projected death rates. The life expectancy at x, e_x., is stated as follows:

$$e_x = \frac{T_x}{l_x} \tag{11}$$

T_x presents the total number of years that the cohort has lived during the age interval and subsequent age intervals, and l_x denotes number of individuals alive at the start of the x age interval from a population of l_0 newborn infants. This is generally expressed as l_0 =100,000 (23).

Error measure

The predictive ability of the model was evaluated by mean absolute percent error (MAPE), using the following formula:

$$MAPE = \left(\frac{1}{H}\sum_{h=1}^{H}|e_{t+h}|\right) \times 100$$

where $e_{t+h} = \frac{\text{actul value−predicted value}}{\text{actual value}}$, and H denotes the number of predicted sample size.

To assess the forecast ability of the model, both within-sample and out-of-sample forecast accuracy were tested. A model is deemed to be well-fit if it delivers a strong fit within-sample to the historical data and good out-of-sample forecasts. As a result, out-of-sample predictive accuracy was investigated to confirm the model's predictive accuracy with consistency. The following steps were taken into account when evaluating forecast accuracy. To begin, we must select the metric of interest, which includes the anticipated variable. Forecasted variable measurements could include death rates, life expectancy, or future survival rates. As this study aims to examine the feasibility of stochastic mortality model on BC mortality data, therefore, we focused on BC mortality rates. We forecasted BC mortality rates from 2011 to 2019 using the fitted model and calculated life expectancy by comparing forecasts with the actual values.

Results

Breast cancer mortality behavior

We found that BC mortality has gradually grown with time when we examined the variations in BC mortality rates related to both age x and period t. Figure 1 depicts the general patterns in BC mortality rates from 1990 to 2019 for two countries to investigate this process. We may also see that death trends are not consistent between ages and throughout time. In both countries, there is an increasing disparity among older age groups (>50 years), particularly around the age of 84 years.

Model estimation

To assess the model's within-sample and out-of-sample performance, we modified the model by removing the last 9 years of data from both countries' data sets. Fitting the stochastic mortality model (LC) for both the early-onset and screen-age/late-onset population is the initial stage in the analytical process. Figure 2

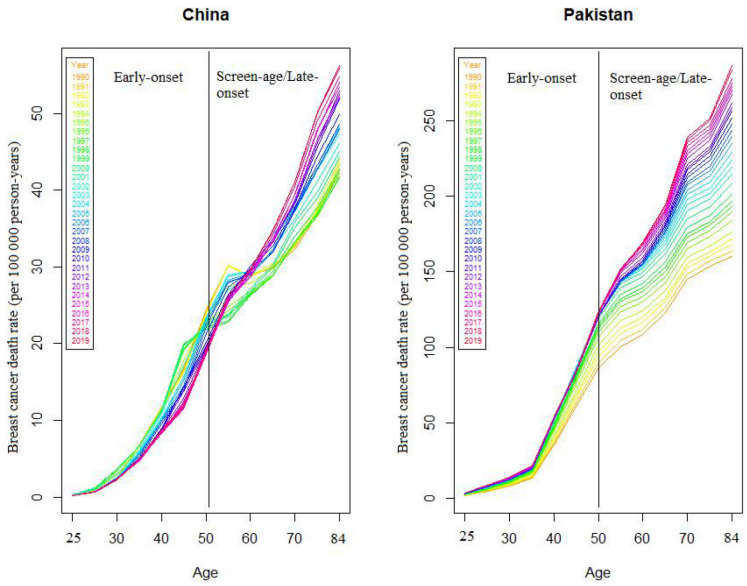

FIGURE 1
Death rates (per 100,000) due to female breast cancer in China and Pakistan, 1990–2019.

shows the estimated parameters of the LC model for China and Pakistan for both the early-onset and screen-age/late-onset population. The model's percentage of variation (PV) was around 86% and 89% between the early-onset and screen-age/late-onset population for the China, and 98% for both the early-onset and screen-age/late-onset population for Pakistan. The variation in PV between two countries' data sets is caused by BC mortality patterns and various data features, as shown in Figure 1. We could show that the BC mortality rates at older ages were less consistent in Pakistani data than in China; as a result, the LC model fit the Pakistan data better and explained the higher PV in the screen-age/late-onset population than in China.

We can observe that the variance trend (b_x) among screen-age/late-onset population is gradually increasing with age for both China and Pakistan, whereas, over time (k_t), these mortality differences are steadily growing after 2000; particularly, these differences were higher for Pakistan than that for China (Figure 2). Moreover, the fitted BC mortality rates by age and year through the LC model for both the early-onset and screen-age/late-onset population for China and Pakistan are depicted in Figure 3.

Model evaluation and forecasting

When the residuals are independent and identically distributed, a matching fit is seen. To validate this condition, the fitted model's residual death rates by age and year were calculated (Figure 4). In the screen-age/late-onset population, residual death rates by age and years were predicted to be more consistent. In Pakistan, these errors were lower than in China. Furthermore, error estimates were produced to confirm the error disparities across different population models, as shown in Table 1. By evaluating the error between the early-onset and screen-age/late-onset population, we noticed that the error measures for screen-age/late-onset model are smaller than the early-onset model.

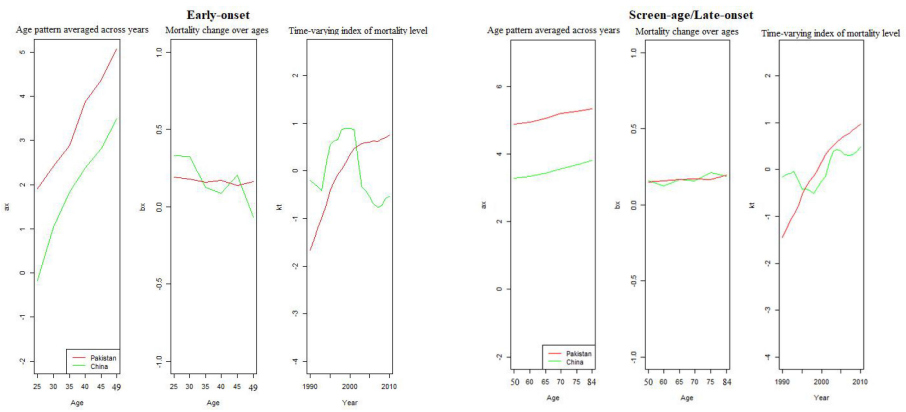

FIGURE 2
Model estimation between the early-onset and screen-age/late-onset population for China and Pakistan.

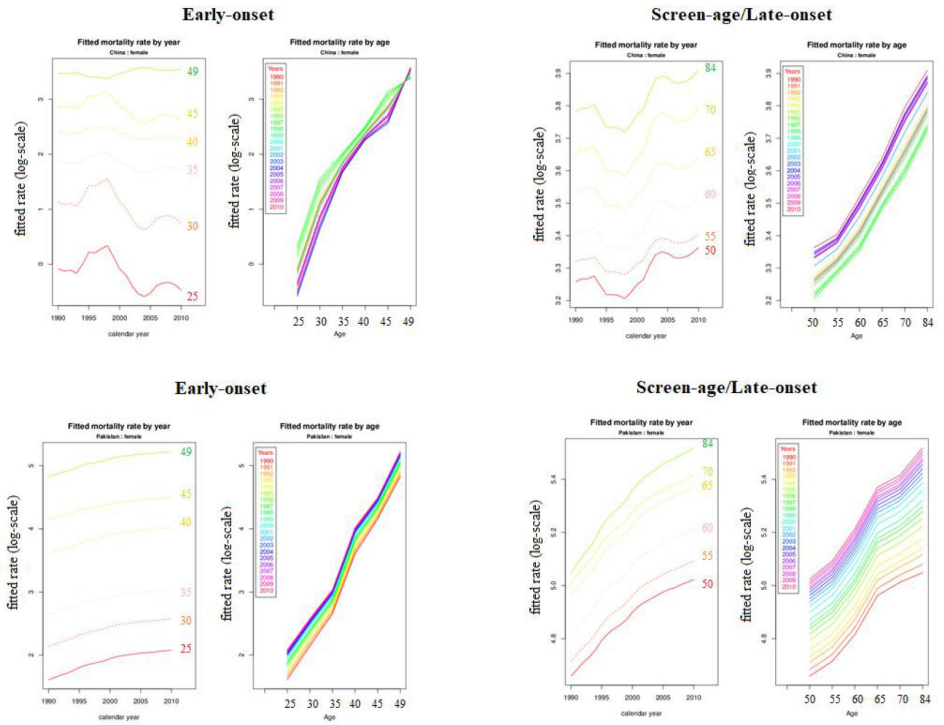

FIGURE 3
Fitted breast cancer mortality rate (log-scale) between the early-onset and screen-age/late-onset population for China and Pakistan.

Between China and Pakistan, these errors were lower in the Pakistan's data set compared with that in China (Table 1).

Forecasts were calculated in our study on the basis of the evolution of time parameter (k_t); and errors in age parameters (a_x and b_x) were not considered because, according to the literature, the standard errors of (a_x) and (b_x) become less significant over forecast time in comparison to the standard error of parameter (k_t) (16). The model predicting ability for both the early-onset and screen-age/late-onset population for China and Pakistan is shown in Figure 5. Overall, we observe that the prediction error for the screen-age/late-onset model was lower than that for the early-onset model for both China and Pakistan. Furthermore, we observed that the LC approach has provided almost comparable results between the early-onset and screen-age/late-onset populations in forecasting accuracy for less invariant mortality behavior over time like in Pakistan (Figure 5). Moreover, the trend in forecast error (test data set) was gradually decreased in the screen-age/late-onset BC population than early-onset for both China and Pakistan (Figure 6).

To confirm the out-of-sample forecast accuracy, we also looked at the mean and variance of life expectancy forecast errors over the projected period. Table 2 demonstrates the minimum variance of life expectancy forecast error for both countries' screen-age/late-onset populations. Finally, according to the model prediction, the BC mortality was predicted to increase by 2030 for both the early-onset and screen-age/late-onset population in Pakistan, whereas, for China, it was expected to decrease in early-onset population (Figure 7).

Discussion

This study presented the application and evaluation of the LC model on age-specific BC death rates between the early-onset and

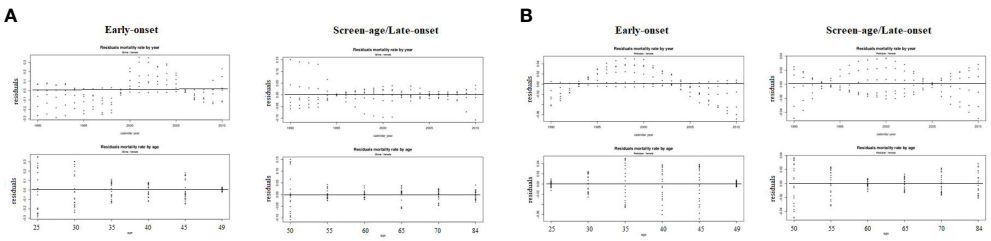

FIGURE 4
Residuals mortality rates by age and year from the LC model between the early-onset and screen-age/late-onset population in **(A)** China and **(B)** Pakistan.

TABLE 1 Error measures from fitted Lee–Carter model of the early-onset and screen-age/late-onset breast cancer population for China and Pakistan.

	China		Pakistan	
	Early-onset	Screen-age/late-onset	Early-onset	Screen-age/late-onset
Averages across ages				
MPE	0.01416	0.00135	0.00039	0.00029
MAPE	0.10212	0.02437	0.01891	0.01371
Averages across years				
IPE	0.34702	0.02743	0.01139	0.0063
IAPE	2.49338	0.51237	0.54902	0.30285

MPE, mean percent error; MAPE, mean absolute percent error; IPE, integrated percent error; IAPE, integrated absolute percent error.

screen-age/late-onset female populations in China and Pakistan for the period 1990–2019. We separated the data set into two parts to study the within-sample and out-of-sample model performance: training data set (1990–2010) and test data set (2011–2019). We test the model on the training data set and assessed its performance using within and outside forecast accuracy. The index of the level of BC mortality between the early-onset and screen-age/late-onset population as well as and shape and sensitivity coefficient by age were found through this approach. The mortality rates for the period 2020 to 2030 were predicted using the ARIMA model between the early-onset and screen-age/late-onset in the female population for each country under study, and it is necessary to highlight that the period under this study represents the maximum period of data availability. The LC approach presented in this study provides the adequate fit on BC mortality data between the early-onset and screen-age/late-onset female populations for China and Pakistan. However, there were some differences in forecast accuracy measure between the early-onset and screen-age/late-onset population, where we have observed the most accurate fit and strong predictive ability of model for screen-age/late-onset population for both countries. The reason might be the more smoothing mortality behavior in this population as compared to the early-onset. In some the previous studies, the LC approach has been suggested for mortality prediction among older populations (13).

According to the recent estimation of Global Burden of Disease GBD, among women, BC caused the most disability-adjusted life years, deaths, and years lived with disability (41). The differences in age-specific BC mortality between the early-onset and screen-age/late-onset female population in China and Pakistan followed a smooth function with minor observational error. Our findings showed that BC has a high variance in older age groups, where the population is lesser, and, among younger age group too, the mortality rates were low. These findings are consistent with the previous studies, which revealed considerable variability in rates based on geography and age group, notably for mortality rates (42, 43). A related study found a similar pattern in US mortality statistics, where statisticians discovered that age-specific mortality was higher than 1.0/100,000 for very small populations (44). Stochastic mortality

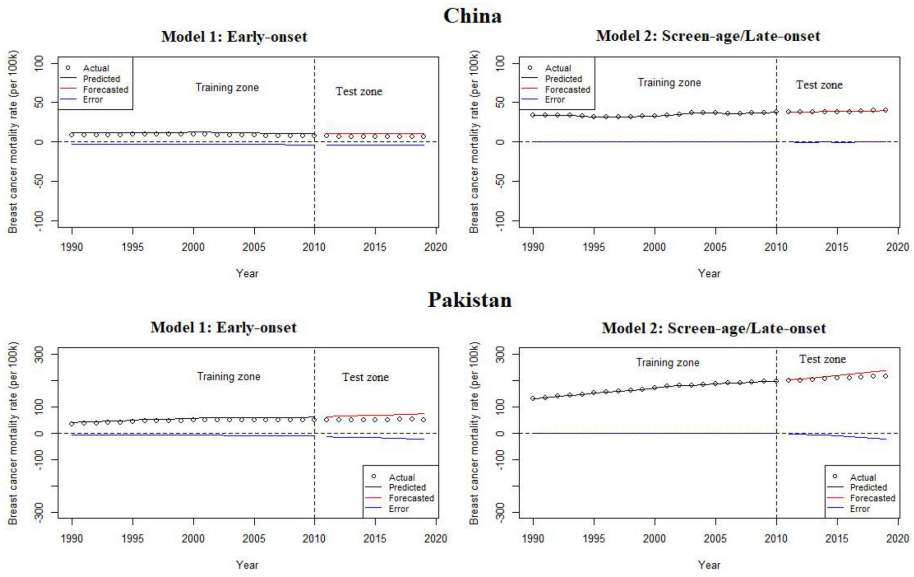

FIGURE 5
Lee–Carter model predicting ability between the early-onset and screen-age/late-onset population in China and Pakistan.

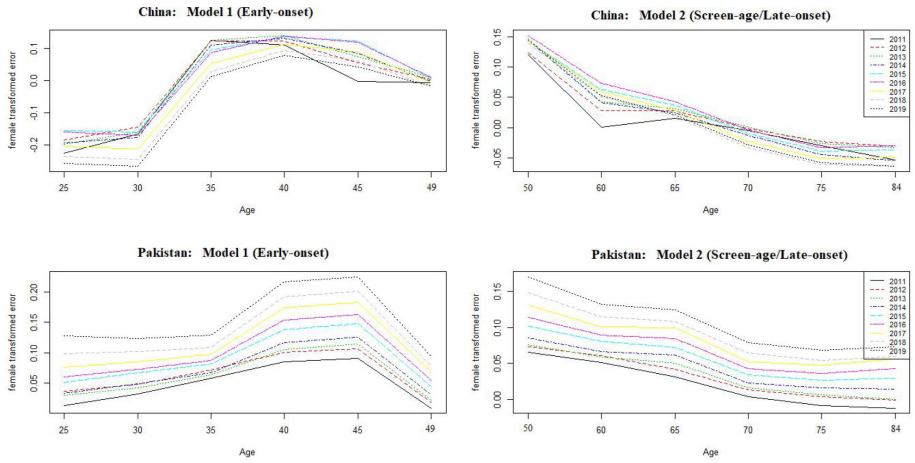

FIGURE 6
Forecast error over ages between the early-onset and screen-age/late-onset population in China and Pakistan.

models represent forecasting mortality trend based on such data pattern, and these approaches have been applied in various studies in different countries for all-cause and cause-specific mortality prediction (28, 44–46).

The general mortality index (k_t) is a time series analysis representing the variability over time. It shows a declining trend in BC mortality for the early-onset Chinese population and increasing trend for the screen-age/late-onset population in both China and Pakistan. The plausible reasons for the predicted decline in BC mortality are not yet clear and demand more research. Proper health infrastructure and therapies availability might explain some portion of predicted reductions in China among the young population. This method increases early detection while also providing efficient treatment. Most women under the age of 50 who work in cities have access to employer-sponsored services such as medical exams and free breast ultrasounds once or twice a year. Previous research has demonstrated that an ultrasound is performed before to Chinese women's mammography to prevent and control BC (47). Mubarik et al. (2020) analyzed the trends and forecasts in BC mortality and predicted greater BC mortality rates among older populations in numerous Asian countries, including Pakistan, in 2030 (13). The rising behaviors in the patterns of BC mortality might be due to lack of BC early screening, diagnosis, and treatment regime, as compared with developed countries (13). The proposed model for risk factors and their roles in triggering BC therapy may be used in future studies to improve healthcare tactics targeting this disease.

This study presents the application and evaluation of the Lee and Carter's approach for BC mortality prediction. As the LC method appears to be a method with probabilistic support, this strategy generates many measurements and outcomes that characterize current and future patterns in BC mortality. As in many other countries, the use of this strategy in China and Pakistan produced better outcomes in terms of least forecast error and diagnostic measures. It is important to note that the study duration is significantly shorter than those of Sweden, the United States, and Chile (16, 35, 48). These three investigations covered time spans of more than 100 years. The amount of projections that can be generated is affected by the time period under consideration. Because the LC model is entirely reliant on historical mortality and population statistics, it is critical to have solid data over a long period of time. This demonstrates the significance of obtaining data efficiently and keeping records up to date in a certain region, country, or sub-national level.

This study has some strengths. First of all, our study examined the applicability of the multi-population random mortality models, the LC dynamic mortality assessment model, in the prediction of BC mortality in China and Pakistan. The LC model is considered as one of the most representative dynamic models in the random prediction methods, but, as far as we know, this is the first time to verify the statistical model of BC mortality prediction in two developing countries. In addition, we further compared the differences in mortality trends of BC between the early-onset and screen-age/late-onset population and verified that the model was more accurate in predicting age/late onset group, filling the

TABLE 2 Mean and variance of forecast error in life expectancy derived from the Lee–Carter model.

Country	Early-onset		Screen-age/late-onset	
	Mean	Variance	Mean	Variance
China	0.034	0.006	0.020	0.0012
Pakistan	0.033	0.004	0.013	0.0010

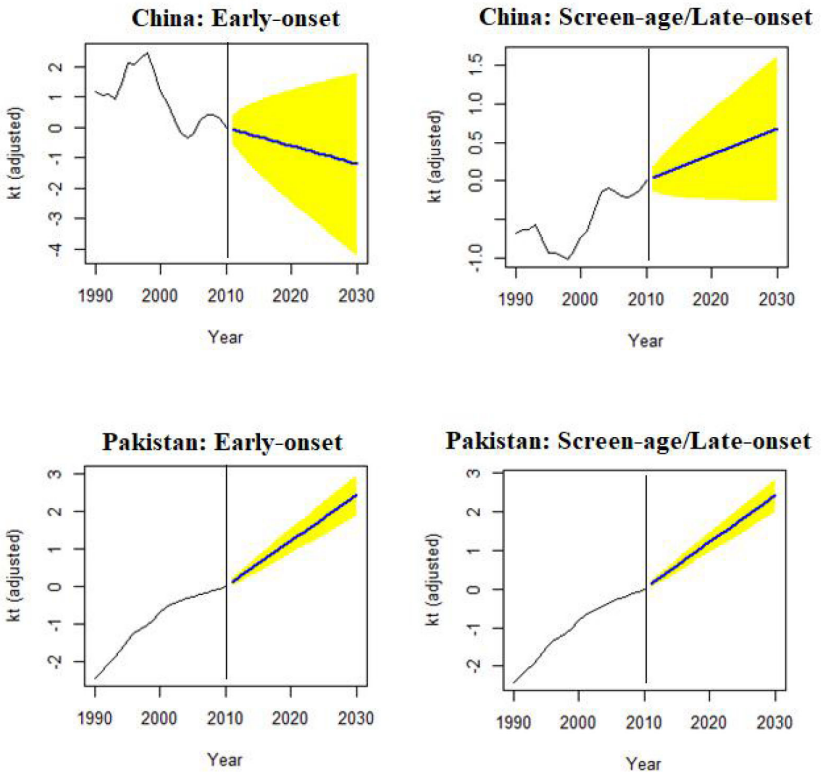

FIGURE 7
Forecast of mortality index (k_t) to 2030, in the early-onset and screen-age/late-onset female breast cancer population for China and Pakistan.

gap in this regard. Similarly, this study has some limitations. First, we conducted our analysis based on secondary data; therefore, the accuracy of the model simulation is limited by the accuracy of GBD estimates. Second, we did not consider other covariates that may affect the risk of death from BC in the two countries in the model evaluation, such as health policies and treatment conditions. Third, our model was trained and tested for different parts of the same data set, and the actual effect may not be as good as the alternative, which is to train on one data set and validated on the other data set, so that the external validation is more able to demonstrate the generality of the model. As, for validation, our work made use of a comparable data set. If screening, diagnostic, and treatment methods change between different centers and over time, further analysis using an independent data set would be helpful to assure adaptability.

Conclusion

The LC model can be considered to forecast BC mortality to project the future life expectancy at birth, particularly among the screen-age/late-onset population. By model prediction, BC mortality is expected to increase to 2030 for both the early-onset and screen-age/late-onset population in Pakistan. In China, it is likely to decrease for the early-onset population. Hence, this approach may be helpful and convenient to predict the cancer related mortality even for insufficient epidemiological and demographic disease data set. According to model prediction to BC mortality, better health facilities in terms of disease diagnosis, control, and prevention are needed to minimize this disease's future burden, particularly in less developing countries.

Data availability statement

Publicly available datasets were analyzed in this study. This data can be found here: The dataset analyzed during the current study are available in the Institute for Health Metrics and Evaluation (IHME): http://ghdx.healthdata.org/gbd-results-tool.

Author contributions

CY supervised the study. SM and CY conceptualized the analysis. SM did the data analysis and wrote the first draft of the paper. FW, LL, and KH reviewed and provided comments on the first draft. All authors reviewed and approved the final manuscript.

Funding

This research was funded by the National Natural Science Foundation of China (Grant No. 82173626) and Health Commission of Hubei Province Scientific Research Project (Grant No. WJ2019H304). The funders had no role in the study design, data collection, analysis, and decision to publish or preparation of the manuscript.

Acknowledgments

We acknowledge the contributions made by GBD study in Data.

Conflict of interest

The authors declare that the research was conducted in the absence of any commercial or financial relationships that could be construed as a potential conflict of interest.

Publisher's note

All claims expressed in this article are solely those of the authors and do not necessarily represent those of their affiliated organizations, or those of the publisher, the editors and the reviewers. Any product that may be evaluated in this article, or claim that may be made by its manufacturer, is not guaranteed or endorsed by the publisher.

References

1. Siegel RL, Miller KD, Fuchs HE, Jemal A. Cancer statistics, 2022. *CA Cancer J Clin* (2022) 72(1):7–33. doi: 10.3322/caac.21708

2. Giaquinto AN, Sung H, Miller KD, Kramer JL, Newman LA, Minihan A, et al. Breast cancer statistics, 2022. *CA Cancer J Clin* (2022) 72(6):524–41. doi: 10.3322/caac.21754

3. Polyak K. Breast cancer: Origins and evolution. *J Clin Invest.* (2007) 117(11):3155–63. doi: 10.1172/JCI33295

4. Agostinetto E, Gligorov J, Piccart M. Systemic therapy for early-stage breast cancer: Learning from the past to build the future. *Nat Rev Clin Oncol* (2022) 19(12):763–74. doi: 10.1038/s41571-022-00687-1

5. Hanahan D, Weinberg RA. Hallmarks of cancer: The next generation. *Cell* (2011) 144(5):646–74. doi: 10.1016/j.cell.2011.02.013

6. Cortazar P, Zhang L, Untch M, Mehta K, Costantino JP, Wolmark N, et al. Pathological complete response and long-term clinical benefit in breast cancer: The CTNeoBC pooled analysis. *Lancet* (2014) 384(9938):164–72. doi: 10.1016/S0140-6736(13)62422-8

7. Savas P, Salgado R, Denkert C, Sotiriou C, Darcy PK, Smyth MJ, et al. Clinical relevance of host immunity in breast cancer: From TILs to the clinic. *Nat Rev Clin Oncol* (2016) 13(4):228–41. doi: 10.1038/nrclinonc.2015.215

8. Arnold M, Morgan E, Rumgay H, Mafra A, Singh D, Laversanne M, et al. Current and future burden of breast cancer: Global statistics for 2020 and 2040. *Breast.* (2022) 66:15–23. doi: 10.1016/j.breast.2022.08.010

9. Wojtyla C, Bertuccio P, Wojtyla A, La Vecchia C. European Trends in breast cancer mortality, 1980–2017 and predictions to 2025. *Eur J Cancer.* (2021) 152:4–17. doi: 10.1016/j.ejca.2021.04.026

10. Zhou C-M, Xue Q, Wang Y, Tong J, Ji M, Yang J-J. Machine learning to predict the cancer-specific mortality of patients with primary non-metastatic invasive breast cancer. *Surg Today* (2021) 51(5):756–63. doi: 10.1007/s00595-020-02170-9

11. Mubarik S, Sharma R, Hussain SR, Iqbal M. Breast cancer mortality trends and predictions to 2030 and its attributable risk factors in East and south Asian countries. *Front Nutr* (2022) 9. doi: 10.3389/fnut.2022.847920

12. Lee S, Zelen M. Chapter 11: A stochastic model for predicting the mortality of breast cancer. *JNCI Monographs.* (2006) 2006(36):79–86. doi: 10.1093/jncimonographs/lgj011

13. Mubarik S, Wang F, Fawad M, Wang Y, Ahmad I, Yu C. Trends and projections in breast cancer mortality among four Asian countries (1990–2017): Evidence from five stochastic mortality models. *Sci Rep* (2020) 10(1):1–12. doi: 10.1038/s41598-020-62393-1

14. Pérez CYG, Guzmán VMG. *Pronósticos estadísticos de mortalidad y su impacto sobre el sistema de Pensiones de México*. Mexico (2007).

15. Gompertz B XXIV. On the nature of the function expressive of the law of human mortality, and on a new mode of determining the value of life contingencies. *In a letter to Francis Baily, Esq. FRS &c. Philosophical transactions of the Royal Society of London* London: Philosophical transactions of the Royal Society (1825) 31(115):513–83. doi: 10.1098/rstl.1825.0026

16. Lee RD, Carter LR. Modeling and forecasting US mortality. *J Am Stat Assoc* (1992) 87(419):659–71. doi: 10.1080/01621459.1992.10475265

17. Bell WR, Monsell B. Using principal components in time series modeling and forecasting of age-specific mortality rates. In: *Proceedings of the American statistical association, social statistics section*. Suitland: US Bureau of the Census. (1991) 154–9 pp.

18. McNown R, Rogers A. Forecasting mortality: A parameterized time series approach. *Demography* (1989) 26(4):645–60. doi: 10.2307/2061263

19. McNown R, Rogers A. Forecasting cause-specific mortality using time series methods. *Int J Forecasting.* (1992) 8(3):413–32. doi: 10.1016/0169-2070(92)90056-F

20. Li N, Lee R, Tuljapurkar S. Using the Lee–carter method to forecast mortality for populations with limited data. *Int Stat Review.* (2004) 72(1):19–36. doi: 10.1111/j.1751-5823.2004.tb00221.x

21. Booth H, Tickle L, Smith L. Evaluation of the variants of the Lee-carter method of forecasting mortality: a multi-country comparison. *New Z Population Review.* (2005) 31 (1):13–34.

22. Dhandevi W, Kang HM, Ponnusamy RR. Lee-Carter Mortality Forecasting: Application to Mauritian Population. no. 2019. *International Journal of Recent Technology and Engineering (IJRTE)* (2019) 7(5S):169–75.

23. Alho JM. Stochastic methods in population forecasting. *International Journal of forecasting.* (1990) 6(4):521–30.

24. Mubarik S, Hu Y, Yu C. A multi-country comparison of stochastic models of breast cancer mortality with p-splines smoothing approach. *BMC Med Res methodol* (2020) 20 (1):1–16. doi: 10.1186/s12874-020-01187-5

25. Booth H, Maindonald J, Smith L. Applying Lee-carter under conditions of variable mortality decline. *Population Stud* (2002) 56(3):325–36. doi: 10.1080/00324720215935

26. Koissi M-C, Shapiro AF, Högnäs G. Evaluating and extending the Lee–carter model for mortality forecasting: Bootstrap confidence interval. *Insurance: Math Economics.* (2006) 38(1):1–20. doi: 10.1016/j.insmatheco.2005.06.008

27. Booth H, Hyndman RJ, Tickle L, De Jong P. Lee-Carter mortality forecasting: A multi-country comparison of variants and extensions. *Demog Res* (2006) 15:289–310. doi: 10.4054/DemRes.2006.15.9

28. D'Amato V, Piscopo G, Russolillo M. The mortality of the italian population: Smoothing techniques on the lee–carter model. *The Annals of Applied Statistics.* Institute of Mathematical Statistics (2011) 5(2A):705–25. doi: 10.1214/10-AOAS394

29. Lyu P, Waegenaere AD, Melenberg B. A multi-population approach to forecasting all-cause mortality using cause-of-Death mortality data. *North Am Actuarial J* (2021) 25 (sup1):S421–56. doi: 10.1080/10920277.2019.1662316

30. Benz CC. Impact of aging on the biology of breast cancer. *Crit Rev Oncol Hematol* (2008) 66(1):65–74. doi: 10.1016/j.critrevonc.2007.09.001

31. Matsuno RK, Anderson WF, Yamamoto S, Tsukuma H, Pfeiffer RM, Kobayashi K, et al. Early- and late-onset breast cancer types among women in the united states and Japan. *Cancer Epidemiol Biomarkers Prev* (2007) 16(7):1437–42. doi: 10.1158/1055-9965.EPI-07-0108

32. Li L, Yi Z, Li C, Guan X, Xu B, Ma F. Integrative clinical genomics of early-onset breast cancer. *Journal of Clinical Oncology* (2018) 36(15_suppl):1541. doi: 10.1200/JCO.2018.36.15_suppl.1541

33. Wang H, Abbas KM, Abbasifard M, Abbasi-Kangevari M, Abbastabar H, Abd-Allah F, et al. Global age-sex-specific fertility, mortality, healthy life expectancy (HALE), and population estimates in 204 countries and territories, 1950–2019: A comprehensive demographic analysis for the global burden of disease study 2019. *Lancet* (2020) 396 (10258):1160–203. doi: 10.1016/S0140-6736(20)30977-6

34. Vos T, Lim SS, Abbafati C, Abbas KM, Abbasi M, Abbasifard M, et al. Global burden of 369 diseases and injuries in 204 countries and territories, 1990–2019: A systematic analysis for the global burden of disease study 2019. *Lancet* (2020) 396 (10258):1204–22. doi: 10.1016/S0140-6736(20)30925-9

35. Wang JZ. *Fitting and forecastin mortality for Sweden: Applying the Lee-carter model: Matematisk statistik*. Stockholms universitet (2007).

36. Jodź K. Mortality in a heterogeneous population-Lee-Carter's methodology. *arXiv preprint* (2018) arXiv:1803.11233. doi: 10.48550/arXiv.1803.11233

37. Alho JM, Spencer BD. *Statistical demography and forecasting*. New York: Springer (2005).

38. Bell WR. Comparing and assessing time series methods for forecasting age-specific fertility and mortality rates. *J Off Statistics.* (1997) 13(3):279.

39. Ortega A. Aplicacion de la tabla de mortalidad en estudios de poblacion. En: *Tablas de mortalidad-LC/DEM/CR/G*. (1987) 16-1987:203–88.

40. Chiang CL. A stochastic study of the life table and its applications: II. Sample variance of the observed expectation of life and other biometric functions. *Human biology*. (1960) 32(3):221–38.

41. Kocarnik JM, Compton K, Dean FE, Fu W, Gaw BL, Harvey JD, et al. Cancer incidence, mortality, years of life lost, years lived with disability, and disability-adjusted life years for 29 cancer groups from 2010 to 2019: A systematic analysis for the global burden of disease study 2019. *JAMA Oncol* (2022) 8(3):420–44. doi: 10.1001/jamaoncol.2021.6987

42. Hu K, Ding P, Wu Y, Tian W, Pan T, Zhang S. Global patterns and trends in the breast cancer incidence and mortality according to sociodemographic indices: an observational study based on the global burden of diseases. *BMJ Open* (2019) 9(10): e028461. doi: 10.1136/bmjopen-2018-028461

43. Lima SM, Kehm RD, Terry MB. Global breast cancer incidence and mortality trends by region, age-groups, and fertility patterns. *EClinicalMedicine* (2021) 38:100985. doi: 10.1016/j.eclinm.2021.100985

44. Booth H, Hyndman RJ, Tickle L. Prospective life tables. In: *Computational Actuarial Science with R*. England and wales: Taylor and Francis group (2014) 319–44.

45. Camarda CG. MortalitySmooth: An r package for smoothing poisson counts with p-splines. *J Stat Software* (2012) 50(1):1–24. doi: 10.18637/jss.v050.i01

46. Currie ID, Durban M, Eilers PH. Smoothing and forecasting mortality rates. *Stat model* (2004) 4(4):279–98. doi: 10.1191/1471082X04st080oa

47. Shen S, Zhou Y, Xu Y, Zhang B, Duan X, Huang R, et al. A multi-centre randomised trial comparing ultrasound vs mammography for screening breast cancer in high-risk Chinese women. *Br J cancer*. (2015) 112(6):998–1004. doi: 10.1038/bjc.2015.33

48. Lee RD, Rofman R. Modeling and projecting mortality in Chile. *Notas poblacion.* (1994) 22(59):183–213.

frontiers | Frontiers in Oncology

TYPE Original Research
PUBLISHED 16 February 2023
DOI 10.3389/fonc.2023.1105649

OPEN ACCESS

EDITED BY
Ming Yi,
Zhejiang University, China

REVIEWED BY
Sreejata Raychaudhuri,
University of Pittsburgh Medical Center, United States
Rakiya Saidu,
University of Cape Town, South Africa

*CORRESPONDENCE
Idris Olasunmbo Ola
gusidrol@student.gu.se;
idrisola234@gmail.com

†PRESENT ADDRESS
Idris Olasunmbo Ola,
Division of Clinical Epidemiology and Aging Research, German Cancer Research Center, Heidelberg, Germany

SPECIALTY SECTION
This article was submitted to Cancer Epidemiology and Prevention, a section of the journal Frontiers in Oncology

RECEIVED 01 December 2022
ACCEPTED 01 February 2023
PUBLISHED 16 February 2023

CITATION
Ola IO, Okunowo AA, Habeebu MY and Miao Jonasson J (2023) Clinical and non-clinical determinants of cervical cancer mortality: A retrospective cohort study in Lagos, Nigeria. *Front. Oncol.* 13:1105649. doi: 10.3389/fonc.2023.1105649

Clinical and non-clinical determinants of cervical cancer mortality: A retrospective cohort study in Lagos, Nigeria

Idris Olasunmbo Ola[1,2*†], Adeyemi Adebola Okunowo[3,4], Muhammad Yaqub Habeebu[5,6,7] and Junmei Miao Jonasson[8,9]

[1]Global Health Program, Institute of Medicine, Sahlgrenska Academy, Gothenburg University, Gothenburg, Sweden, [2]Departments of Clinical and Community Service, The Blue-Pink Center for Women's Health, Lagos, Nigeria, [3]Department of Obstetrics & Gynaecology, College of Medicine University of Lagos, Lagos, Nigeria, [4]Department of Obstetrics & Gynaecology, Lagos University Teaching Hospital, Lagos, Nigeria, [5]Department of Radiotherapy, College of Medicine, University of Lagos, Lagos, Nigeria, [6]Department of Radiotherapy, Lagos University Teaching Hospital, Lagos, Nigeria, [7]Lead Oncologist, NSIA-LUTH Cancer Centre (NLCC), Lagos, Nigeria, [8]School of Public Health and Community Medicine, Institute of Medicine, Sahlgrenska Academy, Gothenburg University, Gothenburg, Sweden, [9]Department of Research and Development, Region Halland, Halmstad, Sweden

Introduction: Cervical cancer (CCa) is the fourth most frequent and a common cause of cancer mortality in women, the majority of whom live in low- and middle-income countries. Data on CCa mortality and its determinants have been poorly studied in Nigeria, resulting in a paucity of information that can assist patient management and cancer control policy.

Aim: The purpose of this study was to assess the mortality rate among CCa patients in Nigeria as well as the major factors influencing CCa mortality.

Study design: Data from the medical records of 343 CCa patients seen at the Lagos University Teaching Hospital and NSIA-LUTH Cancer Center from 2015 to 2021 were used in a retrospective cohort analysis. The hazard ratios (HR) and confidence intervals (CI) associated with the exposure variables and CCa mortality were calculated using Cox proportional hazard regression.

Results: The CCa mortality rate was 30.5 per 100 women-years after 2.2 years of median follow-up. Clinical factors such as HIV/AIDS (adjusted HR [aHR]: 11.9; 95% CI: 4.6, 30.4), advanced clinical stage (aHR: 2.7; 95% CI: 1.5, 4.7), and anemia at presentation (aHR: 1.8; 95% CI: 1.1, 3.0) were associated with a higher mortality risk, as were non-clinical factors such as age at diagnosis >50 years (aHR: 1.4; 95% CI: 1.0, 1.9) and family history of CCa (aHR: 3.5; 95%CI: 1.1, 11.1)

Conclusion: CCa has a high mortality rate in Nigeria. Incorporating these clinical and non-clinical factors into CCa management and control policies may improve women's outcomes.

KEYWORDS

cervical cancer, cancer mortality, determinants of mortality, Nigeria, cancer epidemiology, cancer control, women's health, oncology

1 Introduction

Cancer of the uterine cervix or simply cervical cancer (CCa) is one of the leading causes of cancer-related mortality in women and a major disease of global public health concern. A recent estimate shows that about three billion women over the age of 15 years are at risk of the disease which is currently the fourth most frequent malignancy affecting women worldwide, after breast, colorectal, and lung cancers (1, 2). Globally, CCa represents about 7% of all cancer types, with significant variation along socioeconomic divides ranging from 2.8% in countries with very high human development index (HDI) to 17.7% in those with low HDI (2).

Mortality from CCa closely follows its incidence pattern, being the fourth major cause of cancer-related deaths, accounting for 7.5% of all cancer mortality in 2018, and with a global average age at death of 59 years (2). The age-standardized mortality rate ranges from 3 per 100,000 women in high-income countries to 20 per 100,000 women in low and middle-income countries (LMICs) (2, 3).

Recently, in the United States and many European countries, the incidence has remained stable, and mortality declined by almost 1% annually, owing to increased attention to prevention and early detection services and increased access to evidence-based treatments (3, 4). Although China and India account for almost one-third of global CCa incidence and mortality (2), a progressive decline in mortality has also been reported, especially in India, mainly due to improvements in their CCa control and healthcare services (5). In contrast, CCa incidence and mortality rates in Sub-Saharan Africa have been steadily increasing over the last 10-25 years, with the annual increase ranging from 1.3% to 9.5% in some countries (6, 7), culminating in about 10.8% of cancer deaths between 2015 and 2019 (8).

Studies in sub-Sahara Africa have reported cumulative mortality during a 2–5-year period ranging from 65% to 68% (9–11). In Nigeria, the 5-year CCa mortality prevalence was estimated at 22.11 per 100,000 women (12) and was responsible for 14.8% of all cancer deaths among Nigerian women in 2018 (13).

Empirical evidence has shown several factors that influence mortality risk from CCa. Late-stage hospital presentation of CCa is very common in sub-Sahara Africa (9, 14–17), and has been reported to generally reduce the 5-year survival rate from 92% in the early-stage presentation to about 17% in the late-stage when metastases has occurred (18, 19). Sociodemographic factors like lack of formal education, rural residence, fear, misconceptions, misinterpretation, ignorance, and longer investigation time are some of the health-seeking and health systems variables predisposing to late stage CCa presentation and its attendant increased mortality chance (17, 20). Dietary and lifestyle practices such as alcohol use, cigarette smoking, high body mass index (BMI), use of other substances of abuse (21), as well as socioeconomic/demographic factors like age at diagnosis, family history of CCa in first degree relatives, history of abortion, and age at first marriage and birth have been described as determinants of CCa mortality (20, 22).

Other clinical factors such as anemia, HIV/AIDS, comorbidity, type of treatment received, and histological type of the disease have also been reported to influence CCa outcome (9–11, 22).

Although these factors have varying influences on CCa mortality risk, to our knowledge, their exact roles in determining CCa outcome among women in Nigeria have been poorly studied. Nigeria has a large population of CCa-at-risk women whose mortality has not been adequately investigated (13). Consequently, there is a scarcity of relevant data on CCa mortality rate and the factors that influence it (2, 23).

This study aimed to estimate the mortality rate and the clinical and non-clinical factors that determine mortality among CCa patients in Lagos, Nigeria.

2 Materials and methods

2.1 Study design and setting

A retrospective cohort study was conducted in the gynecological oncology unit of Lagos University Teaching Hospital (LUTH) and the NSIA-LUTH Cancer Center (NLCC) both in Lagos, Nigeria.

LUTH is an 800 bedded tertiary teaching and referral hospital in Lagos, Nigeria. Through a public-private partnership model, LUTH, in partnership with the NSIA Healthcare Development and Investment Company opened the NLCC, an advanced cancer treatment center that has synchronized cancer treatment services in LUTH since May 29, 2019 (24).

Medical records of CCa patients diagnosed between January 1st, 2015, and December 31st, 2021, were retrieved from the medical records department through manual sorting of all the gynecological cancer cases seen in LUTH and NLCC during the period. Retrieval of records was supported by trained staff of the medical record units of both the LUTH and the NLCC.

Records of participants who were newly diagnosed with CCa or referred from other hospitals on account of CCa, whose clinical diagnoses were ascertained with a histological report and attended the gyne-oncology unit of LUTH or the NLCC between January 1st, 2015, and December 31st, 2021, were included in the study.

2.1.1 Exposure variables

Data were extracted from medical records using a pretested structured questionnaire. Socio-demographic, family, and social history data were used as non-clinical exposure variables, whereas clinical and histopathology data were used as clinical exposure variables.

Data on histology was derived from the histology report of pathologists. Three categories were derived based on the frequency of occurrence of the different histo-types: squamous cell carcinoma, adenocarcinoma, and other types including adenosquamous and small cell carcinoma.

Data on comorbidity was based on the Deyo modification of the Charlson Comorbidity Index after excluding cervical cancer (25).

Data on anemia was obtained using the patient's packed cell volume (PCV) and classified according to WHO recommendations for non-pregnant women 15 years or older. Severe anemia was PCV <24%, moderate anemia 24–32.9%, mild anemia 33–35.9%, and PCV 36% or higher constitute no anemia (26).

Clinical staging of the disease was based on the International Federation of Gynecology and Obstetrics (FIGO) 2018 classification into early and late disease (27). For this study, we also explored

further categorization into early (FIGO I—IIA), late (FIGO IIB—IIIC), and advanced disease (FIGO IVA and IVB) to observe more clearly the effect of these stages on CCa death. Treatment data were also obtained from the oncologists/surgeon's management plan and the nursing report of medications and treatments administered for those that were admitted during their treatment. Data were classified based on whether the patient had chemotherapy, radiotherapy, or surgery only, and varying combinations of the three modalities.

Information on HIV/AIDS status was extracted from the laboratory investigation reports usually carried out as part of baseline investigations at hospital presentation.

Information about age, location/residence, occupation, religion, ethnicity, educational level, and marital status were extracted from the biodata section of the records. Age at diagnosis was categorized broadly as age 50 years or younger and age older than 50 years based on previous research (10). Data on occupation was classified as either unemployed or based on skill levels derived using the latest versions of the International Labor Organization's International Standard Classification of Occupations 2008 [ISCO-08 and ISCO-88] (28). Participants who were engaged in some forms of occupation were sub-classified as high-skilled, medium-skilled, or low-skilled occupation, armed forces, or not elsewhere classified.

The family and social history section of the medical records provided information on the family history of CCa in a first-degree relative, cigarette smoking, alcohol intake, use of other substances, including herbal preparations, and parity, defined by the number of pregnancies carried to viability, irrespective of whether the child was alive or not.

2.1.2 Outcome variable

Mortality during the follow-up period was the dependent, binary outcome variable, and was confirmed through the death register, death summary form, or phone calls to the next of kin of patients whose outcomes could not be ascertained through existing records. Empirical evidence has proven verbal confirmation of mortality to be accurate and reliable in resource-constrained settings with low coverage of vital registrations, including death registration (29).

Follow-up started from the first histological diagnosis of CCa and ended on the date of death of the participant, referral for the continuation of care outside LUTH or NLCC (often due to proximity to their location), or the common closing date on December 31st, 2021, whichever came first.

2.2 Statistical analysis

Descriptive analysis was conducted using frequencies, means, and percentages. Inferential statistics were obtained using the Cox proportional hazards regression model. Hazard ratios (HRs) and their confidence intervals were used as measures of association between CCa diagnosis and mortality.

Univariate analyses were conducted for all exposure/independent variables of CCa mortality using the log-rank tests of equality. Variables such as family history of cervical cancer, cigarette smoking, educational level, alcohol, and other substances use, HIV/AIDS status, anemia, stage of the disease, and types of treatment received with a p-value less than 0.25 (30) were considered relevant and were included in the multivariable Cox regression model. In the multivariable analysis, the p-value of anemia was statistically insignificant (p-value = 0.856), however, we retained anemia in the model because the overall p-value for the model was <0.001 and previous research showed that anemia was relevant in the model (9, 10).

Proportionality assumption was checked using the Schoenfeld and scaled Schoenfeld residuals and the goodness of fit of the final model was checked using the Cox-Snell residuals plotted in a Nelson-Aalen cumulative hazard function.

All statistical tests were 2-tailed, and type-1 error was set at 0.05 level of significance. The power of the study was 80%. Missing data were handled using complete case analysis for each variable of interest and the low level of missing data increased the validity of the results.

2.3 Ethical considerations

Ethical approval for study was granted by the ethical review committee of LUTH with approval number ADM/DSCST/HREC/APP/4939. This approval was used to gain permission from the gyne-oncology unit and the medical records department to access the medical records. A secondary approval was also granted by the administrative boards of NSIA-LUTH Cancer Center to access medical records in the center.

3 Results

Out of 420 cases of CCa seen during the study period, a total of 343 (81.7%) women with complete records were included in the analysis.

3.1 Non-clinical characteristics of women with cervical cancer

The mean age at CCa diagnosis (entry) was 55.3 years (SD 12.5 years) with age range between 28 and 88 years. The age group 55–64 years recorded the highest number of cases of CCa during the study period.

Two-thirds of the study population were suburban residents, and more than one-thirds had a secondary level of education. Fifty-six (16.6%) were unemployed and about 55% (185) were engaged in various low-skill occupations. Approximately 25% (65) had a history of substance use, with alcohol intake responsible for the highest substance use at 17.6% (57) while only about 5% (16) smoked cigarette (Table 1). Other non-clinical characteristics are described in Table 1.

3.2 Clinical characteristics of women with cervical cancer

A total of 202 (59%) CCa deaths were recorded during the follow-up period with a mean age of 57.6 years (SD 13.0 years) at death. Nearly 10% (33) of the study population was still alive, and the

TABLE 1 Non-clinical characteristics of the study population including results of univariate analysis.

Variables	Categories	Frequency N (%)	Total CCa Mortality N (%)	p-value in univariate analysis (log-rank test)(<0.25)
Age (years)	50 years or less >50 years Missing	119 (34.7) 214 (62.4) 10 (2.9)	70 (58.8) 132 (61.7) 0	0.0337* #
Ethnicity	Yoruba Igbo Others Missing	172 (50.2) 85 (24.8) 86 (25) 0	108 (62.8) 47 (55.3) 47 (54.7) 0	0.3207
Residence	Rural Suburban Urban Missing	9 (3.5) 158 (61.2) 91 (35.3) 85 (24.8)	3 (33.3) 102 (64.6) 56 (61.5) 0	0.3953
Education	Primary Secondary Tertiary No formal education Missing	78 (24.8) 106 (33.6) 75 (23.8) 56 (17.8) 28 (8.2)	47 (60.3) 61 (57.5) 37 (49.3) 37 (66.1) 0	0.0173*
Occupation	Unemployed High-Skill Occupation Medium-Skill Low-Skill Occupation Armed forces Unclassified Missing	56 (16.6) 32 (9.5) 54 (16.0) 185 (54.9) 2 (0.6) 8 (2.4) 6 (1.7)	34 (60.7) 15 (46.9) 33 (61.1) 109 (58.9) 1 (50) 5 (62.5) 0	0.4003
Religion	Islam Christianity Missing	74 (21.6) 269 (78.4) 0	46 (62.2) 156 (58.0) 0	0.6590
Marital Status	Single Married Missing	7 (2.2) 307 (97.8) 29 (8.5)	5 (71.4) 181 (59.0) 0	0.5130
Parity	0-3 4-7 8-11 >11 Missing	71 (23.5) 169 (56.0) 61 (20.2) 1 (0.3) 41 (12)	42 (59.2) 100 (59.2) 36 (59.0) 0 (0.0) 0	0.9256
Family History of CCa	Yes No Missing	5 (1.6) 313 (98.4) 25 (7.3)	4 (80.0) 190 (60.7) 0	0.0210* #
Cigarette smoking	Cigarette Smoking No smoking Missing	16 (5.0) 301 (87.8) 26 (7.6)	13 (81.3) 185 (61.5) 0	0.0469*
Alcohol	Alcohol intake No alcohol intake Missing	56 (17.7) 261 (82.3) 26 (7.6)	40 (71.4) 158 (60.5) 0	0.0794*
Other substances use	Yes No Missing	11 (4.4) 240 (95.6) 83 (24.2)	11 (100) 148 (61.7) 0	0.0207*
Overall treatment outcomes	Alive Dead Referred Loss to follow-up Missing	33 (9.9) 202 (59) 35 (10.5) 62 (18.6) 10 (2.9)		

*Statistically significant variables in univariate analysis that were included in multivariate analysis.
Variables significantly associated with CCa mortality in multivariate analysis ($p < 0.05$).

outcome could not be ascertained in over one-quarter of the study population due to either referral to other centers, short-term management at LUTH and NLCC, 35 (10%) or loss to follow-up 62 (18.6%). Attempts to contact these women and their relatives *via* phone call were not successful.

Of the cases reviewed, 245 (86.3%) presented in late stages (FIGO stage IIB-IVB) and about 5% (15) were diagnosed with HIV/AIDS during treatment. Squamous cell carcinoma accounted for over four-fifths (82.6%) of all CCa histologic types seen in the cohort. Over 83% (241) of the study participants were anemic, approximately a quarter of these women had severe anemia. Less than half [45.4%, (117)] of the participants had comorbid conditions and most patients in the cohort 149 (55.6%) received combination therapy involving chemotherapy and radiotherapy. (Table 2).

3.3 Cervical cancer mortality

The crude all-cause mortality rate was 30.5 per 100 person-years with 2.2 years median follow-up time, corresponding to a cumulative mortality of 59%.

Relative disparities in CCa mortality were most pronounced for very advanced stage disease (FIGO IVA and IVB) with only 17.1% survival after 7 years of diagnosis, which increased by almost four-folds (61.5%) when diagnosis was made at early stages (FIGO I and IIA). Mortality was lowest [10 (40%)] among those that received three combination therapies involving surgery, chemotherapy, and radiotherapy, but highest among those that received either chemotherapy alone [22 (73.3%)] or in combination with surgery [3 (75%)]. Histologically, adenocarcinoma had the lowest proportional survival from the disease 11(33.3%). Approximately nine in 10 CCa mortality had some form of anemia and HIV/AIDS was responsible for a disproportionately higher mortality (85.7%) compared to 62% among those without HIV/AIDS. (Table 2).

3.4 Non-clinical determinants of cervical cancer mortality

In the analysis of non-clinical determinants of CCa mortality, the gradient was especially noticeable in patients who had family history of CCa in a first degree relative, with more than four-folds increase in risk of dying from the disease (Age-adjusted hazard ratio [aHR]: 4.1, 95% CI: 1.8, 10.0). Being older than 50 years of age at diagnosis was also associated with a 40% higher chance of dying from CCa than those who presented at 50 or younger age (HR: 1.4, 95% CI: 1.0, 1.9). (Table 3)

TABLE 2 Clinical characteristics of the study population, mortality pattern within each group, and results of univariate analysis.

Variables	Categories	Frequency N (%)	CCa Mortality N (%)	p-value in univariate analysis (log-rank test) (<0.25)
Clinical Stage	Early	39 (13.7)	15 (38.5)	0.0002* #
	Advanced/Late	245 (86.3)	159 (64.9)	
	Late (IIb-IIIc)	167 (58.8)	96 (59.6)	
	Very Advanced (>=IVa)	78 (27.5)	63 (82.9)	
	Missing	59 (17.2)	0	
Anemia	No anemia	48 (16.6)	18 (37.5)	0.0247* #
	Anemia	241 (83.4)	164 (68.0)	
	Mild	50 (17.4)	28 (56.0)	
	Moderate	131 (45.5)	93 (71.0)	
	Severe	59 (20.5)	42 (71.2)	
	Missing	54 (15.7)	0	
Histology	Squamous	263 (83)	152 (57.8)	0.5224
	Adenocarcinoma	34 (10.7)	22 (64.7)	
	Adenosquamous	8 (2.5)	4 (50)	
	Others	12 (3.8)	6 (50)	
	Missing	26 (7.6)	0	
HIV/AIDS	Negative	300 (95.2)	181(60.3)	0.0000* #
	Positive	15 (4.8)	12(80.0)	
	Missing	28 (8.2)	0	
Comorbidity	No	141(54.7)	91(64.5)	0.5282
	Yes	117 (45.3)	67(57.3)	
	Missing	85 (24.8)	0	
Treatment	Chemotherapy	30 (11.2)	22 (73.3)	0.1160*
	Radiotherapy	45 (16.8)	28 (62.2)	
	Surgery	9 (3.4)	5 (55.6)	
	Chemo+Radio	149 (55.6)	90 (60.4)	
	Surgery+Radio	4 (1.5)	0 (0.0)	
	Surgery+Chemo	5 (1.9)	3 (60.0)	
	Surgery+Radio+Chemo	26 (9.7)	10 (38.5)	
	Missing	75 (21.9)	0	

*Statistically significant variables in univariate analysis that were included in multivariate analysis.
Variables significantly associated with CCa mortality in multivariate analysis ($p < 0.05$).

3.5 Clinical determinants of cervical cancer mortality

When clinical stage of the disease at diagnosis was explored, clinical presentation at late or advanced stages (FIGO IIB-IVB) correlated with a three-folds increase in mortality risk (aHR: 2.7, 95% CI: 1.5-4.7). On further analysis, there was a sharp upward gradient in the risk from the baseline early stage (FIGO I-IIA) disease to advanced (FIGO IVA-IVB) disease. (Table 3)

The chances of CCa death rose by almost three-folds when a CCa patient had underlying or recently diagnosed HIV/AIDS disease (aHR: 2.7, 95% CI: 1.5, 4.8). Anemia conferred approximately 80% increased risk of CCa mortality (aHR: 1.8, 95% CI: 1.1, 3.0). However, the pattern observed along the levels of anemia was similar to that of clinical stage of the disease, with a steep upward gradient from mild to severe. (Table 3)

4 Discussion

This study investigated the clinical and non-clinical factors that influence mortality from CCa in Nigeria. The cumulative prevalence of CCa mortality over the 7-year period was 59%, with an all-cause mortality rate of 30.5 per 100 women-years and a median follow-up time of 2.2 years. The risk of CCa mortality increases with clinical factors such as anemia, advanced clinical stage of CCa at presentation, and coexisting HIV/AIDS. Few non-clinical factors including family history of CCa in a first-degree relative and older age over 50 years at diagnosis were associated with increased mortality risk.

The mortality rate in this study is substantial, but very strongly correlated with the recent estimate of 31 per 100-women years in Ethiopia (9). However, it also varies widely from estimates in other previous studies with the rates ranging from 15.6 to as high as 79.8 per 100 women-years (10, 11). This may be due to the selection of the study population as mortality from hospital-based data are usually higher than that of the population. Similarly, variations in the sample size, study period, and focus of the study may also contribute to the wide variation observed (11). Another factor that could possibly explain the disparities is the poor and inconsistent record of mortality in most LMICs especially sub-Saharan Africa where national vital statistics including death registers are grossly inadequate or absent (31). Thus, the reported mortality rates were entirely dependent on how much of the mortality and outcome data could be retrieved by various researchers.

Overall, most of the factors revealed in this study corroborate the findings from previous studies (9–11, 23), but also find many of the previously documented factors insignificant in our study cohort.

Anemia was found in over four-fifths of CCa patients in our study. This estimate was significantly higher relative to earlier reports in Ethiopia (51.2%), Kenya (56.5%), Northern Nigeria (51%) and Korea (36.4%) (11, 14, 32, 33). In the United States, however, Hufnagel and colleagues (34) found up to 64% of gynecologic cancer (including CCa) patients developed anemia within six months of their diagnosis while the European Cancer Anemia Survey (ECAS) found up to 68% prevalence of anemia among European cancer patients during a 6-month survey period (35).

Anemia in cancer patients has a complex etiopathogenesis. The probable contributing causes include bleeding, dietary inadequacies, hemolysis, diminished erythropoietin levels, inflammation with increased hepcidin activity, and chemotherapy toxicity in marrow precursors (for those already commenced on chemotherapy) (36). In addition to population characteristics, stage of disease, and treatment modality received, presence of other comorbidities could significantly influence the incidence and severity of anemia, leading to considerable variation in its estimation (37).

In Nigeria, the rate of anemia among healthy women of reproductive age is high and it varies widely across regions ranging between 21% and 55% according to recent estimates (38, 39). This high pre-morbid anemia among women increases the risk of symptomatic anemia when cancer sets in, thus further explaining

TABLE 3 Age-adjusted and unadjusted hazard ratios for CCa mortality.

Variables	Categories	Unadjusted HR (95% CI)	p-value	Age-adjusted HR (95% CI)	p-value
Clinical Determinants					
HIV/AIDS	Negative	1.0		1.0	
	Positive	2.6 (1.4, 4.7)	0.002	2.7 (1.5, 4.8)	0.001
Clinical Stage	Early	1.0		1.0	
	Late/Advanced	2.8 (1.6, 4.8)	<0.001	2.7 (1.5, 4.7)	<0.001
	Early (I-IIA)	1.0		1.0	
	Late stage (IIB-IIIC)	2.4 (1.4, 4.2)	0.003	2.3 (1.3, 4.0)	0.005
	Advanced (IVA-IVB)	3.7 (2.1, 6.8)	<0.001	3.7 (2.1, 6.7)	<0.001
Anemia	No anemia	1.0		1.0	
	Anemia	1.7 (1.1, 2.8)	0.027	1.8 (1.1, 3.0)	0.017
	Mild	1.0		1.0	
	Moderate	1.8 (1.2, 2.8)	0.006	1.8 (1.2, 2.8)	0.006
	Severe	2.4 (1.5, 3.9)	<0.001	2.4 (1.4, 3.9)	0.001
Non-Clinical Determinants					
Age	≤50 years	1.0		1.0	
	>50 years	1.4 (1.0, 1.9)	0.035	1.4 (1.0, 1.9)	0.035
Family History of CCa	No	1.0		1.0	
	Yes	3.5 (1.1, 11.1)	0.031	4.1 (1.8, 13.0)	0.017

the high prevalence observed in our study. Of note is that most of the previous studies used a lower PCV cutoff value of 30% as normal blood levels (11), contrary to the WHO-recommended 36% for non-pregnant, reproductive-aged women (26). Most clinicians and researchers in Nigeria use the 30% cutoff for the general population because most people are asymptomatic at that level (40, 41).

Anemia at presentation in cancer patients could be due to anemia of chronic disease (ACD) which are often exacerbated by chronic blood loss and nutritional deficiencies, especially Iron deficiency (42). ACD is caused by a malfunction in Iron metabolism induced by excessive release of the Iron transport modulator hepcidin, resulting in a paradoxical Iron deficiency and anemia (43).

Our study shows that anemia significantly reduces disease-specific survival by more than 80%. A possible mechanism responsible for this is anemia-induced hypoxia which is associated with decreased tumor susceptibility to anticancer medications and increased morbidity in general (10, 44).

Over 86% of our study cohort were diagnosed at advanced stage of the disease. This is close to the East African estimates in Kenya and Ethiopia (14, 15). However, this estimate is significantly higher than the global average of about 60% and the African average of 62% (20). It also differs from other estimates such as in Nepal (65.5%), Northern Nigeria (72.3%), Ethiopia (60.4), and Brazil (70.6%) (11, 16, 45, 46).

The stage of CCa at diagnosis could partly reflect the accessibility and uptake of cancer screening services (47). Generally, most LMICs lack efficient national cancer screening and control programs that cover a substantial proportion of eligible women. In Nigeria, only 0.7–8% of reproductive-age women had been screened at least once in their lifetime (48, 49) similar to findings in Ghana (2.4%) but contrary to findings in Uganda (20.6%), and Malawi (40.2%) (50–52).

Healthcare system inadequacies could also be a significant contributor to late-stage diagnosis of CCa. For example, the prevalence of misdiagnosis especially among the cases referred from private health facilities was reported to be as high as 87.6%, and prolonged investigation time and degree of secondary (facility-based) delays could be responsible for delay in early diagnosis and commencement of appropriate care (17).

Our study showed that late-stage presentation was significantly associated with a higher chance of mortality, and this agrees with previous reports (18, 19). The mechanism of this effect is multifactorial, and probably due to multi organs involvement, distant spread to multiple vital organs, obstructive effect on the urinary system leading to kidney disorders, increasing risk of severe anemia, and overall higher morbidity.

HIV/AIDS confers significantly increased mortality risk up to three-folds among CCa patients. Similarly, other findings have reported a 2 to 3-fold increase in the risk of mortality among CCa patients living with HIV/AIDS (9, 53).

The association of HIV/AIDS with immunosuppression has been shown to cause poor clearance of high-risk HPV oncotypes and facilitate its infection of the cervical basal cells (54). These mechanisms enhance susceptibility of HIV patients to CCa. However, its effect on survival from CCa is complex and still insufficiently understood. Current understanding shows that HIV primarily impairs the ability of the cellular immune system to clear cancerous cells after treatment and in fact, could directly lead to poorer response to CCa therapy (53, 55). In other words, it leads to increased susceptibility to early cancer recurrence and severity. A recent study in Brazil showed that HIV infection did not affect initial treatment response or early mortality in women with cervical cancer, but it did increase relapse after achieving a complete response or remission, and late mortality (56). Similarly, the immunosuppression linked with HIV/AIDS also increases the susceptibility of CCa patients to other life-threatening AIDS-defining infections and cancers (57) which adds significant morbidity and increase their mortality risk.

In our study, about 5% of the patients had HIV/AIDS compared to previous studies that reported approximately 8% incidence (9, 11). This is a substantially higher HIV/AIDS prevalence than the recent national estimate of 1.4% in Nigeria (58), showing the higher propensity of women living with HIV/AIDS to develop CCa.

The mean age at diagnosis and death in our study is consistent with reported global estimates (2) and a large population-based estimate from an African study (59). These mean ages are, however, slightly higher at diagnosis and lower at mortality than the mean ages reported in the United States and Europe (3, 4).

As shown in our study, and in consonance with previous studies, being older than 50 years at time of diagnosis, was associated with a substantially higher risk of death from CCa (9, 10). However, no consistent pattern was observed when 13 African countries were studied (57). Conversely, age at diagnosis was found to be protective in an Ethiopian study (15), however, the cohort used for the study had younger women with mean cohort age of 49 years which might have impacted the study finding.

A risk level of about 46% has been reported among the age group 50–69 years, including an almost three-fold higher risk among CCa patients older than 70 years (60). This is consistent with the findings in our study.

Age has multiple effects on CCa outcome, and it is an independent negative prognostic factor irrespective of clinical stage, ethnicity or histological type of the disease (60). Older women are more likely to receive less-aggressive treatments (60) such as surgery and chemotherapy because of concern for their overall tolerability of stress of surgery or the ability of their organs to effectively metabolize anticancer medications. Older age also correlates with an increasing risk of other comorbidities and anemia which increases the morbidity and mortality from the disease (61).

The most common understanding of the role of family history in CCa is the increased risk of occurrence of the disease usually at genetic level. However, our study suggests that family history of CCa might also play a role in the outcome of CCa. A time-to-death analysis conducted among Ethiopian women supported this finding (22). However, caution should be applied in interpreting this finding due to the relatively small number of patients with family history of CCa in our data. It is also important to note that all the patients in our study who had family history of CCa presented at advanced stage mostly stage IVA or IVB. This could have significantly influenced the findings observed.

The biological mechanism of effect of family history on CCa mortality is still unclear as no previous descriptions were found in the literature at the time of reporting this study.

4.1 Study strengths and limitations

This study's categorization of the factors into clinical and non-clinical determinants helps to put further clarity on the type of interventions that would be appropriate to address the factors. The

study was based on relatively accurate and reliable data collected by trained health personnel and with high consistency because of multiple reviews by more than one medical personnel during management of the patients. We also achieved a relatively high complete follow-up rate of about 71% of the study population and were able to compile comprehensive information on the variables despite the prevailing challenges to record keeping, retrieval, data collection and follow-up in our environment. The strict reliance on histological diagnosis of CCa conferred high level of diagnostic accuracy and consistent determination of the follow-up time.

In the evaluation of women with family history of CCa in first-degree relatives, the power of the study was limited due to the small number of women who had family history of the disease. Being an institution-based study data, its interpretation may also partly reflect on institutional factors and may be difficult to completely extrapolate the findings to the general population. The lack of a national or regional database of death records is a major impediment for studies on cancer mortality in many LMICs, as observed in our study. The results of our study could have been bolstered even further by the confirmation of every death through such a database.

5 Conclusions

The study of clinical and non-clinical factors influencing cervical cancer mortality in Lagos, Nigeria, shows that mortality rate from the disease is very high. Clinical factors such as presence of anemia, HIV/AIDS, and advanced clinical stage disease, in addition to non-clinical factors like age above 50 years at diagnosis and family history of the disease in a first-degree relative were associated with higher CCa mortality risk. Consideration of these clinical and non-clinical factors during CCa management and control may improve the outcome for Nigerian women.

Data availability statement

The raw data supporting the conclusions of this article will be made available by the authors, without undue reservation.

Ethics statement

Ethical approval for study was granted by the ethical review committee of Lagos University Teaching Hospital (LUTH) with approval number ADM/DSCST/HREC/APP/4939. Written informed consent for participation was not required for this study in accordance with the institutional requirements

Author contributions

IO conceptualized the topic and research methodology, conducted data analysis, and prepared the first drafts of the manuscript and subsequent co-authors inputs. AO was involved in data curation and provided supervision. MH was involved in data curation. IO, AO, and MH were involved in securing ethical approval for the study. JM provided supervision. All authors contributed to the article and approved the submitted version.

Funding

The data collection for the research was supported by the Sahlgrenska Academy Travel Grant for data collection as part of Idris Olasunmbo Ola's study at Gothenburg University.

Acknowledgments

This publication has been produced during IO's scholarship period at Gothenburg University, Sweden, which is funded by the Swedish Institute. We are grateful to the staff at LUTH's medical records department as well as the management and staff at the NSIA-LUTH Cancer Center for allowing us access to the patient records during the review period.

Conflict of interest

The authors declare that the research was conducted in the absence of any commercial or financial relationships that could be construed as a potential conflict of interest.

Publisher's note

All claims expressed in this article are solely those of the authors and do not necessarily represent those of their affiliated organizations, or those of the publisher, the editors and the reviewers. Any product that may be evaluated in this article, or claim that may be made by its manufacturer, is not guaranteed or endorsed by the publisher.

References

1. Bruni L, Albero G, Serrano B, Mena M, Collado JJ, Gómez D, et al. *ICO/IARC information centre on HPV and cancer (HPV information centre). human papillomavirus and related diseases in the world. summary report 22 October 2021* (Accessed November 23, 2021).

2. Arbyn M, Weiderpass E, Bruni L, de Sanjose S, Saraiya M, Ferlay J, et al. Estimates of incidence and mortality of cervical cancer in 2018: A worldwide analysis. *Lancet Glob Health* (2020) 8:e191–203. doi: 10.1016/S2214-109X(19)30482-6

3. Surveillance, Epidemiology, and End Results Program [SEER]. *Cancer stat facts: Cervical cancer* (2022). Available at: https://seer.cancer.gov/statfacts/html/cervix.html (Accessed April 16, 2022).

4. European Cancer Information System. *Cervical cancer factsheet* (2021). Available at: https://ecis.jrc.ec.europa.eu/pdf/factsheets/cervical_cancer_en-Nov_2021.pdf (Accessed April 16, 2022).

5. Singh M, Jha RP, Shri N, Bhattacharyya K, Patel P, Dhamnetiya D. Secular trends in incidence and mortality of cervical cancer in India and its states, 1990-2019: Data from the global burden of disease 2019 study. *BMC Cancer* (2022) 22:149–9. doi: 10.1186/s12885-022-09232-w

6. Jedi-Agba E, Joko WY, Liu B, Buziba NG, Borok M, Korir A, et al. Trends in cervical cancer incidence in sub-Saharan Africa. *Brit J Cancer* (2020) 123:148–54. doi: 10.1038/s41416-020-0831-9

7. Chokunonga E, Borok MZ, Chirenje ZM, Nyakabu AM, Parkin DM. Trends in the incidence of cancer in the black population of Harare, Zimbabwe 1991-2010. *Int J Cancer* (2013) 133:721–9. doi: 10.1002/ijc.28063

8. GLOBOCAN. *Africa* (2020) (Accessed April 24, 2022).

9. Seifu B, Fikru C, Yilma D, Tessema F. Predictors of time to death among cervical cancer patients at tikur anbesa specialized hospital from 2014 to 2019: A survival analysis. *PLos One* (2022) 17:e0264369. doi: 10.1371/journal.pone.0264369

10. Wassie M, Fentie B, Asefa T. Determinants of mortality among cervical cancer patients attending in tikur anbessa specialized hospital, Ethiopia: Institutional-based retrospective study. *J Oncol* (2021) 2021:9916050. doi: 10.1155/2021/9916050

11. Musa J, Nankat J, Achenbach CJ, Shambe IH, Taiwo BO, Mandong B, et al. Cervical cancer survival in a resource-limited setting-north central Nigeria. *Infect Agent Cancer.* (2016) 11:15. doi: 10.1186/s13027-016-0062-0

12. GLOBOCAN. *Nigeria* (2020) (Accessed November 21, 2021).

13. World Health Organization. *Nigeria; cancer country profile* (2020). Available at: https://www.who.int/cancer/country-profiles/ NGA_2020.pdf?ua=1?subject=https://www.who.int/cancer/country-profiles/ NGA_2020.pdf?ua=1 (Accessed May 7, 2022).

14. Maranga IO, Hampson L, Oliver AW, Gamal A, Gichangi P, Opiyo A, et al. Analysis of factors contributing to the low survival of cervical cancer patients undergoing radiotherapy in Kenya. *PLos One* (2013) 8:e78411. doi: 10.1371/journal.pone.0078411

15. Begoihn M, Mathewos A, Aynalem A, Wondemagegnehu T, Moelle U, Gizaw M, et al. Cervical cancer in Ethiopia- predictors of advanced stage and prolonged time to diagnosis. *Infect Agents Cancer* (2019) 14:36. doi: 10.1186/s13027-019-0255-4

16. Dereje N, Gebremariam A, Addissie A, Worku A, Assefa M, Abraha A, et al. Factors associated with advanced stage at diagnosis of cervical cancer in Addis Ababa, Ethiopia: a population-based study. *BMJ Open* (2020) 10:e040645. doi: 10.1136/bmjopen-2020-040645

17. Awofeso O, Roberts AA, Salako O, Balogun L, Okediji P. Prevalence and pattern of late-stage presentation in women with breast and cervical cancers in Lagos university teaching hospital, Nigeria. *Nigerian Med J* (2018) 59:74. doi: 10.4103/nmj.NMJ11217

18. Fowler JR, Maani EV, Jack BW. Cervical cancer, in: *StatPearls* (2022). Treasure Island (FL: StatPearls Publishing. Available at: https://www.ncbi.nlm.nih.gov/books/NBK431093/ (Accessed May 10, 2022).

19. American Cancer Society. *Cancer facts figures* (2018). Available at: https://cancer.org/content/dam/cancer-org/research/cancer-facts-and-statistics/annual-cancer-facts-and-figures/2018/cancer-facts-and-figures-2018.pdf (Accessed May 4, 2022).

20. Tekalign T, Teshome M. Prevalence and determinants of late-stage presentation among cervical cancer patients, a systematic review and meta-analysis. *PLos One* (2022) 17:e0267571. doi: 10.1371/journal.pone.0267571

21. WHO Africa. *Burden of cancer*. Available at: https://www.who.int/countries/nga/ (Accessed April 18, 2022).

22. Gurmu SE. Assessing survival time of women with cervical cancer using various parametric frailty models: A case study at tikur anbessa specialized hospital, Addis Ababa, Ethiopia. *Ann Data Sci* (2018) 5:513–27. doi: 10.1007/s40745-018-0150-7

23. Shrestha AD, Neupane D, Vedsted P, Kallestrup P. Cervical cancer prevalence, incidence and mortality in low and middle income countries: A systematic review. *Asian Pacific J Cancer Prev* (2018) 19:319–24. doi: 10.22034/APJCP.2018.19.2.319

24. NSIA-LUTH Cancer Center. Available at: https://www.nhdic.ng/facility/nlcc/ (Accessed May 6, 2022).

25. Pylväläinen J, Talala K, Murtola T, Taari K, Raitanen J, Tammela TL, et al. Charlson comorbidity index based on hospital episode statistics performs adequately in predicting mortality, but its discriminative ability diminishes over time. *Clin Epidemiol* (2019) 11:923–32. doi: 10.2147/CLEP.S218697

26. World Health Organization. *Haemoglobin concentrations for the diagnosis of anaemia and assessment of severity. vitamin and mineral nutrition information system* (2011). Available at: http://www.who.int/vmnis/indicators/ haemoglobin.pdf ?subject=http://www.who.int/vmnis/indicators/ haemoglobin.pdf (Accessed May 6, 2022).

27. Bhatla N, Berek JS, Cuello Fredes M, Denny LA, Grenman S, Karunaratne K, et al. Revised FIGO staging for carcinoma of the cervix uteri. *Intl J gynaecol obstet* (2019) 145:129–35. doi: 10.1002/ijgo.12749

28. International Labor Organization. *International standard classification of occupations (ISCO)*. Available at: https://ilostat.ilo.org/resources/concepts-and-definitions/classificationoccupation/ (Accessed May 3, 2022).

29. Khademi H, Etemadi A, Kamangar F, Nouraie M, Shakeri R, Abaie B, et al. Verbal autopsy: reliability and validity estimates for causes of death in the golestan cohort study in Iran. *PLos One* (2010) 5:e11183. doi: 10.1371/journal.pone.0011183

30. UCLA. *Survival analysis with stata* . UCLA Statistical Consulting Group. Available at: https://stats.oarc.ucla.edu/stata/seminars/stata-survival/ (Accessed May 5, 2022).

31. Yokobori Y, Obara H, Sugiura Y, Kitamura T. Gaps in the civil registration and vital statistics systems of low- and middle-income countries and the health sector's role in improving the situation. *Global Health Med* (2021) 3:243–5. doi: 10.35772/ghm.2020.01103

32. Lim S, Lee CM, Park JM, Jung SY, Lee KB. An association between preoperative anemia and poor prognostic factors and decreased survival in early-stage cervical cancer patients. *Obstet Gynecol Sci* (2014) 57:471–7. doi: 10.5468/ogs.2014.57.6.471

33. Wassie M, Aemro A, Fentie B. Prevalence and associated factors of baseline anemia among cervical cancer patients in tikur anbesa specialized hospital, Ethiopia. *BMC Women's Health* (2021) 21. doi: 10.1186/s12905-021-01185-9

34. Hufnagel DH, Mehta ST, Ezekwe C, Brown AJ, Beeghly-Fadiel A, Prescott LS. Prevalence of anemia and compliance with NCCN guidelines for evaluation and treatment of anemia in patients with gynecologic cancer. *J Nat Compr Cancer Network* (2021) 19:513–20. doi: 10.6004/jnccn.2020.7638

35. Ludwig H, Van Belle S, Barrett-Lee P, Birgegård G, Bokemeyer C, Gascón P, et al. The European cancer anaemia survey (ECAS): A large, multinational, prospective survey defining the prevalence, incidence, and treatment of anaemia in cancer patients. *Eur J Cancer* (2004) 40:2293–306. doi: 10.1016/j.ejca.2004.06.019

36. Anand S, Burkenroad A, Glaspy J. Workup of anemia in cancer. *Clin Adv Hematol Oncol* (2020) 10:640–6.

37. Grotto HZ. Anaemia of cancer: an overview of mechanisms involved in its pathogenesis. *Med Oncol* (2008) 25:12–21. doi: 10.1007/s12032-007-9000-8

38. Ogunsakin RE, Akinyemi O, Babalola BT, Adetoro G. Spatial pattern and determinants of anemia among women of childbearing age in Nigeria. *Spatial Spatio-temporal Epidemiol* (2021) 36:100396. doi: 10.1016/j.sste.2020.100396

39. The World Bank. *Prevalence of anemia among women of reproductive age (% of women ages 15–49) – Nigeria* (2019). Available at: https://data.worldbank.org/indicator/SH.ANM.ALLW.ZS?locations=NG (Accessed May 23, 2022).

40. Akinbami A, Popoola A, Adediran A, Dosunmu A, Oshinaike O, Adebola P, et al. Full blood count pattern of pre-chemotherapy breast cancer patients in Lagos, Nigeria. *Caspian J Intern Med* (2013) 4:574–9.

41. Alani A, Vincent O, Adewumi A, Titilope A, Onogu E, Ralph A, et al. Plasma folate studies in HIV-positive patients at the Lagos university teaching hospital, Nigeria. *Indian J Sex Transm Dis AIDS.* (2010) 31:99–103. doi: 10.4103/0253-7184.74995

42. Aapro M, Österborg A, Gascón P, Ludwig H, Beguin Y. Prevalence and management of cancer-related anaemia, iron deficiency and the specific role of i.v. iron. *Ann Oncol* (2012) 23:1954–62. doi: 10.1093/annonc/mds112

43. Nemeth E, Ganz T. The role of hepcidin in iron metabolism. *Acta haematologica* (2009) 122:78–86. doi: 10.1159/000243791

44. Madeddu C, Gramignano G, Astara G, Demontis R, Sanna E, Atzeni V, et al. Pathogenesis and treatment options of cancer related anemia: Perspective for a targeted mechanism-based approach. *Front Physiol* (2018) 9:1294. doi: 10.3389/fphys.2018.01294

45. Ojha N, Jha M, Shrestha E, Dangal G. Late-stage cervical cancer among confirmed cervical cancer cases in a tertiary care centre: A descriptive cross-sectional study. *J Nepal Med Asso* (2021) 59:630–4. doi: 10.31729/jnma.6630

46. Thuler L CS, Aguiar SSD, Bergmann A. Determinantes do diagnóstico em estadio avançado do câncer do colo do útero no brasil. *Rev Bras Ginecologia e Obstetrícia* (2014) 36:237–43. doi: 10.1590/S0100-720320140005010

47. Shand L, Burney S, Fletcher J. Knowledge of cervical cancer, pap testing and the human papillomavirus among young Australian women. *Health Promotion J Aust* (2010) 21:202–7. doi: 10.1071/he10202

48. Idowu A, Olowookere SA, Fagbemi AT, Ogunlaja OA. Determinants of cervical cancer screening uptake among women in ilorin, north central Nigeria: A community-based study. *J Cancer Epidemiol* (2016) 2016:6469240. doi: 10.1155/2016/6469240

49. Olubodun T, Odukoya OO, Balogun MR. Knowledge, attitude and practice of cervical cancer prevention, among women residing in an urban slum in Lagos, southwest, Nigeria. *Pan Afr Med J* (2019) 32:130. doi: 10.11604/pamj.2019.32.130.14432

50. Calys-Tagoe BN, Aheto JM, Mensah G, Biritwum RB, Yawson AE. Cervical cancer screening practices among women in Ghana: evidence from wave 2 of the WHO study on global AGEing and adult health. *BMC Women's Health* (2020) 20:1–9. doi: 10.1186/s12905-020-00915-9

51. Isabirye A, Mbonye MK, Kwagala B. Predictors of cervical cancer screening uptake in two districts of central Uganda. *PLos One* (2020) 15:e0243281. doi: 10.1371/journal.pone.0243281

52. Gerstl S, Lee L, Nesbitt RC, Mambula C, Sugianto H, Phiri T, et al. Cervical cancer screening coverage and its related knowledge in southern Malawi. *BMC Public Health* (2022) 22:295. doi: 10.1186/s12889-022-12547-9

53. Dryden-Peterson S, Medhin H, Kebabonye-Pusoentsi M, Seage GR, Suneja G, Kayembe MK, et al. Cancer incidence following expansion of HIV treatment in Botswana. *PLos One* (2015) 10:e0135602. doi: 10.1016/j.virol.2013.08.018

54. Tugizov SM, Herrera R, Chin-Hong P, Veluppillai P, Greenspan D, Michael Berry J, et al. HIV-Associated disruption of mucosal epithelium facilitates paracellular penetration by human papillomavirus. *Virology* (2013) 446:378–88. doi: 10.1016/j.virol.2013.08.018

55. Nkwanyana NN, Gumbi PP, Roberts L, Denny L, Hanekom W, Soares A, et al. Impact of human immunodeficiency virus 1 infection and inflammation on the composition and yield of cervical mononuclear cells in the female genital tract. *Immunology* (2009) 128:e746–e757. doi: 10.1111/j.1365-2567.2009.03077.x

56. Ferreira MP, Coghill AE, Chaves CB, Bergmann A, Thuler LC, Soares EA, et al. Outcomes of cervical cancer among HIV-infected and HIV-uninfected women treated at the Brazilian national institute of cancer. *AIDS* (2017) 31:523–31. doi: 10.1097/QAD.0000000000001367

57. Reinhardt SW, Spec A, Meléndez J, Alonzo Cordon A, Ross I, Powderly WG, et al. AIDS-defining illnesses at initial diagnosis of HIV in a Large Guatemalan cohort. *Open Forum Infect Dis* (2017) 4:249. doi: 10.1093/ofid/ofx249

58. National Agency for the Control of AIDS (NACA). *Nigeria Prevalence rate* (2019). Available at: https://naca.gov.ng/nigeria-prevalence-rate/ (Accessed May 26, 2022).

59. Sengayi-Muchengeti M, Joko-Fru WY, Miranda-Filho A, Egue M, Akele-Akpo MT, N'da G, et al. Cervical cancer survival in sub-Saharan Africa by age, stage at diagnosis and human development index: A population-based registry study. *Int J Cancer* (2020) 147:3037–48. doi: 10.1002/ijc.33120

60. Quinn BA, Deng X, Colton A, Bandyopadhyay D, Carter JS, Fields EC. Increasing age predicts poor cervical cancer prognosis with subsequent effect on treatment and overall survival. *Brachytherapy* (2019) 18:29–37. doi: 10.1016/j.brachy.2018.08.016

61. Michalak SS, Rupa-Matysek J, Gil L. Comorbidities, repeated hospitalizations, and age ≥ 80 years as indicators of anemia development in the older population. *Ann Hematol* (2018) 97:1337–47. doi: 10.1007/s00277-018-3321-x

frontiers | Frontiers in Medicine

TYPE Review
PUBLISHED 21 February 2023
DOI 10.3389/fmed.2023.1111269

OPEN ACCESS

EDITED BY
Ming Yi,
Zhejiang University,
China

REVIEWED BY
Manuela Tamburro,
University of Molise,
Italy
Matteo Pavone,
Agostino Gemelli University Polyclinic (IRCCS),
Italy

*CORRESPONDENCE
Lina Zhang
✉ linazhang@njmu.edu.cn

SPECIALTY SECTION
This article was submitted to Obstetrics and Gynecology, a section of the journal Frontiers in Medicine

RECEIVED 29 November 2022
ACCEPTED 26 January 2023
PUBLISHED 21 February 2023

CITATION
Zhou Y, Shi X, Liu J and Zhang L (2023) Correlation between human papillomavirus viral load and cervical lesions classification: A review of current research.
Front. Med. 10:1111269.
doi: 10.3389/fmed.2023.1111269

Correlation between human papillomavirus viral load and cervical lesions classification: A review of current research

Yilu Zhou, Xiaoyu Shi, Jiaxin Liu and Lina Zhang*

Center for Diagnosis and Treatment of Cervical Diseases, Changzhou Maternity and Child Health Care Hospital, Changzhou Medical Center, Nanjing Medical University, Changzhou, China

Cervical cancer is the fourth largest malignant tumor among women in the world. Human papillomavirus (HPV) infection can lead to cervical intraepithelial neoplasia (CIN) and cervical cancer. Active papillomavirus infection occurs when the infected basal cells replicate and fill a certain area. Persistent HPV infection can lead to squamous intraepithelial lesions, which are divided into CIN1, CIN2, and CIN3 according to how much epithelium is impacted. Different types of HPV have different possibilities of causing cervical cancer, and high-risk HPV is the main cause of cervical cancer. Research showed that viral load may be an indicator of the progression of cervical precancerous lesions, but this association does not seem to be universal. This article aims to summarize different genotypes, multiple infections, especially viral load, in cervical precancerous lesions, to guide early intervention.

KEYWORDS

human papillomavirus, viral load, HPV genotyping, multiple infections, cervical lesions

1. Introduction

Cervical cancer is a leading cause of mortality among women. In 2020, an estimated 604,000 women were diagnosed with cervical cancer worldwide and about 342,000 women died from the disease (1). According to epidemiological research statistics, in the United States, 75% of people aged 15–50 are infected with human papillomavirus (HPV) in their lifetime, of which 60% are only temporary infections, 10% are persistent infections (the habitual targets of the HPV), 4% have slight cytological changes, and only 1% have clinical cytological damage. Persistent infection with about 15 types of hrHPV is the main risk factor for cervical cancer, of which HPV16 and HPV18 infections account for about 70% of the total cases (2). In the summary analysis of 11 case–control studies (3), HPV 16, 18, 45, 31, 33, 52, 58, and 35 accounted for 95% of HPV DNA-positive squamous cell carcinoma.

Two decades ago, hrHPV testing was proposed as a potential alternative to repeated cytology or immediate colposcopy for the triage of women with Atypical Squamous Cells of Undetermined Significance (ASCUS) cytology (4). In the last few years, the superiority of hrHPV testing compared to cytology to detect high-grade lesions has been demonstrated (5). However, for young women aged 21–24, the specificity of the HPV mRNA test in defining CIN2 lesions in women with ASCUS or Low-grade Squamous Intraepithelial Lesion (LSIL) is much higher than hrHPV DNA test (6). Recently, a Cochrane review (7) pointed out that relevant triage strategies are needed to manage hrHPV-positive women. Biomarkers have been assessed to manage hrHPV-positive women that include HPV genotyping, p16/Ki67 dual-staining, or the methylation status of HPV and some human genes (8–10). According to recent longitudinal studies, hrHPV viral loads can affect cervical diseases to varying degrees. This article summarizes the research progress on the correlation between

hrHPV viral load, HPV genotyping, and cervical lesions and provides guidance for the screening of cervical cancer.

2. Human papillomavirus genome

Human papillomavirus is a DNA virus in the papillomavirus subgroup. The shell consists of 72 5-polymers, 20 polyhedra, no envelope, 45–55 nm in diameter, and 5 × 106 Da. The HPV genome is an annular double-stranded DNA molecule with about 7,800–7,900 base pairs (bp), whose DNA composition accounts for about 12% of the mass of the virus (11). The complete genome can be divided into 3 coding regions (Figure 1): (1) early region (open reading box): including six genes in total, including E1, E2, E3, E4, E5, and E6, with a total length of about 4,500 bp, which can participate in the replication, transcription, and cell transformation of viral genes; (2) advanced regions (late stage) Coding area: contains a total of 2 genes, L1 and L2, of which L1 is the main capsid protein and L2 is the secondary capsid protein, which can be self-assembled into viral-like particles to induce the body's immune response and promote the production of protective antibodies. It belongs to the late expression of viral replication; (3) Upstream regulatory area (long control) control area, non-coding area: Located between the L1 gene and the E6 gene, it contains multiple binding sites and can participate in the regulation of virus replication and transcription (12).

3. Human papillomavirus genotyping

Of the approximately 30 types of HPV that infect the anogenital tract, 15 types of HPV, classified as "high-risk" types (HPV types 16, 18, 31, 33, 35, 39, 45, 51, 52, 56, 58, 59, 68, 73, and 82), are associated with high-grade lesions and invasive cervical cancer (13). On the other hand, 11 different HPV types, classified as "low-risk" HPV types (HPV types 6, 11, 40, 42, 43, 44, 54, 61, 70, and 81), are mainly associated with genital warts and benign cervical lesions (14). In the list of type 1 carcinogens published by the International Agency for Research on Cancer of the World Health Organization, there are types 16, 18, 31, 33, 35, 39, 45, 51, 52, 56, 58, and 59 of high-risk HPV (11).

3.1. Single HPV infection

The global prevalence of five top hrHPV types among women (15) is reported to be HPV 16: 55.4 (95% CI; 55.0–55.8), HPV 18: 14.6 (95% CI; 14.3–14.9), HPV 45: 4.8 (95% CI; 4.6–5.0), HPV 33: 4.2 (95% CI; 4.1–4.4), HPV 58: 3.8 (95% CI; 3.7–4.0), and HPV 31: 3.5 (95% CI; 3.4–3.7). A global study on HPV genotypes (16), published in the Lancet in 2010, found that genotypes HPV 16, HPV 18, HPV 31, HPV 33, HPV 35, HPV 45, HPV 52, and HPV 58 are easily capable of causing moisturizing cervical cancer. As previously stated, HPV 16/18 is the primary virus of cervical intraepithelial neoplasia (CIN). However, Ma L (17), on the other hand, found that CIN2+ accounted for 31.02% of 648 HPV-positive histopathological data, with HPV16 having the highest infection rate and HPV18 having only 3.75%, but HPV18 can play an important role in severe cervical lesions, with CIN3 and cervical adenocarcinoma being closely related to HPV18 single infection. A recent systematic synthesis (18) showed that individual HPV genotypes carry distinct risk values for high-grade cervical disease. HPV16 consistently carries the highest risk for CIN 3 or worse, HPV31, 18, and 33 carry intermediate-high CIN 3 or worse risk. Beyond HPV 16, 31, 18, and 33, HPV 52, 58, and 45 carry moderate risks, with 35, 39, 51, 56, 59, 66, and 68 consistently having the lowest CIN 3 or worse risks.

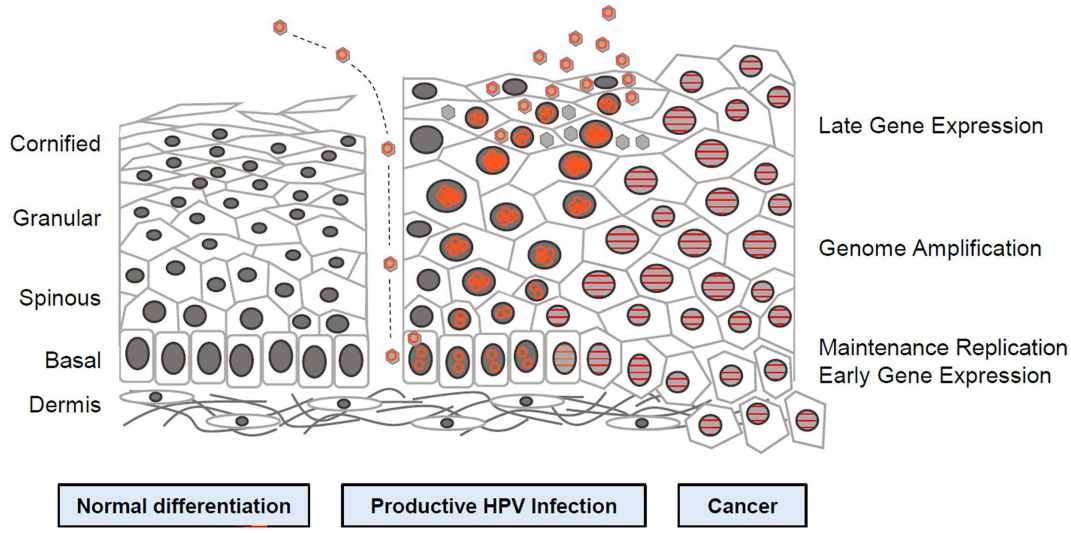

FIGURE 1
Human papillomavirus (HPV) life cycle and cancer (12). Cartoon depicting normal stratified cervical epithelium (left), HPV infected epithelium (center), and HPV induced cancer (right). Epithelial layers are indicated on the far left and HPV life cycle stages are indicated on the far right. Episomal genomes are shown as orange circles and integrated genomes shown as orange stripes. Left: Normal keratinocyte differentiation. Basal cells divide and daughter cells migrate upward, beginning the differentiation program. As differentiation proceeds, cells exit the cell cycle. Fully keratinized squames slough off from the apical surface. Middle: Productive HPV Infection: HPV virions gain access to basal cells *via* microwounds. The viral genomes migrate to the nucleus, where they are maintained at approximately100 copies/cell. As daughter cells begin differentiation, viral genomes are amplified. Cell nuclei are retained and chromatin is activated to support viral DNA replication. Right: Cancer. Viral genomes often integrate into the host genome and E6/E7 expression is increased, leading to enhanced proliferation and accumulation of cellular mutations. Cellular differentiation is lost and cancerous cells invade into the dermal layer along with neighboring tissues (12).

3.2. Multiple HPV infections

Women may be infected with multiple HPV infections with different genotypes throughout their lives (3). It is reported that among HPV-positive women, the prevalence rate of multiple HPV infections is between 18.5 and 46% (19–21). A variety of HR-HPV types infect synergistically in the occurrence of cervical cancer, according to prospective research (22). Fife et al. (23) reported that infection with multiple HR-HPV types tends to increase the severity of cervical diseases. However, other reports provided controversial conclusions. Muñoz et al. (3) found that there is no significant difference in the risk of cervical cancer among women with multiple and single HPV infections. Herrero et al. (24) have shown that multiple infections may be related to the persistence of HPV and increase the duration of infection and the risk of cervical disease, but some studies (25–27) still showed no impact. Recently, Iacobone et al. (28) confirmed that multiple HPV infections are significantly associated with reduced CIN2+ risk, while cervical cancer and changes in precancerous diseases may occur in single infections. Another hrHPV test through Cobas4800 showed that the risk of HPV16 co-infection with other types of CIN3 seems to be lower than that of a single HPV16 infection (29). A study (30) from Beijing, China, also indicated that the incidence of CIN2+ in patients with a single HPV 16 infection (62.2%) is higher than that of patients mixed with other HPV genotypes (52.4%). At the same time, the incidence of CIN2+ in patients infected with HPV 16 may be higher than that of patients with a single HPV 52 and other genotypes. Recently, a study published by Song et al. (31) suggested that co-infection with lower-grade HPV types has little impact on the CIN2+ risk associated with a single hrHPV infection, which confirms the above conclusion.

4. Human papillomavirus viral load

4.1. hrHPV viral load and cervical lesions

Most scholars (32–41) believe that there is a clear correlation between HPV viral load and the degree of cervical lesion, that is, as the viral load increases, the risk of cervical lesions increases. A large Chinese retrospective study (34), compared the viral load of ≤CIN1 and CIN2+ patients in eight high-risk HPV genotypes (HPV16/18/31/33/45/52/58/82). The results showed that statistical significance was only found in HPV16 genotypes; there was no such difference in the other seven genotypes. Zhao et al. (36) conducted a 15-year prospective cohort study in China and found a significant correlation between the change in HPV viral load over time and the probability of CIN2+ in patients. Women with an increased viral load (15.3%) had a 38-fold higher risk of CIN2+ than HPV-negative women (0.4%). We summarized some longitudinal studies (Table 1) published in the past 5 years and found that the HPV viral load is indeed related to the CIN level of cervical lesions, but this law is not universal. It needs to be reflected in a specific genotype. For example, in the cohort of French women (42), only the viral load of HPV16 can predict CIN2+, and this association has not been found in HPV18 and other genotypes. This rule has also been found in the Chinese female cohort (34). More interestingly, a cohort study from Canada (33) showed that the HPV 16/18/31 viral load is related to higher levels of cervical lesions. In the Mexican women's cohort (35), we found that women in LSIL and HSIL have a higher HPV 16 viral load. In contrast, Del Río-Ospina L et al. (44) study in Colombia has documented that a higher level of cervical lesions in women corresponds to a lower HPV 16 viral load. Wang W et al. (39) have shown that the HPV16 viral load can gradually increase with the development of the lesion, and there is no obvious correlation between the HPV18 viral load and histopathology. At the same time, the viral load of subtypes close to HPV16 (HPV52, HPV58, etc.) can increase with the development of the disease, while the viral load of subtypes close to HPV18 (HPV45, HPV59, etc.) does not change significantly. Unlike the general description of viral load two decades ago, the description of viral loads of different HPV genotypes in recent years has helped us better understand the relationship between viral load and CIN classification.

However, some experts (45–47) do not think that HPV viral load is associated with the degree of cervical lesions (48). They said that CIN1 was in the acute stage of HPV infection, and HPV's self-replication ability was significantly more prominent in other stages. When CIN1 developed into CIN2-3, there was a significant downward trend in HPV viral load because HPV's self-replication ability was relatively stable. When it developed from CIN2-3 to cervical cancer stage I again, the HPV gene was integrated into the DNA of the host cell and had the ability to transform cells, causing the cervical lesion to gradually transform into cervical *in situ* cancer and even infiltrating cancer (48, 49). From this perspective, the viral load may underestimate the severity of the disease, thus delaying treatment.

When we reviewed these studies, we also found that the viral load is also related to age. Compared with women under the age of 30, the relationship between viral load and cervical lesions in women older than 30 years old is stronger (33).

4.2. Viral load as a triage biomarker

At present, many countries around the world use HPV testing for primary cervical cancer screening. Clinical trials (50) showed that HPV detection and screening of high-level lesions are more sensitive than cytological testing. The randomized clinical trial published in JAMA Oncology (51) indicated that genotyping for hrHPV with cytology triage significantly reduced the colposcopy referral rate compared with cytology for urban women. However, many HPV-positive women have no potential cervical lesions. To avoid overburdening colposcopy services and reduce the harm caused by over-referral, HPV-positive women must undergo a second test. Whether the HPV viral load can be used as a biomarker for triage is a question worth discussing at present. Luo et al.'s (52) research used the viral load as a triage indicator for cervical cancer screening. It is recommended that colposcopy be performed immediately when the viral load is >10 RLU/CO, and cytological testing should be carried out at >1 RLU/CO or <10 RLU/CO to optimize sensitivity, specificity, and the referral rate. This proved that the viral load can be used as a triage indicator. However, The HPV viral load can only predict the risk of cervical lesions under specific HPV typing. This may not apply to all HPV-positive women.

In December 2021, the World Health Organization issued guidelines for the screening and treatment of cervical precancerous lesions, proposing the use of mRNA testing for cervical cancer screening. Even if the viral load cannot be used as a method for secondary triage, it can be used as an indicator of virus replication to predict condition tracking and subsequent treatment.

5. Discussion

Due to the close relationship between HPV and cervical cancer, cervical cancer becomes a unique type of cancers. Its etiology is clear, and early prevention and diagnosis can achieve complete eradication. In May

TABLE 1 Longitudinal studies.

Author	Year	Country	Participants	Findings
Xiang (34)	2022	China	17,235	• The most prevalent hrHPV genotype for study patients who had ASC-US cervical cytology results were HPV52 (16%), HPV16 (11.3%), HPV58 (10.2%), and HPV53 (8.4%). The least prevalent hrHPV genotypes were HPV26, HPV82, HPV73 and HPV45, each with a prevalence < 1.5%.
				• Only the viral load difference between < CIN1 and CIN2+ groups ($p = 0.001$) was found in HPV16, and there was no such difference in the other seven genotypes.
Liu (32)	2021	China	256	• Higher high-risk HPV viral load in cervical lesions is related to higher risk of high-level cervical lesions.
Baumann (42)	2021	French	885	• HPV16 DNA load may independently predict the development of CIN2+.
				• On the contrary, compared with other hrHPVs, contracting HPV 18 does not increase the risk of high-level cervical disease development.
Oyervides (35)	2020	Mexican	294	• The predominant HPV type was 16 (33.7%), followed by 18 (25.3%) and 39 (22.5%).
				• We found associations between HPV 18, 51, and 56 and high viral loads (p-values of 0.012, 0.034, and 0.005, respectively).
				• Significant difference was also not found when we analyzed HPV 18 and HPV52.
Zhao (36)	2019	China	1,479	• Individuals with medium/high virus loads, especially those whose HPV load remains stable, as well as individuals with increased HPV loads, are at greater risk of high-level lesions in the future and may be used as triage indicators for HPV-positive women.
Talía (33)	2019	Canada	1,611	• Viral load varied by HPV type and by diagnosis. The geometric mean viral load was highest for HPV16 and lowest for HPV45.
				• Higher HPV16/18/31 viral load was associated with a higher likelihood of being diagnosed with CIN and cancer.
Long (43)	2017	America	2,902	• The viral load of subtypes close to HPV16 can increase with the development of the disease.
				• The viral load of other types appeared slightly lower among women with HSIL compared to those with LSIL.
Del L (44)	2015	Colombian	180	• The increased viral load of HPV-18 and HPV-33 is directly proportional to the degree of cervical lesions.
				• High frequency of cervical lesions in women with low HPV-16 load.

2018, the Director-General of WHO called on countries to take action to jointly achieve the global goal of eliminating cervical cancer. Vaccinating adolescents against HPV is now the primary cervical cancer prevention strategy (53). However, HPV vaccination is not recommended instead of cervical cancer screening (54), although the vaccine can greatly reduce the risk of cervical cancer (55). Regardless of the relationship between HPV viral load and cervical lesions, viral load must be combined with other methods to maximize sensitivity and specificity in cervical cancer screening. Therefore, we need to further study the many factors that may influence the occurrence and development of cervical lesions, to achieve the combined application of multiple methodological detections in the early screening of cervical cancer, which is conducive to the early detection, early diagnosis, and early treatment of cervical cancer, so as to achieve the elimination of cervical cancer by the World Health Organization by 2030.

Author contributions

LZ and YZ conceived the review study. YZ drafted the manuscript. All authors contributed to the article and approved the submitted version.

Funding

This study was funded by grants from The Maternal and Child Health Research Project in Jiangsu Province (F202166) and The Changzhou Health Commission Guidance Project (WZ202217).

Acknowledgments

We thank our supervisor for her help in the initial stage of the review study, we gratefully acknowledge the financial supports by The Maternal and Child Health Research Project in Jiangsu Province number F202166 and The Changzhou Health Commission Guidance Project number WZ202217.

Conflict of interest

The authors declare that the research was conducted in the absence of any commercial or financial relationships that could be construed as a potential conflict of interest.

Publisher's note

References

1. Sung, H, Ferlay, J, Siegel, RL, Laversanne, M, Soerjomataram, I, Jemal, A, et al. Global cancer statistics 2020: globocan estimates of incidence and mortality worldwide for 36 cancers in 185 countries. *CA Cancer J Clin*. (2021) 71:209–49. doi: 10.3322/caac.21660

2. Sammarco, ML, Del Riccio, I, Tamburro, M, Grasso, GM, and Ripabelli, G. Type-specific persistence and associated risk factors of human papillomavirus infections in women living in Central Italy. *Eur J Obstet Gynecol Reprod Biol*. (2013) 168:222–6. doi: 10.1016/j.ejogrb.2013.01.012

3. Muñoz, N, Bosch, FX, de Sanjosé, S, Herrero, R, Castellsagué, X, Shah, KV, et al. Epidemiologic classification of human papillomavirus types associated with cervical cancer. *N Engl J Med*. (2003) 348:518–27. doi: 10.1056/NEJMoa021641

4. Group, A.L.T.S.A. Results of a randomized trial on the management of cytology interpretations of atypical squamous cells of undetermined significance. *Am J Obstet Gynecol*. (2003) 188:1383–92. doi: 10.1067/mob.2003.457

5. Ronco, G, and Giorgi, RP. Role of hpv dna testing in modern gynaecological practice. *Best Pract Res Clin Obstet Gynaecol*. (2018) 47:107–18. doi: 10.1016/j.bpobgyn.2017.08.002

6. Frega, A, Pavone, M, Sesti, F, Leone, C, Bianchi, P, Cozza, G, et al. Sensitivity and specificity values of high-risk hpv dna, p16/ki-67 and hpv mrna in young women with atypical squamous cells of undetermined significance (ascus) or low-grade squamous intraepithelial lesion (lsil). *Eur Rev Med Pharmacol Sci*. (2019) 23:10672–7. doi: 10.26355/eurrev_201912_19765

7. Koliopoulos, G, Nyaga, VN, Santesso, N, Bryant, A, Martin-Hirsch, PP, Mustafa, RA, et al. Cytology versus hpv testing for cervical cancer screening in the general population. *Cochrane Database Syst Rev*. (2017) 8:CD008587. doi: 10.1002/14651858.CD008587.pub2

8. Schiffman, M, Burk, RD, Boyle, S, Raine-Bennett, T, Katki, HA, Gage, JC, et al. A study of genotyping for management of human papillomavirus-positive, cytology-negative cervical screening results. *J Clin Microbiol*. (2015) 53:52–9. doi: 10.1128/JCM.02116-14

9. Stoler, MH, Baker, E, Boyle, S, Aslam, S, Ridder, R, Huh, WK, et al. Approaches to triage optimization in hpv primary screening: extended genotyping and p16/ki-67 dual-stained cytology-retrospective insights from athena. *Int J Cancer*. (2020) 146:2599–607. doi: 10.1002/ijc.32669

10. Verhoef, VMJ, Bosgraaf, RP, van Kemenade, FJ, Rozendaal, L, Heideman, DAM, Hesselink, AT, et al. Triage by methylation-marker testing versus cytology in women who test hpv-positive on self-collected cervicovaginal specimens (prohtect-3): a randomised controlled non-inferiority trial. *Lancet Oncol*. (2014) 15:315–22. doi: 10.1016/S1470-2045(14)70019-1

11. Wang, X, Huang, X, and Zhang, Y. Involvement of human papillomaviruses in cervical cancer. *Front Microbiol*. (2018) 9:2896. doi: 10.3389/fmicb.2018.02896

12. Langsfeld, E, and Laimins, LA. Human papillomaviruses: research priorities for the next decade. *Trends cancer*. (2016) 2:234–40. doi: 10.1016/j.trecan.2016.04.001

13. Shukla, S, Bharti, AC, Mahata, S, Hussain, S, Kumar, R, Hedau, S, et al. Infection of human papillomaviruses in cancers of different human organ sites. *Indian J Med Res*. (2009) 130:222–33.

14. Castellsagué, X, Díaz, M, de Sanjosé, S, Muñoz, N, Herrero, R, Franceschi, S, et al. Worldwide human papillomavirus etiology of cervical adenocarcinoma and its cofactors: implications for screening and prevention. *J Natl Cancer Inst*. (2006) 98:303–15. doi: 10.1093/jnci/djj067

15. Pimple, S, and Mishra, G. Cancer cervix: epidemiology and disease burden. *Cytojournal*. (2022) 19:21. doi: 10.25259/CMAS_03_02_2021

16. de Sanjose, S, Quint, WG, Alemany, L, Geraets, DT, Klaustermeier, JE, Lloveras, B, et al. Human papillomavirus genotype attribution in invasive cervical cancer: a retrospective cross-sectional worldwide study. *Lancet Oncol*. (2010) 11:1048–56. doi: 10.1016/S1470-2045(10)70230-8

17. Ma, L, Cong, X, Shi, M, Wang, X, Liu, H, and Bian, M. Distribution of human papillomavirus genotypes in cervical lesions. *Exp Ther Med*. (2017) 13:535–41. doi: 10.3892/etm.2016.4000

18. Bonde, JH, Sandri, M, Gary, DS, and Andrews, JC. Clinical utility of human papillomavirus genotyping in cervical cancer screening: a systematic review. *J Low Genit Tract Dis*. (2020) 24:1–13. doi: 10.1097/LGT.0000000000000494

19. Vaccarella, S, Franceschi, S, Snijders, PJF, Herrero, R, Meijer, CJLM, Plummer, M, et al. Concurrent infection with multiple human papillomavirus types: pooled analysis of the iarc hpv prevalence surveys. *Cancer Epidemiol Biomarks Prev*. (2010) 19:503–10. doi: 10.1158/1055-9965.EPI-09-0983

20. Chaturvedi, AK, Katki, HA, Hildesheim, A, Rodríguez, AC, Quint, W, Schiffman, M, et al. Human papillomavirus infection with multiple types: pattern of coinfection and risk of cervical disease. *J Infect Dis*. (2011) 203:910–20. doi: 10.1093/infdis/jiq139

21. Dickson, EL, Vogel, RI, Bliss, RL, and Downs, LSJ. Multiple-type human papillomavirus (hpv) infections: a cross-sectional analysis of the prevalence of specific types in 309,000 women referred for hpv testing at the time of cervical cytology. *Int J Gynecol Cancer*. (2013) 23:1295–302. doi: 10.1097/IGC.0b013e31829e9fb4

22. Trottier, H, Mahmud, S, Costa, MC, Sobrinho, JP, Duarte-Franco, E, Rohan, TE, et al. Human papillomavirus infections with multiple types and risk of cervical neoplasia. *Cancer Epidemiol Biomarks Prev*. (2006) 15:1274–80. doi: 10.1158/1055-9965.EPI-06-0129

23. Fife, KH, Cramer, HM, Schroeder, JM, and Brown, DR. Detection of multiple human papillomavirus types in the lower genital tract correlates with cervical dysplasia. *J Med Virol*. (2001) 64:550–9. doi: 10.1002/jmv.1085

24. Herrero, R, Castle, PE, Schiffman, M, Bratti, MC, Hildesheim, A, Morales, J, et al. Epidemiologic profile of type-specific human papillomavirus infection and cervical neoplasia in Guanacaste, Costa Rica. *J Infect Dis*. (2005) 191:1796–807. doi: 10.1086/428850

25. Wentzensen, N, Schiffman, M, Dunn, T, Zuna, RE, Gold, MA, Allen, RA, et al. Multiple human papillomavirus genotype infections in cervical cancer progression in the study to understand cervical cancer early endpoints and determinants. *Int J Cancer*. (2009) 125:2151–8. doi: 10.1002/ijc.24528

26. Adcock, R, Cuzick, J, Hunt, WC, McDonald, RM, and Wheeler, CM. Role of hpv genotype, multiple infections, and viral load on the risk of high-grade cervical neoplasia. *Cancer Epidemiol Biomarkers Prev*. (2019) 28:1816–24. doi: 10.1158/1055-9965.EPI-19-0239

27. Schmitt, M, Depuydt, C, Benoy, I, Bogers, J, Antoine, J, Arbyn, M, et al. Multiple human papillomavirus infections with high viral loads are associated with cervical lesions but do not differentiate grades of cervical abnormalities. *J Clin Microbiol*. (2013) 51:1458–64. doi: 10.1128/JCM.00087-13

28. Iacobone, AD, Bottari, F, Radice, D, Preti, EP, Franchi, D, Vidal Urbinati, AM, et al. Distribution of high-risk human papillomavirus genotypes and multiple infections in preneoplastic and neoplastic cervical lesions of unvaccinated women: a cross-sectional study. *J Low Genit Tract Dis*. (2019) 23:259–64. doi: 10.1097/LGT.0000000000000487

29. Wu, P, Xiong, H, Yang, M, Li, L, Wu, P, Lazare, C, et al. Co-infections of hpv16/18 with other high-risk hpv types and the risk of cervical carcinogenesis: a large population-based study. *Gynecol Oncol*. (2019) 155:436–43. doi: 10.1016/j.ygyno.2019.10.003

30. Li, M, du, X, Lu, M, Zhang, W, Sun, Z, Li, L, et al. Prevalence characteristics of single and multiple hpv infections in women with cervical cancer and precancerous lesions in Beijing, China. *J Med Virol*. (2019) 91:473–81. doi: 10.1002/jmv.25331

31. Song, F, Yan, P, Huang, X, Wang, C, Du, H, Qu, X, et al. Roles of extended human papillomavirus genotyping and multiple infections in early detection of cervical precancer and cancer and hpv vaccination. *BMC Cancer*. (2022) 22:42. doi: 10.1186/s12885-021-09126-3

32. Liu, Y, Xu, C, Pan, J, Sun, C, Zhou, H, and Meng, Y. Significance of the viral load of high-risk hpv in the diagnosis and prediction of cervical lesions: a retrospective study. *BMC Womens Health*. (2021) 21:353. doi: 10.1186/s12905-021-01493-0

33. Malagón, T, Louvanto, K, Ramanakumar, AV, Koushik, A, Coutlée, F, Franco, EL, et al. Viral load of human papillomavirus types 16/18/31/33/45 as a predictor of cervical intraepithelial neoplasia and cancer by age. *Gynecol Oncol*. (2019) 155:245–53. doi: 10.1016/j.ygyno.2019.09.010

34. Tao, X, Austin, RM, Yu, T, Zhong, F, Zhou, X, Cong, Q, et al. Risk stratification for cervical neoplasia using extended high-risk hpv genotyping in women with asc-us cytology: a large retrospective study from China. *Cancer Cytopathol*. (2022) 130:248–58. doi: 10.1002/cncy.22536

35. Oyervides-Muñoz, MA, Pérez-Maya, AA, Sánchez-Domínguez, CN, Berlanga-Garza, A, Antonio-Macedo, M, Valdéz-Chapa, LD, et al. Multiple hpv infections and viral load association in persistent cervical lesions in mexican women. *Viruses*. (2020) 12:12. doi: 10.3390/v12040380

36. Zhao, X, Zhao, S, Hu, S, Zhao, K, Zhang, Q, Zhang, X, et al. Role of human papillomavirus dna load in predicting the long-term risk of cervical cancer: a 15-year prospective cohort study in China. *J Infect Dis*. (2019) 219:215–22. doi: 10.1093/infdis/jiy507

37. Basu, P, Muwonge, R, Mittal, S, Banerjee, D, Ghosh, I, Panda, C, et al. Implications of semi-quantitative hpv viral load estimation by hybrid capture 2 in colposcopy practice. *J Med Screen*. (2016) 23:104–10. doi: 10.1177/0969141315606483

38. Wang, SM, Colombara, D, Shi, JF, Zhao, FH, Li, J, Chen, F, et al. Six-year regression and progression of cervical lesions of different human papillomavirus viral loads in varied histological diagnoses. *Int J Gynecol Cancer*. (2013) 23:716–23. doi: 10.1097/IGC.0b013e318286a95d

39. Wang, W, Zhang, XH, Li, M, Hao, CH, Zhao, ZM, and Liang, HP. Association between viral loads of different oncogenic human papillomavirus types and the degree of cervical lesions in the progression of cervical cancer. *Clin Chim Acta*. (2018) 483:249–55. doi: 10.1016/j.cca.2018.05.016

40. Mittal, S, Basu, P, Muwonge, R, Banerjee, D, Ghosh, I, Sengupta, MM, et al. Risk of high-grade precancerous lesions and invasive cancers in high-risk hpv-positive women with normal cervix or cin 1 at baseline-a population-based cohort study. *Int J Cancer*. (2017) 140:1850–9. doi: 10.1002/ijc.30609

41. Manawapat-Klopfer, A, Wang, L, Haedicke-Jarboui, J, Stubenrauch, F, Munk, C, Thomsen, LT, et al. Hpv16 viral load and physical state measurement as a potential immediate triage strategy for hr-HPV-infected women: a study in 644 women with single hpv16 infections. *Am J Cancer Res*. (2018) 8:715–22.

42. Baumann, A, Henriques, J, Selmani, Z, Meurisse, A, Lepiller, Q, Vernerey, D, et al. Hpv16 load is a potential biomarker to predict risk of high-grade cervical lesions in high-risk HPV-infected women: a large longitudinal french hospital-based cohort study. *Cancers*. (2021) 13:4149. doi: 10.3390/cancers13164149

43. Fu, XL, Schiffman, M, Ke, Y, Hughes, JP, Galloway, DA, He, Z, et al. Type-dependent association between risk of cervical intraepithelial neoplasia and viral load of oncogenic human papillomavirus types other than types 16 and 18. *Int J Cancer*. (2017) 140:1747–56. doi: 10.1002/ijc.30594

44. del Río-Ospina, L, Soto-de León, SC, Camargo, M, Moreno-Pérez, DA, Sánchez, R, Pérez-Prados, A, et al. The dna load of six high-risk human papillomavirus types and its association with cervical lesions. *BMC Cancer*. (2015) 15:100. doi: 10.1186/s12885-015-1126-z

45. Andersson, S, Safari, H, Mints, M, Lewensohn-Fuchs, I, Gyllensten, U, and Johansson, B. Type distribution, viral load and integration status of high-risk human papillomaviruses in pre-stages of cervical cancer (cin). *Br J Cancer*. (2005) 92:2195–200. doi: 10.1038/sj.bjc.6602648

46. Lorincz, AT, Castle, PE, Sherman, ME, Scott, DR, Glass, AG, Wacholder, S, et al. Viral load of human papillomavirus and risk of cin3 or cervical cancer. *Lancet*. (2002) 360:228–9. doi: 10.1016/S0140-6736(02)09463-1

47. Castle, PE, Schiffman, M, and Wheeler, CM. Hybrid capture 2 viral load and the 2-year cumulative risk of cervical intraepithelial neoplasia grade 3 or cancer. *Am J Obstet Gynecol*. (2004) 191:1590–7. doi: 10.1016/j.ajog.2004.05.018

48. Constandinou-Williams, C, Collins, SI, Roberts, S, Young, LS, Woodman, CBJ, and Murray, PG. Is human papillomavirus viral load a clinically useful predictive marker? A longitudinal study. *Cancer Epidemiol Biomarks Prev*. (2010) 19:832–7. doi: 10.1158/1055-9965.EPI-09-0838

49. Pett, M, and Coleman, N. Integration of high-risk human papillomavirus: a key event in cervical carcinogenesis? *J Pathol*. (2007) 212:356–67. doi: 10.1002/path.2192

50. Bottari, F, Iacobone, AD, Radice, D, Preti, EP, Preti, M, Franchi, D, et al. Hpv tests comparison in the detection and follow-up after surgical treatment of cin2+ lesions. *Diagnostics*. (2022) 12:2359. doi: 10.3390/diagnostics12102359

51. Zhang, J, Zhao, Y, Dai, Y, Dang, L, Ma, L, Yang, C, et al. Effectiveness of high-risk human papillomavirus testing for cervical cancer screening in China: a multicenter, open-label, randomized clinical trial. *JAMA Oncol*. (2021) 7:263–70. doi: 10.1001/jamaoncol.2020.6575

52. Luo, H, Belinson, JL, Du, H, Liu, Z, Zhang, L, Wang, C, et al. Evaluation of viral load as a triage strategy with primary high-risk human papillomavirus cervical cancer screening. *J Low Genit Tract Dis*. (2017) 21:12–6. doi: 10.1097/LGT.0000000000000277

53. Human Papillomavirus Vaccination. Committee opinion no. 704: human papillomavirus vaccination. *Obstet Gynecol*. (2017) 129:1. doi: 10.1097/AOG.0000000000002052

54. Okunade, KS, Sunmonu, O, Osanyin, GE, and Oluwole, AA. Knowledge and acceptability of human papillomavirus vaccination among women attending the gynaecological outpatient clinics of a university teaching hospital in Lagos, Nigeria. *J Trop Med*. (2017) 2017:8586459. doi: 10.1155/2017/8586459

55. Lei, J, Ploner, A, Elfström, KM, Wang, J, Roth, A, Fang, F, et al. Hpv vaccination and the risk of invasive cervical cancer. *N Engl J Med*. (2020) 383:1340–8. doi: 10.1056/NEJMoa1917338

frontiers | Frontiers in Oncology

TYPE Original Research
PUBLISHED 16 March 2023
DOI 10.3389/fonc.2023.1092602

OPEN ACCESS

EDITED BY
Yujiao Deng,
The Second Affiliated Hospital of Xi'an Jiaotong University, China

REVIEWED BY
Zohre Momenimovahed,
Qom University of Medical Sciences, Iran
Sumaira Mubarik,
Wuhan University, China

*CORRESPONDENCE
Haomin Yang
haomin.yang@fjmu.edu.cn
Yulin Zhou
zhou_yulin@126.com

†These authors have contributed equally to this work

SPECIALTY SECTION
This article was submitted to Cancer Epidemiology and Prevention, a section of the journal Frontiers in Oncology

RECEIVED 05 December 2022
ACCEPTED 27 February 2023
PUBLISHED 16 March 2023

CITATION
Chen Y, Song M, Zhang Y, Yu X, Zou S, Zhu P, Zhou Y and Yang H (2023) The temporal trend of women's cancer in Changle, China and a migrant epidemiological study.
Front. Oncol. 13:1092602.
doi: 10.3389/fonc.2023.1092602

The temporal trend of women's cancer in Changle, China and a migrant epidemiological study

Yu Chen[1†], Mengjie Song[1†], Yanyu Zhang[1], Xingxing Yu[1], Shuqing Zou[1], Pingxiu Zhu[1], Yulin Zhou[2*] and Haomin Yang[1,3*]

[1]Department of Epidemiology and Health Statistics, School of Public Health, Fujian Medical University, Fuzhou, China, [2]United Diagnostic and Research Center for Clinical Genetics, Women and Children's Hospital, School of Medicine and School of Public Health, Xiamen University, Xiamen, Fujian, China, [3]Department of Medical Epidemiology and Biostatistics, Karolinska Institutet, Stockholm, Sweden

Background: Although the etiology of women's cancer has been extensively studied in the last few decades, there is still little evidence comparing the temporal pattern of these cancers among different populations.

Methods: Cancer incidence and mortality data from 1988 to 2015 were extracted from the Changle Cancer Register in China, and cancer incidence data for Los Angeles were extracted from Cancer Incidence in Five Continents plus database. A Joinpoint regression model was used to analyze the temporal trends of incidence and mortality for breast, cervical, corpus uteri and ovarian cancers. The standardized incidence ratios were applied to compare the cancer risk across populations.

Results: An increasing trend of incidence rate for breast, cervical, corpus uteri and ovarian cancer was observed in Changle, although the rate leveled off for breast and cervical cancer after 2010, although not statistically significant. The mortality rate of breast and ovarian cancer was slightly increased during this period, while we found a decreased mortality of cervical cancer from 2010. The mortality of corpus uteri cancer showed a decreasing and then increasing trend. The incidence of breast, corpus uteri and ovarian cancer in Chinese American immigrants in Los Angeles was significantly higher than indigenous Changle Chinese and lower than Los Angeles whites. However, the incidence of cervical cancer in Chinese American immigrants shifted from significantly exceeding to lower than Changle Chinese.

Conclusion: The incidence and mortality of women's cancers in Changle were generally on the rise, and this study concluded that environmental changes were important factors affecting the occurrence of these cancers. Appropriate preventive measures should be taken to control the occurrence of women's cancers by addressing different influencing factors.

KEYWORDS

women's cancer, incidence, mortality, joinpoint analysis, Chinese immigrant

Introduction

Women's cancers involve cancers of the breast, ovaries, uterus, cervix, vagina, and vulva. Breast cancer is the most common cancer among women world-wide, followed by cervical cancer, while ovarian cancer is the deadliest gynecological malignancy worldwide (1, 2). In high-income countries, incidences of the breast, cervical and ovarian cancers are all on a downward trend, while the incidence of corpus uteri cancer has increased from 1976 to 2012 (3). In China, the medical expenses of the three gynecological cancers increased instead of decreasing, which caused a heavy economic burden (4).

In the past few decades, the etiology of women's cancers has been researched extensively. For example, a large number of epidemiological studies have manifested that socioeconomic status has a considerable impact on the occurrence and development of these cancers (5, 6). A subtle difference in certain genes can explain a part of the observed disparities in breast and gynecological cancers between various populations in numerous genetic studies (7, 8). The true etiology of women's cancers is difficult to understand, given that it has become increasingly clear that cancer development cannot be viewed as purely genetic or purely environmental.

Studies of migrants are classic tools for exploring the significance of environmental, social, and genetic traits in disease etiology and have been particularly important for disentangling the etiology of cancer (9). Earlier studies, which initially focused on individuals in one region, found that the incidence of women's cancers varies significantly between different ethnic groups (10–12). Studies of migrants from China, Japan and the Philippines to the USA have shown that increased rates of breast cancer are first observed after 10 years of residence in the USA, whilst the maximum increase is not seen until the offspring of migrants have been resident for a generation or two (13). However, evidence for gynecological cancers in Chinese immigrants is scarce.

Chinese immigrants are the largest Asian ethnic group in the USA, accounting for about 36.2% of immigrants in California, and they are among the groups with the oldest immigration history (14). Meanwhile, Changle is a district in southeast China with a long history of immigration, and most of the immigrants went to the USA. In 2003, there were 170,000 immigrants from Changle in the USA together with their families, which is one fifth of the original population (15). Therefore, Chinese women in Changle could be considered an appropriate reference for migrant study of women's cancers. At present, breast cancer is one of the leading diseases that threatens the health of women, and cervical and ovarian cancers also ranked among top ten causes of cancer death in women in Changle (16).

However, previous study showing the rising trend of women's cancer in Changle was updated until 2002 (17), and it is still unknown about the temporal trend of women's cancer risk in recent years, when China has experienced rapid economic growth. Moreover, the few studies on the differences in risk of women's cancer between Chinese and other ethnicity mainly focused on breast cancer (18, 19), while the only migrant study comparing breast cancer risk among indigenous Chinese, Chinese Americans and White Americans was conducted during 1968-1981 (20). Considering the changing social and environmental factors in China after the reform and opening up, it is necessary to investigate the temporal risk pattern of women's cancer in indigenous Chinese in the recent 30 years, and compare it with other populations.

In the current study, we compared the incidence rates and standardized incidence ratios of breast and gynecologic cancers among indigenous Chinese in Changle, Chinese Americans and Los Angeles whites. The temporal trends in women's cancers were investigated in Changle Chinese population. Findings in this study can not only provide the fundamental information for cancer prevention and control, but also explore the etiology by comparing three populations.

Materials and methods

Study data

The data for women's cancer in Changle District were extracted from the Changle Cancer Register in southeast China, from 1988-2015. The Changle Cancer Registry was established in 1986, with the support from Changle Institute for Cancer Research, Fujian Medical University and The University of Hong Kong. All medical facilities that diagnose and treat cancer in the region are required to report all newly diagnosed cancers and deaths resulting from cancer, using a standardized notification card and medical certification of death. The demographic information was registered by calendar year, sex and 5-year age group. The quality of the registration was relatively good (21), and it had reported data to National Central Cancer Registry of China and Cancer Incidence in Five Continents from 1988.

Cancer incidence for Chinese Americans and white Americans who were residents of Los Angeles, the USA were extracted from Cancer Incidence in Five Continent Vol. Plus (CI5plus, http://ci5.iarc.fr/CI5plus) from 1988 to 2012. Since 1972, the Cancer Surveillance Program has routinely collected and analyzed information on all cancer diagnoses made among residents of the county. The original cancer data is categorized by gender, age and cancer sites, which are identified *via* the International Classifications of Diseases, 10th version (ICD-10).

With the available cancer data in Changle, Chinese Americans in Log Angles and Los Angles whites, the study analyzed age-standardized incidence and age-standardized mortality of women's cancer, including breast [C50], cervical uteri [C53], corpus uteri [C54], and ovarian [C56] cancers.

Patient and public involvement

Patients or the public were not involved in the design, or conduct, or reporting, or dissemination plans of our research.

Statistical analysis

The segi's standard world population was used to estimate the age standardized rates of women's cancers per 100,000 person years, for all groups. The annual percentage change (APC) and average annual percent change (AAPC) were used to quantify the trends for age standardized incidence and age standardized mortality. A regression model was calculated by Joinpoint Regression Program 4.3.1.0 which was developed by the Statistical Research and Applications Branch, National Cancer Institute (https://surveillance.cancer.gov/joinpoint/). The model fitted the natural logarithm of the age-standardized incidence and age-standardized mortality. The independent variable is the calendar year. Analysis starts with the minimum number of joinpoints (*i.e.*, 0 joinpoint, representing a straight line) and tests for model fit with a maximum of 2 or 3 joinpoints. R^2 was calculated to choose the best fit model for the joinpoint regression. We also calculated AAPC for each 5-year interval period as a sensitivity analysis.

The standardized incidence ratio (SIR), a ratio of observed to expected number of cases, was used to compare the incidence of women's cancers among the three populations, using Chinese Americans as the reference population. The expected number of cases was calculated by multiplying the number of population in age (5-year categories) and calendar-specific strata of the Changle Chinese and Los Angles white women by the incidence rate of each outcome in the corresponding strata of Chinese Americans. The ninety-five percent confidence interval (CI) of the SIR was calculated based on the Poisson distribution method described by Vandenbroucke (22), and potential heterogeneity of SIRs by populations was examined using Chi-Square tests. A p value <0.05 was considered statistically significant.

Results

The temporal trend of women's cancer in Changle district

Tables 1, 2 show the crude incidence rate, the crude mortality rate, age standardized incidence rate and age standardized mortality rate by cancer site at the beginning (1988) and end (2015) of the study period, together with results of Joinpoint analysis for age standardized incidence and mortality in women, respectively.

Overall, for people in Changle, the age-standardized incidence of breast, cervical, corpus uteri and ovarian cancers markedly increased during the study period (Figure 1 and Supplementary Table 1), with the most obvious increase observed in cervical cancer (AAPC=10.7, 95%CI=7.5-14.1). For breast cancer, the trend fluctuated, increasing by 5.6% per year from 1988 to 2004, declining by 7.7% per year from 2004 to 2008, rising by 13.7% per year from 2008 to 2011, and stabilizing from 2011 to 2015. The trend of cervical cancer was divided into two segments, clear consecutive increasing by 18.3% from 1988 to 2005, and slowly rising by 1.8% from 2005 to 2015. Whereas, the age standardized

TABLE 1 Crude incidence rates, age standardized incidence and Joinpoint analyses for 1988 through 2015 in Changle.

Site	Year1988-1992		Year 2015		Joinpoint analysis (1988-2015)
	Crude rate (/100 000)	Std. Rate (/100 000)	Crude rate (/100 000)	Std. rate (/100 000)	AAPC(95%CI)
Breast	4.60	5.40	20.21	13.93	3.3*(-4.7,12.0)
Cervix	0.90	1.20	12.78	8.59	10.7**(7.5,14.1)
Corpus uteri	2.10	2.50	5.35	3.57	5.1**(1.8,8.6)
Ovary	0.90	0.80	3.86	3.24	5.1**(3.0,7.2)

AAPC, average annual percent change (%); CI, confidence interval; Std. rate, age standardized rate.
*The average annual percent change is significantly different from 0 (two-side p<0.1).
**The average annual percent change is significantly different from 0 (two-side p < 0.05).

TABLE 2 Crude mortality rates, age standardized mortality and Joinpoint analyses for 1988 through 2015 in Changle.

Site	Year1988-1992		Year 2015		Joinpoint analysis (1988-2015)
	Crude rate (/100 000)	Std. Rate (/100 000)	Crude rate (/100 000)	Std. Rate (/100 000)	AAPC
Breast	2.80	3.40	5.35	3.55	0.6(-0.6,1.9)
Cervix	0.50	0.70	2.68	1.92	5.1(-1.9,12.7)
Corpus uteri	1.90	2.40	3.57	2.34	0.7(-15.7,20.3)
Ovary	0.50	0.40	1.78	1.28	3.7(-4.8,12.9)

AAPC, average annual percent change (%); CI, confidence interval; Std. rate, age standardized rate.

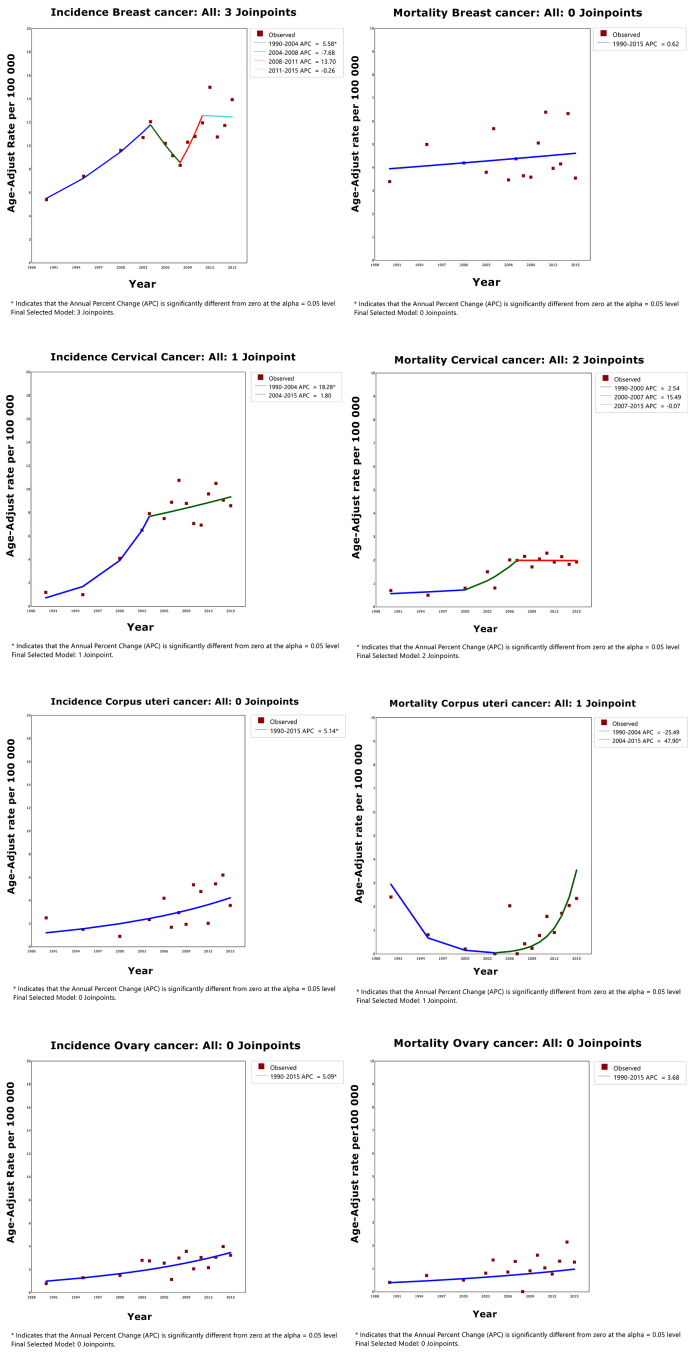

FIGURE 1
Trends in cancer incidence and mortality in Changle.

incidence for cancers of the corpus uteri and ovary continued an upward trend from 1988 to 2015.

From 1988 to 2015, there was no significant change in the standardized mortality rates for women's cancer (Supplementary Table 2). In cervical cancer, the trend is divided into three parts, with age standardized mortality increasing during the study period. On the contrary, the tendency of the age-standardized mortality of corpus uteri cancer showed a U-shaped curve, decreasing by 25.5% per year from 1988 to 2005, and rising by 47.9% per year from 2005 to 2015.

As sensitivity analyses, when the maximum number of joinpoints varied between 2 and 3, majority of the results did not change. However, the number of connections for the standardized incidence rate of breast cancer (maximum of joinpoint=2, R^2 = 0.70; maximum of joinpoint=3, R^2 = 0.92) and the standardized mortality rate of cervical cancer (maximum of joinpoint=2, R^2 = 0.86; maximum of joinpoint=3, R^2 = 0.74) differed a lot. Therefore, to make a better fit for the data, the maximum of joinpoint for the standardized incidence rate was set to 3 and the mortality rate was

set to 2. In addition, AAPCs of the four cancers for each 5-year interval period were also presented in Supplementary Table 3.

The disparities in women's cancer among different populations

During the study period (1988-1992 and 2008-2012), the age standardized incidence of breast, corpus uteri and ovarian cancers were highest in Los Angeles White, intermediate in Chinese Americans and lowest in indigenous Changle Chinese populations, regardless of years (Figures 2, 3). For example, Los Angeles whites had a significantly 2 times higher risk of breast cancer from 1988 to 1992 when compared with the Chinese American population (SIR=2.361, 95% CI 2.286-2.438), whereas women in Changle had a significantly lower risk of developing breast cancer, (SIR =0.144, 95% CI 0.078-0.230). In 2008-2012, the effect size was slightly attenuated with a1.5-fold increased risk in Los Angeles whites (SIR=1.524, 95% CI 1.478-1.572), and an 80% reduced risk in Changle (SIR=0.207, 95% CI 0.153-0.269). For ovarian cancer, the disparities in age standardized incidence were also statistically significant among the three populations. These results suggested that over the past 20 years, the incidence of breast and ovarian cancer among these three populations has trending closer to each other. For corpus uteri cancer, the incidence rate in Los Angeles whites was also close to that in Chinese Americans, but the gap between the incidence rate in Changle residents and Chinese Americans has slightly widened. However, the difference is not statistically significant.

Los Angeles Whites had a nearly 40% increased risk of cervical cancer, compared to that in Chinese Americans in both time periods (1988-1992: SIR= 1.376, 95% CI 1.250-1.508; 2008-2012: SIR= 1.404, 95% CI 1.256-1.560). In 1988-1992, even more striking discrepancies were detected between Changle residents and their counterparts among Chinese Americans in Los Angeles (SIR= 0.143, 95% CI 0.023-0.366). However, in 2008-2012, the age-standardized incidence of Changle residents had obviously risen for cervical cancer, with a risk increase of 1.6-fold (SIR= 1.603, 95% CI 0.130-2.160), compared to the Chinese American population.

Discussion

Key results

Generally speaking, age standardized incidence and mortality for women's cancer in Changle have been rising for the majority of cancers. The few exceptions showed an increase after decrease in mortality of corpus uteri cancer. For breast, corpus uteri and ovarian cancers, we found a higher incidence in Los Angeles Whites than in Chinese Americans, and lower incidence in Changle residents than in Chinese Americans. We also observed a changing difference between cervical cancer incidence in Chinese Americans and the Changle Chinese. Overall the incidence of women's cancers among Chinese-Americans is closer to that of Los Angeles whites. This suggests that changes in lifestyle and living environment are associated with increased incidence of breast, cervical,corpus uteri and ovarian cancers.

In general, for women's cancers, the risk in migrants from China has reached a medium level between the country of origin and the country of new residence. Similar patterns of change have been reported in studies previously limited to other Asian-American immigrants, such as immigrants from Japan (23), South Korea (24) and the Philippines (25). In our study, we also showed that Los Angeles white residents had a significantly higher risk of women's cancer than Chinese Americans and Changle Chinese. This result is supported by other studies showing that cancers of the breast, corpus uteri, and ovary are more common in high-income countries than in middle- or low-income countries (26–28).While these disparities have persisted over period, the gap between the three groups has narrowed to varying degrees, suggesting a changing of associated social and environmental factors.

In the current study, we found an increased incidence and mortality of breast and ovarian cancer in Changle, which was

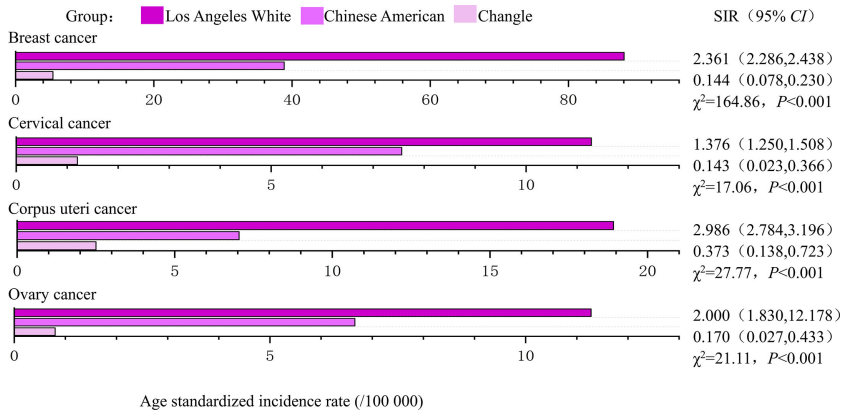

FIGURE 2
The age-standardized incidences and disparities in women's cancer in 1988-1992. SIR, standardized incidence rate.

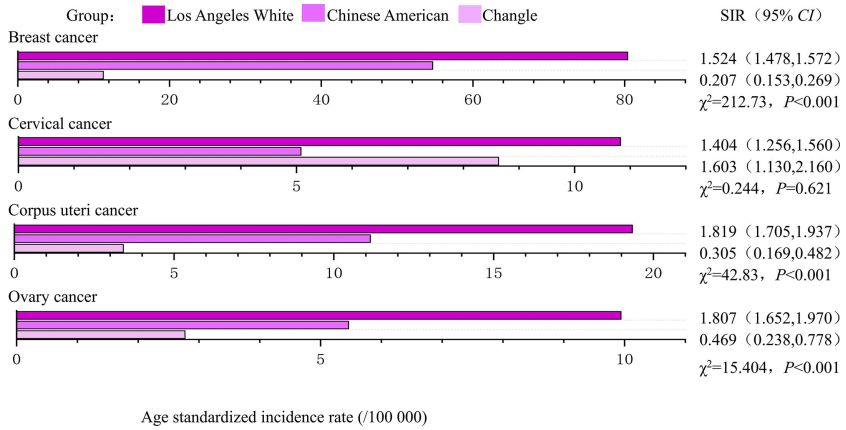

FIGURE 3
The age-standardized incidences and disparities in women's cancer in 2008-2012. SIR, standardized incidence rate.

similar to the trend in other rural areas of China (29, 30). In addition, the incidence of breast and ovarian cancer increased after Chinese women migrated to the USA and was closer to that of white Los Angeles. Although breast and ovarian cancer have a heritability of 30-40% and BRCA1/2 mutations are well known for both cancers (31), these results in our study suggested more pronounced effect from social and environmental risk factors for breast and ovarian cancers, while genetic factors may have a smaller contribution to breast and ovarian cancer in Chinese women (32).

The incidence of corpus uteri cancer increased each year during the study period. Notably, its mortality rate showed a decreasing trend from 1988-2005, and an increasing trend from 2005-2015, but not statistically significant. Improvements in treatment techniques and increased incidence might contribute to this trend in mortality. Considering the increasing incidence of corpus uteri cancer in Changle and Chinese Americans approaching to the incidence of Los Angeles whites, it is reasonable to believe that patterns of corpus uteri cancer may change as the environment changes.

For cervical cancer, the incidence and mortality rates increased by an average of 10.7% and 5.1% per year, respectively. The magnitude of its change is greater than the average level in China (33). This may be explained by increased HPV exposure, inadequately compensated for by the benefit from cytological screening (12). Notably, the incidence rate of cervical cancer among Changle residents was significantly lower than that of Chinese Americans from 1988 to 1992, but gradually exceeded that of Chinese Americans from 2008 to 2012. This changing trend might not only reflect the prevention and control efforts for cervical cancer, but also suggest the present and future public health concern in terms of this cancer in Changle district. A review of the relevant literature revealed that routine cervical cancer screening by cervical cytology was introduced in the United States in 1950 (34) and California launched a universal free cervical cancer screening program and treatment for precancerous lesions in 2002 (35). As of 2010, the rates of cervical cancer screening completed in the past three years among whites in the United States and American Chinese were 83.4% and 71.6% respectively (36). HPV vaccination has been a priority for cervical cancer prevention in the United States since 2008 (37). However, The free cervical cancer screening program in Changle district only started in 2012 and has limited coverage of the population (38). The screening rate of cervical cancer in China was only 26.7% in 2013 (39). Therefore, the cervical cancer screening process might play a role in the cancer incidence trend.

Some limitations of our study should be mentioned here. First, improvements in medical treatment and cancer registration system, and the increase in cancer diagnosis rate and reporting rate might have affected the long-term trend analysis. Second, we don't have individual level information on the study participants, which means it is impossible to accurately link shifts in cancer patterns to specific environmental changes. Third, there is no information on the generational (e.g., first, second, or third generation) or immigration status of Chinese in Los Angeles, which may pose a comparability problem to some extent. Fourth, time of migration was not available in the dataset and we did not take into account the "healthy migration effect", in which new immigrant populations are healthier than native populations in their countries of origin and places of migration, which may introduce bias when comparing cancer incidence rates between immigrant populations and their native populations and populations in places of migration. However, the observed higher risk of cancer in those women who migrated compared to the native population argued against the potential healthy migration effect between them. Considering these limitations, our results should be interpreted with caution.

Conclusions

In summary, in the current study, we analyzed the trend of women's cancer incidence in the Changle district, and compared the incidences of these cancers among Chinese Americans, Los Angeles whites and Chinese populations in the Changle district. These results suggest that the risk of women's cancers in Changle is increasing year by year and environmental factors might have an indelible impact on these cancers, thereby providing new insights into cancer genesis and prevention.

Data availability statement

The raw data supporting the conclusions of this article will be made available by the authors, without undue reservation.

Ethics statement

The study was based on publicly available data of population sizes and aggregated number of cancer cases. Therefore, ethics approval or consent to participate was not necessary.

Author contributions

YC and MS had full access to all data, and take responsibility for the integrity of the data and the accuracy of the analysis. Study concept and design: HY and YZhou. Acquisition, analysis, and interpretation of data: YZhag, MS, HY, and YC. Drafting of the manuscript: YC and YZhou. Critical revision of the manuscript for important intellectual content: All authors. Statistical analysis: YC and MS. Funding: HY. All authors contributed to the article and approved the submitted version.

Funding

Haomin Yang is supported by the Natural Science Foundation of Fujian Province (grant no: 2021J01721), Startup Fund for high-level talents of Fujian Medical University (grant no: XRCZX2020007), Startup Fund for scientific research, Fujian Medical University (grant no: 2019QH1002).

Conflict of interest

The authors declare that the research was conducted in the absence of any commercial or financial relationships that could be construed as a potential conflict of interest.

Publisher's note

All claims expressed in this article are solely those of the authors and do not necessarily represent those of their affiliated organizations, or those of the publisher, the editors and the reviewers. Any product that may be evaluated in this article, or claim that may be made by its manufacturer, is not guaranteed or endorsed by the publisher.

Supplementary material

The Supplementary Material for this article can be found online at: https://www.frontiersin.org/articles/10.3389/fonc.2023.1092602/full#supplementary-material

References

1. Siegel RL, Miller KD, Jemal A. Cancer statistics, 2019. *CA: Cancer J Clin* (2019) 69 (1):7–34. doi: 10.3322/caac.21551

2. Sung H, Ferlay J, Siegel RL, Laversanne M, Soerjomataram I, Jemal A, et al. Global cancer statistics 2020: GLOBOCAN estimates of incidence and mortality worldwide for 36 cancers in 185 countries. *CA: Cancer J Clin* (2021) 71(3):209–49. doi: 10.3322/caac.21660

3. Torre LA, Islami F, Siegel RL, Ward EM, Jemal A. Global cancer in women: Burden and TrendsGlobal cancer in women: Burden and trends. *Cancer Epidemiol Biomarkers Prev* (2017) 26(4):444–57. doi: 10.1158/1055-9965.EPI-16-0858

4. Di J, Rutherford S, Chu C. Review of the cervical cancer burden and population-based cervical cancer screening in China. *Asian Pacific J Cancer Prev* (2015) 16 (17):7401–7. doi: 10.7314/APJCP.2015.16.17.7401

5. Alsolami FJ, Azzeh FS, Ghafouri KJ, Ghaith MM, Almaimani RA, Almasmoum HA, et al. Determinants of breast cancer in Saudi women from makkah region: A case-control study (breast cancer risk factors among Saudi women). *BMC Public Health* (2019) 19(1):1–8. doi: 10.1186/s12889-019-7942-3

6. Karadag Arli S, Bakan AB, Aslan G. Distribution of cervical and breast cancer risk factors in women and their screening behaviours. *Eur J Cancer Care* (2019) 28(2): e12960. doi: 10.1111/ecc.12960

7. Yuzhalin AE, Kutikhin AG. ABO and Rh blood groups in relation to ovarian, endometrial and cervical cancer risk among the population of south-East Siberia. *Asian Pacific J Cancer Prev* (2012) 13(10):5091–6. doi: 10.7314/APJCP.2012.13.10.5091

8. Bafligil C, Thompson DJ, Lophatananon A, Ryan NA, Smith MJ, Dennis J, et al. Development and evaluation of polygenic risk scores for prediction of endometrial cancer risk in European women. *Genet Med* (2022) 24(9):1847–56. doi: 10.1016/j.gim.2022.05.014

9. Parkin DM, Khlat M. Studies of cancer in migrants: Rationale and methodology. *Eur J Cancer* (1996) 32(5):761–71. doi: 10.1016/0959-8049(96)00062-7

10. Quirk JT, Natarajan N. Ovarian cancer incidence in the united states, 1992–1999. *Gynecol Oncol* (2005) 97(2):519–23. doi: 10.1016/j.ygyno.2005.02.007

11. Permuth-Wey J, Besharat A, Sellers TA. Epidemiology of ovarian cancer: An update. In: *Advances in diagnosis and management of ovarian cancer*. Boston, MA: Springer (2014). p. 1–21.

12. Arbyn M, Weiderpass E, Bruni L, de Sanjosé S, Saraiya M, Ferlay J, et al. Estimates of incidence and mortality of cervical cancer in 2018: A worldwide analysis. *Lancet Global Health* (2020) 8(2):e191–203. doi: 10.1016/S2214-109X(19)30482-6

13. Key TJ, Verkasalo PK, Banks E. Epidemiology of breast cancer. *Lancet Oncol* (2001) 2(3):133–40. doi: 10.1016/S1470-2045(00)00254-0

14. Jones NA, Chief RS. The Asian population in the united states: Results from the 2010 census. In: *Meeting of the 2010 Asian profile America event*, vol. 2012. Washington, DC (2012).

15. Zhuang G. Motives and conditions of emigration from changle to U.S. @ in last 20 years. *J Overseas Chin History Stud* (2006) 06):1–11.

16. Chen C. *Fujian cancer registry annual report in 2021* (2021). FuZhou: Fujian Science & Technology Publishing House.

17. Mingang Y, Jianshun C, Xiao J. An analysis of temporal trend with cancer incidence from 1988 to 2002 in changle *China*. *Cancer* (2005) 14(1):32–4.

18. Sung H, Rosenberg PS, Chen WQ, Hartman M, Lim WY, Chia KS, et al. Female breast cancer incidence among Asian and Western populations: More similar than expected. *J Natl Cancer Inst* (2015) 107(7):djv107. doi: 10.1093/jnci/djv107

19. Ziegler RG, Hoover RN, Pike MC, Hildesheim A, Nomura AM, West DW, et al. Migration patterns and breast cancer risk in Asian-American women. *JNCI: J Natl Cancer Inst* (1993) 85(22):1819–27. doi: 10.1093/jnci/85.22.1819

20. Yu H, Harris RE, Gao YT, Gao R, Wynder EL. Comparative epidemiology of cancers of the colon, rectum, prostate and breast in shanghai, China versus the united states. *Int J Epidemiol* (1991) 20(1):76–81. doi: 10.1093/ije/20.1.76

21. Feng G. *The evaluation and quality control of the high risk areas for cancer in China*. Beijing, China: BeiJing University (2008).

22. Vandenbroucke JP. A shortcut method for calculating the 95 per cent confidence interval of the standardized mortality ratio. *Am J Epidemiol* (1982) 115(2):303–4. doi: 10.1093/oxfordjournals.aje.a113306

23. Tominaga S. Cancer incidence in Japanese in Japan, Hawaii, and Western united states. *Natl Cancer Inst Monogr* (1985) 69:83–92.

24. Gomez SL, Le GM, Clarke CA, Glaser SL, France A-M, West DW. Cancer incidence patterns in koreans in the US and in kangwha, south Korea. *Cancer Causes Control* (2003) 14(2):167–74. doi: 10.1023/A:1023046121214

25. Kolonel LN. Cancer incidence among filipinos in Hawaii and the Philippines. *Natl Cancer Inst Monogr* (1985) 69:93–8.

26. Bosch F, Munoz N, De Sanjose S, Izarzugaza I, Gili M, Viladiu P, et al. Risk factors for cervical cancer in Colombia and Spain. *Int J Cancer* (1992) 52(5):750–8. doi: 10.1002/ijc.2910520514

27. Porter PL. Global trends in breast cancer incidence and mortality. *Salud Publica Mexico* (2009) 51:s141–6. doi: 10.1590/S0036-36342009000800003

28. Lortet-Tieulent J, Ferlay J, Bray F, Jemal A. International patterns and trends in endometrial cancer incidence, 1978–2013. *JNCI: J Natl Cancer Inst* (2018) 110(4):354–61. doi: 10.1093/jnci/djx214

29. He M-Y, Zhu B-Q, Zhong Y, Wang L, Yang L, Liao X-Z, et al. Analysis of the incidence and mortality trend of breast cancer in Chinese women from 2005 to 2013. *Chin J Dis Control Prev* (2019) 23(1):10–4. doi: 10.16462/j.cnki.zhjbkz.2019.01.003

30. Xu J, Yang Q, Chen L. Analysis on the incidence and mortality trend of ovraian cancer in Chinese women from 2005 to 2015. *Chin J Cancer Prev Treat* (2022) 29 (03):163–7. doi: 10.16073/j.cnki.cjcpt.2022.03.01

31. Mucci LA, Hjelmborg JB, Harris JR, Czene K, Havelick DJ, Scheike T, et al. Familial risk and heritability of cancer among twins in Nordic countries. *JAMA J Am Med Assoc* (2016) 315(1):68–76. doi: 10.1001/jama.2015.17703

32. Suter NM, Ray RM, Hu YW, Lin MG, Porter P, Gao DL, et al. BRCA1 and BRCA2 mutations in women from shanghai China. *Cancer Epidemiol Biomarkers Prev* (2004) 13(2):181–9. doi: 10.1158/1055-9965.EPI-03-0196

33. Jinyao W, Nianping Z, Zhiqiang B, Zhenkun W. Age-Period-Cohort analysis of secular trends of cervical cancer incidence and mortality in China, 1993–2017. *Chin Gen Pract* (2022) 25(13):1564. doi: 10.12114/j.issn.1007-9572.2022.0074

34. Kessler TA. Cervical cancer: Prevention and early detection. *Seminars in oncology nursing*, (2017) 33(2):172–83. doi: 10.1016/j.soncn.2017.02.005

35. Hoste G, Vossaert K, Poppe W. The clinical role of HPV testing in primary and secondary cervical cancer screening. *Obstetr Gynecol Int* (2013) 2013:610373. doi: 10.1155/2013/610373

36. Centers for Disease Control and Prevention (CDC). Cancer screening-united states, 2010. *MMWR Morbidity Mortality Weekly Rep* (2012) 61(3):41–5.

37. Scarinci IC, Garcia FA, Kobetz E, Partridge EE, Brandt HM, Bell MC, et al. Cervical cancer prevention: New tools and old barriers. *Cancer: Interdiscip Int J Am Cancer Soc* (2010) 116(11):2531–42. doi: 10.1002/cncr.25065

38. *Free screening of "two cancers" for rural women in changle kicked off*. Available at: http://women.fjsen.com/2012-10/10/content_9550923.htm.

39. Chen Q. *The study on the evaluation of primary health care from 2008 to 2010 in fujian*. Fuzhou, China: Fujian Medical University (2012).

frontiers | Frontiers in Medicine

TYPE Original Research
PUBLISHED 20 March 2023
DOI 10.3389/fmed.2023.1161835

OPEN ACCESS

EDITED BY
Yujiao Deng,
The Second Affiliated Hospital of Xi'an Jiaotong University, China

REVIEWED BY
Xiaodi Huang,
Peking Union Medical College Hospital (CAMS), China
Shengnan Yu,
First Affiliated Hospital of Chongqing Medical University, China
Yingkun Xu,
Chongqing Medical University, China

*CORRESPONDENCE
Jianwei Zhou
✉ 2195045@zju.edu.cn

SPECIALTY SECTION
This article was submitted to Obstetrics and Gynecology, a section of the journal Frontiers in Medicine

RECEIVED 08 February 2023
ACCEPTED 27 February 2023
PUBLISHED 20 March 2023

CITATION
Li T, Feng R, Chen B and Zhou J (2023) EREG is a risk factor for the prognosis of patients with cervical cancer. *Front. Med.* 10:1161835. doi: 10.3389/fmed.2023.1161835

EREG is a risk factor for the prognosis of patients with cervical cancer

Tianye Li[1], Ruijing Feng[2], Bingxin Chen[3] and Jianwei Zhou[1]*

[1]Department of Gynecology, The Second Affiliated Hospital, School of Medicine, Zhejiang University, Hangzhou, China, [2]Department of Obstetrics and Gynecology, The Central Hospital of Wuhan, Wuhan, China, [3]Department of Gynecologic Oncology, Women's Hospital, Zhejiang University School of Medicine, Hangzhou, Zhejiang, China

Background: Cervical cancer continues to threaten women's health worldwide. Identifying critical oncogenic molecules is important to drug development and prognosis prediction for patients with cervical cancer. Recent studies have demonstrated that epiregulin (EREG) is upregulated in various cancer types, which contributes to cancer progression by triggering the EGFR signaling pathway. However, the role of EREG is still unclear.

Methods: In this study, we first conducted a comprehensive biological analysis to investigate the expression of EREG in cervical cancer. Then, we investigated the correlations between EREG expression level and clinicopathological features. In addition, we validated the effects of EREG expression on the proliferation and apoptosis of cervical cancer cells.

Results: Based on the public database, we found that the expression of EREG was higher in advanced cervical cancer samples. Survival analysis showed that EREG was a risk factor for the prognosis of cervical cancer. *In vitro* experiments demonstrated that EREG knockdown undermined proliferation and promoted apoptosis in cancer cells.

Conclusion: EREG plays a vital role in the progression of cervical cancer, which contributes to hyperactive cell proliferation and decreased cell apoptosis. It might be a valuable target for prognosis prediction and drug development for cervical cancer in the future.

KEYWORDS

EREG, prognosis prediction, biomarker, proliferation, apoptosis, cervical cancer

1. Background

Cervical cancer remains a conundrum for gynecology clinicians and poses a serious threat to women's health worldwide (1). It is estimated that cervical cancer leads to 342,000 deaths, accounting for 7.7% of all deaths from malignancies in women (2). Due to human papillomavirus (HPV) vaccination and the use of cervical cancer screening, the incidence of cervical cancer in developed countries has been decreasing year by year. However, in low-income and developing countries, the incidence and mortality rates of cervical cancer are still high. The number of cervical cancer deaths in these regions accounts for more than 90%

of global cervical cancer deaths (3). Although the overall survival of early stage cervical cancer is satisfactory after standardized treatment, the outcome of patients with locally advanced or metastatic cervical cancer is still poor (4). At the present stage, chemotherapy and radiotherapy cannot meet the unmet clinical needs (5, 6). Meanwhile, the development of novel targeted agents such as tyrosine kinase inhibitors (TKI), poly (ADP-ribose) polymerase inhibitors (PARPi), and immune checkpoint inhibitors has altered the standard treatment paradigm for cancer (7–10). Identifying key genes or signaling pathways in cervical cancer is important for risk stratification and drug development.

Hyperactivated epidermal growth factor receptor (EGFR) signaling has been reported in multiple cancer types, including but not limited to non-small cell lung cancer (NSCLC), breast cancer, bladder cancer, and colorectal cancer (11, 12). In addition, EGFR signaling is a key component driving the initiation and progression of cervical cancer. The coexistence of HPV infection and active EGFR signaling has been reported in multiple studies (13). The E5 protein of HPV could bind to the subunit of the protein pump ATPase, reduce EGFR degradation, and increase EGFR expression, eventually promoting the activation of the EGFR signaling pathway (14, 15). Moreover, the E6 protein of HPV also increases the expression of EGFR (16). Additionally, the alteration in the E6/E7 protein of HPV interferes with cervical cancer cell proliferation by decreasing EGFR stability at the posttranscriptional level (17). It has been identified that EGFR has seven ligands: EGF, EREG, amphiregulin (AREG), heparin-binding EGF-like growth factor (HB-EGF), epigen (EPGN), betacellulin (BTC), and transforming growth factor-α (TGF-α) (18). After binding with ligands, EGFR triggers the phosphorylation of downstream pathways, such as MAPK, PI3K-AKT, JAK-STAT, and PLCγ1-PKC pathways, mainly supporting cancer cell survival and proliferation (19).

As the ligand of EGFR, EREG is commonly upregulated in cancer types, such as non-small cell lung cancer, breast cancer, gastric cancer, head and neck cancer, ovarian cancer, colorectal cancer, brain cancer, and bladder cancer (20). The EREG–EGFR axis participates in tumor progression by regulating several biological functions, including cell survival, proliferation, migration, and angiogenesis (21). In NSCLC, increased EREG is robustly associated with aggressive tumor phenotypes and poor outcomes (22, 23). Similarly, in gastric cancer and colorectal cancer, upregulated EREG also predicts the shorter survival of patients (24, 25). Generally, EREG is an unfavorable factor for the outcomes of patients with tumors. However, there are still rare studies investigating the role of EREG in cervical cancer.

Abbreviations: EREG, epiregulin; HPV, human papillomavirus; TKI, tyrosine kinase inhibitor; PARPi, poly (ADP-ribose) polymerase inhibitor; EGFR, epidermal growth factor receptor; AREG, amphiregulin; HBEGF, heparin-binding EGF-like growth factor; EPGN, epigen; BTC, betacellulin; TGF-α, transforming growth factor-α; TCGA, The Cancer Genome Atlas; GTEx, Genotype Tissue-Expression; GO, The Gene Ontology; KEGG, Kyoto Encyclopedia of Genes and Genomes; DMEM, Dulbecco's Modified Eagle Medium; FBS, fetal bovine serum; CCK8, Counting Kit-8; OD value, the optical density value.

In this study, we calculated the correlations between EREG expression and clinical-pathological characteristics and prognosis of patients with cervical cancer. Moreover, we measured the effects of EREG knockdown on the proliferation and apoptosis of cervical cancer cells. Collectively, we showed that EREG might be a promising prediction biomarker and treatment target for cervical cancer in the future.

2. Materials and methods

2.1. Data available source

All expression profiles and clinicopathological parameters were obtained from The Cancer Genome Atlas (TCGA) and TCGA TARGET GTEx, a combined cohort of TCGA, TARGET, and Genotype Tissue-Expression (GTEx) databases, and downloaded from the UCSC website (https://xenabrowser.net/). The web addresses of online websites and online analysis tools are presented in the context.

2.2. Expression level analysis

The expression level of EREG in 44 different types of cancer was collected. The survival data were extracted from a previous follow-up study (26). Samples with a follow-up duration of <30 days were excluded. Cancer types with <10 cases were omitted. Log2 (x + 0.001) transformation was performed for each expression value. Coxph function of R package survival (version 3.2-7) was used to establish a Cox proportional hazards regression model, and a forest map was conducted. The correlation between expression and clinicopathological parameters was calculated and analyzed using the online tool Kaplan-Meier Plotter (http://kmplot.com/analysis/) and the GraphPad Prism software (version 8.0).

2.3. Functional enrichment analysis and correlation analysis

The RNA-seq data were derived from the TCGA.CESC.SampleMap HiSeqV2 dataset and downloaded from http://xena.ucsc.edu/. Genes with a correlation coefficient R > 0.3 were identified as EREG-related members. The online tool Database for Annotation, Visualization, and Integrated Discovery (DAVID) (https://david.ncifcrf.gov/) was used for enrichment analysis. The Gene Ontology (GO) and the Kyoto Encyclopedia of Genes and Genomes (KEGG) were adopted in enrichment analysis.

2.4. Protein interaction analysis

A protein interaction network analysis was employed to investigate EREG-associated proteins. The online tool STRING was used in protein interaction network analysis (https://cn.string-db.org/).

2.5. RNA methylation analysis

A uniformly normalized Pan-Cancer online dataset TCGA-TARGET-GTEx derived from the UCSC (https://xenabrowser.net/) database was downloaded. Subsequently, we extracted the EREG and 44 marker genes of three types of RNA modifications. The primary solid tumor, primary tumor, primary blood-derived cancer bone marrow, and primary blood-derived cancer peripheral blood samples were collected and analyzed, while normal samples were excluded from the analysis. Then, further log2 (x + 0.001) transformation was performed for the expression matrix. Finally, Pearson correlations for RNA methylation modification marker genes and EREG were calculated.

2.6. Immune-associated analysis

The correlation between EREG expression and immunoregulatory genes was investigated using the SangerBox online platform (http://sangerbox.com/tool.html). Ultimately, the Pearson correlations between EREG and five immune pathway marker genes were calculated. In addition, the TIMER online platform (http://timer.comp-genomics.org/) was adopted to explore the relationship between EREG and immune cells in cervical cancer.

2.7. Cell culture

SiHa (cervical squamous cancer cell line) and Caski (omentum-metastasized cervical cancer cell line) were purchased from the American Type Culture Collection (ATCC, Manassas, VA, USA) and maintained at the Second Affiliated Hospital, School of Medicine, Zhejiang University Laboratory (Hangzhou, China). SiHa cells were cultured with Dulbecco's Modified Eagle Medium (DMEM), and Caski were cultured in RPMI 1640 containing a concentration of 10% fetal bovine serum (FBS). All of the cells were cultured in the incubator with 5% CO_2 at a temperature of 37°C.

2.8. RNA interference

The small interference RNA (siRNA) was structured by Guangzhou RiboBio. The interference RNA sequences were as follows: siEREG#1 (CCACCAACCTTTAAGCAAA), siEREG#2 (GCATCTATCTGGTGGACAT), and siEREG#3 (GGCTCAAGTGTCAATAACA).

2.9. Quantitative analysis with RT-PCR

The sample was disrupted and solubilized using Trizol (Takara Bio.). Then trichloromethane was used to extract the RNA. The aqueous phase containing total RNA was further purified by isopropanol and ethanol. The resulting product was resolved by 0.1% DEPC, and residual DNA was wiped off with a gDNA wiper (a component of HiScript III RT SuperMix). Sample mRNA was reverse-transcribed into cDNA with HiScript III RT SuperMix for qPCR (Vazyme, Nanjing, China). Then, cDNA was quantitatively analyzed by RT-PCR using an iTaqTM Universal SYBR Green Supermix (Bio-Rad, #1725125) and a 7,500 real-time PCR instrument (Applied Biosystems). The primer sequences used are as follows: GAPDH Forward Primer, 5′-TGTGGGCATCAATGGATTTGG-3′; Reverse Primer, 5′-ACACCATGTATTCCGGGTCAAT-3′; EREG Forward Primer, 5′-GTGATTCCATCATGTATCCCAGG-3′; and EREG Reverse Primer, 5′-GCCATTCATGTCAGAGCTACACT-3′.

2.10. Cell counting kit-8 and clone formation assay

The 96-well plate was seeded with 2,500 cervical cancer cells per well. Using the Cell Counting Kit-8, the optical density value (OD value) at 450 nm wavelength, reflecting the vitality of the cells, was discovered after being treated for 48 h (DOJINDO). Utilizing GraphPad Prism 8, data analysis for the cell viability experiments was carried out (San Diego, CA). Data were fitted using the four-parameter logistic equation to derive the log (concentration)-response curves (for IC50 values). In a 12-well plate, 1,000 cells, after transfected with siRNA for 24 h, were put into each well. The clonal cell aggregation was given medication or a new medium after being grown for 48 h. siRNA was transfected into the cell aggregation at 7 days again for guaranteeing the effect of RNA interference. The cultured plate was then collected after 7 days, and the clones were dyed with crystal violet. The stained clonal cell aggregation was processed and analyzed using ImageJ software. Statistical differences were analyzed using Student's *t*-test, and a *P*-value of <0.05 was considered significant.

2.11. Cell apoptosis assay

The cells were collected after being treated for 24 h. The AnnexinV-FITC/PI Apoptosis Detection Kit (BD556547) was subsequently used to dye the cells, and a flow cytometry device (Beckman) was used to measure the cell apoptosis rate. In each sample, three accessory wells were present. The apoptosis rate differences across groups were compared pairwise by an unpaired *t*-test, and a *P*-value of <0.05 was regarded as statistically significant. The flow cytometry data were analyzed using the FlowJo V software.

2.12. Statistical analysis

Data in this study were all statistically processed and analyzed using GraphPad 8.0 software, and all data were presented as "mean ± standard deviation" (x ± SD) with at least three independent repeated experiments. The independent sample *t*-test method was used to compare the control group and experimental group. The chi-square test was used to compare the ratio's statistical

significance. A *P*-value of <0.05 was considered statistically significant. The Pearson correlation analysis was used to analyze the correlation between the two genes.

3. Results

3.1. The clinical significance of EREG in cervical cancer

The standardized datasets and prognostic outcomes (overall survival) were collected. An increased level of EREG was a risk prognostic factor in the following types of cancer: glioma, adrenocortical carcinoma, kidney renal clear cell carcinoma, cervical cancer, pancreatic adenocarcinoma, Pan-kidney cohort, lung adenocarcinoma, bladder urothelial carcinoma, glioblastoma multiforme, acute lymphoblastic leukemia, lung squamous cell carcinoma, and liver hepatocellular carcinoma (Figure 1A; Supplementary Table 1). Using the Kaplan-Meier Plotter curve [Kaplan-Meier Plotter (kmplot.com)], we investigated the relationship between survival data (overall survival and relapse-free survival) and the EREG expression condition of cervical cancer (Figure 1B). The findings revealed that EREG overexpression was associated with a poor prognosis in patients with cervical cancer. Furthermore, we investigated the relationship between the EREG expression condition of patients with cervical cancer and clinical significance, including stage status and T status. The clinical stage analysis showed that EREG expression was increased in Stages 3–4 and T3–4 tumors rather than in the early stage (Figures 2A, B). It also showed that increased EREG expression resulted in worse clinical outcomes in cervical cancer.

3.2. Functional analysis and correlation analysis of EREG in cervical cancer

Enrichment analyses of the KEGG and GO pathways were performed using the DAVID online platform. The findings suggested that EREG may play a role in a number of cancer-related molecular pathways, including those involving the EGFR biological process, the extracellular matrix structure, the interaction between cytokines and their receptors, and the PI3K-AKT, JAK-STAT, MAPK, and NK-B intracellular biological processes (Figures 3, 4A–C). Besides, protein interaction network analysis showed that the EREG could interact with or combine with the RAS family (H-Ras and K-Ras) and the ERBB family (ERBB2, ERBB3, and ERBB4), as well as its receptor EGFR (Figure 4D). In addition, genetic alteration analysis was carried out to investigate the underlying mutation-derived biological process alternatives. The findings revealed that cervical cancer tissue with a higher EREG level had higher mutative frequencies of HECTD4, NBAS, THSD7A, BRCA2, CENPE, VWF, STK11, NBEAL2, STAB1, DMXL1, GOLGA4, GANAB, and KIAA1549. Meanwhile, the cervical cancer tissue with a lower level of EREG just harbored higher mutative frequencies of KNTC1 and RTL1 (Figure 5A). Furthermore, the RNA modification analysis revealed that EREG expression was significantly correlated with the RNA methylation modification reader genes, including m1A reader (YTHDF1, YTHDF2, YTHDF3, and YTHDC1), m5C reader (ALYREF), and m6A reader (YTHDF1, YTHDF2, YTHDF3, YTHDC1, YTHDC2, and HNRNPA2B1) (Figure 5B). The aforementioned results delineate a potential biological process that, through RNA methylation regulation, EREG triggered various signaling factors dysregulation. The aforementioned factors collectively caused adverse prognostic events in cervical cancer.

3.3. Immune-associated analysis of EREG in cervical cancer

Epiregulin was positively correlated with most chemokines, such as CXCL1, CXCL2, CXCL3, CXCL5, CXCL6, CXCL8, and CCL20, in most types of cancer, including cervical cancer. However, it was negatively correlated with some kinds of chemotactic cytokines, such as CXCL14, CCL14, CXCL17, and CX3CL1. The prognostic analysis showed that the overall survival of CXCL1, CXCL2, CXCL3, CLCL6, CXCL8, and CCL20 were all risk factors in cervical cancer, with the hazard ratios of 2.29 ($p = 0.00072$), 2.41 ($p = 0.00016$), 2.41 ($p = 0.00021$), 2.29 ($p = 0.00034$), 1.61 ($p = 0.045$), 2.97 ($p =$ 1.2e-5), and 2.02 ($p = 0.0071$), respectively. In contrast, CXCL14, CCL14, CXCL17, and CX3CL1 were favorable factors, whose hazard ratios were 0.41 ($p = 0.00017$), 0.67 ($p = 0.12$), 0.61 ($p = 0.0397$), and 0.46 ($p = 0.00095$). A lot of studies have illustrated that the expression of chemokines in cervical cancer could result in different tumoral biological effects that strikingly affect the outcomes of patients (27–31). The results of the analysis showed that the expression of EREG was commonly positive relative to the adverse chemokine clusters. Besides, EREG was related to immunostimulator pathway genes rather than immunosuppressor genes (Figure 6A; Supplementary Figure 1). Furthermore, the TIMER analysis showed the relationship between EREG and immune cells. HPV-positive head and neck squamous cancer, which was considered to share the same etiology and pathology as cervical cancer, was also presented to explore the potential immune-associated mechanisms. The TIMER analysis suggested that the expression of EREG seemed negative relative to the infiltration level of most types of immune cells, including B lymphocytes, CD8+ T cells, CD4+ T cells, macrophages, neutrophil cells, and dendritic cells, both in cervical cancer and head and neck squamous cancer (Figures 6B, C). The results indicated that EREG might diminish the immune cell infiltration in the tumor microenvironment. Additionally, head and neck squamous cancer also shared the same immune regulation characteristics with cervical cancer (Figure 6A; Supplementary Figure 1), which indicated that the HPV infection might interact with EREG and together lead to cancer immune regulation dysfunction. The contradiction between the immune regulation gene analysis and immune cell infiltration analysis of EREG in cervical cancer reflected the dual character of immune regulation. However, more investigation into how EREG plays a role in the tumor immune microenvironment is needed, both *in vivo* and *in vitro*.

A

CancerCode	pvalue	Hazard Ratio(95%CI)
TCGA-GBMLGG(N=619)	8.4e-10	1.19(1.13,1.26)
TCGA-ACC(N=77)	2.7e-7	1.24(1.13,1.36)
TCGA-KIRC(N=515)	5.7e-7	1.17(1.10,1.24)
TCGA-CESC(N=273)	9.2e-6	1.18(1.09,1.27)
TCGA-PAAD(N=172)	1.2e-5	1.20(1.11,1.30)
TCGA-KIPAN(N=855)	6.2e-4	1.07(1.03,1.11)
TCGA-LUAD(N=490)	5.4e-3	1.06(1.02,1.10)
TCGA-BLCA(N=398)	8.9e-3	1.06(1.01,1.10)
TCGA-GBM(N=144)	0.01	1.10(1.02,1.19)
TARGET-ALL-R(N=99)	0.01	1.09(1.02,1.17)
TCGA-LUSC(N=468)	0.02	1.06(1.01,1.11)
TCGA-LIHC(N=341)	0.03	1.06(1.01,1.11)
TCGA-STES(N=547)	0.06	1.04(1.00,1.09)
TCGA-LAML(N=209)	0.06	1.05(1.00,1.10)
TCGA-STAD(N=372)	0.07	1.06(1.00,1.12)
TCGA-THYM(N=117)	0.09	1.25(0.96,1.64)
TCGA-UVM(N=74)	0.09	1.33(0.94,1.87)
TCGA-SKCM-P(N=97)	0.10	1.09(0.98,1.21)
TCGA-KICH(N=64)	0.13	1.21(0.94,1.56)
TCGA-HNSC(N=509)	0.14	1.03(0.99,1.08)
TARGET-LAML(N=142)	0.15	1.05(0.98,1.11)
TARGET-ALL(N=86)	0.16	1.10(0.97,1.25)
TCGA-SKCM(N=444)	0.18	1.02(0.99,1.06)
TCGA-CHOL(N=33)	0.20	1.09(0.95,1.26)
TCGA-TGCT(N=128)	0.25	1.28(0.82,2.02)
TCGA-UCEC(N=166)	0.46	1.04(0.94,1.15)
TCGA-DLBC(N=44)	0.46	1.09(0.86,1.38)
TCGA-THCA(N=501)	0.47	1.06(0.91,1.22)
TARGET-WT(N=80)	0.58	1.04(0.91,1.19)
TCGA-UCS(N=55)	0.58	1.03(0.92,1.16)
TCGA-LGG(N=474)	0.65	1.02(0.94,1.10)
TCGA-OV(N=407)	0.71	1.01(0.96,1.07)
TCGA-PRAD(N=492)	0.72	1.04(0.82,1.33)
TCGA-SARC(N=254)	0.77	1.01(0.95,1.08)
TCGA-MESO(N=84)	0.86	1.01(0.93,1.09)
TCGA-ESCA(N=175)	0.87	1.01(0.93,1.09)
TCGA-SKCM-M(N=347)	0.97	1.00(0.96,1.04)
TARGET-NB(N=151)	1.00	1.00(0.93,1.07)
TCGA-COADREAD(N=368)	0.02	0.91(0.85,0.98)
TCGA-COAD(N=278)	0.06	0.92(0.85,1.00)
TCGA-READ(N=90)	0.09	0.84(0.68,1.03)
TCGA-BRCA(N=1044)	0.27	0.97(0.93,1.02)
TCGA-KIRP(N=276)	0.40	0.97(0.89,1.05)
TCGA-PCPG(N=170)	0.92	0.99(0.74,1.31)

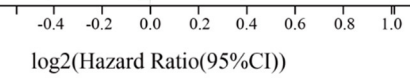

B

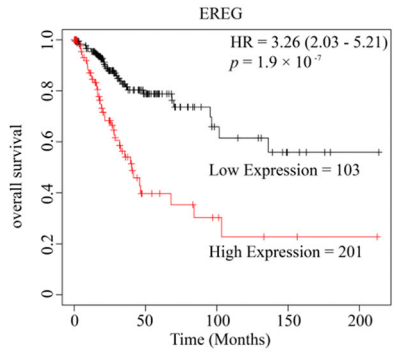

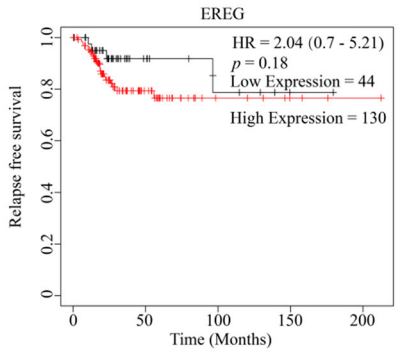

FIGURE 1
Prognosis analysis of EREG in Pan-Cancer and patients with cervical cancer. **(A)** The forest map delineated the relationship between EREG expression and overall survival in 44 types of cancer. The cancer codes and corresponding full terms are listed in Supplementary Table 1. **(B)** The overall survival and relapse-free survival of EREG in patients with cervical squamous cell carcinoma and endocervical adenocarcinoma were presented by Kaplan–Meier Plotter (http://kmplot.com/analysis/).

10.3389/fmed.2023.1161835

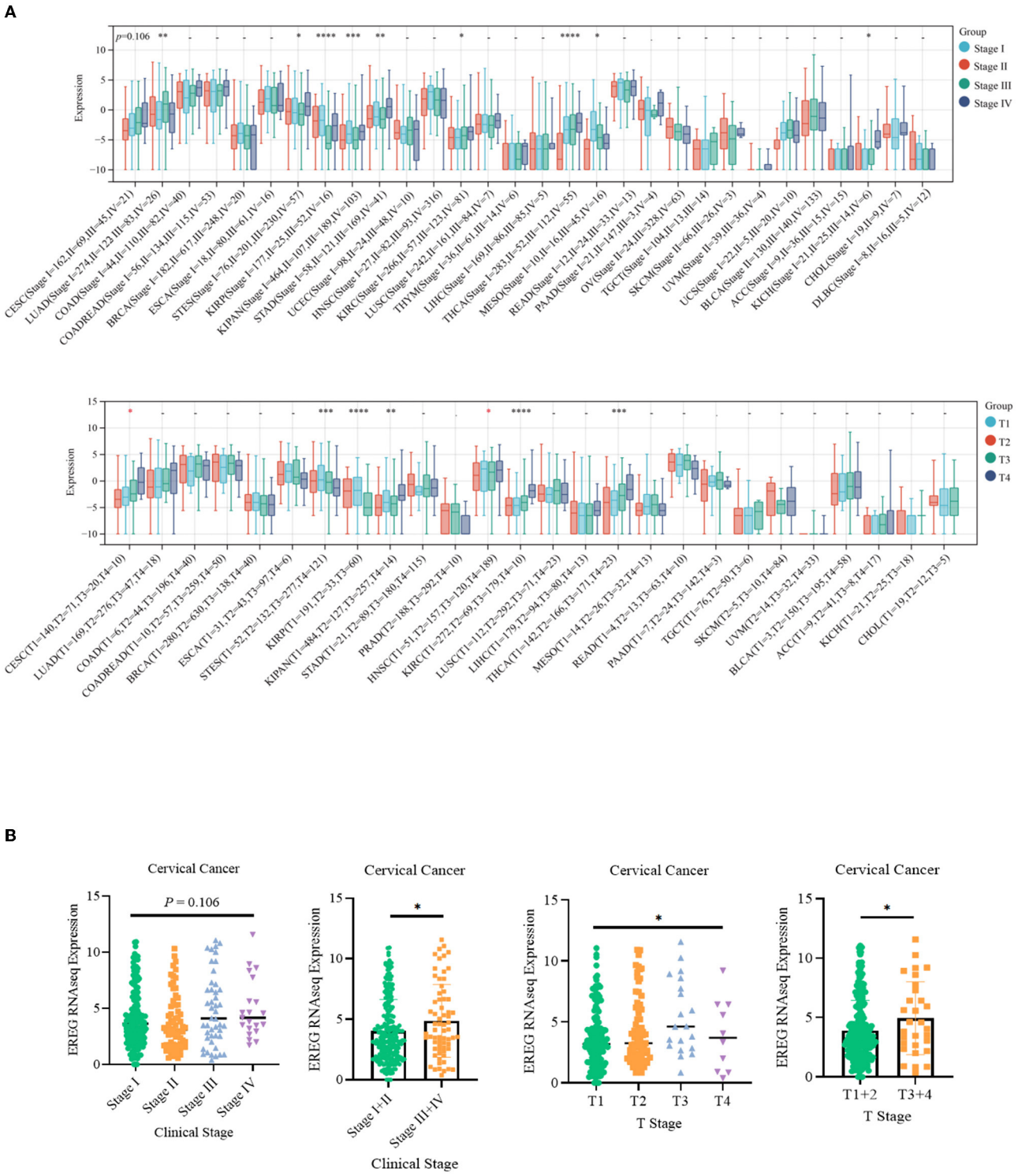

FIGURE 2
Clinical feature analysis of EREG in Pan-Cancer and patients with cervical cancer. **(A)** The relationship between EREG expression and clinical features (clinical stage and T stage) in Pan-Cancer. **(B)** The relationship between EREG expression and clinical features in cervical cancer. "*" represented $p < 0.05$, indicated statistically significant.

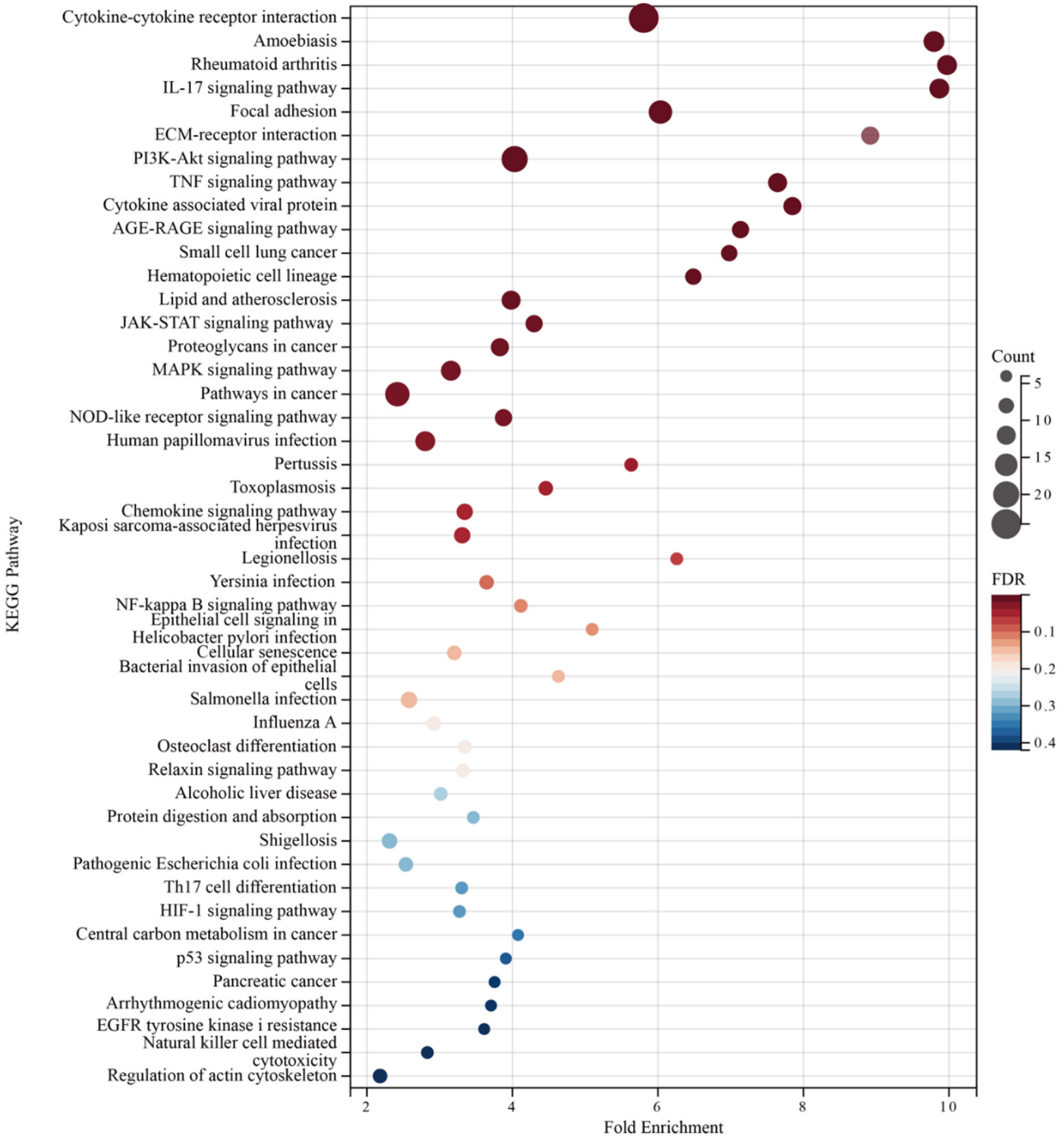

FIGURE 3
KEGG pathway enrichment analysis of EREG-correlated genes. The bubble diagram shows the enriched KEGG pathway terms for the genes correlated with EREG in the TCGA CESC dataset. The size of the bubble represents the number of associated genes included in the term. The shade of the color represents the FDR (false discovery rates).

3.4. Knockdown of EREG undermined the proliferation of cervical cancer

siRNA was used to downregulate the expression of EREG in SiHa and CaSki, and the most effective siEREG#1 was selected for further experiments (Figure 7A). EGFR, which is robustly associated with EREG, is a crucial biological factor in cell proliferation. Therefore, it is apparent to detect the proliferation of cervical cancer with different EREG expression statuses. The proliferation assay using CCK8 showed that the knockdown of EREG could impede cervical cancer cell proliferation (Figure 7B). Additionally, the clone formation assay confirmed the phenomenon (Figures 7E, G, H).

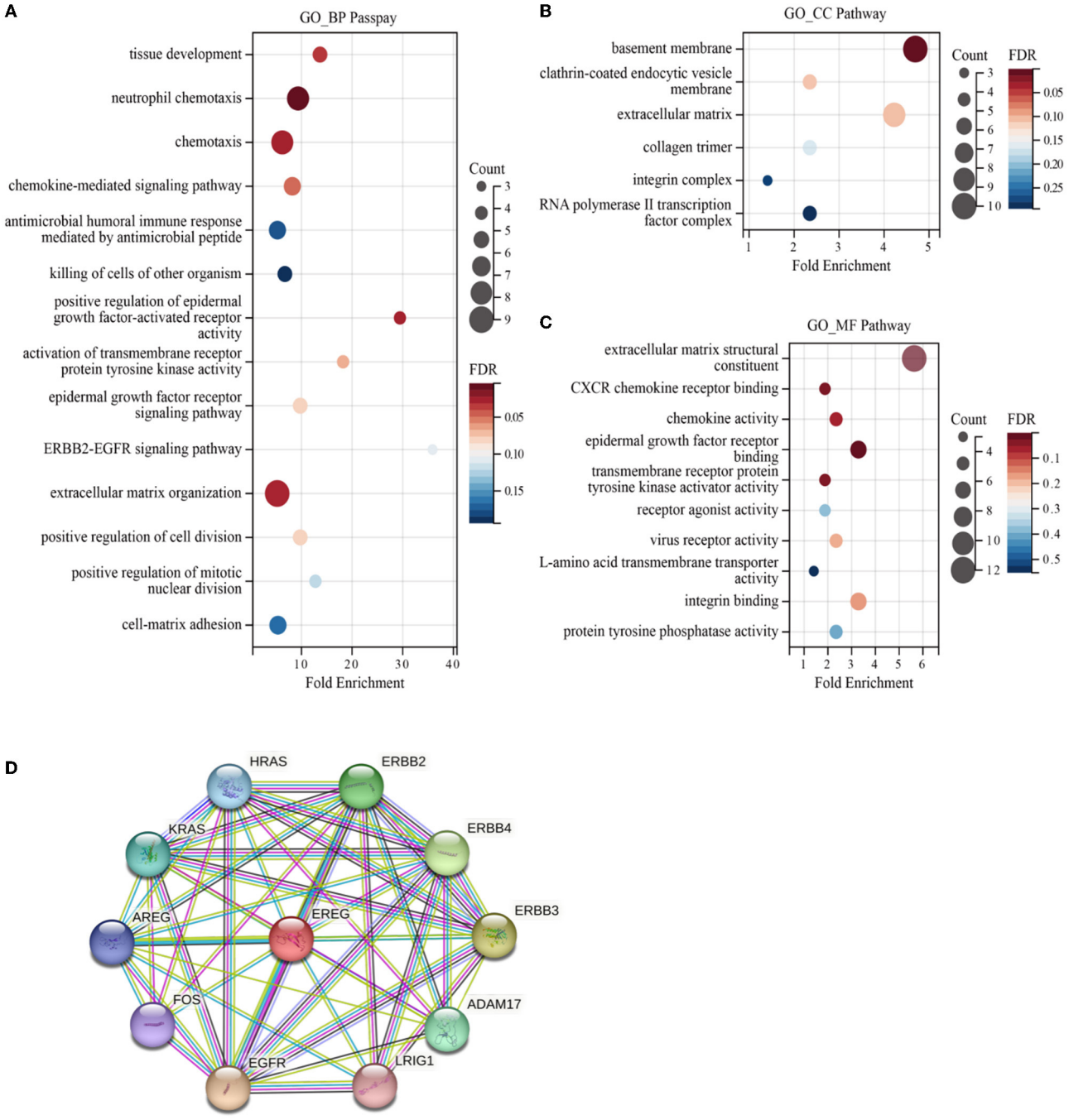

FIGURE 4
GO enrichment of EREG-correlated genes and protein interaction analysis of EREG. The bubble diagrams show the GO_BP (biological process) **(A)**, GO_CC (cellular component) **(B)**, and GO_MF (molecular function) pathway terms **(C)** of the genes correlated with EREG in the TCGA CESC dataset, respectively. The size of the bubble represents the number of associated genes included in the term. The shade of the color represents the FDR (false discovery rates). **(D)** Protein interaction network sketch map in STRING [STRING: functional protein association networks (string-db.org)]. The center of the map was EREG, and the periphery sphere represents the proteins predicted to interact with EREG.

3.5. Knockdown of EREG-induced apoptosis in cervical cancer

Using the pathway enrichment analysis and protein interaction of EREG (Figures 3, 4), multiple signaling factors were identified. Therein, EREG/Ras was a potential protein interaction (Figure 4D). It was reported that the downregulation of the EREG/Ras pathway could induce cell cycle arrest and finally trigger apoptosis in hepatoma cells (32). Therefore, the apoptosis analysis was undertaken to detect the apoptosis rate of cervical cancer cells with different EREG expression levels. The results verified the putative EREG pathway and indicated the cervical cancer cells would trend to apoptosis when the EREG declined (Figures 8A, B, E, F, I, J).

10.3389/fmed.2023.1161835

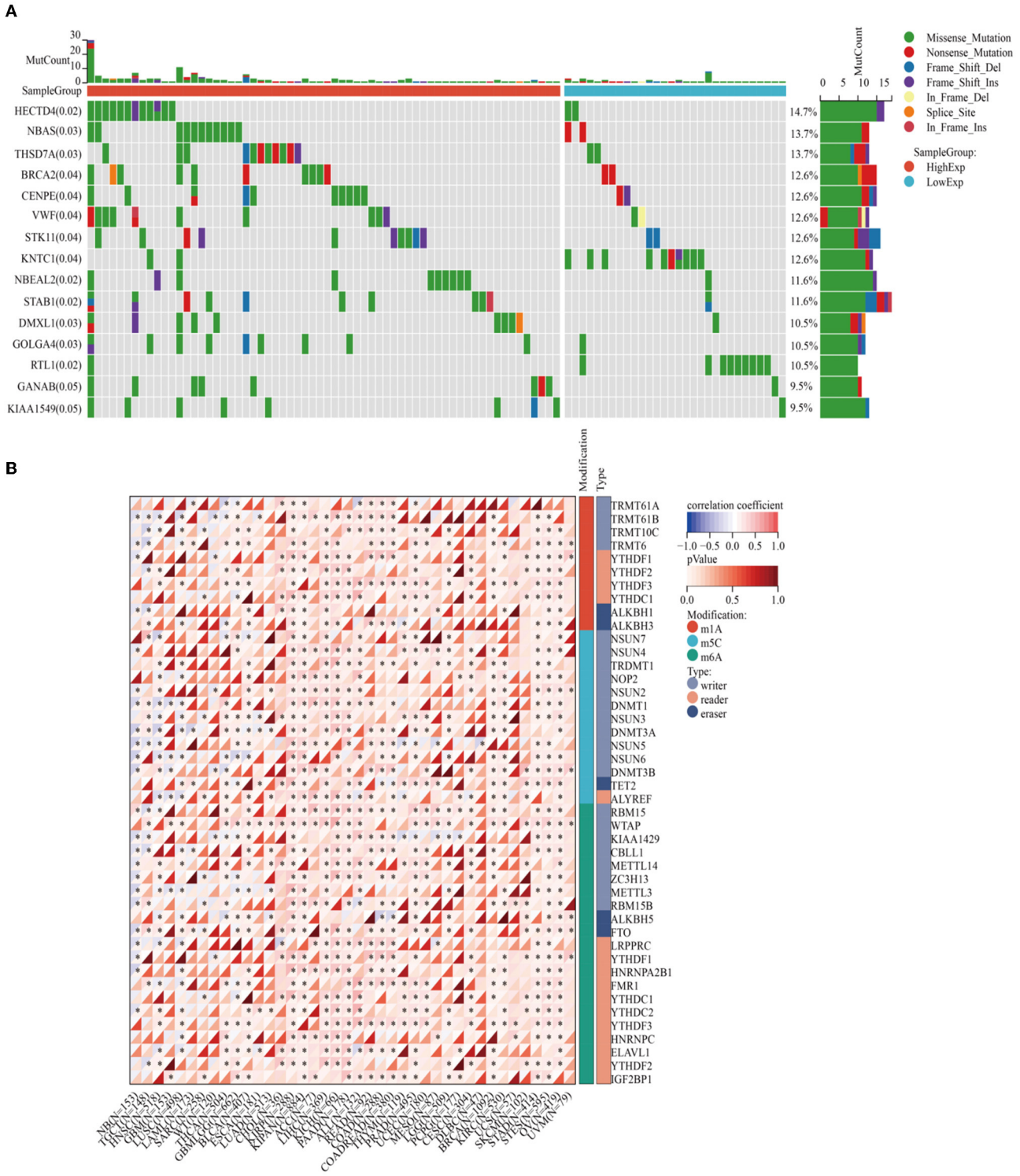

FIGURE 5
Genetic alteration analysis and RNA methylation analysis of EREG in cervical cancer. **(A)** The waterfall plot represents the genetic mutation discrepancies in a different expression of EREG in cervical cancer. The annotations in parentheses behind the gene symbol represent the *p*-value of the mutation discrepancy. **(B)** The map represents the relationship between EREG expression and the distribution of crucial RNA methylation modification genes. "*" represented $p < 0.05$, which indicated statistical significance.

10.3389/fmed.2023.1161835

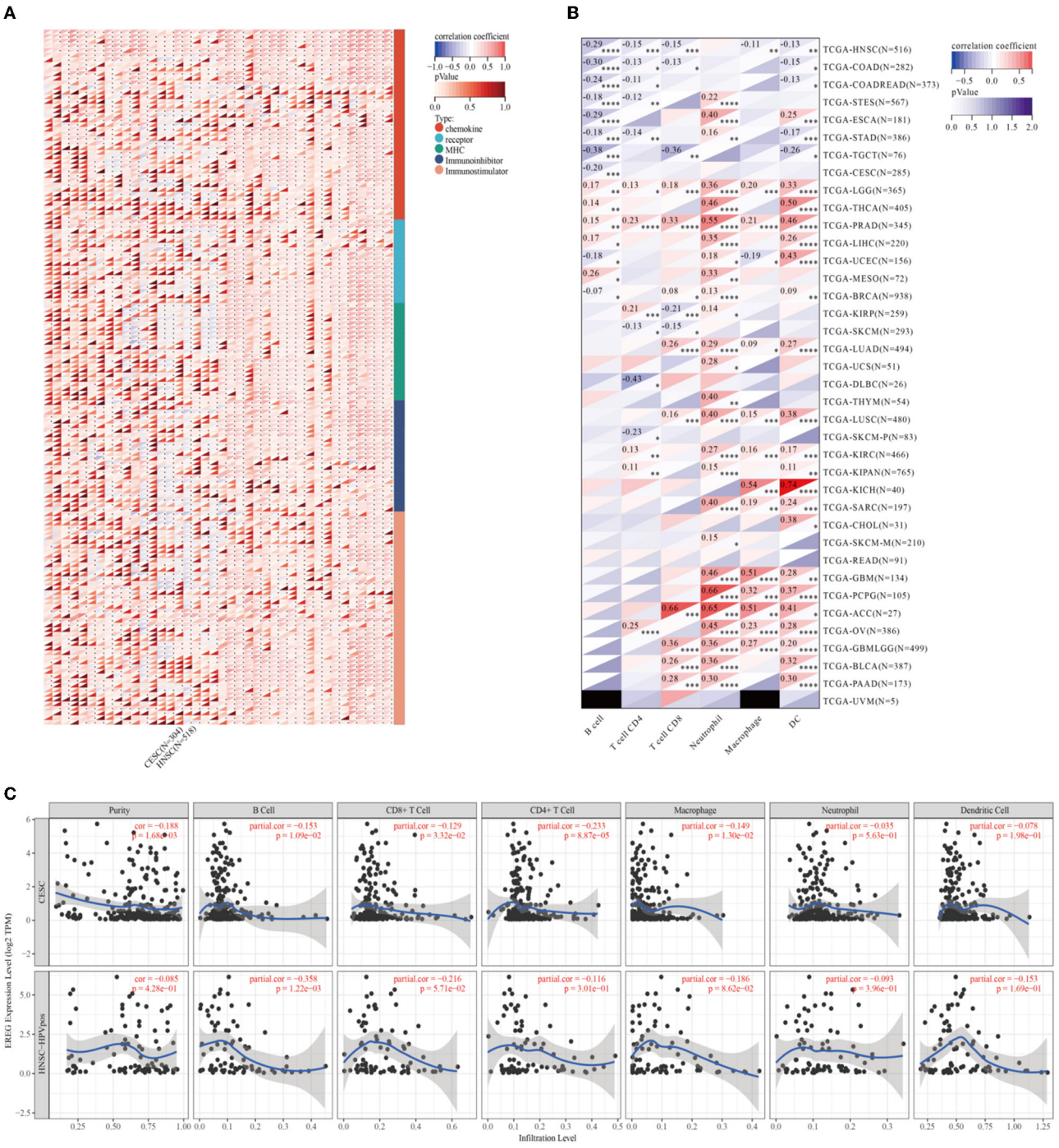

FIGURE 6
Immune-associated analysis of EREG in Pan-Cancer, cervical cancer, and HPV positive head and neck squamous cell cancer. **(A)** The map represents the relationship between EREG expression and the expression of immune regulatory genes. The types of genes were divided into chemokine, receptor, immunoinhibitory, and immunostimulator. **(B)** The correlation between immunocyte infiltration and expression of EREG in Pan-Cancer. **(C)** The correlation between immunocyte infiltration and expression of EREG in cervical cancer and HPV-positive head and neck squamous cell cancer. "*" represents $p < 0.05$, "**" represents $p < 0.01$, "***" represents $p < 0.001$, and "****" represents $p < 0.0001$.

3.6. Knockdown of EREG-sensitized cervical cancer to cisplatin

Since EREG downregulation could trigger cervical cancer apoptosis, it is logical that declining EREG could be a promising therapy for cervical cancer. However, the single gene's interference usually makes no difference because of the compensation of other signaling pathways (33). As is well known, cisplatin is the canonical chemotherapy for cervical cancer. Therefore, to further explore the effect variation of cisplatin on cervical cancer cells

10.3389/fmed.2023.1161835

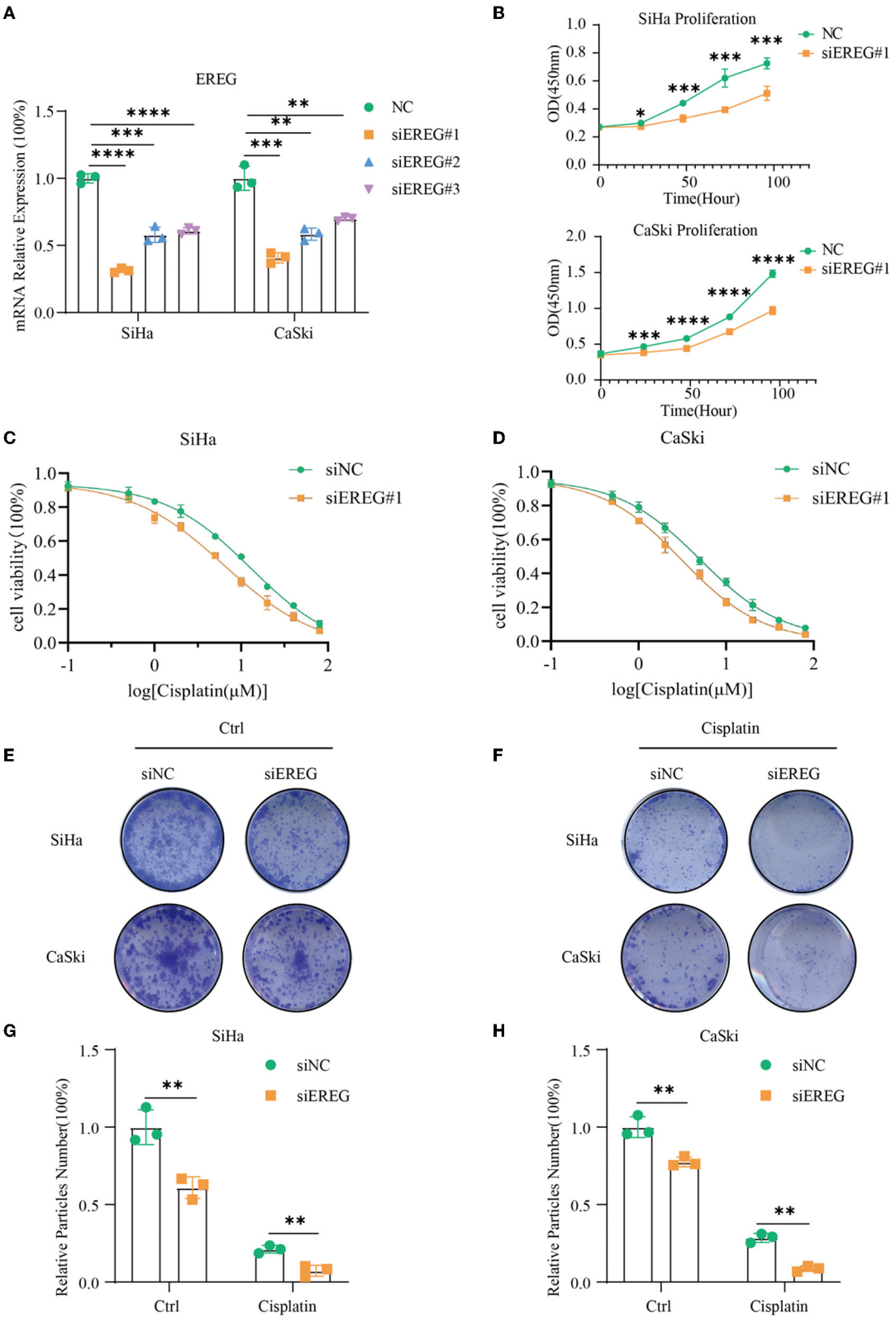

FIGURE 7
The alterations in biological behavior when EREG was knocked down in cervical cancer. **(A)** Real-time PCR was used to detect mRNA levels in SiHa and CaSki cells transfected with siEREG at 48 h. **(B)** The CCK8 cell viability curve was used to detect the proliferation of cervical cancer cells with different EREG expression levels. The CCK8 cell viability curve was used to detect the relative cell viability of SiHa **(C)** and CaSki cells **(D)** transfected with siEREG at different cisplatin concentration gradients after 48 h. **(E)** The clone formation of SiHa and CaSki transfected with siEREG. **(F)** The clone formation of SiHa and CaSki transfected with siEREG was followed by cisplatin treatment for 48 h. Histogram meant the relative clone particle numbers of SiHa **(G)** and CaSki **(H)** with or without cisplatin treatment. "*" represents $p < 0.05$, "**" represents $p < 0.01$, "***" represents $p < 0.001$, and "****" represents $p < 0.0001$.

10.3389/fmed.2023.1161835

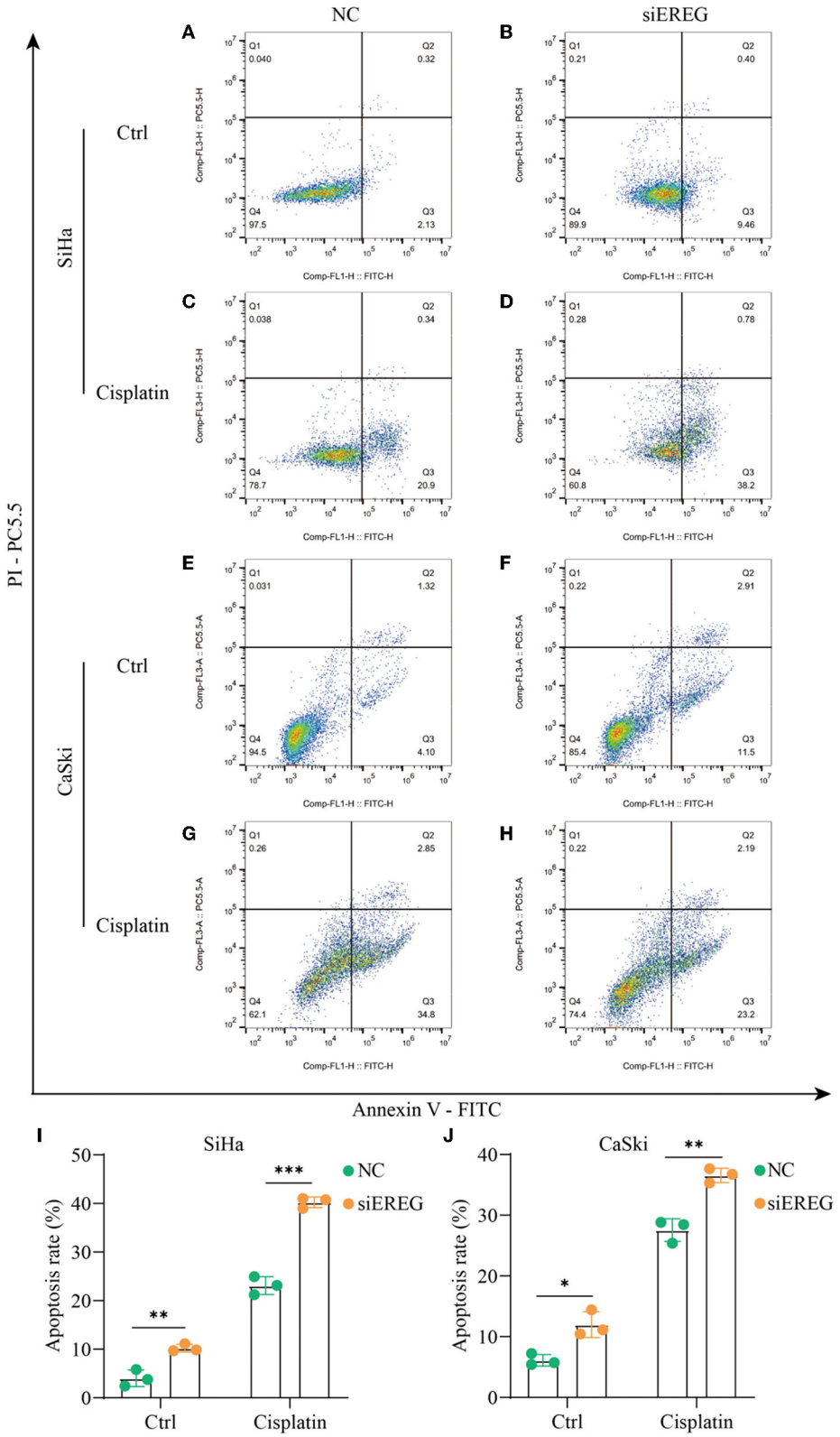

FIGURE 8
The changes in apoptosis when EREG was knocked down in cervical cancer cells with or without cisplatin treatment. Flow cytometry showed the apoptosis rate of SiHa cells after siRNA transfection, followed by treatment with 10 μM cisplatin **(C, D)** or not **(A, B)** for 48 h. Flow cytometry exhibited the apoptosis rate of CaSki cells after siRNA transfection, followed by treatment with 5 μM cisplatin **(G, H)** or not **(E, F)** for 48 h. The histogram showed the apoptosis rate of SiHa **(I)** and CaSki **(J)** with different treatments. "*" represents $p < 0.05$, "**" represents $p < 0.01$, and "***" represents $p < 0.001$.

TABLE 1 The four-parameter logistic equation of GraphPad Prism was used to determine the IC50 of cisplatin for each type of cervical cancer cell, taking into account their divergent EREG expression.

	Cisplatin concentration of IC50 (95% confidence interval) (μM)
SiHa-NC	12.9 (10.57–17.10)
SiHa-siEREG	6.395 (5.255–8.168)
CaSki-NC	5.011 (4.406–5.754)
CaSki-siEREG	3.123 (2.770–3.523)

as the expression of EREG is downregulated, the CCK8 cell viability assay was conducted (Figures 7C, D). Both SiHa and CaSki with downregulated EREG displayed more vulnerability to cisplatin than the negative control ones through IC50 value analysis (Table 1). Meanwhile, the number of clone formation particles in cervical cancer cells with EREG knocked down was robustly less than the negative control ones following the cisplatin treatment (Figures 7F–H). Furthermore, the apoptosis rate of cervical cancer cells with EREG downregulated was significantly higher than the negative control ones in the treatment with cisplatin (Figures 8C, D, G, H–J). The results suggested that the knockdown of EREG could induce the sensibilization of cervical cancer on cisplatin and indicated a promising synergistic therapeutic regimen of cisplatin and EREG inhibitors.

4. Discussion

As a well-established protumorigenic signaling pathway, EGFR is frequently mutated in various types of cancer. EGFR drives tumorigenesis by enhancing pro-survival, antiapoptotic responses, proliferation, migration, invasion, angiogenesis, and vascular mimicry (34–36). Moreover, hyperactivated EGFR signaling leads to the upregulation of stemness markers, including Oct4, Nanog, CD44, and CXCR4. Upon binding with its ligands, such as EREG, the conformation of the tyrosine kinase domain of EGFR is altered, triggering autophosphorylation and intracellular signaling cascades. Besides acting as a cell surface receptor, EGFR could locate in the nucleus and function as a co-transcriptional activator or nuclear kinase (nuclear EGFR, also termed nEGFR). It has been validated that nEGFR promotes the expression of multiple oncogenes, such as *Cyclin D1*, *AurkA*, *c-Myc*, and *BCRP/ABCG2* (19). Additionally, nEGFR contributes to the resistance to chemotherapy, radiotherapy, and EGFR-targeting therapy (37–40). Nowadays, EGFR tyrosine kinase inhibitors, such as gefitinib and erlotinib, have been widely used in the clinic (41).

Epiregulin is the ligand of EGFR, eliciting a variety of biological functions mainly through EGFR-mediated tyrosine kinase activity. In the tumor microenvironment, autocrine and paracrine EREG activates the downstream pathways of EGFR to promote tumorigenesis (20). In a COX2-overexpressed bladder cancer model, EREG is identified as the most highly expressed EGF, supporting tumor cell proliferation (42). EREG promotes motility capability by activating MAPK and PI3K-AKT pathways in salivary adenoid cystic carcinoma cells (43). In head and neck squamous cell carcinoma, EREG enhances malignant transformation by activating the MAPK pathway and inducing C-Myc expression (44). Notably, fibroblast-derived EREG could support the growth of the colitis-associated neoplasm by activating the MAPK pathway in intestinal epithelial cells (45). In parallel, EREG/RAS dual knockdown leads to cycle arrest and retards liver cancer growth by regulating MAPK, PI3K-AKT, and Rb pathways (32). Although EREG expression has no significant relationship to clinicopathological features in gastric cancer, a high EREG level is an independent predictor of poor clinical outcomes for patients receiving curative surgery (46). However, there are rare studies estimating the role of EREG in cervical cancer.

In the present study, we found that high EREG expression was associated with the poor survival of patients with cervical cancer. In addition, EREG expression was increased in Stages T3–4 and 3–4 tumors. Enrichment analysis demonstrated that EREG was highly associated with cytokine–cytokine receptor interaction, PI3K-AKT signaling, TNF signaling, JAK-STAT signaling, MAPK signaling, and NK-κB signaling. Notably, EREG was also related to HPV infection. As mentioned earlier, HPV infection could trigger the EGFR pathway by upregulating EGFR expression. EREG, as well, plays an important role in tumoral immune regulation. It was found to be increased in myeloid cells across the progression of cancer (47). In this study, EREG was also found to take part in the negative immune regulation, mainly *via* chemokine processes and probably impeding immune cell infiltration, through which EREG eventually resulted in the adverse clinical event. Besides, *in vitro* experiments indicated that EREG knockdown limited cell proliferation and promoted cell apoptosis. Moreover, EREG knockdown relieved the resistance to cisplatin in cervical cancer cells. In conclusion, our data showed that EREG functioned as a driving factor in cervical cancer progression and contributed to chemotherapy resistance. However, the mechanistic investigation of how EREG contributed to the phenotype was limited, while EREG was considered to act through nEGFR and downstream pathways. A further mechanistic investigation was needed. In conclusion, it is logical that targeting EREG could be a potential strategy for cervical cancer treatment.

5. Conclusion

Collectively, high EREG expression predicts poor prognostic outcomes for patients with cervical cancer. EREG knockdown impairs proliferation and promotes apoptosis of cervical cancer cells. EREG would be a promising target for risk classification and drug development for patients with cervical cancer.

Data availability statement

The original contributions presented in the study are included in the article/Supplementary material, further inquiries can be directed to the corresponding author.

Author contributions

The study was conceived and designed by JZ. TL performed the most statistical analysis and experiments and wrote the

manuscript. RF and BC participated in collecting literature and helped in revising the manuscript. All authors read and approved the manuscript.

Funding

This research was supported by the Natural Science Foundation of Zhejiang Province (Grant Number: LY20H160028).

Conflict of interest

The authors declare that the research was conducted in the absence of any commercial or financial relationships that could be construed as a potential conflict of interest.

Publisher's note

All claims expressed in this article are solely those of the authors and do not necessarily represent those of their affiliated organizations, or those of the publisher, the editors and the reviewers. Any product that may be evaluated in this article, or claim that may be made by its manufacturer, is not guaranteed or endorsed by the publisher.

Supplementary material

The Supplementary Material for this article can be found online at: https://www.frontiersin.org/articles/10.3389/fmed.2023.1161835/full#supplementary-material

SUPPLEMENTARY FIGURE 1
The map shows the relationship between EREG and immune regulatory genes. The clearer map presented the relationship between EREG expression and the expression of immune regulatory genes. The types of genes were divided into chemokine, receptor, immunoinhibitory, and immunostimulator. In addition, the official gene symbols of each type were listed right on the map.

SUPPLEMENTARY TABLE 1
Cancer codes and corresponding full terms.

References

1. Yi M, Li T, Niu M, Luo S, Chu Q, Wu K. Epidemiological trends of women's cancers from 1990 to 2019 at the global, regional, and national levels: a population-based study. *Biomark Res.* (2021) 9:55. doi: 10.1186/s40364-021-00310-y

2. Sung H, Ferlay J, Siegel RL, Laversanne M, Soerjomataram I, Jemal A, et al. Global cancer statistics 2020: GLOBOCAN estimates of incidence and mortality worldwide for 36 cancers in 185 countries. *CA Cancer J Clin.* (2021) 71:209–49. doi: 10.3322/caac.21660

3. Fitzmaurice C, Abate D, Abbasi N, Abbastabar H, Abd-Allah F, Abdel-Rahman O, et al. Global, regional, and national cancer incidence, mortality, years of life lost, years lived with disability, and disability-adjusted life-years for 29 cancer groups, 1990 to 2017: a systematic analysis for the global burden of disease study. *JAMA Oncol.* (2019) 5:1749–68. doi: 10.1001/jamaoncol.2019.2996

4. Cohen PA, Jhingran A, Oaknin A, Denny L. Cervical cancer. *Lancet.* (2019) 393:169–82. doi: 10.1016/S0140-6736(18)32470-X

5. Sun Q, Wang L, Zhang C, Hong Z, Han Z. Cervical cancer heterogeneity: a constant battle against viruses and drugs. *Biomark Res.* (2022) 10:85. doi: 10.1186/s40364-022-00428-7

6. Small WJr, Bacon MA, Bajaj A, Chuang LT, Fisher BJ, Harkenrider MM, et al. Cervical cancer: a global health crisis. *Cancer.* (2017) 123:2404–12. doi: 10.1002/cncr.30667

7. Yi M, Dong B, Qin S, Chu Q, Wu K, Luo S. Advances and perspectives of PARP inhibitors. *Exp Hematol Oncol.* (2019) 8:29. doi: 10.1186/s40164-019-0154-9

8. Li A, Yi M, Qin S, Chu Q, Luo S, Wu K. Prospects for combining immune checkpoint blockade with PARP inhibition. *J Hematol Oncol.* (2019) 12:98. doi: 10.1186/s13045-019-0784-8

9. Yi M, Zhang J, Li A, Niu M, Yan Y, Jiao Y, et al. The construction, expression, and enhanced anti-tumor activity of YM101: a bispecific antibody simultaneously targeting TGF-β and PD-L1. *J Hematol Oncol.* (2021) 14:27. doi: 10.1186/s13045-021-01045-x

10. Yi M, Wu Y, Niu M, Zhu S, Zhang J, Yan Y, et al. Anti-TGF-β/PD-L1 bispecific antibody promotes T cell infiltration and exhibits enhanced antitumor activity in triple-negative breast cancer. *J Immunother Cancer.* (2022) 10:e005543. doi: 10.1136/jitc-2022-005543

11. Sigismund S, Avanzato D, Lanzetti L. Emerging functions of the EGFR in cancer. *Mol Oncol.* (2018) 12:3–20. doi: 10.1002/1878-0261.12155

12. Shi K, Wang G, Pei J, Zhang J, Wang J, Ouyang L, et al. Emerging strategies to overcome resistance to third-generation EGFR inhibitors. *J Hematol Oncol.* (2022) 15:94. doi: 10.1186/s13045-022-01311-6

13. Ilahi NE, Bhatti A. Impact of HPV E5 on viral life cycle via EGFR signaling. *Microb Pathog.* (2020) 139:103923. doi: 10.1016/j.micpath.2019.103923

14. Zhang B, Srirangam A, Potter DA, Roman A. HPV16 E5 protein disrupts the c-Cbl-EGFR interaction and EGFR ubiquitination in human foreskin keratinocytes. *Oncogene.* (2005) 24:2585–8. doi: 10.1038/sj.onc.1208453

15. Straight SW, Hinkle PM, Jewers RJ, McCance DJ. The E5 oncoprotein of human papillomavirus type 16 transforms fibroblasts and effects the downregulation of the epidermal growth factor receptor in keratinocytes. *J Virol.* (1993) 67:4521–32. doi: 10.1128/jvi.67.8.4521-4532.1993

16. Morgan EL, Scarth JA, Patterson MR, Wasson CW, Hemingway GC, Barba-Moreno D, et al. E6-mediated activation of JNK drives EGFR signalling to promote proliferation and viral oncoprotein expression in cervical cancer. *Cell Death Differ.* (2021) 28:1669–87. doi: 10.1038/s41418-020-00693-9

17. Hu G, Liu W, Mendelsohn J, Ellis LM, Radinsky R, Andreeff M, et al. Expression of epidermal growth factor receptor and human papillomavirus E6/E7 proteins in cervical carcinoma cells. *J Natl Cancer Inst.* (1997) 89:1271–6. doi: 10.1093/jnci/89.17.1271

18. Harris RC, Chung E, Coffey RJ. EGF receptor ligands. *Exp Cell Res.* (2003) 284:2–13. doi: 10.1016/S0014-4827(02)00105-2

19. Levantini E, Maroni G, Del Re M, Tenen DG, EGFR. signaling pathway as therapeutic target in human cancers. *Semin Cancer Biol.* (2022) 85:253–75. doi: 10.1016/j.semcancer.2022.04.002

20. Cheng WL, Feng PH, Lee KY, Chen KY, Sun WL, Van Hiep N, et al. The role of EREG/EGFR pathway in tumor progression. *Int J Mol Sci.* (2021) 22:12828. doi: 10.3390/ijms222312828

21. Riese DJ2nd, Cullum RL. Epiregulin: roles in normal physiology and cancer. *Semin Cell Dev Biol.* (2014) 28:49–56. doi: 10.1016/j.semcdb.2014.03.005

22. Zhang J, Iwanaga K, Choi KC, Wislez M, Raso MG, Wei W, et al. Intratumoral epiregulin is a marker of advanced disease in non-small cell lung cancer patients and confers invasive properties on EGFR-mutant cells. *Cancer Prev Res.* (2008) 1:201–7. doi: 10.1158/1940-6207.CAPR-08-0014

23. Sunaga N, Kaira K, Imai H, Shimizu K, Nakano T, Shames DS, et al. Oncogenic KRAS-induced epiregulin overexpression contributes to aggressive phenotype and is a promising therapeutic target in non-small-cell lung cancer. *Oncogene.* (2013) 32:4034–42. doi: 10.1038/onc.2012.402

24. Xia Q, Zhou Y, Yong H, Wang X, Zhao W, Ding G, et al. Elevated epiregulin expression predicts poor prognosis in gastric cancer. *Pathol Res Pract.* (2019) 215:873–9. doi: 10.1016/j.prp.2019.01.030

25. Stahler A, Heinemann V, Giessen-Jung C, Crispin A, Schalhorn A, Stintzing S, et al. Influence of mRNA expression of epiregulin and amphiregulin on outcome of patients with metastatic colorectal cancer treated with 5-FU/LV plus irinotecan or irinotecan plus oxaliplatin as first-line treatment (FIRE 1-trial). *Int J Cancer.* (2016) 138:739–46. doi: 10.1002/ijc.29807

26. Liu J, Lichtenberg T, Hoadley KA, Poisson LM, Lazar AJ, Cherniack AD, et al. An integrated TCGA pan-cancer clinical data resource to drive high-quality survival outcome analytics. *Cell.* (2018) 173:400–16. doi: 10.1016/j.cell.2018.02.052

27. Sun J, Yuan J. Chemokine (C-X-C motif) ligand 1/chemokine (C-X-C motif) receptor 2 autocrine loop contributes to cellular proliferation, migration and apoptosis in cervical cancer. *Bioengineered.* (2022) 13:7579–91. doi: 10.1080/21655979.2022.2036896

28. Kadomoto S, Izumi K, Mizokami A. The CCL20-CCR6 axis in cancer progression. *Int J Mol Sci.* (2020) 21:5186. doi: 10.3390/ijms21155186

29. Zhang JJ, Liu W, Xing GZ, Xiang L, Zheng WM, Ma ZL. Role of CC-chemokine ligand 2 in gynecological cancer. *Cancer Cell Int.* (2022) 22:361. doi: 10.1186/s12935-022-02763-z

30. Xu L, Li C, Hua F, Liu X. The CXCL12/CXCR7 signalling axis promotes proliferation and metastasis in cervical cancer. *Med Oncol.* (2021) 38:58. doi: 10.1007/s12032-021-01481-2

31. Kodama J. Hasengaowa, Kusumoto T, Seki N, Matsuo T, Ojima Y, et al. Association of CXCR4 and CCR7 chemokine receptor expression and lymph node metastasis in human cervical cancer. *Ann Oncol.* (2007) 18:70–6. doi: 10.1093/annonc/mdl342

32. Zhao M, He HW, Sun HX, Ren KH, Shao RG. Dual knockdown of N-ras and epiregulin synergistically suppressed the growth of human hepatoma cells. *Biochem Biophys Res Commun.* (2009) 387:239–44. doi: 10.1016/j.bbrc.2009.06.128

33. Uda S, Saito TH, Kudo T, Kokaji T, Tsuchiya T, Kubota H, et al. Robustness and compensation of information transmission of signaling pathways. *Science.* (2013) 341:558–61. doi: 10.1126/science.1234511

34. Weihua Z, Tsan R, Huang WC, Wu Q, Chiu CH, Fidler IJ, et al. Survival of cancer cells is maintained by EGFR independent of its kinase activity. *Cancer Cell.* (2008) 13:385–93. doi: 10.1016/j.ccr.2008.03.015

35. Sato M, Shames DS, Gazdar AF, Minna JD. A translational view of the molecular pathogenesis of lung cancer. *J Thorac Oncol.* (2007) 2:327–43. doi: 10.1097/01.JTO.0000263718.69320.4c

36. Peter Y, Comellas A, Levantini E, Ingenito EP, Shapiro SD. Epidermal growth factor receptor and claudin-2 participate in A549 permeability and remodeling: implications for non-small cell lung cancer tumor colonization. *Mol Carcinog.* (2009) 48:488–97. doi: 10.1002/mc.20485

37. Traynor AM, Weigel TL, Oettel KR, Yang DT, Zhang C, Kim K, et al. Nuclear EGFR protein expression predicts poor survival in early stage non-small cell lung cancer. *Lung Cancer.* (2013) 81:138–41. doi: 10.1016/j.lungcan.2013.03.020

38. Kwak EL, Sordella R, Bell DW, Godin-Heymann N, Okimoto RA, Brannigan BW, et al. Irreversible inhibitors of the EGF receptor may circumvent acquired resistance to gefitinib. *Proc Natl Acad Sci U S A.* (2005) 102:7665–70. doi: 10.1073/pnas.0502860102

39. Nishimura Y, Yoshioka K, Bereczky B, Itoh K. Evidence for efficient phosphorylation of EGFR and rapid endocytosis of phosphorylated EGFR via the early/late endocytic pathway in a gefitinib-sensitive non-small cell lung cancer cell line. *Mol Cancer.* (2008) 7:42. doi: 10.1186/1476-4598-7-42

40. Li C, Iida M, Dunn EF, Ghia AJ, Wheeler DL. Nuclear EGFR contributes to acquired resistance to cetuximab. *Oncogene.* (2009) 28:3801–13. doi: 10.1038/onc.2009.234

41. Li S, Zhu S, Wei H, Zhu P, Jiao Y, Yi M, et al. The prospect of combination therapies with the third-generation EGFR-TKIs to overcome the resistance in NSCLC. *Biomed Pharmacother.* (2022) 156:113959. doi: 10.1016/j.biopha.2022.113959

42. Wang X, Colby JK, Rengel RC, Fischer SM, Clinton SK, Klein RD. Overexpression of cyclooxygenase-2 (COX-2) in the mouse urinary bladder induces the expression of immune- and cell proliferation-related genes. *Mol Carcinog.* (2009) 48:1–13. doi: 10.1002/mc.20449

43. Hu K, Li SL, Gan YH, Wang CY, Yu GY. Epiregulin promotes migration and invasion of salivary adenoid cystic carcinoma cell line SACC-83 through activation of ERK and Akt. *Oral Oncol.* (2009) 45:156–63. doi: 10.1016/j.oraloncology.2008.04.009

44. Liu S, Wang Y, Han Y, Xia W, Zhang L, Xu S, et al. EREG-driven oncogenesis of head and neck squamous cell carcinoma exhibits higher sensitivity to Erlotinib therapy. *Theranostics.* (2020) 10:10589–605. doi: 10.7150/thno.47176

45. Neufert C, Becker C, Türeci Ö, Waldner MJ, Backert I, Floh K, et al. Tumor fibroblast-derived epiregulin promotes growth of colitis-associated neoplasms through ERK. *J Clin Invest.* (2013) 123:1428–43. doi: 10.1172/JCI63748

46. Suematsu H, Hashimoto I, Hiroshima Y, Watanabe H, Kano K, Takahashi K, et al. Clinical significance of EREG gene expression in gastric cancer tissue after curative surgery. *Anticancer Res.* (2022) 42:3873–8. doi: 10.21873/anticanres.15880

47. Zhao X, Li H, Lyu S, Zhai J, Ji Z, Zhang Z, et al. Single-cell transcriptomics reveals heterogeneous progression and EGFR activation in pancreatic adenosquamous carcinoma. *Int J Biol Sci.* (2021) 17:2590–605. doi: 10.7150/ijbs.58886

frontiers | Frontiers in Oncology

TYPE Systematic Review
PUBLISHED 22 March 2023
DOI 10.3389/fonc.2023.1103146

OPEN ACCESS

EDITED BY
Ming Yi,
Zhejiang University, China

REVIEWED BY
Marcus Vetter,
University Hospital of Basel, Switzerland
Nan Wen,
Radboud University Medical Centre, Netherlands
Yin Tao,
The People's Hospital of Jianyang City, China

*CORRESPONDENCE
Ji-Qiao Yang
jqyangscu@163.com

†These authors share first authorship

SPECIALTY SECTION
This article was submitted to Breast Cancer, a section of the journal Frontiers in Oncology

RECEIVED 20 November 2022
ACCEPTED 10 March 2023
PUBLISHED 22 March 2023

CITATION
Jin T, Chen Y, Chen Q-Y, Xiong Y and Yang J-Q (2023) Circulating tumor cells in peripheral blood as a diagnostic biomarker of breast cancer: A meta-analysis. *Front. Oncol.* 13:1103146. doi: 10.3389/fonc.2023.1103146

Circulating tumor cells in peripheral blood as a diagnostic biomarker of breast cancer: A meta-analysis

Tao Jin[1,2†], Yao Chen[3†], Qing-Yan Chen[4], Yang Xiong[5] and Ji-Qiao Yang[3*]

[1]Department of Gastrointestinal Surgery, West China Hospital, Sichuan University, Chengdu, China, [2]Laboratory of Gastric Cancer, State Key Laboratory of Biotherapy/Collaborative Innovation Center of Biotherapy and Cancer Center, West China Hospital, Sichuan University, Chengdu, China, [3]Breast Center, West China Hospital, Sichuan University, Chengdu, China, [4]Medical college, Hebei University of Engineering, Hebei, China, [5]Department of Urology, West China Hospital, Sichuan University, Chengdu, China

Purpose: Studies have reported that breast cancer (BC) patients' circulating tumor cells (CTCs) have varying results for their diagnostic role. Thus, we conducted a meta-analysis to systematically assess the accuracy of CTCs in the diagnosis of BC.

Methods: A meta-analysis was conducted to evaluate the overall accuracy of CTC detection. A pooled analysis of sensitivity (SEN), specificity (SPE), positive likelihood ratio (PLR), negative likelihood ratio (NLR), and diagnostic advantage ratio (DOR) was used to measure diagnostic accuracy. In addition, the area under the summary receiver operating characteristic curve (AUC) was used to discriminate BC from non-BC. An analysis of the threshold effect was calculated using the Spearman correlation coefficient. We calculated the Q and I2 statistics to determine whether the studies were heterogeneous. Sensitivity analysis was performed by removing studies one by one. Publication bias was assessed by Deeks' funnel plot asymmetry test.

Results: Studies from the PubMed, Cochrane Library, Embase, Web of Science, Wanfang, Vip, and CNKI databases were collected for diagnosing BC from January 2000 to April March 2023. Finally, 8 publications were retrieved in total containing 2014 cases involved in the study. Based on a random-effects model, it was found that the pooled SEN was 0.69 (0.55 - 0.80), SPE was 0.93 (0.60 - 0.99), PLR was 9.5 (1.4 - 65.9), NLR was 0.33 (0.23 - 0.48), DOR was 29 (4 - 205) and the AUC of the summary receiver operating characteristic (SROC) curve was 0.81 (0.77 - 0.84). Some heterogeneity was found in the article, but there was no threshold effect to account for it (P = 0.27). Deek's funnel plot asymmetry test indicated that no publication bias was observed in this meta-analysis (P = 0.52).

Conclusion: The results of this meta-analysis confirmed that CTCs were an important component of noninvasive methods of confirming BC with SEN of 0.69 (0.55 - 0.80), SPE of 0.93 (0.60 - 0.99) and AUC of 0.81 (0.77 - 0.84).

KEYWORDS

breast cancer, diagnosis, circulating tumor cells, CTCs, meta - analysis

Background

Among women, BC is the most prevalent cancer and is influenced by lifestyle factors, hormonal factors, reproductive factors, and iatrogenic factors. Furthermore, recent data from 185 countries reported 2.3 million new cases (more than 10% of all cancers) of breast cancer and a mortality rate of 6.9%, and BC ranked the second leading cause of death from cancer among women globally (1, 2). During the past few decades, the morbidity of BC has continued to increase around the world (3). Furthermore, a study showed a significant increase in breast cancer mortality rate in low-income regions, while the decreasing rate mostly belongs to Western Europe, with 37.57 in 1990 to 36.00 in 2015 (4). Due to advances in screening methods and breakthroughs in early diagnosis and treatment, BC survival rates have improved. The conventional diagnostic methodologies of BC include breast biopsy, which is regarded as the gold standard, and imaging methods without high sensitivity to detect BC in the early stage (5). In addition, molecular markers, including CA15-3 and CEA, are common markers for monitoring and follow-up of patients by testing BC patient blood samples, but they have low SEN and SPE (6–8). Thus, it was not suitable for the detection of BC. To improve BC cure rates and reduce BC mortality, early diagnosis remains essential. Thus, it is necessary to explore a new test with high SEN and SPE to diagnose BC in the early stage. Recently, a hot research topic about tumors has been the clinical application of CTCs. CTCs, a subset of tumor cells that circulate within the body due to tumor tissue instability or external physical stimulation, participate in the body's circulation and then integrate into the peripheral blood circulation (9, 10). The Fourth Edition of the National Comprehensive Cancer Network (NCCN) guidelines has added a new M0 (i+) category, which is defined as "no clinical or radiographic evidence of distant metastases, but the presence of detected tumor cells in the circulation fluids" (11). In addition, CTCs have demonstrated efficacy in the screening of malignant cancers such as prostate, lung, and colorectal cancers (9). In a recent study, CTCs were found to be 76.56% sensitive and 95.4% specific for diagnosing breast cancer using the CytoSorter® (12). Nonetheless, several studies have been conducted on CTCs to diagnose BC with varied results by testing peripheral blood. In addition, current studies have shown that CTC detection positive rates (≥ 1 CTC/7.5 ml) range from 11%~54% for early breast cancer, while ≥1 CTC can be detected in approximately 70% of stage IV BC patients. Thus, a meta-analysis was performed to determine whether CTCs are particularly useful as a diagnostic tool in patients with BC.

Methods

This study was conducted according to the Preferred Reporting Items for Systematic Reviews and Meta-analyses (PRISMA) guidelines (13).

Literature search

We conducted a comprehensive computer literature search of abstracts from human studies to identify articles about the effectiveness of CTC tests for diagnosing BC by two independent individuals (Tao Jin and Yao Chen). Electronic databases such as PubMed, Embase, Cochrane Library, Web of Science, Wanfang, CNKI, and Vip were used with the following search terms: "CTCs", "circulating tumor cells", "breast cancer", "breast carcinoma", "accuracy", "sensitivity and specificity", from January 2000 to March 2023, without language limitation. We manually searched references in the included literature to identify studies that met our eligibility criteria, and gray literature was also included in the study.

Literature eligibility

The included studies were screened according to the following criteria: (1) Type of trial: studies applying the method of detecting CTCs to diagnose breast cancer; (2) Diagnostic gold standard: histopathological examination or biopsy results; (3) The literature should include sufficient study data including true positive (TP), false positive (FP), true negative (TN), false negative (FN); (4) patients without other malignant tumors; (5) we chose the article with the most detail or the most recent when more than one article presented the same data or subset of data. Exclusion criteria were (1) insufficient information in the literature to obtain complete diagnostic data from the full text of the literature and (2) reports on cases, reviews, letters, single-arm trials, editorials, and duplicate studies.

Data extraction and quality assessment

Two independent researchers (Tao Jin and Yao Chen) reviewed all studies. Disagreements between researchers were resolved through discussion and consensus. In the case of disputes, an independent third researcher was responsible for resolving disagreements. The main data information included author, year of publication, country, tumor stage, isolation enrichment method, assay identification method, CTC cutoff, TP, FP, FN, and TN. Data for results not directly reported were derived from estimates of SEN and SPE, along with positive and negative predictive values. Primary outcome measures were pooled estimates of SEN and SPE. Evaluation of the quality of the included literature was carefully conducted using the Quality Assessment of Diagnostic Accuracy Studies-2 (QUADAS-2) (14) by two independent reviewers. The inconsistent evaluation was decided by discussion.

Statistical analysis

The diagnostic accuracy of CTC detection in BC was determined using Stata (version 15.0). Pooled analysis of SEN, SPE, PLR, NLR, and DOR and the corresponding 95% confidence interval (CI) was used to evaluate diagnostic accuracy. The SROC was performed using a bivariate regression approach to identify abnormal examinations that resulted in the expected trade-off between SEN and SPE. In addition, the AUC can summarize the inherent capacity of a test for discriminating BC from non-BC. The threshold effect was analyzed using Spearman correlation coefficients in the heterogeneity analysis. The heterogeneity of the studies was evaluated by the Q test and I2

statistics. I^2 values ≥50% indicated substantial heterogeneity; additionally, we considered the difference to be statistically significant at $P < 0.05$. Sensitivity analysis was performed by a one-by-one exclusion method to determine whether the hypothesis had a significant effect on the results. Deeks' funnel plot asymmetry was used to assess publication bias, and a significance level of $P < 0.05$ was considered significant.

Results

Literature search results

A total of 3225 pieces of literature were retrieved through electronic databases. After excluding duplicates and irrelevant studies, we carefully and independently reviewed the titles and abstracts. Finally, eight studies (12, 15–21), including 2014 cases, met the requirements through careful screening by two independent researchers after reading the full text in detail. The flow diagram in Figure 1 illustrates the process of searching for eligible studies.

Basic characteristics and quality assessment

A summary of the basic characteristics of the included studies is provided in Table 1. All patients were diagnosed with stage I to IV disease. Seven studies were from Asia, and one study was from Western countries. Four, three, and one articles set the CTC cutoff as 2, 1, and 1.5, respectively. The enrichment methods of CTCs included negative enrichment, density gradient centrifugation, CytoSorter, immunomagnetic bead, and CellSearch. Most of the articles used imFISH to identify CTCs. Table 2 presents the results of the QUADAS-2 assessment. Patient selection and index tests accounted for the majority of bias risks.

Accuracy of CTCs in the diagnosis of BC

The overall accuracy of CTCs in diagnosing BC was as follows: SEN, 0.69 (0.55 - 0.80); SPE, 0.93 (0.60 - 0.99) (Figure 2); PLR, 9.5 (1.4 - 65.9); NLR, 0.33 (0.23 - 0.48); and DOR, 29 (4 - 205). Figure 3 shows the SROC plot with a 95% CI. The AUC for BC was 0.81

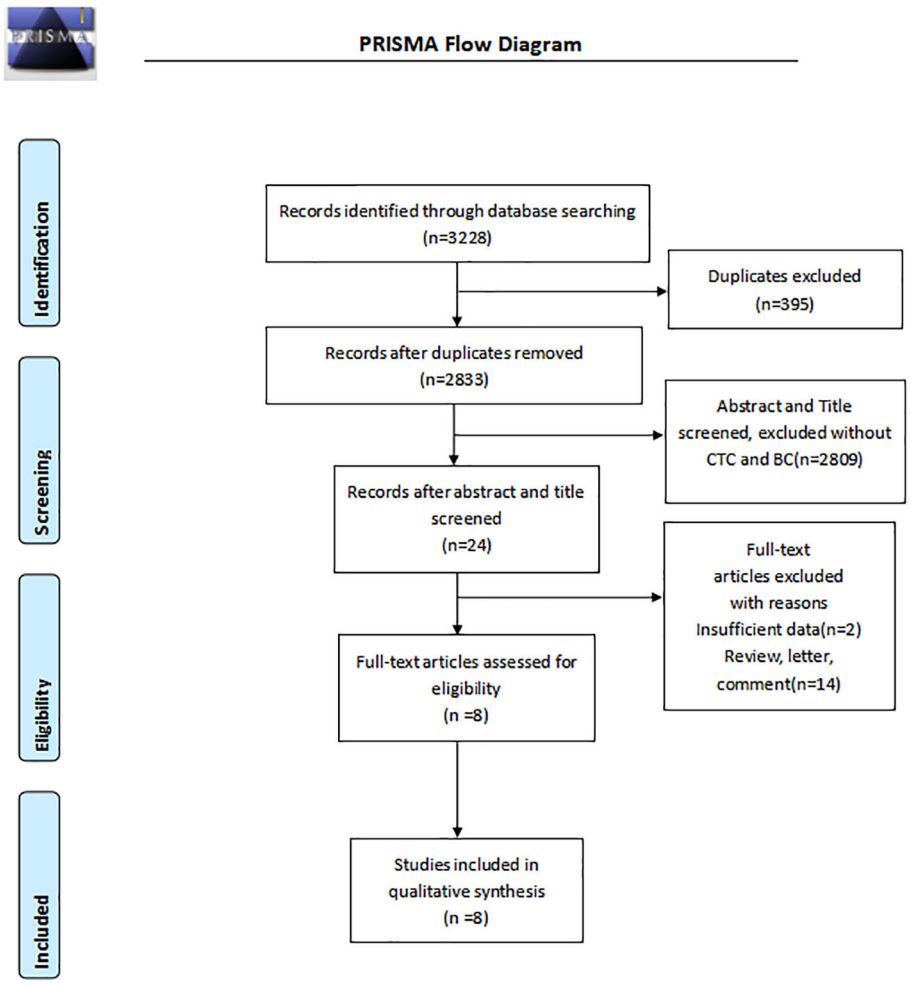

FIGURE 1
A flow chart of the search and selection of relevant studies.

TABLE 1 Main characteristics of studies included in the meta-analysis of the diagnostic accuracy of CTCs detection in BC.

Author	Year	Country	Stage	Enrichment method	Identification method	CTC cut-off	TP	FP	FN	TN
Qiu	2020	China	I-IV	Negative enrichment	ImFISH	2	105	2	34	346
Wang	2020	China	I-IV	Density gradient centrifugation	ImFISH	2	102	59	27	4
Ji	2020	China	I-IV	Density gradient centrifugation	Nucleic acid testing	1.5	23	0	37	50
Wang	2018	China	I-IV	Immunomagnetic bead	ImFISH	1	25	0	20	10
Gao	2021	China	I-IV	CytoSorter	ImFISH	2	199	76	39	161
Jin	2019	China	I-IV	CytoSorter	ImFISH	2	109	38	19	223
Murray	2015	Chile	NA	Density gradient centrifugation	ImFISH	1	58	6	20	60
Xue	2021	China	I-IV	CellSearch	CellSearch	1	16	18	26	102

(0.77 - 0.84). The percentage of heterogeneity caused by the threshold effect was 0.27, while the coefficient of correlation in the mixed model was -0.52, which meant no significant influence of the threshold effect. Figure 4 presents the Fagan plot, showing that the prior-test probability of BC was 50%. Furthermore, the posttest probability of BC, given a negative result, was 25%, while 91% had a positive result for CTC detection in this meta-analysis. Deek's funnel plot asymmetry test demonstrated that the slope coefficient P value was 0.52, suggesting that there was no significant publication bias (Figure 5). Sensitivity analysis (Table 3) showed a slight change when removing articles one by one, indicating that the results were robust.

Discussion

Breast ultrasound and mammography are currently the main methods for screening BC, but with low SEN, they are easily influenced by breast density, and the incidence of false negatives and false positives is high (22). Serological markers such as carbohydrate antigen CA153 and carcinoembryonic antigen (CEA) have the characteristics of noninvasiveness, nonradiation, and low price but still have low SEN and SPE. Thus, they are not suitable for the early diagnosis of BC (23). CTCs are cancer cells that contain unique biomarkers and are commonly found in blood samples from individuals with solid tumors but often not in healthy populations. The prognostic relevance of CTCs in many types of metastatic cancer has already been demonstrated (24–26). According to the eighth AJCC cancer staging manual, BC patients with CTCs are at a greater risk for poor outcomes (27). In recent years, CTC detection has been proven to be helpful in the diagnosis of lung cancer (28), bladder cancer, urothelial cancer (29), pancreatic cancer (30), and so on. Furthermore, CTCs in peripheral blood have been used to diagnose BC in a limited number of studies, with varying results. Consequently, we conducted the first meta-analysis to assess the diagnostic value of CTC detection in the peripheral blood of BC patients.

The results of the study, including 2014 individuals from 8 diagnostic accuracy studies, proved that CTCs had high clinical utility in the diagnosis of breast cancer, with a pooled SEN of 0.69 (0.55-0.80), a pooled SPE of 0.93 (0.60-0.99), a pooled LNR of 9.5 (1.4-65.9), a pooled NLR of 0.33 (0.23-0.48), and a total AUC of the

TABLE 2 The results of quality assessment of included studies in the meta-analysis.

Study	Risk of Bias				Applicability Concerns		
	Patient Selection	Index Test	Reference Standard	Flow and Timing	Patient Selection	Index Test	Reference Standard
Qiu 2020	low	unclear	low	low	low	low	low
Wang 2020	low	unclear	low	low	low	low	low
Ji 2020	high	unclear	low	low	low	low	low
Wang 2018	high	unclear	low	low	high	low	low
Gao 2021	high	high	low	low	high	low	low
Jin 2019	low	high	low	low	high	low	low
Murray 2015	low	unclear	low	low	low	low	low
Xue 2021	low	unclear	low	low	low	low	low

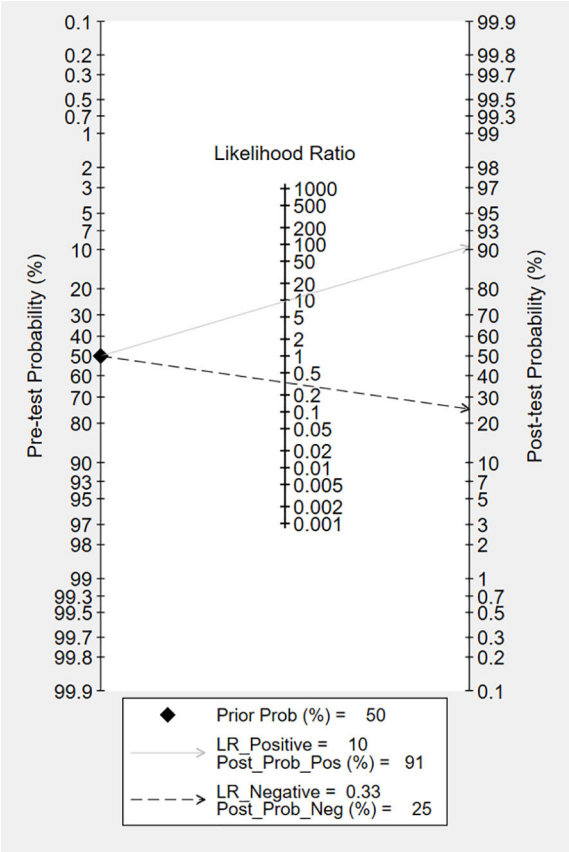

FIGURE 2
Forest plots depicting the SEN and SPE of CTCs in BC diagnosis.

SROC curve of 0.81. These results show that the overall accuracy of CTCS in the early diagnosis of BC is relatively good. After sensitivity analysis, the results of the literature we included were stable, indicating that our meta-analysis results are of reference significance. By using the DOR, a diagnostic test evaluation indicator, we could compare the likelihood of positive results between patients with and without the condition. In the present analysis, the pooled DOR was 29 (95% CI, 4–205), indicating that in comparison to patients who do not test positive for CTCs, those who test positive have 29 times the likelihood of developing BC. Based on the above results, CTCs might be helpful as a diagnostic method for BC screening, which is in accordance with a prior study (12). However, the included studies have different CTC detection methodologies, as well as different sensitivity levels, resulting in a varying CTC cutoff value for the same clinical application (31). To date, CellSearch® has been the only CTC system approved by the Food and Drug Administration (FDA). However, CellSearch® had low rates of CTC detection in BC, approximately 40–50% in metastatic BC and just under 30% in early-stage BC (32). There was only one study (21) using CellSearch® in our meta-analysis. Another study (12) reported the CytoSorter® CTC detection system. CytoSorter® was shown to be superior to CellSearch® in detecting CTCs in BC patients at stages II and III, with a detection rate of over 90% (32). Due to the lack of uniform detection standards for CTCs, clinical practice does not consider CTCs to be a standard routine diagnostic tool. Thus, more research is required to determine the criteria for CTC detection. Based on the use of different threshold values in the included studies, we used Spearman's correlation coefficient to analyze threshold effects and found that there was no connection between thresholds and heterogeneity.

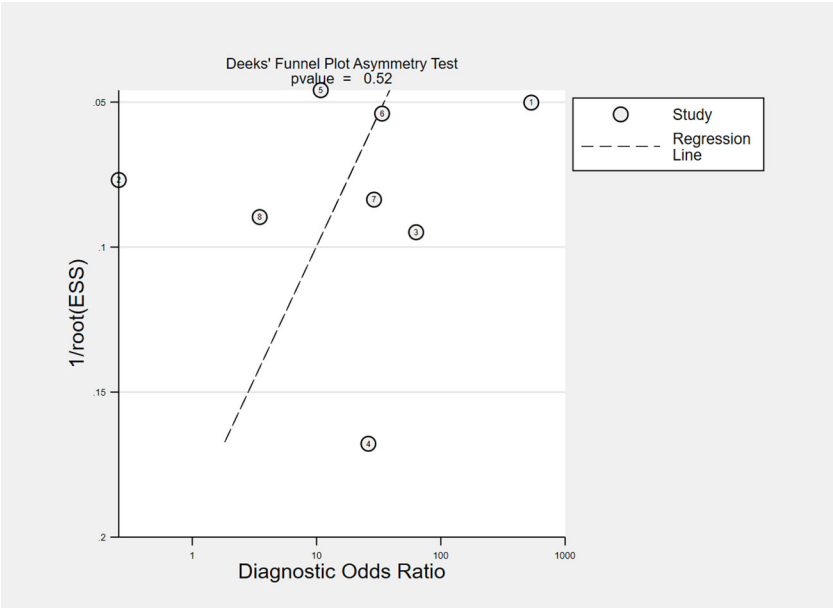

FIGURE 3
SROC of CTCs in the diagnosis of BC.

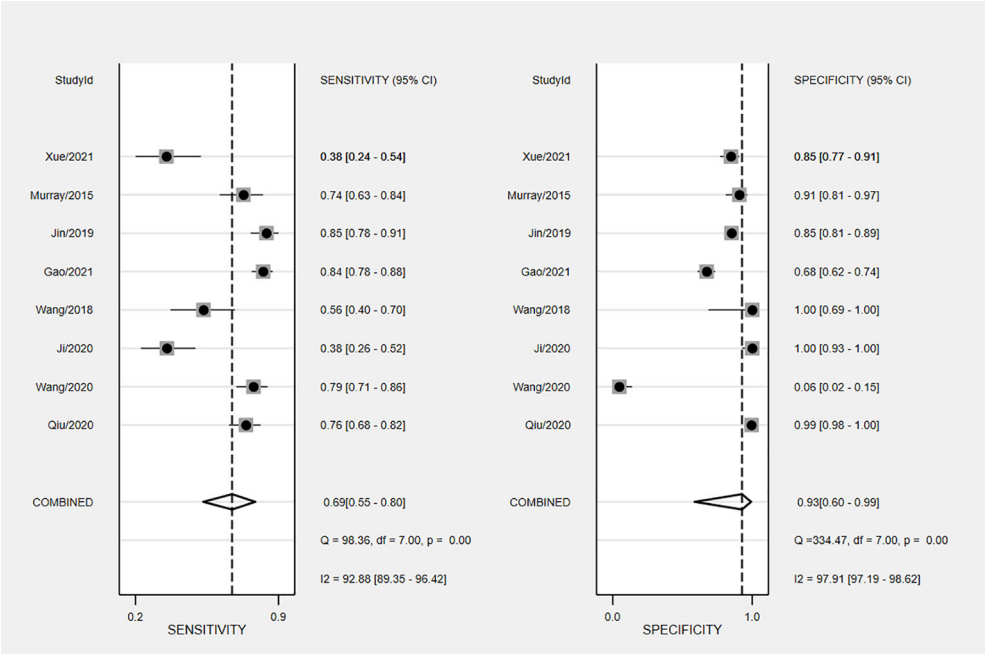

FIGURE 4
Fagan nomogram plot analysis for the evaluation of CTCs as a diagnostic tool for detecting BC.

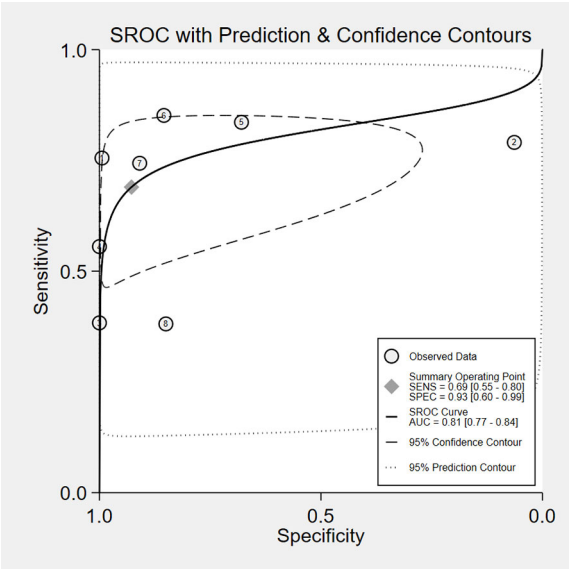

FIGURE 5
Deeks' funnel plot for detecting publication bias. ESS, effective sample size.

This study has some limitations. First, on account of the relatively small number of cases in this study, we failed to determine the potential source of this study due to the relatively high heterogeneity of this study. Second, in various studies, cutoff values differ, which has an impact on our results, and there is a need for further research on CTCS's optimal cutoff point. In addition, seven out of eight studies were conducted in Asia, and the electronic databases included regional databases, which could cause bias in the

TABLE 3 Meta-analysis sensitivity analysis for included studies.

Without study	Heterogeneity (*I*2,%)	Sensitivity (95%CI)	Heterogeneity (*I*2,%)	Specificity (95%CI)
None	92.88	0.69 [0.55-0.80]	97.91	0.93[0.60-0.99]
Qiu 2020	93.83	0.68 [0.52-0.80]	97.07	0.88 [0.48-0.98]
Wang 2020	93.46	0.67 [0.52-0.80]	95.14	0.95 [0.81-0.99]
Ji 2020	90.18	0.73 [0.61-0.82]	98.1	0.87 [0.51-0.98]
Wang 2018	93.66	0.71 [0.56-0.82]	98.22	0.90 [0.51-0.99]
Gao 2021	92.04	0.66 [0.52-0.78]	98.26	0.95 [0.59-1.00]
Jin 2019	92.93	0.66 [0.52-0.78]	98.13	0.94 [0.54-1.00]
Murray 2015	93.86	0.68 [0.52-0.80]	98.13	0.93 [0.52-0.99]
Xue 2021	91.80	0.73 [0.68-0.82]	98.15	0.97 [0.41-1.00]

results. It would be beneficial to conduct more international prospective multicenter research on this topic.

Conclusion

This meta-analysis showed that CTCs can be used as a helpful tool in BC screening and early diagnosis, with better sensitivity and specificity. To clarify the accuracy of CTCs as BC diagnostic indicators, more high-quality prospective studies are needed.

Data availability statement

The original contributions presented in the study are included in the article/supplementary material. Further inquiries can be directed to the corresponding author.

Author contributions

All authors contributed to the study conception and design. Material preparation, data collection and analysis were performed by TJ, YC and J-QY. The first draft of the manuscript was written by TJ, and all authors commented on previous versions of the manuscript. All authors contributed to the article and approved the submitted version.

Conflict of interest

The authors declare that the research was conducted in the absence of any commercial or financial relationships that could be construed as a potential conflict of interest.

Publisher's note

References

1. Loibl S, Poortmans P, Morrow M, Denkert C, Curigliano G. Breast cancer. *Lancet* (2021) 397(10286):1750–69. doi: 10.1016/S0140-6736(20)32381-3

2. Daly AA, Rolph R, Cutress RI, Copson ER. A review of modifiable risk factors in young women for the prevention of breast cancer. *Breast Cancer (Dove Med Press)* (2021) 13:241–57. doi: 10.2147/BCTT.S268401

3. Siegel RL, Miller KD, Jemal A. Cancer statistics, 2019. *CA Cancer J Clin* (2019) 69 (1):7–34. doi: 10.3322/caac.21551

4. Azamjah N, Soltan-Zadeh Y, Zayeri F. Global trend of breast cancer mortality rate: A 25-year study. *Asian Pac J Cancer Prev* (2019) 20(7):2015–20. doi: 10.31557/APJCP.2019.20.7.2015

5. Zhao S, Gai X, Wang Y, Liang W, Gao H, Zhang K, et al. Diagnostic values of carcinoembryonic antigen, cancer antigen 15-3 and cancer antigen 125 levels in nipple discharge. *Chin J Physiol* (2015) 58(6):385–92. doi: 10.4077/CJP.2015.BAD336

6. Chu WG, Ryu DW. Clinical significance of serum CA15-3 as a prognostic parameter during follow-up periods in patients with breast cancer. *Ann Surg Treat Res* (2016) 90(2):57–63. doi: 10.4174/astr.2016.90.2.57

7. Wu SG, He ZY, Zhou J, Sun JY, Li FY, Lin Q, et al. Serum levels of CEA and CA15-3 in different molecular subtypes and prognostic value in Chinese breast cancer. *Breast* (2014) 23(1):88–93. doi: 10.1016/j.breast.2013.11.003

8. Brooks M. Breast cancer screening and biomarkers. *Methods Mol Biol* (2009) 472:307–21. doi: 10.1007/978-1-60327-492-0_13

9. Farshchi F, Hasanzadeh M. Microfluidic biosensing of circulating tumor cells (CTCs): Recent progress and challenges in efficient diagnosis of cancer. *BioMed Pharmacother* (2021) 134:111153. doi: 10.1016/j.biopha.2020.111153

10. Zhong X, Zhang H, Zhu Y, Liang Y, Yuan Z, Li J, et al. Circulating tumor cells in cancer patients: Developments and clinical applications for immunotherapy. *Mol Cancer* (2020) 19(1):15. doi: 10.1186/s12943-020-1141-9

11. Gradishar WJ, Anderson BO, Balassanian R, Blair SL, Burstein HJ, Cyr A, et al. Breast cancer, version 4.2017, NCCN clinical practice guidelines in oncology. *J Natl Compr Canc Netw* (2018) 16(3):310–20. doi: 10.6004/jnccn.2018.0012

12. Jin L, Zhao W, Zhang J, Chen W, Xie T, Wang L, et al. Evaluation of the diagnostic value of circulating tumor cells with CytoSorter(®) CTC capture system in patients with breast cancer. *Cancer Med* (2020) 9(5):1638–47. doi: 10.1002/cam4.2825

13. Liberati A, Altman DG, Tetzlaff J, Mulrow C, Gøtzsche PC, Ioannidis JP, et al. The PRISMA statement for reporting systematic reviews and meta-analyses of studies that evaluate healthcare interventions: Explanation and elaboration. *Bmj* (2009) 339: b2700. doi: 10.1136/bmj.b2700

14. Whiting PF, Rutjes AW, Westwood ME, Mallett S, Deeks JJ, Reitsma JB, et al. QUADAS-2: A revised tool for the quality assessment of diagnostic accuracy studies. *Ann Intern Med* (2011) 155(8):529–36. doi: 10.7326/0003-4819-155-8-201110180-00009

15. Murray NP, Miranda R, Ruiz A, Droguett E. Diagnostic yield of primary circulating tumor cells in women suspected of breast cancer: The BEST (Breast early screening test) study. *Asian Pac J Cancer Prev* (2015) 16(5):1929–34. doi: 10.7314/APJCP.2015.16.5.1929

16. Gao Y, Fan WH, Duan C, Zhao W, Zhang J, Kang X. Enhancing the screening efficiency of breast cancer by combining conventional medical imaging examinations with circulating tumor cells. *Front Oncol* (2021) 11:643003. doi: 10.3389/fonc.2021.643003

17. Fuqing J, Mengwan L, Yulong Y, Yonggang L. CTCs, ctDNA detection and diagnostic value in breast cancer patients. *Hainan Med [Chinese Journal]* (2020) 31 (07):838–41.

18. Ruijuan W, Xueming X, Huanhong Z, Qiang L, Linfang S, Junjie Z, et al. Clinical value of peripheral blood circulation tumor cell detection in breast cancer patients. *Fujian Med Journal[Chinese Journal]* (2020) 42(05):42–5.

19. Xiaoyang Q, Xuan W, Jun L, Xiaofen Z, Zhiqiang C. The application value of peripheral blood circulation tumor cells combined with CA153 detection in breast cancer screening and staging prediction. *J Huazhong Univ Sci Technol (Medical Edition)[Chinese Journal]* (2020) 49(03):331–7.

20. Jian W, Xu L, Li WZJ, Tao Z, Rongjin S. A study on the relationship between peripheral blood circulation tumor cells and the clinical pathological features of breast cancer. *Chin J Oncol Surgery[Chinese Journal]* (2021) 13(03):242–5.

21. Paizura S, Ayyu E, Irina Wenting X, Chenguang Z, Weihua J, et al. Clinical value study of peripheral blood circulation of tumor cells with different fragment length cf DNA in the diagnosis of breast cancer. *J Clin Military Medicine[Chinese Journal]* (2021) 49(12):1372–4.

22. Oeffinger KC, Fontham ET, Etzioni R, Herzig A, Michaelson JS, Shih YC, et al. Breast cancer screening for women at average risk: 2015 guideline update from the American cancer society. *Jama* (2015) 314(15):1599–614. doi: 10.1001/jama.2015.12783

23. Gao J, Zhang Q, Xu J, Guo L, Li X. Clinical significance of serum miR-21 in breast cancer compared with CA153 and CEA. *Chin J Cancer Res* (2013) 25(6):743–8.

24. Wang H, Stoecklein NH, Lin PP, Gires O. Circulating and disseminated tumor cells: diagnostic tools and therapeutic targets in motion. *Oncotarget* (2017) 8(1):1884–912. doi: 10.18632/oncotarget.12242

25. Giordano A, Giuliano M, De Laurentiis M, Arpino G, Jackson S, Handy BC, et al. Circulating tumor cells in immunohistochemical subtypes of metastatic breast cancer: lack of prediction in HER2-positive disease treated with targeted therapy. *Ann Oncol* (2012) 23(5):1144–50. doi: 10.1093/annonc/mdr434

26. Liu XR, Shao B, Peng JX, Li HP, Yang YL, Kong WY, et al. Identification of high independent prognostic value of nanotechnology based circulating tumor cell enumeration in first-line chemotherapy for metastatic breast cancer patients. *Breast* (2017) 32:119–25. doi: 10.1016/j.breast.2017.01.007

27. Xie N, Hu Z, Tian C, Xiao H, Liu L, Yang X, et al. In vivo detection of CTC and CTC plakoglobin status helps predict prognosis in patients with metastatic breast cancer. *Pathol Oncol Res* (2020) 26(4):2435–42. doi: 10.1007/s12253-020-00847-7

28. Maly V, Maly O, Kolostova K, Bobek V. Circulating tumor cells in diagnosis and treatment of lung cancer. *In Vivo* (2019) 33(4):1027–37. doi: 10.21873/invivo.11571

29. Msaouel P, Koutsilieris M. Diagnostic value of circulating tumor cell detection in bladder and urothelial cancer: Systematic review and meta-analysis. *BMC Cancer* (2011) 11:336. doi: 10.1186/1471-2407-11-336

30. Chang Y, Min J, Jarusiewicz JA, Actis M, Yu-Chen Bradford S, Mayasundari A, et al. Degradation of janus kinases in CRLF2-rearranged acute lymphoblastic leukemia. *Blood* (2021) 138(23):2313–26. doi: 10.1182/blood.2020006846

31. Krawczyk N, Banys M, Hartkopf A, Hagenbeck C, Melcher C, Fehm T. Circulating tumor cells in breast cancer. *Ecancermedicalscience* (2013) 7:352. doi: 10.3332/ecancer.2013.352

32. Eroglu Z, Fielder O, Somlo G. Analysis of circulating tumor cells in breast cancer. *J Natl Compr Canc Netw* (2013) 11(8):977–85. doi: 10.6004/jnccn.2013.0118

frontiers | Frontiers in Oncology

TYPE Original Research
PUBLISHED 29 March 2023
DOI 10.3389/fonc.2023.1134149

OPEN ACCESS

EDITED BY
Yujiao Deng,
The Second Affiliated Hospital of Xi'an Jiaotong University, China

REVIEWED BY
Junlin Lu,
Sun Yat-sen Memorial Hospital, China
YuTing Jiang,
Guangxi Medical University Cancer Hospital, China

*CORRESPONDENCE
Ya Xie
fccxiey@zzu.edu.cn

†These authors have contributed equally to this work

SPECIALTY SECTION
This article was submitted to Breast Cancer, a section of the journal Frontiers in Oncology

RECEIVED 30 December 2022
ACCEPTED 20 March 2023
PUBLISHED 29 March 2023

CITATION
Jiao Y, Li S, Gong J, Zheng K and Xie Y (2023) Comprehensive analysis of the expression and prognosis for RAI2: A promising biomarker in breast cancer. *Front. Oncol.* 13:1134149. doi: 10.3389/fonc.2023.1134149

Comprehensive analysis of the expression and prognosis for RAI2: A promising biomarker in breast cancer

Ying Jiao[1,2†], Shiyu Li[1,2†], Juejun Gong[3], Kun Zheng[4,5] and Ya Xie[6*]

[1]Department of Oncology, Tongji Hospital of Tongji Medical College, Huazhong University of Science and Technology, Wuhan, China, [2]Department of Medicine and Therapeutics, State Key Laboratory of Digestive Disease, Institute of Digestive Disease, Li Ka Shing Institute of Health Sciences, CUHK-Shenzhen Research Institute, The Chinese University of Hong Kong, Hong Kong, Hong Kong SAR, China, [3]Department of Oncology, The Central Hospital of Wuhan, Tongji Medical College, Huazhong University of Science and Technology, Wuhan, China, [4]Biological Sciences, Faculty of Environmental and Life Sciences, University of Southampton, Southampton, United Kingdom, [5]Institute for Life Sciences, University of Southampton, Southampton, United Kingdom, [6]Department of Gynecology, The First Affiliated Hospital of Zhengzhou University, Zhengzhou, China

Introduction: Retinoic acid-induced 2 (RAI2) was initially related to cell differentiation and induced by retinoic acid. RAI2 has been identified as an emerging tumor suppressor in breast cancer and colorectal cancer.

Methods: In this study, we performed systematic analyses of RAI2 in breast cancer. Meta-analysis and Kaplan-Meier survival curves were applied to identify the survival prediction potential of RAI2. Moreover, the association between RAI2 expression and the abundance of six tumor-infiltrating immune cells was investigated by TIMER, including B cells, CD8+ T cells, CD4+ T cells, B cells, dendritic cells, neutrophils, and macrophages. The expression profiles of high and low RAI2 mRNA levels in GSE7390 were compared to identify differentially expressed genes (DEGs) and the biological function of these DEGs was analyzed by R software, which was further proved in GSE7390.

Results: Our results showed that the normal tissues had more RAI2 expression than breast cancer tissues. Patients with high RAI2 expression were related to a favorable prognosis and more immune infiltrates. A total of 209 DEGs and 182 DEGs were identified between the expression profiles of high and low RAI2 mRNA levels in the GSE7390 and GSE21653 databases, respectively. Furthermore, Gene Ontology (GO) enrichment indicated that these DEGs from two datasets were both mainly distributed in "biological processes" (BP), including "organelle fission" and "nuclear division". Kyoto Encyclopedia of Genes and Genomes (KEGG) pathways analysis demonstrated that these DEGs from two datasets were both significantly enriched in the "cell cycle". Common hub genes between the DEGs in GSE7390 and GSE21653 were negatively associated with RAI2 expression, including CCNA2, MAD2L1, MELK, CDC20, and CCNB2.

Discussions: These results above suggested that RAI2 might play a pivotal role in preventing the initiation and progression of breast cancer. The present study may contribute to understanding the molecular mechanisms of RAI2 and enriching biomarkers to predict patient prognosis in breast cancer.

KEYWORDS

RAI2, biomarker, breast cancer, prognosis, tumor progression

1 Background

Breast cancer (BRCA), which accounts for approximately 30% of female cancers, is the first leading cause of cancer death for women aged 20 to 59 years (1). Several major molecular subtypes in BRCA are defined by the presence or absence of hormone receptors (estrogen receptors (ER) or progesterone receptors (PR) and human epidermal growth factor receptor 2 (HER2) (2). Over the decades, molecular classification exerts a critical role in predicting tumor behavior and guiding therapeutic strategies (3). Nearly 75% of BRCA patients express hormone receptors, which results in the potent effects of endocrine therapy (2). However, some patients get primary or acquired resistance to endocrine therapy (4). Moreover, approximately 20-30% of BRCAs patients overexpress HER2 and have poorer prognoses with more aggressive tumors (5). Although anti-HER2 treatment has shown some achievements for HER2-positive BRCAs, continuing high mortality of HER2-overexpressed BRCAs demands new therapies (6). Thus, it is crucial to investigate further novel biomarkers and emerging agents to treat BRCA.

Retinoic acid (RA) is one of the metabolic products of retinol (vitamin A) and exerts activity in distinct isometric forms, including 9-cis-RA, 13-cis-RA as well as all-trans-RA (7). Retinoic acid-induced 2 (RAI2) is induced by RA in embryonal carcinoma cells and involved in cellular differentiation (8, 9). Stefan Werner et al. found that RAI2 acts as a transcriptional regulator that contributes to the expression of some critical regulators of breast epithelial integrity (10). Low RAI2 expression was significantly associated with early hematogenous metastasis of BRCA cells to bone marrow, especially in ER^+ BRCA (10). Moreover, RAI2 inhibited AKT signaling to suppress CRC progression, and methylated RAI2 indicated poor prognosis in CRC (11).

Abbreviations: BRCA, breast cancer; BP, biological processes; CC, cellular component; CCNA2, CyclinA2; CI, confidence interval; DEGs, differentially expressed genes; ER, estrogen receptor; EMT, epithelial-mesenchymal transitions; GEO, Gene Expression Omnibus; GO, Gene Ontology; HER2, human epidermal growth factor receptor 2; HR, hazard ratio; KEGG, Kyoto Encyclopedia of Genes and Genomes; MAD2L1, mitotic arrest deficient 2-like 1; MF, molecular function; MFS, metastasis-free survival; OR, odds ratio; OS, overall survival; PPI, protein-protein interaction; PR, progesterone receptor; RA, Retinoic acid; RAI2, retinoic acid-induced 2; RFS, relapse-free survival; STRING, Search Tool for Retrieval of Interacting Genes database; TCGA, The Cancer Genome Atlas; TIMER, Tumor Immune Estimation Resource.

Some studies used invasive breast cancer tissues to indicate that lower RAI2 mRNA and protein were independent risk factors for lower shorter disease-free survival (DFS), and breast-cancer-specific survival (BCSS) (12). However, there are not sufficient studies to explain the biological function of RAI2 in BRCA. Furthermore, more samples are needed to validate the effects of RAI2 on prognosis for breast cancer patients and RAI2-related pathways should be clarified. More investigations on RAI2 might provide novel therapeutic strategies for clinicians (13).

2 Materials and methods

2.1 Search strategy of the GEO datasets

The datasets of human BRCA with RAI2 mRNA expression were searched in the GEO databases (https://www.ncbi.nlm.nih.gov/geo/), up to December 10, 2015. The search terms "breast cancer" ("breast neoplasm," "breast tumor," "breast carcinoma," and "mammary cancer") were used and the search scope was based on homo sapiens. Only the databases that met the inclusion criteria were chosen in the following analysis.

2.2 Inclusion criteria

Based on the PRISMA statement criteria, we chose databases that matched the following inclusion criteria: 1) the databases were about BRCA or normal breast tissues, and homo sapience rather than cell lines; 2) the datasets were about mRNA rather than DNA or microRNA and included RAI2 mRNA expression; 3) the sample capacity was more than 45; 4) it was available for clinic-pathological and prognosis information of BRCA patients in these databases, such as T stage, N stage, TNM stage, grade, molecular subtypes, and clinical outcome. 5) when several databases shared specific patient identification, we chose the latest and most complete datasets.

2.3 Data extraction

We performed in silico validation of RAI2, using 30 publicly available breast datasets with 4863 samples. Data analysis and technical graphics were performed independently by two individuals. We extracted data from every dataset to a predefined table with a

standardized data collection form, with information recorded as follows: first author's name, publication year, country or area, follow-up duration, tumor stage, patient number, detection methods, and platform. The median of RAI2 mRNA expression was used for cutoff values. The probe with the maximum mRNA expression value was extracted while there was more than one probe for RAI2. Overall survival (OS), metastasis-free survival (MFS), and relapse-free survival (RFS) were evaluated by Cox proportional hazard ratio (HR) and 95% confidence interval (CI) using the extracted data. These data were shown in Supplemental Table 1.

2.4 Meta-analysis

The meta-analysis was performed using the STATA software (Version 12.0; StataCorp LP, College Station, TX, USA). The heterogeneity of publication was assessed by the inconsistency index (I^2) statistic. The random-effect model was employed on the condition that the I^2 value was more than 50%, which indicated that heterogeneity was shown. The fixed-effect model was used on the condition that the I^2 value was less than 50%, which demonstrated that homogeneity was presented. The publication bias was evaluated by Begg's and Egger's tests. To evaluate the association between RAI2 expression level and clinicopathological parameters, the odds ratio (OR) and its corresponding 95% CI were calculated. To evaluate the effects of RAI2 expression level on the survival outcome of BRCAs, we assessed the hazard ratio (HR) and its corresponding 95% CI. HR > 1 indicated that higher expression of RAI2 predicted worse survival.

2.5 Survival analysis

We performed Kaplan-Meier survival curves with HR and log-rank *p*-value for the RAI2 mRNA expression level of BRCAs by the online analysis tool (http://www.kmplot.com/analysis/). The Affymetrix probe ID for RAI2 was 219440_at. The patients were divided into two groups according to the median expression value. We chose 120 months as the follow-up threshold. Every intrinsic subtype of BRCA was conducted, including luminal A, luminal B, $HER2^+$, and basal-like types.

2.6 Analysis of TIMER datasets

The online tool, Tumor Immune Estimation Resource (TIMER, https://cistrome.shinyapps.io/timer/) included RNA-seq profiles of 10897 samples from 32 cancers in The Cancer Genome Atlas (TCGA) (14). The association of RAI2 expression with the abundance of six tumor-infiltrating immune cells could be evaluated based on silico deconvolution approaches *via* gene module in TIMER, including CD8+ T cells, CD4+ T cells, B cells, dendritic cells, neutrophils, and macrophages. The results were demonstrated in scatterplots with *p*-value and purity-corrected partial Spearman's correlation (partial-cor).

2.7 Identification of DEGs

Based on the databases of GSE7390 and GSE21653, we compared the two expression profiles of high and low RAI2 mRNA expression in BRCAs, which were divided according to the median expression by R software (version 3.6.3; https://www.r-project.org/) to identify DEGs. The results were obtained using limma package (version 3.42.2) (15) and pheatmap package (version 1.0.12). The limma package was employed to determine DEGs with log |fold change| > 1 and adj. $p < 0.05$ in unpaired t-test as cut-off levels. Subsequently, we used pheatmap package to generate a heatmap, demonstrating the differential expression levels of the top 40 DEGs directly, and a volcano plot was produced to show all DEGs in this dataset.

2.8 GO enrichment and KEGG pathways analysis

To discover the biological functions of DEGs, the GO enrichment, and KEGG pathways analysis were performed by R software (16, 17). Colorspace package (version 1.4-1), stringi package (version 1.4.6), ggplot2 package (version 3.3.0), and Bioconductor packages, such as DOSE package (version 3.12.0) (18), clusterProfiler package (version 3.14.3) (19) and enrichplot package (version 1.6.1), were used to get bubble plot and barplot. $p < 0.05$ was statistically significant.

2.9 PPI network construction

The PPIs of the DEGs were identified using the online Search Tool for Retrieval of Interacting Genes (STRING) database (version 11.0). All DEGs were mapped into this database to evaluate the interactive relations, showing nodes with the confidence score >0.4 and hiding disconnected nodes in the network. Subsequently, the Cytoscape software (version 3.7.2; National Resource for Network Biology) was employed to get PPI networks (20). The criteria for disease module searching were set as follows: Molecular COmplex DEtection (MCODE) score > 3, and each module must have more than four nodes. $p < 0.05$ was considered a statistically significant difference. Besides, the top 10 hub genes ranking by degree were identified using cytoHubba application on Cytoscape with the shortest path displaying (21).

2.10 The relation between RAI2 and several genes

The correlation of RAI2 and several hub genes were shown by GraphPad Prism (version 8.0.1). We chose the datasets of GSE7390 with 198 primary BRCA patients and GSE21653 with 266 patients to present the relation between RAI2 and hub genes, including CCNA2, CDC20, CDC6, MAD2L1, TTK, MELK, and CCNB2.

3 Results

3.1 RAI2 expression relates to the molecular subtypes of BRCA

A total of ten studies with GEO datasets indicated that RAI2 mRNA expression in BRCA samples was reduced when compared with healthy control samples (pooled OR: 0.42, 95% CI: 0.28-0.65; Cochran's *Q* test $p = 0.176$ and $I^2 = 29.2\%$; Figure 1A). Then, some studies were adopted to further evaluate the relation between RAI2 mRNA expression and clinicopathological features of BRCA. The results showed that RAI2 mRNA expression in mammary cancer had a negative relation with T stage (pooled OR: 0.76, 95% CI: 0.61-0.96; Cochran's Q test, $p = 0.753$ and $I^2 = 0.0\%$; Figure 1B), N status (pooled OR: 0.82, 95% CI: 0.71-0.96;

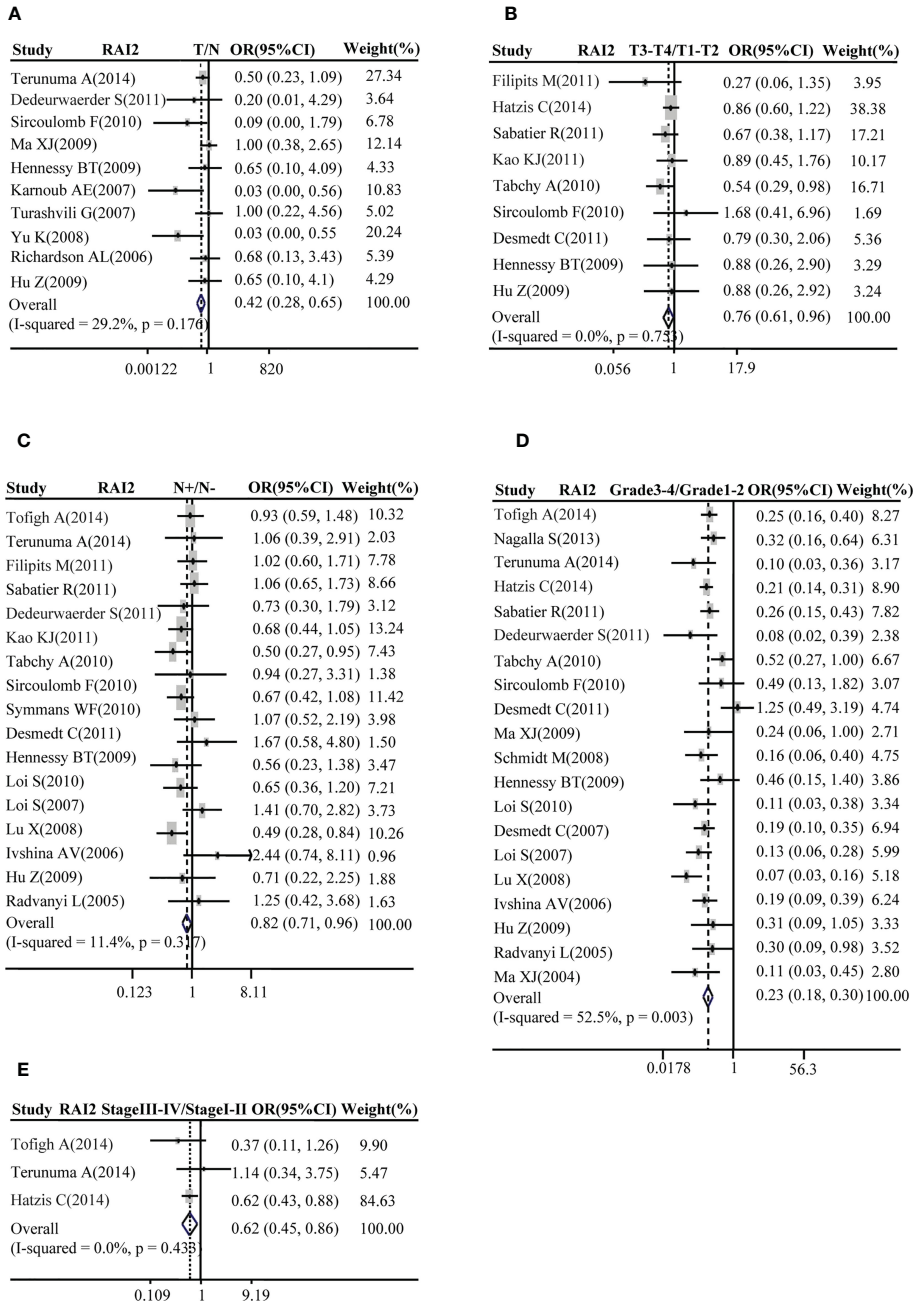

FIGURE 1
Correlation between RAI2 mRNA expression and breast cancer as evaluated by the OR. Relation of RAI2 mRNA expression with breast cancer risk compared with normal breast tissues **(A)**. Association between RAI2 mRNA expression and breast cancer risk compared with T stage **(B)**, N status **(C)**, histological grade **(D)**, and clinical TNM stage **(E)**. RAI2, retinoic acid-induced 2; CI, confidence interval; OR, odds ratio; TNM, tumor–node–metastasis.

Cochran's Q test, $p = 0.317$ and $I^2 = 11.4\%$; Figure 1C), histological grade (pooled OR: 0.23, 95% CI: 0.18-0.30; Cochran's Q test, $p = 0.003$ and $I^2 = 52.5\%$; Figure 1D) and TNM stage (pooled OR: 0.62, 95% CI: 0.45-0.86; Cochran's Q test, $p = 0.433$ and $I^2 = 0.0\%$; Figure 1E).

Subsequently, the relation between RAI2 mRNA expression and ER, PR, HER2 status, luminal type, and basal-like BRCA was further evacuated by meta-analysis in GEO datasets. Our results demonstrated that the elevated expression of RAI2 was positively related to BRCA with ER^+ subtype (pooled OR =4.27, 95% CI: 2.98–6.13, Cochran's Q test, $p = 0.000$, and $I^2 = 67.8\%$; Figure 2A) and PR^+ subtype (pooled OR = 3.16, 95% CI: 2.52–3.96, Cochran's Q test, $p = 0.614$, and $I^2 = 0.0\%$; Figure 2B), but it was negatively correlated with BRCA with $HER2^+$ subtype (pooled OR =0.68, 95% CI: 0.52–0.89, Cochran's Q test, $p = 0.505$, and $I^2 = 0.0\%$; Figure 2C). Besides, there was a positive association between the increased RAI2 expression and luminal subtype of tumors rather than basal-like cancers (pooled OR = 6.95, 95% CI: 5.07–9.51, Cochran's Q test, $p = 0.39$, and $I^2 = 4.6\%$; Figure 2D).

3.2 RAI2 expression relates to patient survival in BRCA

The association of RAI2 mRNA expression with survival was evaluated in a total of BRCA patients. Our analysis showed that patients with BRCA with higher RAI2 mRNA level tended to have better OS (pooled OR = 0.69, 95% CI: 0.55–0.87, Cochran's Q test, $p = 0.146$, and $I^2 = 34.0\%$; Figure 3A). Moreover, there was a significant association of high RAI2 expression with prolonged RFS (pooled OR = 0.67, 95% CI: 0.56–0.80, Cochran's Q test, $p = 0.102$, and $I^2 = 37.2\%$; Figure 3B) and MFS (pooled OR = 0.80, 95% CI: 0.66–0.97, Cochran's Q test, $p = 0.766$, and $I^2 = 0.0\%$; Figure 3C).

In order to evaluate the prognosis value of RAI2 in distinct molecular subtypes, Kaplan-Meier survival curves were plotted in BRCA patients in Figure 4. Our results showed that RAI2 expression was positively associated with the OS (HR = 0.6, 95% CI: 0.48-0.76, $p < 0.01$; Figure 4A), RFS (HR = 0.55, 95% CI: 0.49-0.61, $p < 0.01$; Figure 4B) and MFS (HR = 0.57, 95% CI: 0.47-0.7, $p < 0.01$; Figure 4C) rate in all BRCA patients, it had distinct prognostic value in different subtypes. Although lower RAI2 mRNA expression predicted poor RFS (HR = 0.55, 95% CI: 0.46-0.66, $p < 0.01$; Figure 4E) and MFS (HR = 0.61, 95% CI: 0.45-0.83, $p < 0.01$; Figure 4F) in patients with luminal A subtype, there was no significant association between RAI2 expression and OS (HR = 0.71, 95% CI: 0.49-1.04, $p = 0.078$; Figure 4D) in the patients. In patients with luminal B subtype, lower RAI2 mRNA expression predicted poor RFS (HR = 0.76, 95% CI: 0.62-0.92, $p < 0.01$; Figure 4H), whereas there was no significant association between RAI2 and OS (HR = 0.94, 95% CI: 0.64-1.37, $p = 0.74$; Figure 4G) and

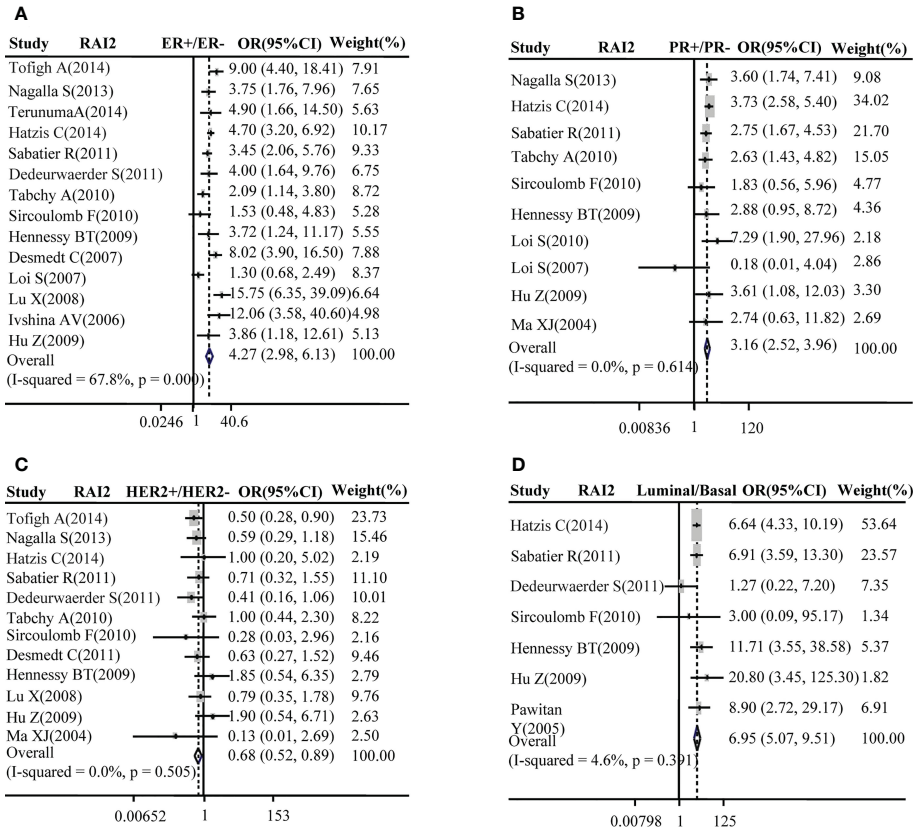

FIGURE 2
Correlation between RAI2 mRNA expression and molecular subtype. Correlation between RAI2 mRNA expression with ER status **(A)**, PR **(B)**, HER2 **(C)**, and luminal-basal **(D)**. CI, confidence interval; ER, estrogen receptor; HER2, human epidermal growth factor receptor-2; OR, odds ratio; PR, progesterone receptor; RAI2, retinoic acid-induced 2.

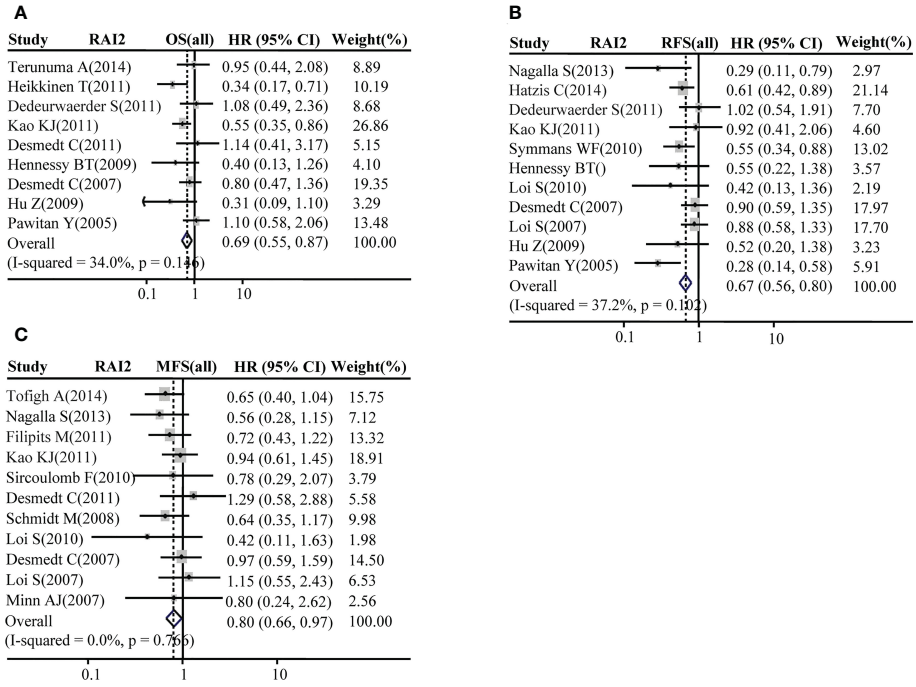

FIGURE 3
Forest plot for the association of RAI2 mRNA expression with breast cancer survival. Associations between RAI2 mRNA expression with breast cancer OS **(A)**, RFS **(B)**, and MFS **(C)** in all populations of breast cancer. CI, confidence interval; HR, hazard ratio; MFS, metastasis-free survival; OS, overall survival; RFS, recurrence-free survival; RAI2, retinoic acid-induced 2.

MFS (HR = 0.92, 95% CI: 0.64-1.31, $p = 0.64$; Figure 4I). In addition, there was no statistically significant effect of RAI2 on promoting OS (HR=1.39, 95% CI: 0.72-2.68, $p = 0.32$; Figure 4J), RFS (HR = 0.86, 95% CI: 0.59-1.27, $p = 0.45$; Figure 4K) and MFS (HR=1.61, 95% CI: 0.86-3.04, $p = 0.31$; Figure 4L) in patients with HER2-overexpressed subtype, and on prolonging OS (HR=1.2, 95% CI: 0.73-1.97, P = 0.46; Figure 4M), RFS (HR = 0.88, 95% CI: 0.68-1.13, P = 0.3; Figure 4N) and MFS (HR = 0.86, 95% CI: 0.52-1.42, P = 0.55; Figure 4O) in patients with basal-like subtype. In all, the analysis of the RAI2 mRNA level and survival showed that higher RAI2 expression predicted a more favorable prognosis for BRCA patients.

3.3 The association of RAI2 expression with six immune infiltrates in BRCA

Some studies had reported that immune infiltrates were closely related to patient prognosis and could predict the status of sentinel lymph node (22, 23). We utilized the gene module of TIMER datasets to determine the relation of RAI2 expression with tumor-infiltrating lymphocytes for BRCA patients. The analyses results indicated that RAI2 expression was negatively related to tumor purity of BRCA ($r = -0.136$, $p < 0.001$), BRCA-basal ($r = -0.401$, $p < 0.001$), BRCA-HER2 ($r = -0.136$, $p < 0.001$) and BRCA-luminal ($r = -0.261$, $p < 0.001$) subtypes. Furthermore, RAI2 expression level was positively associated with infiltrating levels of CD8+ T cells ($r = 0.078$, $p = 0.015$), CD4+ T cells ($r = 0.069$, $p = 0.032$), and macrophages ($r = 0.17$, $p < 0.001$) in BRCA (Figure 5A). In BRAC-basal subtypes (Figure 5B), there were a positive association of RAI2 expression within filtrating levels of B cells ($r = 0.186$, $p = 0.039$), CD8+ T cells ($r = 0.264$, $p = 0.003$), CD4+ T cells ($r = 0.268$, $p = 0.003$), macrophages ($r = 0.298$, $p < 0.001$), neutrophils ($r = 0.202$, $p = 0.035$) and DCs ($r = 0.222$, $p = 0.018$). However, there was no relation of RAI2 expression with immune infiltrating levels in BRAC-HER2 subtypes (Figure 5C). In addition, RAI2 expression had no association with immune infiltrating levels of B cells, CD8+ T cells, macrophages, neutrophils, and dendritic cells except for CD4+ T cells ($r = 0.124$, $p = 0.004$) in BRAC-luminal subtypes (Figure 5D).

3.4 Different expression and pathway analysis for DEGs of $RAI2^{high}$ versus $RAI2^{low}$ group

The datasets of GSE7390 and GSE21653 were respectively divided into two groups ($RAI2^{high}$ and $RAI2^{low}$) by median expression of RAI2 to identify DEGs by R software. Based on the Limma package, a total of 209 DEGs (120 upregulated and 89 downregulated DEGs) in GSE7390 and a total of 182 DEGs (100 upregulated and 82 downregulated DEGs) in GSE21653 were obtained. With GSE7309, a volcano map was employed to show all DEG distribution (Figure 6A) and the expression heatmap for 40 genes, comprising the top 20 upregulated and the top 20 downregulated DEGs, was shown in Figure 6B. Additionally, the enriched GO terms and KEGG pathways were analyzed for DEGs. In the biological process terms of GO (Supplemental Table 2A), our analysis indicated that most of the DEGs in GSE7390 were enriched in "organelle fission"

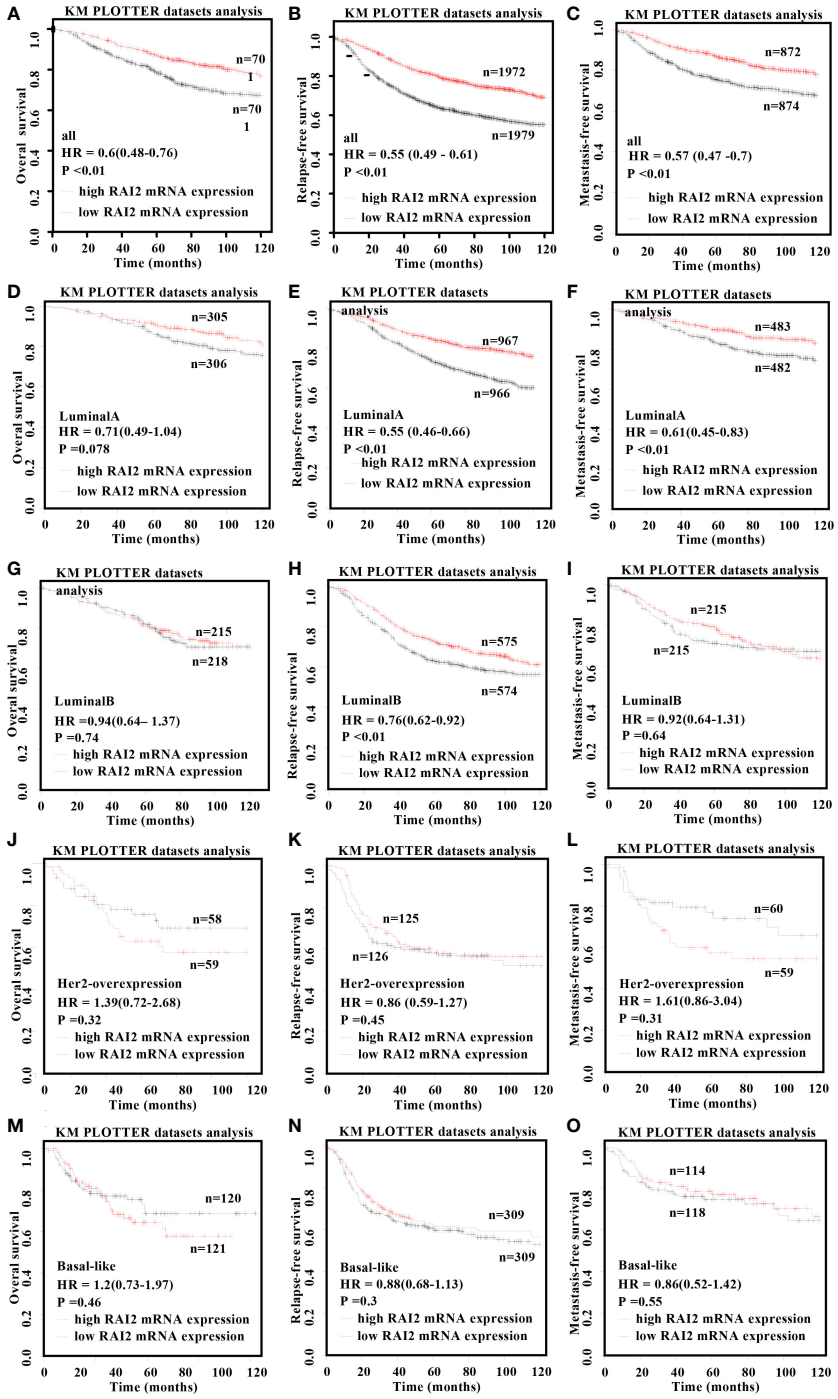

FIGURE 4
Kaplan–Meier survival curves for the correlation of RAI2 mRNA expression with breast cancer. Overexpression of RAI2 predicted favorable survival in patients with BRCA. The relation of RAI2 expression level in all **(A-C)**, luminal-A **(D-F)**, luminal-B **(G-I)**, her2-overexpression **(J-L)**, and basal-like **(M-O)** breast cancer patients with OS, RFS, and MFS. Her2, human epidermal growth factor receptor 2; MFS, metastasis-free survival; OS, overall survival; RFS, recurrence-free survival; RAI2, retinoic acid-induced 2.

(GO:0048285), "chromosome segregation" (GO:0007059), and "nuclear division" (GO:0000280) (Figure 6C). In the KEGG analysis (Supplemental Table 3A), our result showed that most of the DEGs in GSE7390 were enriched in the "cell cycle" (hsa04110) and "cellular senescence" (hsa04218) (Figure 6D). Using the same analysis strategies, we showed the results of GSE21653 in Supplemental Figure 1 and Supplemental Tables 2B, 3B. The top 20 upregulated and the top 20 downregulated DEGs in GSE7390 (Supplemental Figure 2A) and GSE21653 (Supplemental Figure 2B) were respectively analyzed for the correlativity among these genes using R software.

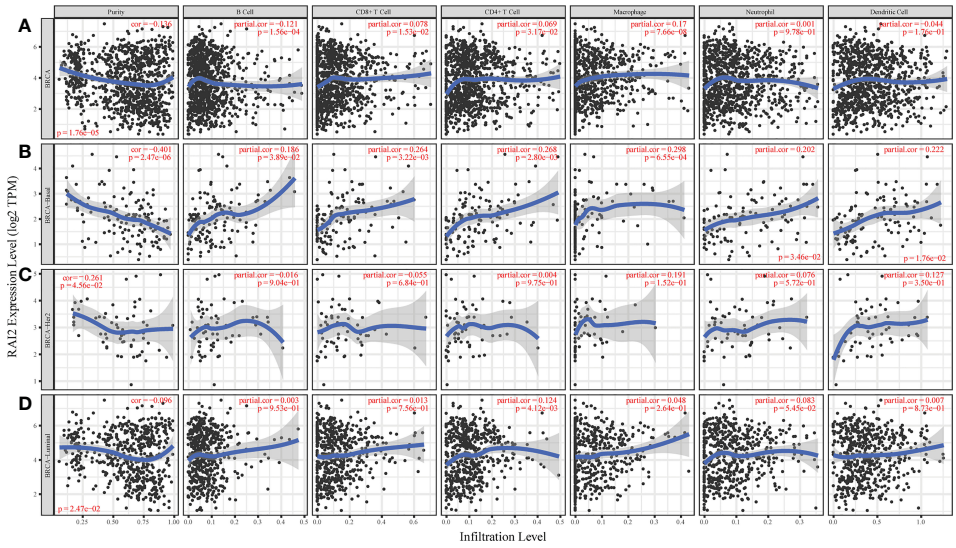

FIGURE 5
Association of RAI2 expression with immune infiltrating levels in breast cancer. **(A)** RAI2 expression is significantly negatively associated with tumor purity and has a significant positive relation with infiltrating immune cells of B cells, CD8+ T cells, CD4+ T cells, and macrophages, other than neutrophils and dendritic cells. **(B)** RAI2 expression has significant negative correlations with tumor purity and positive infiltrating levels of B cells, CD8+ T cells, CD4+ T, macrophages, neutrophils, and dendritic cells in the BRCA-basal subtype. **(C)** RAI2 expression is negatively related to tumor purity and showed a very weak correlation with infiltrating B cells, CD8+ T cells, CD4+ T, macrophages, neutrophils, and dendritic cells in BRCA-her2 subtype. **(D)** RAI2 expression has negative correlations with tumor purity and positive with infiltrating levels of CD4+ T cells but no significant association with infiltrating level of B cells, CD8+ T cells, macrophages, neutrophils, and dendritic cells in the BRCA-luminal subtype. Her2, human epidermal growth factor receptor 2; RAI2, retinoic acid-induced 2.

3.5 Disease module from the PPI network

The PPIs network of DEGs was screened in the STRING database (24). Genes were included in the network with a medium interaction score (confidence > 0.4) and disconnected nodes were hidden. However, for the two databases, the gene of RAI2 was not shown in the PPI network. Then, the PPI networks were exported to the Cytoscape for visualized results. Most of the up-regulated genes with red and down-regulated genes with blue color were interactional in the PPI visualized network. Analyzing a total of 155 nodes and 860 edges, we discovered the top five largest-size modules of GSE7390 utilizing the MCODE application in Cytoscape (Figures 7A–E). KEGG enrichment analysis of the modules indicated that these genes in modules 1–3 were mainly related to "cell cycle" (hsa04110), "viral protein interaction with cytokine and cytokine receptor" (hsa04061), "estrogen signaling pathway" (hsa04915). Analyzing a total of 131 nodes and 1551 edges, we acquired the top three largest size modules of GSE21653 (Figures 7F–H). KEGG analysis of the modules showed that these genes in modules 1–2 were implicated with "cell cycle" (hsa04110), and "Viral protein interaction with cytokine and cytokine receptor" (hsa04061). The "cell cycle" (hsa04110) was the common pathway of GSE7390 and GSE21653 in KEGG analysis, with the common genes of CCNA2, CDC20, CDC6, MAD2L1, and TTK. Then, the cytoHubba application in Cytoscape was used to identify the ten hub nodes with the highest degrees and shortest path. The 10 hub genes in GSE7390 contained CDK1, CCNA2, FOXM1, MAD2L1, BIRC5, MELK, CDC20, CDC6, RRM2, CCNB2 (Figure 7I; Supplemental Table 4A). The ten hub genes in GSE21653 contained UBE2C, CCNB1, CCNA2, MELK, MAD2L1, MKI67, PBK, TOP2A, BIRC5, CDC20 (Figure 7J; Supplemental Table 4B). In summary, the genes of CCNA2, MAD2L1, MELK, CDC20, and CCNB2 were the common and down-regulated hub genes in the $RAI2^{high}$ group of the two datasets.

3.6 The relation of RAI2 expression with several core genes

We performed scatter diagrams and linear regression to show the relations between RAI2 mRNA expression and some core gene mRNA expression in the datasets of GSE7390 and GSE21653. According to the results above, we chose some core genes to estimate their relationship with RAI2. Correlation analysis in GSE7390 demonstrated that RAI2 mRNA expression was negatively correlated with CCAN2 (r = -0.5725, P < 0.001; Figure 8A), CDC20 (r = -0.5885, P < 0.001; Figure 8B), CDC6 (r = -0.5181, P < 0.001; Figure 8C), MAD2L1 (r = -0.5601, P < 0.001; Figure 8D), TTK (r = -0.5989, P < 0.001; Figure 8E), MELK (r = -0.5647, P < 0.001; Figure 8F), CCNB2 (r = -0.6154, P < 0.001; Figure 8G) mRNA expression. Additionally, correlation analysis in GSE21653 of RAI2 mRNA expression and these genes further proved the results that RAI2 was negatively correlated with CCAN2 (r = -0.5622, P < 0.001; Supplemental Figure 3A),

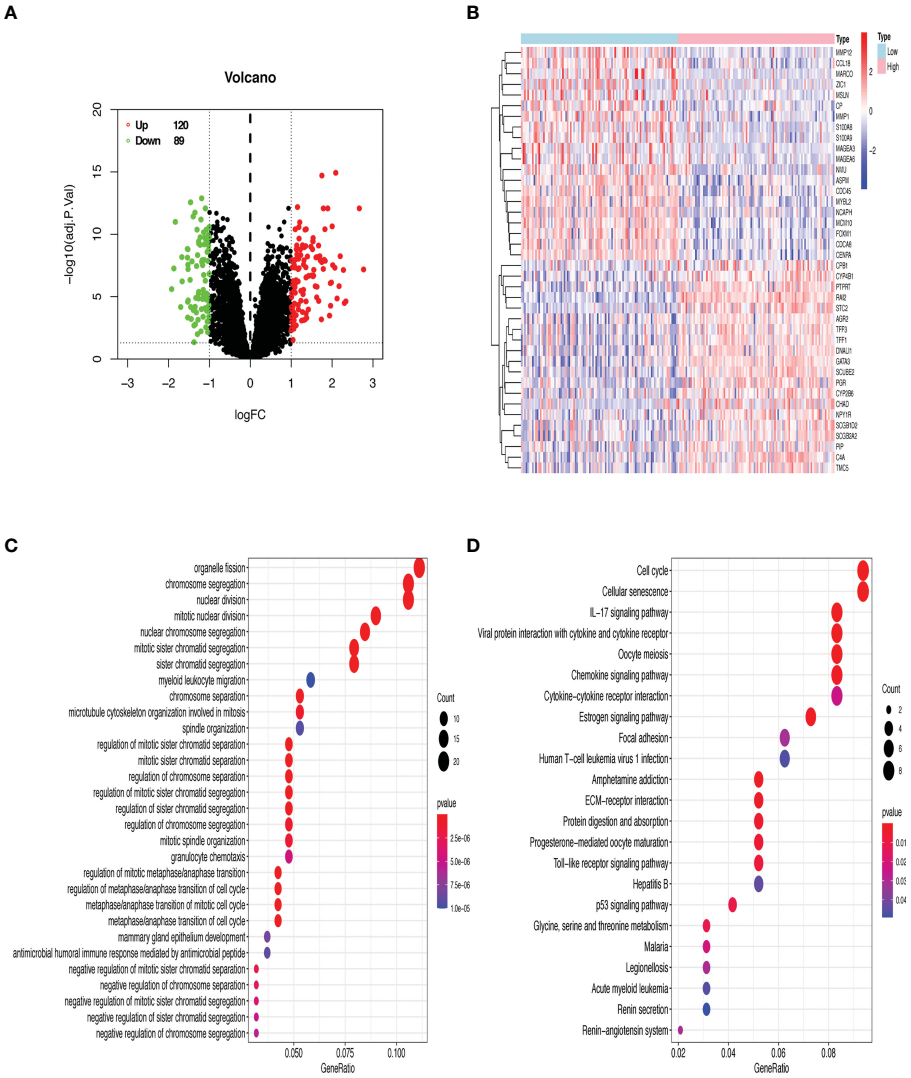

FIGURE 6
GO and KEGG enrichment analyses of DEGs from the microarray dataset GSE7390. **(A)** 209 DEGs are shown in a volcano plot. 120 upregulated genes are shown in red, and 89 downregulated genes are shown in green. **(B)** Heatmap of the top 20 upregulated and downregulated DEGs. Red denotes upregulated genes, and blue represents downregulated genes. **(C)** The top 30 enriched terms of GO analysis. **(D)** The top 23 enriched terms of the KEGG pathway. The size of dots indicates the count of DEGs enriched under each term.

CDC20 (r = -0.5446, P < 0.001; Supplemental Figure 3B), CDC6 (r = -0.4985, P < 0.001; Supplemental Figure 3C), MAD2L1 (r = -0.4984, P < 0.001; Supplemental Figure 3D), TTK (r = -0.5531, P < 0.001; Supplemental Figure 3E), MELK (r = -0.5150, P < 0.001; Supplemental Figure 3F), CCNB2 (r = -0.5920, P < 0.001; Supplemental Figure 3G) mRNA expression.

4 Discussion

RAI2 has been proven to suppress early hematogenous dissemination of breast cancer and indicate favorable prognosis by analyzing hundreds of breast cancer patient samples. However, these results need further validation with more patient samples (10, 12). Our results showed that high RAI2 expression could be regarded as an independent and favorable prognostic biomarker for BRCA patients, which predicts tumor invasion and metastasis.

Previous studies found that there was no relation between RAI2 level and lymph node metastasis (10). However, the meta-analysis of 17 GEO datasets in our results showed that lymph node metastasis status had a lower RAI2 mRNA expression level than lymph node non-metastasis status. There was positive relation of RAI2 expression with immune infiltrating levels, including B cells, CD8+ T cells, CD4 + T cells, B cells, and dendritic cells in the BRCA, especially in the BRCA-basal subtype. In addition, our result also showed that RAI2 was positively associated with CX3CR1 and negatively related to CXCL8, respectively. CXCL8 was a well-known chemokine involved in tumorigenesis, tumor progression and immune suppression, and CX3CR1 was regarded as a novel cancer targeted therapeutic strategy due to its immune activation capacity (25, 26). However, the ligands

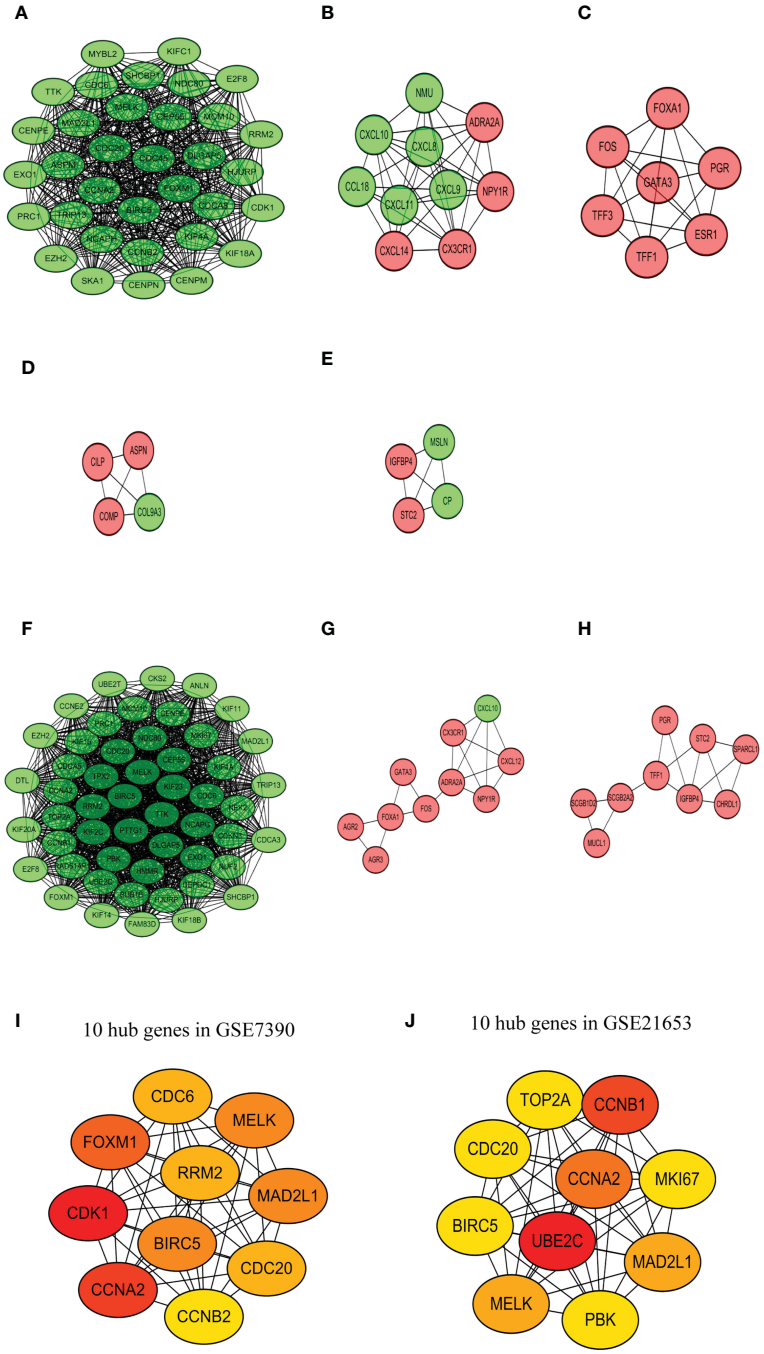

FIGURE 7
PPI network analysis. Top 5 largest size modules of GSE7390 **(A-E)** and top 3 largest size modules of GSE21653 **(F-H)** from the high-score protein-protein interactive network. 10 hub genes in GSE7390 **(I)** and GSE21653 **(J)**.

of CX3CR1, CXCL9, 10, and 11 were downregulated by RAI2, which is not consistent with their well-established immunostimulatory function. There may be two explanations for the bias. On the one hand, CXCL9, 10, and 11 promoted immune response by paracrine signal, while tumor-derived autocrine signal will induce tumor cell proliferation and metastasis (26). We could not investigate whether the downregulated expressions of CXCL9, 10, and 11 were induced by paracrine or autocrine axis. On the other hand, divergent immune response occurred in distinct breast cancer subtypes. Generally, any tumor features that oscillated a tumor toward a more aggressive "basal-like" state will typically elicit a stronger immune reaction (27), which is consistent with our result (Figure 5B). In the PPI network analysis, we performed the correlation based on the overall BRCA subtypes, which could not visualize and restore the true immune state for each subtype. Therefore, there will be some biases in immune-related chemokines. In general, it was reported that immune infiltrates could predict the status of sentinel lymph nodes and were closely associated with survival (22, 23). Therefore, the high

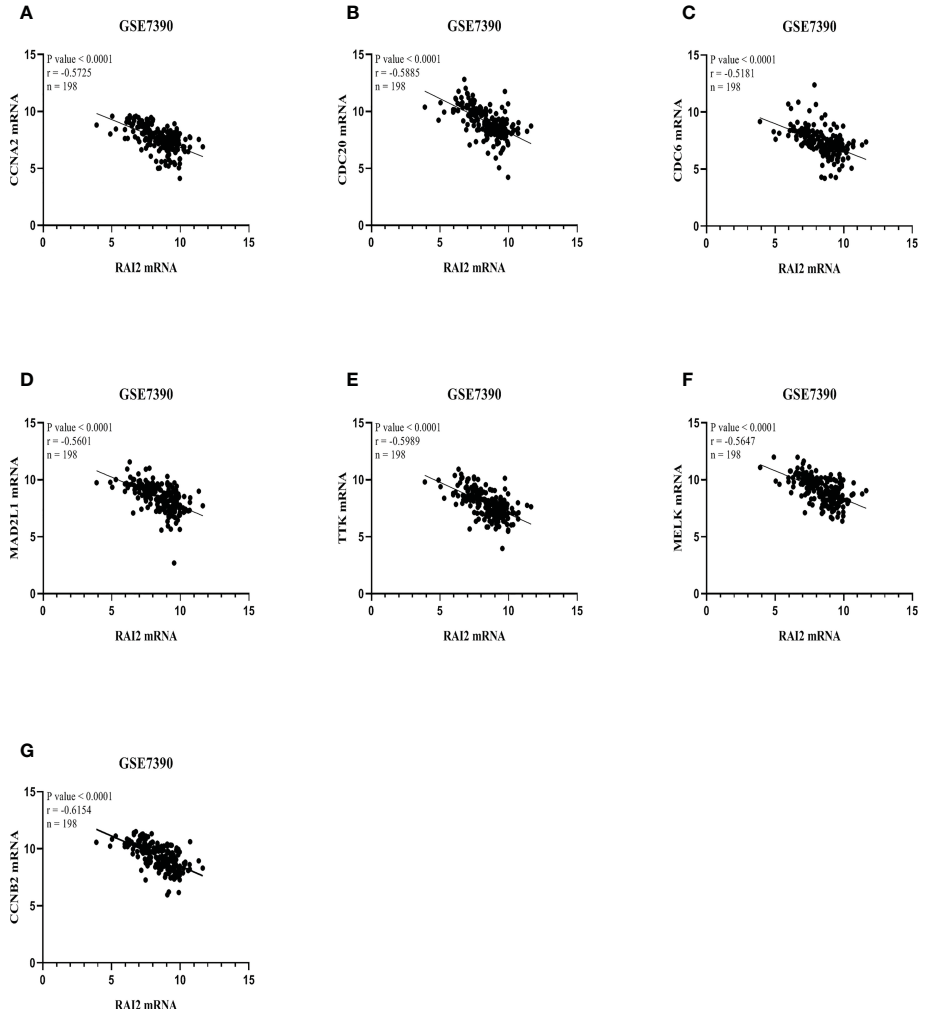

FIGURE 8
RAI2 expression was associated with several core genes in GSE7390. Association between mRNA expressions of RAI2 with several core genes, including CCNA2 **(A)**, CDC20 **(B)**, CDC6 **(C)**, MAD2L1 **(D)**, TTK **(E)**, MELK **(F)**, and CCNB2 **(G)**. CCNA2, CyclinA2; CCNB2, cyclin B2; CDC6, cell division cycle 6; CDC20, cell division cycle 20; MAD2L1, mitotic arrest deficient 2-like 1; MELK, maternal embryonic leucine zipper kinase; TTK, TTK protein kinase; RAI2, retinoic acid-induced 2.

immune infiltrates might contribute to the favorable prognosis in patients with high RAI2 expression.

The results of the functional enrichment of RAI2 mentioned above indicated that RAI2 may be involved in the process of cell proliferation and cell cycle. The common genes in the cell cycle pathway were downregulated in the $RAI2^{high}$ group, including CCNA2, CDC20, CDC6, MAD2L1, and TTK, which suggested that RAI2 expression might regulate the cell cycle by suppressing these gene expressions. Moreover, the common hub genes of DEGs from the two datasets were identified as CCNA2, MAD2L1, MELK, CDC20, and CCNB2.

CCNA2, one of the highly conserved cyclin family, was significantly overexpressed in some cancer cells and had a close relation with tumorigenesis and progression (28). It had been proved that CCNA2 might be implicated in the epithelial-mesenchymal transitions (EMT) and cancer metastasis (29). Furthermore, Gao et al. suggested that high CCNA2 expression predicted poor survival and was also implicated with tamoxifen resistance in ER^+ mammary cancer patients by bioinformatic analysis (30). Based on TCGA datasets, Tang et al. indicated that CCNB2 was implicated with poor prognosis in BRCA and was significantly up-regulated expressed in the advanced cancer stage (31). CDC20, the cell division regulator, was significantly overexpressed in mammary cancer cells and indicated poor survival (32, 33). Moreover, a preclinical study held that CDC20 in ER^+ BRCA predicted inadequate response to endocrine therapy and poor survival (34). Cheng et al. firstly proved the association of CDC20 with BRCA metastasis in preclinical research (35). In ER^+ BRCA, CCNA2, CCNB2, and CDC20 could be inhibited by O6-benzylguanine, an MGMT inhibitor (36). In addition, CDC6 got involved in regulating DNA replication and expressed at a high level in BRCA cells, especially in ER^- BRCA, compared with

normal breast cells (37). By producing chromosomal instability and aneuploidy, the abnormal expression of MAD2L1 might induce malignant transformation and progression of BRCA (38). TTK, a dual serine/threonine kinase, exerted a vital role in spindle assembly checkpoint signaling and mitotic checkpoint (39, 40). Additionally, by regulating the phosphorylation of p53, CHK2, and MDM2, TTK got involved in DNA damage repair (41–43). Previous studies have shown that TTK was up-regulated in triple-negative BRCA, compared to the other BRCA tissues and healthy cells. Furthermore, TTK regulated EMT and proliferative phenotypes through TGF-β and KLF5 signaling (44, 45). Related research indicated that higher MELK expression was a gene signature in BRCA than in normal tissues (46–48). Giuliano et al. found that MELK expression was related to tumor mitotic activity but was not required for tumor development (49). Deng et al. regarded CCNA2 and MELK as part of potential key genes in the process of mitotic cell cycle and EMT pathway for the progression of BRCA by bioinformatic analysis (50).

From the results above, we suggested that RAI2 might get involved in inhibiting the proliferation, invasion, and metastasis of BRCA cells and improving the immune infiltrating levels in BRAC. Moreover, in the development process of BRCA, the lower expression of RAI2 was implicated in the higher expression of CCNA2, CCNB2, CDC20, CDC6, MAD2L1, TTK, and MELK. To discover the role of RAI2 in BRCA, the specific biological mechanisms of the interaction of these genes need further research.

5 Conclusion

Taken together, we estimated the predictive value of RAI2 for BRCA patients. RAI2 could be conceived as a promising prognostic biomarker in each subtype of BRCA. Therefore, our analyses might support RAI2 as the potential prognostic biomarker and contribute to further research of RAI2 as the candidate for therapy target in BRCA diagnosis and treatment.

Data availability statement

Publicly available datasets in this study can be found in TIMER https://cistrome.shinyapps.io/timer/) and GEO (https://www.ncbi.nlm.nih.gov/geo/).

Author contributions

YJ prepared the figures and drafted the manuscript. SL collected data and revised the manuscript and participated in the discussion. JG, KZ, and YX participated in the discussion. All authors contributed to the article and approved the submitted version.

Funding

This research was sponsored by the Medical Science and Technology Project of Henan Province (2018020056), the National Natural Science Foundation of China (81802770), and the Young and Middle-aged Health Science and Technology Innovation Talents Program (YXKC2020036).

Acknowledgments

All authors appreciate TIMER datasets and GEO databases for offering the data on BRCA.

Conflict of interest

The authors declare that the research was conducted in the absence of any commercial or financial relationships that could be construed as a potential conflict of interest.

Publisher's note

Supplementary material

The Supplementary Material for this article can be found online at: https://www.frontiersin.org/articles/10.3389/fonc.2023.1134149/full#supplementary-material

SUPPLEMENTARY FIGURE 1
GO and KEGG enrichment analyses of DEGs from the microarray dataset GSE21653. **(A)** 182 DEGs are shown in a volcano plot. 100 upregulated genes are shown in red, and 82 downregulated genes are shown in green. **(B)** Heatmap of the top 20 upregulated and downregulated DEGs. Red denotes upregulated genes, and blue represents downregulated genes. **(A)** The top 30 enriched terms of GO analysis. **(B)** The top 9 enriched terms of the KEGG pathway. The size of dots indicates the count of DEGs enriched under each term.

SUPPLEMENTARY FIGURE 2
The correlativity of the top 20 upregulated and the top 20 downregulated DEGs in GSE7390 **(A)** and GSE21653 **(B)**.

SUPPLEMENTARY FIGURE 3
RAI2 expression was associated with several core genes in GSE21653. Association between mRNA expressions of RAI2 with several core genes, including CCNA2 **(A)**, CDC20 **(B)**, CDC6 **(C)**, MAD2L1 **(D)**, TTK **(E)**, MELK **(F)**, and CCNB2 **(G)**. CCNA2, CyclinA2; CCNB2, cyclin B2; CDC6, cell division cycle 6; CDC20, cell division cycle 20; MAD2L1, mitotic arrest deficient 2-like 1; MELK, maternal embryonic leucine zipper kinase; TTK, TTK protein kinase; RAI2, retinoic acid-induced 2.

References

1. Siegel RL, Miller KD, Jemal A. Cancer statistics, 2020. *CA Cancer J Clin* (2020) 70 (1):7–30. doi: 10.3322/caac.21590

2. DeSantis CE, Ma J, Gaudet MM, Newman LA, Miller KD, Goding Sauer A, et al. Breast cancer statistics. *CA Cancer J Clin* (2019) 69(6):438–51. doi: 10.3322/caac.21583

3. Imyanitov EN, Kuligina ES. Systemic investigations into the molecular features of bilateral breast cancer for diagnostic purposes. *Expert Rev Mol Diagn* (2020) 20(1):41–7. doi: 10.1080/14737159.2020.1705157

4. Araki K, Miyoshi Y. Mechanism of resistance to endocrine therapy in breast cancer: The important role of PI3K/Akt/mTOR in estrogen receptor-positive, HER2-negative breast cancer. *Breast Cancer* (2018) 25(4):392–401. doi: 10.1007/s12282-017-0812-x

5. Slamon DJ, Clark GM, Wong SG, Levin WJ, Ullrich A, McGuire WL. Human breast cancer: Correlation of relapse and survival with amplification of the HER-2/neu oncogene. *Science* (1987) 235(4785):177–82. doi: 10.1126/science.3798106

6. Loibl S, Gianni L. HER2-positive breast cancer. *Lancet* (2017) 389(10087):2415–29. doi: 10.1016/S0140-6736(16)32417-5

7. Ghyselinck NB, Duester G. Retinoic acid signaling pathways. *Development* (2019) 146(13). doi: 10.1242/dev.167502

8. Walpole SM, Hiriyana KT, Nicolaou A, Bingham EL, Durham J, Vaudin M, et al. Identification and characterization of the human homologue (RAI2) of a mouse retinoic acid-induced gene in Xp22. *Genomics* (1999) 55(3):275–83. doi: 10.1006/geno.1998.5667

9. Jonk LJ, de Jonge ME, Vervaart JM, Wissink S, Kruijer W. Isolation and developmental expression of retinoic-acid-induced genes. *Dev Biol* (1994) 161 (2):604–14. doi: 10.1006/dbio.1994.1056

10. Werner S, Brors B, Eick J, Marques E, Pogenberg V, Parret A, et al. Suppression of early hematogenous dissemination of human breast cancer cells to bone marrow by retinoic acid-induced 2. *Cancer Discov* (2015) 5(5):506–19. doi: 10.1158/2159-8290.CD-14-1042

11. Yan W, Wu K, Herman JG, Xu X, Yang Y, Dai G, et al. Retinoic acid-induced 2 (RAI2) is a novel tumor suppressor, and promoter region methylation of RAI2 is a poor prognostic marker in colorectal cancer. *Clin Epigenet* (2018) 10:69. doi: 10.1186/s13148-018-0501-4

12. Nishikawa S, Uemoto Y, Kim TS, Hisada T, Kondo N, Wanifuchi-Endo Y, et al. Low RAI2 expression is a marker of poor prognosis in breast cancer. *Breast Cancer Res Treat* (2021) 187(1):81–93. doi: 10.1007/s10549-021-06176-w

13. Smith SC, Theodorescu D. Learning therapeutic lessons from metastasis suppressor proteins. *Nat Rev Cancer* (2009) 9(4):253–64. doi: 10.1038/nrc2594

14. Li T, Fan J, Wang B, Traugh N, Chen Q, Liu JS, et al. TIMER: A web server for comprehensive analysis of tumor-infiltrating immune cells. *Cancer Res* (2017) 77(21): e108–10. doi: 10.1158/1538-7445.AM2017-108

15. Ritchie ME, Phipson B, Wu D, Hu Y, Law CW, Shi W, et al. Limma powers differential expression analyses for RNA-sequencing and microarray studies. *Nucleic Acids Res* (2015) 43(7):e47. doi: 10.1093/nar/gkv007

16. The Gene Ontology Consortium. The gene ontology resource: 20 years and still GOing strong. *Nucleic Acids Res* (2019) 47(D1):D330–8. doi: 10.1093/nar/gky1055

17. Kanehisa M, Goto S, Sato Y, Furumichi M, Tanabe M. KEGG for integration and interpretation of large-scale molecular data sets. *Nucleic Acids Res* (2012) 40(Database issue):D109–114. doi: 10.1093/nar/gkr988

18. Yu G, Wang LG, Yan GR, He QY. DOSE: an R/Bioconductor package for disease ontology semantic and enrichment analysis. *Bioinformatics* (2015) 31(4):608–9. doi: 10.1093/bioinformatics/btu684

19. Yu G, Wang LG, Han Y, He QY. clusterProfiler: An r package for comparing biological themes among gene clusters. *Omics* (2012) 16(5):284–7. doi: 10.1089/omi.2011.0118

20. Shannon P, Markiel A, Ozier O, Baliga NS, Wang JT, Ramage D, et al. Cytoscape: A software environment for integrated models of biomolecular interaction networks. *Genome Res* (2003) 13(11):2498–504. doi: 10.1101/gr.1239303

21. Chin CH, Chen SH, Wu HH, Ho CW, Ko MT, Lin CY. cytoHubba: identifying hub objects and sub-networks from complex interactome. *BMC Syst Biol* (2014) 8 Suppl 4(Suppl 4):S11. doi: 10.1186/1752-0509-8-S4-S11

22. Ohtani H. Focus on TILs: Prognostic significance of tumor infiltrating lymphocytes in human colorectal cancer. *Cancer Immun* (2007) 7:4.

23. Azimi F, Scolyer RA, Rumcheva P, Moncrieff M, Murali R, McCarthy SW, et al. Tumor-infiltrating lymphocyte grade is an independent predictor of sentinel lymph node status and survival in patients with cutaneous melanoma. *J Clin Oncol* (2012) 30 (21):2678–83. doi: 10.1200/JCO.2011.37.8539

24. Szklarczyk D, Gable AL, Lyon D, Junge A, Wyder S, Huerta-Cepas J, et al. STRING v11: Protein-protein association networks with increased coverage, supporting functional discovery in genome-wide experimental datasets. *Nucleic Acids Res* (2019) 47(D1):D607–d613. doi: 10.1093/nar/gky1131

25. Xiong X, Liao X, Qiu S, Xu H, Zhang S, Wang S, et al. CXCL8 in tumor biology and its implications for clinical translation. *Front Mol Biosci* (2022) 9:723846. doi: 10.3389/fmolb.2022.723846

26. Tokunaga R, Zhang W, Naseem M, Puccini A, Berger MD, Soni S, et al. CXCL9, CXCL10, CXCL11/CXCR3 axis for immune activation - a target for novel cancer therapy. *Cancer Treat Rev* (2018) 63:40–7. doi: 10.1016/j.ctrv.2017.11.007

27. Onkar SS, Carleton NM, Lucas PC, Bruno TC, Lee AV, Vignali DAA, et al. The great immune escape: Understanding the divergent immune response in breast cancer subtypes. *Cancer Discov* (2023) 13(1):23–40. doi: 10.1158/2159-8290.CD-22-0475

28. Uhlen M, Oksvold P, Fagerberg L, Lundberg E, Jonasson K, Forsberg M, et al. Towards a knowledge-based human protein atlas. *Nat Biotechnol* (2010) 28(12):1248–50. doi: 10.1038/nbt1210-1248

29. Bendris N, Arsic N, Lemmers B, Blanchard JM. Cyclin A2, rho GTPases and EMT. *Small GTPases* (2012) 3(4):225–8. doi: 10.4161/sgtp.20791

30. Gao T, Han Y, Yu L, Ao S, Li Z, Ji J. CCNA2 is a prognostic biomarker for ER+ breast cancer and tamoxifen resistance. *PloS One* (2014) 9(3):e91771. doi: 10.1371/journal.pone.0091771

31. Tang J, Kong D, Cui Q, Wang K, Zhang D, Gong Y, et al. Prognostic genes of breast cancer identified by gene Co-expression network analysis. *Front Oncol* (2018) 8:374. doi: 10.3389/fonc.2018.00374

32. Yuan B, Xu Y, Woo JH, Wang Y, Bae YK, Yoon DS, et al. Increased expression of mitotic checkpoint genes in breast cancer cells with chromosomal instability. *Clin Cancer Res* (2006) 12(2):405–10. doi: 10.1158/1078-0432.CCR-05-0903

33. Karra H, Repo H, Ahonen I, Löyttyniemi E, Pitkänen R, Lintunen M, et al. Cdc20 and securin overexpression predict short-term breast cancer survival. *Br J Cancer* (2014) 110(12):2905–13. doi: 10.1038/bjc.2014.252

34. Alfarsi LH, Ansari RE, Craze ML, Toss MS, Masisi B, Ellis IO, et al. CDC20 expression in oestrogen receptor positive breast cancer predicts poor prognosis and lack of response to endocrine therapy. *Breast Cancer Res Treat* (2019) 178(3):535–44. doi: 10.1007/s10549-019-05420-8

35. Cheng S, Castillo V, Sliva D. CDC20 associated with cancer metastasis and novel mushroom–derived CDC20 inhibitors with antimetastatic activity. *Int J Oncol* (2019) 54(6):2250–6. doi: 10.3892/ijo.2019.4791

36. Bobustuc GC, Kassam AB, Rovin RA, Jeudy S, Smith JS, Isley B, et al. MGMT inhibition in ER positive breast cancer leads to CDC2, TOP2A, AURKB, CDC20, KIF20A, cyclin A2, cyclin B2, cyclin D1, ERα and survivin inhibition and enhances response to temozolomide. *Oncotarget* (2018) 9(51):29727–42. doi: 10.18632/oncotarget.25696

37. Mahadevappa R, Neves H, Yuen SM, Bai Y, McCrudden CM, Yuen HF, et al. The prognostic significance of Cdc6 and Cdt1 in breast cancer. *Sci Rep* (2017) 7(1):985. doi: 10.1038/s41598-017-00998-9

38. Zhu XF, Yi M, He J, Tang W, Lu MY, Li T, et al. Pathological significance of MAD2L1 in breast cancer: An immunohistochemical study and meta analysis. *Int J Clin Exp Pathol* (2017) 10(9):9190–201.

39. Hiruma Y, Sacristan C, Pachis ST, Adamopoulos A, Kuijt T, Ubbink M, et al. CELL DIVISION CYCLE. competition between MPS1 and microtubules at kinetochores regulates spindle checkpoint signaling. *Science* (2015) 348(6240):1264–7. doi: 10.1126/science.aaa4055

40. Ji Z, Gao H, Jia L, Li B, Yu H. A sequential multi-target Mps1 phosphorylation cascade promotes spindle checkpoint signaling. *Elife* (2017) 6:e22513. doi: 10.7554/eLife.22513

41. Huang YF, Chang MD, Shieh SY. TTK/hMps1 mediates the p53-dependent postmitotic checkpoint by phosphorylating p53 at Thr18. *Mol Cell Biol* (2009) 29 (11):2935–44. doi: 10.1128/MCB.01837-08

42. Maachani UB, Kramp T, Hanson R, Zhao S, Celiku O, Shankavaram U, et al. Targeting MPS1 enhances radiosensitization of human glioblastoma by modulating DNA repair proteins. *Mol Cancer Res* (2015) 13(5):852–62. doi: 10.1158/1541-7786.MCR-14-0462-T

43. Yu ZC, Huang YF, Shieh SY. Requirement for human Mps1/TTK in oxidative DNA damage repair and cell survival through MDM2 phosphorylation. *Nucleic Acids Res* (2016) 44(3):1133–50. doi: 10.1093/nar/gkv1173

44. Maire V, Baldeyron C, Richardson M, Tesson B, Vincent-Salomon A, Gravier E, et al. TTK/hMPS1 is an attractive therapeutic target for triple-negative breast cancer. *PloS One* (2013) 8(5):e63712. doi: 10.1371/journal.pone.0063712

45. King JL, Zhang B, Li Y, Li KP, Ni JJ, Saavedra HI, et al. TTK promotes mesenchymal signaling *via* multiple mechanisms in triple negative breast cancer. *Oncogenesis* (2018) 7(9):69. doi: 10.1038/s41389-018-0077-z

46. Pickard MR, Green AR, Ellis IO, Caldas C, Hedge VL, Mourtada-Maarabouni M, et al. Dysregulated expression of fau and MELK is associated with poor prognosis in breast cancer. *Breast Cancer Res* (2009) 11(4):R60. doi: 10.1186/bcr2350

47. Komatsu M, Yoshimaru T, Matsuo T, Kiyotani K, Miyoshi Y, Tanahashi T, et al. Molecular features of triple negative breast cancer cells by genome-wide gene expression profiling analysis. *Int J Oncol* (2013) 42(2):478–506. doi: 10.3892/ijo.2012.1744

48. Liu R, Guo CX, Zhou HH. Network-based approach to identify prognostic biomarkers for estrogen receptor-positive breast cancer treatment with tamoxifen. *Cancer Biol Ther* (2015) 16(2):317–24. doi: 10.1080/15384047.2014.1002360

49. Giuliano CJ, Lin A, Smith JC, Palladino AC, Sheltzer JM. MELK expression correlates with tumor mitotic activity but is not required for cancer growth. *Elife* (2018) 7:e32838. doi: 10.7554/eLife.32838

50. Deng JL, Xu YH, Wang G. Identification of potential crucial genes and key pathways in breast cancer using bioinformatic analysis. *Front Genet* (2019) 10:695. doi: 10.3389/fgene.2019.00695

frontiers | Frontiers in Medicine

TYPE Original Research
PUBLISHED 17 April 2023
DOI 10.3389/fmed.2023.1153537

OPEN ACCESS

EDITED BY
Yujiao Deng,
The Second Affiliated Hospital of Xi'an Jiaotong University, China

REVIEWED BY
Hoda Elkafas,
University of Illinois Chicago, United States
Junying Tang,
First Affiliated Hospital of Chongqing Medical University, China
Qiwei Yang,
Second Military Medical University, China

*CORRESPONDENCE
Hanwang Zhang
✉ hwzhang605@126.com

†These authors have contributed equally to this work

SPECIALTY SECTION
This article was submitted to Precision Medicine, a section of the journal Frontiers in Medicine

RECEIVED 01 February 2023
ACCEPTED 29 March 2023
PUBLISHED 17 April 2023

CITATION
Cai L, Li J, Long R, Liao Z, Gong J, Zheng B and Zhang H (2023) An autophagy-related diagnostic biomarker for uterine fibroids: FOS. *Front. Med.* 10:1153537. doi: 10.3389/fmed.2023.1153537

An autophagy-related diagnostic biomarker for uterine fibroids: FOS

Lei Cai[1†], Jie Li[1†], Rui Long[1], Zhiqi Liao[1], Juejun Gong[2], Bowen Zheng[3] and Hanwang Zhang[1*]

[1]Reproductive Medicine Center, Tongji Hospital, Tongji Medical College, Huazhong University of Science and Technology, Wuhan, China, [2]Department of Oncology, The Central Hospital of Wuhan, Tongji Medical College, Huazhong University of Science and Technology, Wuhan, China, [3]Medical Record Department, Women and Children's Hospital of Chongqing Medical University, Chongqing, China

Uterine fibroids (UFs) are the most common benign gynecologic tumors in reproductive-aged women. The typical diagnostic strategies of UFs are transvaginal ultrasonography and pathological feature, while molecular biomarkers are considered conventional options in the assessment of the origin and development of UFs in recent years. Here, we extracted the differential expression genes (DEGs) and differential DNA methylation genes (DMGs) of UFs from the Gene Expression Omnibus (GEO) database, GSE64763, GSE120854, GSE45188, and GSE45187. 167 DEGs with aberrant DNA methylation were identified, and further Gene Ontology (GO) enrichment and Kyoto Encyclopedia of Genes and Genomes (KEGG) were performed by the relevant R package. We next discerned 2 hub genes (FOS, and TNFSF10) with autophagy involvement by overlapping 167 DEGs and 232 autophagic regulators from Human Autophagy Database. FOS was identified as the most crucial gene through the Protein–Protein Interactions (PPI) network with the correlation of the immune scores. Moreover, the down-regulated expression of FOS in UFs tissue at both mRNA and protein levels was validated by RT-qPCR and immunohistochemistry respectively. The area under the ROC curve (AUC) of FOS was 0.856, with a sensitivity of 86.2% and a specificity of 73.9%. Overall, we explored the possible biomarker of UFs undergoing DNA—methylated autophagy and provided clinicians with a comprehensive assessment of UFs.

KEYWORDS

uterine fibroids, autophagy, FOS, bioinformatics analysis, biomarker

1. Introduction

Uterine fibroids (UFs), also known as uterine leiomyoma, are the most common solid neoplasm in women with an estimated incidence of up to 70% (1). The established risk factors of UFs include increased age until menopause, premenopausal status, hypertension, obesity, or other chronic psychological stress, etc. (2–4). The symptomatic fibroids can manifest with prolonged or heavy menstrual bleeding and the sequelae of uterine enlargement, for instance, pelvic pressure, urinary frequency, and constipation, and it can be associated with infertility and other poor obstetrical outcomes (5). UFs caused the deterioration of the quality of life in women at reproductive age (6) and caused an extremely high economic burden on society (7, 8). Although transvaginal ultrasonography

and pathological feature are the main diagnostic tools of UFs (9), molecular biomarkers are considered conventional strategies in the assessment of the origin and development of UFs in recent years (10). The highly prevalent condition of UFs restricted the biomarkers in a strict sensitivity and specificity to ensure their effectiveness. The efficacious biomarker should guarantee sensitivity >75% and specificity >99.6% (11). Thus, the accuracy biomarkers of UFs diagnosis still needed to be explored.

Autophagy is an evolutionarily conserved process that delivered a portion of the cytoplasm, such as ruptured lysosomes, intracellular microbes, and damaged mitochondria, into lysosomes for degradation via autophagosome formation (12). This process plays a crucial role in the pathogenesis of many diseases including uterine fibroids (13–15). The attenuation of autolysosomes in UFs tissue illustrated the defection of the fusion of the autophagosome with a lysosome in the late stages of autophagy (14). The primary uterine fibroids cells exhibited autophagic response after the stimulation with estradiol (E2) or ulipristal acetate, which is represented by required autophagy-related proteins (ATGs), MAP1LC3 (LC3), and P62, indicating that autophagy significantly involved in the pathophysiology of UFs (15–17). The regulation of autophagy is complex and dynamic, while epigenetics are considered to be the conspicuous machinery regulator of this process, particularly DNA methylation (18–20). DNA methylation is an important epigenetic mechanism of the transfer of a methyl (-CH3) group to the fifth carbon of a cytosine to form 5-methylcytosine (5mC) which induced the modification of gene expression (21). This process is generally presented as transcriptional silencing and occurs predominantly in cytosine guanine dinucleotide (CpG) dinucleotides (22). The genomic maps of DNA methylation, based on CpG site detection, provide information on regulatory regions of genes, those genes are functionally categorized in both ATGs and signal molecule genes that regulate autophagy (18).

The DNA methylation status of UFs is exhibited in the decreasing of DNA methyltransferases (DNMTs), subtypes DNMT3A (DNA methyltransferase 3 alpha) and DNMT3B (DNA methyltransferase 3 beta) (23). The genome-wide DNA methylation status in UFs tissue is distinguished from normal myometrium and the differential methylated genomic locus was also presented in UFs (24–27). The hypomethylated/hypermethylated genes are proven to participate in the proliferation, apoptosis, metabolism, and extracellular matrix formation of UFs (25). Nevertheless, whether the autophagic dysregulation in UFs is regulated by DNA methylation is still unknown.

In the present study, we extracted the hub genes in both differential expression and differential DNA methylation profiles in UFs from Gene Expression Omnibus (GEO) datasets. Identified the autophagic regulators from Human Autophagy Database throughout those hub genes. And the candidate was validated by further RT-qPCR, and immunohistochemistry. We aimed to explore the possible biomarker of UFs undergoing DNA-methylated autophagy, the diagnostic value was performed by the receiver operating characteristic (ROC) curve.

2. Materials and methods

2.1. Data collection

All datasets were downloaded from Gene Expression Omnibus (GEO) database[1] with keywords: "uterine myoma," "fibroid" or "leiomyoma," and "DNA methylation." The inclusion criteria included: (1) The organism was limited to UFs and normal myometrium. (2) All datasets were genome-wide gene expression profiles. (3) Case and control study. The exclusion criteria was another tissue. Four datasets (GSE64763, GSE120854, GSE45188, and GSE45187) were selected. Samples of UFs and normal myometrium were used for subsequent analysis. The gene expression profile and the genome-wide DNA methylation profile were extracted from GSE64763 and GSE120854 respectively as the discovery cohorts. And GSE45187 and GSE45188 were presented as the validation cohorts. The detailed information of all the datasets were summarized in **Table 1**.

2.2. Data processing

The "limma" package was used to analyze mRNA expression data and the "ChAMP" package was used to analyze DNA methylation data (28–30). All mRNA expression data were normalized by "normalizeBetweenArrays()" function. The DNA methylation expression data were normalized by "champ.norm()" function. The "pheatmap" package was used to cluster samples and discard outliers (**Supplementary Figure 1**). Outliers included GSM1579399 and GSM1579420 for mRNA, GSM3417163, GSM3417156, GSM3417160, GSM3417145, GSM417146, GSM417147, and GSM417148 for DNA methylation.

2.3. Identified the differentially expressed genes (DEGs)

The DEGs between the uterine fibroid and normal myometrium samples were identified using "limma" package (version 3.50.0) and the threshold for identifying DEGs was set to |log2fold change (log2FC)| > 1 and adjusted P value < 0.05 (30).

2.4. Identified differentially methylation genes (DMGs)

Identification of DMGs between uterine fibroid and normal myometrium was analyzed by "ChAMP" package (version 3.50.0) (29). The results of DMGs were filtered with |log2FC| > 0.1 and adjust P value < 0.05.

1 https://www.ncbi.nlm.nih.gov/geo/

TABLE 1 Gene Expression Omnibus (GEO) data sets.

Dataset	Organism	Platform	Data type	Sample type	Purpose
GSE64763	*Homo sapiens*	GPL571	Expression profiling by array	Uterine fibroid (n = 25)	Discovery cohort
				Normal myometrium (n = 29)	
GSE120854	*Homo sapiens*	GPL23976	Methylation profiling by array	Uterine fibroid (n = 24)	Discovery cohort
				Normal myometrium (n = 10)	
GSE45187	*Homo sapiens*	GPL13534	Methylation profiling by array	Uterine fibroid (n = 3)	Validation cohort
				Normal myometrium (n = 3)	
GSE45188	*Homo sapiens*	GPL6244	Expression profiling by array	Uterine fibroid (n = 3)	Validation cohort

2.5. Gene Ontology (GO) and Kyoto Encyclopedia of Genes and Genomes (KEGG) enrichment

The GO and KEGG enrichment analysis of the DEGs were performed by the "clusterProfiler" (version 4.2.1) package (31). We filtered the results with a threshold set to P value < 0.05 and false discovery rate (FDR) < 0.05.

2.6. Protein–Protein Interaction network (PPI)

STRING[2] is an online database for predicting interactions between proteins encoded by DEGs. We constructed the PPI network based on the STRING database and Cytoscape (version 3.8.2) software was used to visualize the results.

2.7. Estimation of stromal and immune scores

The scores of immune cells/stromal cells for the uterine fibroid and normal myometrium samples were calculated using the "ESTIMATE" package (version 1.0.13) based on the gene expression data extracted from GSE64763 dataset. Wilcoxon test was used to test the scoring results. The threshold was set to $P < 0.05$ as significant.

2.8. Relationship between key genes and immune status

The correlation coefficient between the key genes and the immune status for uterine fibroid and normal myometrium samples was calculated. Spearman correlation analysis was conducted after excluding the data from normal distribution. The statistical significance was set as $P < 0.05$.

2.9. Patients

This study included patients who were histologically diagnosed with uterine fibroids and underwent subsequent myomectomy or hysterectomy in Tongji Hospital from 2018 to 2022. The participants were excluded if they had been diagnosed with major medical problems, such as cardiovascular disease, diabetes, and autoimmune disease. The patients who were diagnosed with other gynecological diseases, such as adenomyosis, abnormal uterine bleeding, or cancers in the reproductive system were also excluded. They were also excluded if they were taking estrogen or progesterone before the surgery. Paired normal myometrium was biopsied at a distance of 2 cm from the fibroids. The basic information about the patients was obtained from the patient information management system of Tongji Hospital. The study was approved by the Ethics Committee of Tongji Medical College, Huazhong University of Science and Technology (2022S068).

2.10. RT-qPCR

Total RNA was isolated from UFs and normal myometrium tissue using RNA-easy Isolation Reagent (Vazyme, R701) according to the manufacturer's instruction. Total RNA was converted to cDNA using PrimeScript^{TM} RT Master Mix (Takara, RR036A). Then, real-time PCR analyses were carried out by using Taq Pro Universal SYBR qPCR Master Mix (Vazyme, Q712-02). The PCR primers were listed as follows: cFOS-F: GGGGCAAGGTGGAACAGTTAT, cFOS-R: CCGCTTGGAGTGTATCAGTCA, GAPDH-F: CTTG AATCGTTGTTGTTATG, GAPDH-R: ATGGTGGTATTTG TAGGC.

2.11. Immunohistochemistry

The 4μm thickness section of paraffin-embedded fibroids and myometrium tissue were deparaffinized and rehydrated using graded xylene and alcohol. The slides were boiled in Tris/EDTA buffer for the unmasking of the antigenic epitopes. Then the endogenous peroxidase activity was quenched by 10% H_2O_2. Goat serum was used to block for 30min, RT. The slides were then incubated with the primary antibody of cFOS (Abcam, ab222699, 1:400) overnight, then following by the HRP-labeled secondary antibody incubation the next morning after 3 times phosphate buffer saline with Tween 20 (PBST) washing. The 3,3-diaminobenzidine tetrahydrochloride (DAB) substrate-chromogen system was used to detect the peroxidase activity. The following calculation of all slides was derived from the previous report (32).

2 https://cn.string-db.org/

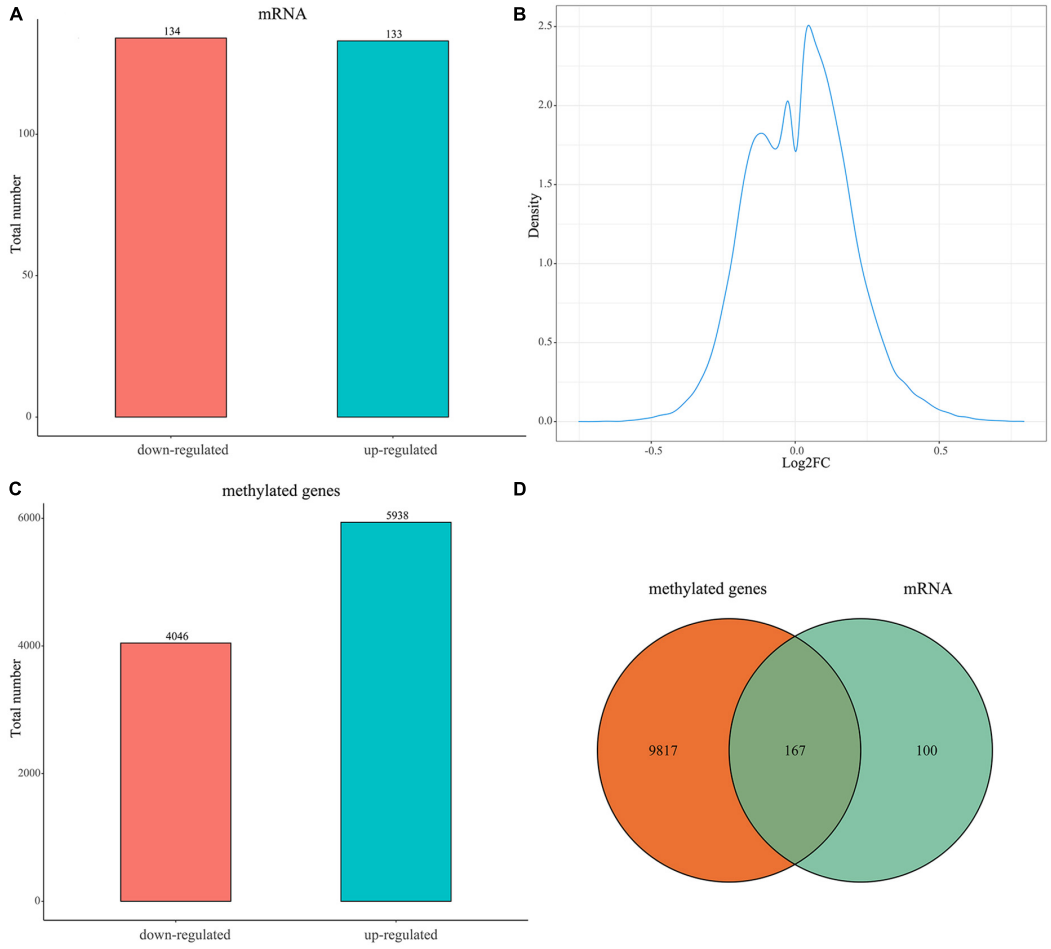

FIGURE 1
Expression of DEGs and DMGs between the uterine fibroid and normal myometrium tissue. **(A)** Bar plot for differentially expressed genes (DEGs) between the two groups. Red bar, down-regulated DEGs in UFs compared with NM; blue bar, up-regulated DEGs in UFs compared with NM. **(B)** Distribution characteristics of log2FC of differential methylation probes. The X-axis is the log2FC value of the differential methylation probe (UFs vs. NM). **(C)** Bar plot for differentially methylated genes (DMGs) between the two groups, Red bar, down-regulated DMGs in UFs; blue bar, up-regulated DMGs in UFs compared with NM. **(D)** Venn diagram of DMGs and DEGs, the overlapped part is used for further analysis. NM, normal myometrium, UFs, uterine fibroids.

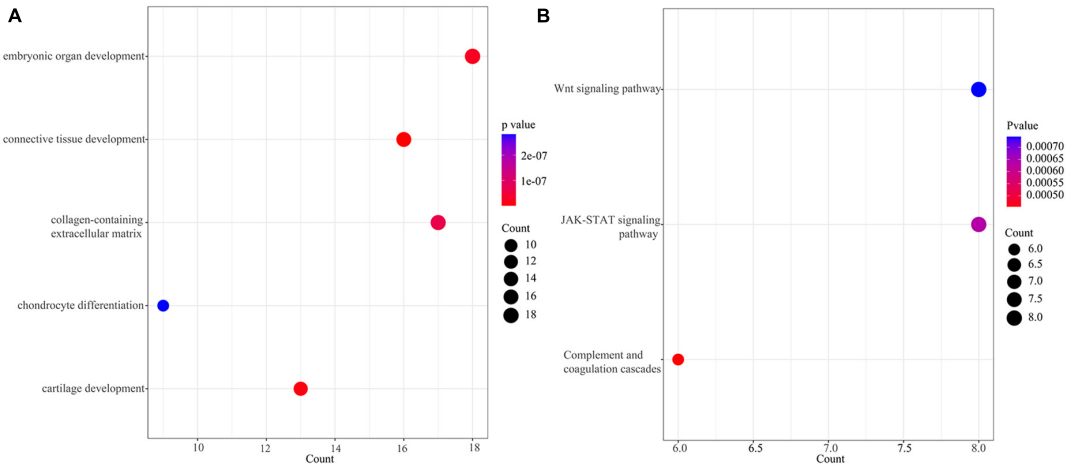

FIGURE 2
Enrichment of methylation related genes (MRGs). **(A)** The top 5 terms (ordered from small to large by FDR) of GO enrichment analysis. **(B)** KEGG of MRGs.

2.12. ROC curve analysis

The "pROC" package (version 1.18.0) was used for ROC curve analysis and the area under the curve (AUC) was used to estimate the diagnostic value of key genes. We verified the expression of key genes in samples at the DNA methylation level and mRNA expression level.

2.13. Statistical analysis

The statistical significance of differences between the two groups in Figures 5, 6 was analyzed using a *t*-test. *P* value less than 0.05 was considered significant. All analyses were conducted on R (version 4.1.2) and SPSS (version 24.0).

3. Results

3.1. Identification of DEGs and DMGs

A total of 267 DEGs between the uterine fibroid and normal myometrium tissue (133 up-regulated and 134 down-regulated) were identified in GSE64763 (Figure 1A and Supplementary Table 1). Differentially methylation probes were identified under the threshold of $|\log2FC| > 0.1$ (Figure 1B). Among them, 4,046 hypomethylation genes and 5938 hypermethylation genes were extracted (Figure 1C). There were 167 genes overlapped in DEGs and DMGs (Figure 1D and Supplementary Table 1). We mainly carried out the follow-up analysis on these 167 genes.

3.2. Enrichment of methylation related genes (MRGs)

The extracted 167 DEGs with distinct methylation levels were defined as methylation related genes (MRGs). We performed functional enrichment analysis on 167 MRGs. Figure 2A showed the top five terms (ordered by FDR) of GO enrichment analysis (Supplementary Table 2). A total of three pathways were enriched under the KEGG analysis, including the "Wnt signaling pathway," "JAK-STAT signaling pathway," and "Complement and coagulation cascades" (Figure 2B and Supplementary Table 2).

3.3. Autophagy and PPI

We extracted 232 autophagy related genes from the autophagy website[3] (Supplementary Table 3), then overlapped 167 MRGs with those 232 autophagy related genes, FOS and TNFSF10 were identified. The mRNA expression of FOS and TNFSF10 in the UFs and myometrium was verified based on the normalized datasets. As shown in Figure 3A, both the FOS and TNFSF10 expression was down-regulated in the UFs group compared with the normal myometrium. The PPI network was visualized based on 167 MRGs with the combined scores of every node restricted over 0.5 (Supplementary Table 4). As shown in Figure 3B, the green-marked FOS and TNFSF10 were illustrated, and FOS connected with more complex interaction network than TNFSF10. Therefore, further analysis was presented with FOS priority.

3.4. Estimation of stromal and immune scores

The stromal and immune scores were further estimated based on the extracted dataset. The immune scores of uterine fibroid samples were significantly lower than that of normal myometrium (Figure 4A), while the stromal scores showed no significant difference between UFs and myometrium (Figure 4B). FOS presented a correlation with immune scores and the immune scores were raising up along with the increase in FOS expression level (Figure 4C). The stromal scores presented no correlation with the FOS expression according to the spearman analysis (Figure 4D).

3.5. Baseline characteristics of the patients

The characteristics of the total of 20 recruited patients were presented in Table 2. The mean age of the patients (±standard deviation) was 44.2 ± 5.75 years, ranging from 31 to 56. The 7(35%) of fibroids were located in the anterior of the uterine in this study. The maximum diameter of fibroids was less than 8 cm in most of the patients (18/20). Most of the patients (18/20) had no history of myomectomy before.

3.6. The expression of FOS in fibroids and normal myometrium from UFs patients

The expression of FOS was investigated using real-time quantitative PCR and IHC in the fibroid and paired myometrium from 20 UFs patients. As shown in Figure 5, FOS was downregulated in the fibroid tissue compared with the normal in both mRNA (Figure 5A) and protein levels (Figure 5B, C). Compared with the partial positive of FOS in the myometrium, fibroid tissue was nearly negative in FOS, only a minority week-stained cell could be captured in the IHC slice, and the IHC score of all samples was shown in Figure 5C.

3.7. Diagnostic value

The diagnosis model of FOS was built based on GSE64763. AUC was 0.856 (95% confidence interval: 75.2–95.9%), and the sensitivity and specificity were 0.862 and 0.739, respectively (Figure 6A). GSE45188 was used as a validation cohort to support the low expression of FOS in the fibroid samples (Figure 6B and Supplementary Table 5). Figures 6C, D showed the differential methylation probes of FOS, indicating that FOS was in the

3 http://www.autophagy.lu/index.html

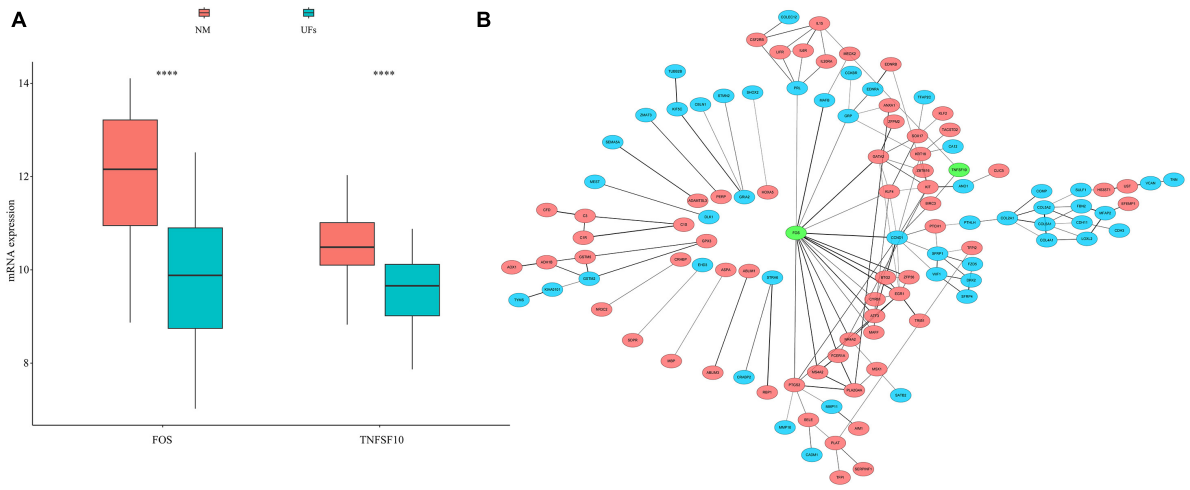

FIGURE 3
Autophagy genes in methylation related genes (MRGs). **(A)** The expression differences of autophagy gene in MRGs. **(B)** PPI network of MRGs and the position of autophagy gene in the network. Red marks down-regulated MRGs, blue marks up-regulated MRGs, and green marks the location of autophagy genes. NM, normal myometrium, UFs, uterine fibroids. ****$P < 0.0001$.

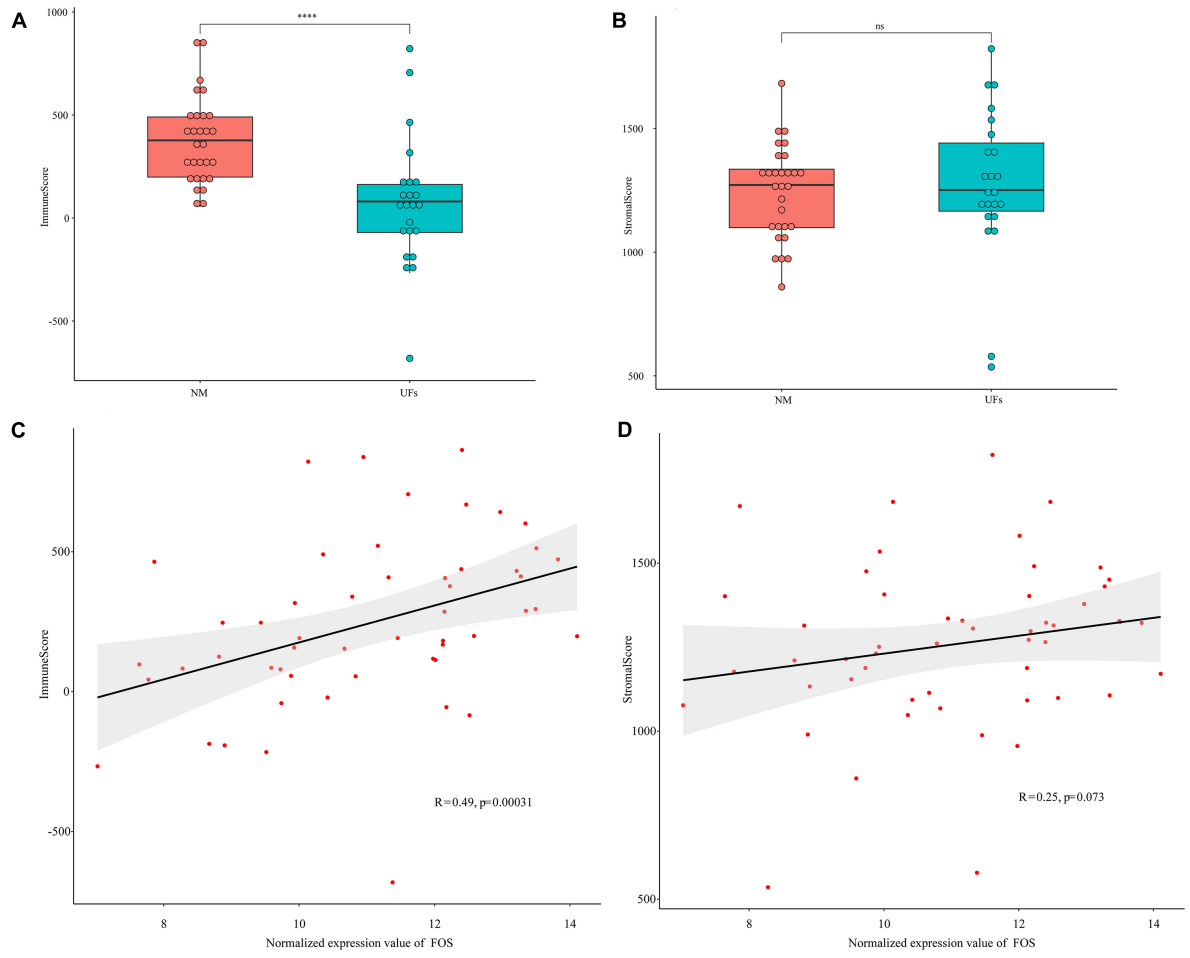

FIGURE 4
Estimation of stromal and immune scores between the fibroid and normal myometrium tissue. **(A)** Immune scores in the two groups. **(B)** Stromal scores in the two groups. **(C,D)** Correlation between FOS and stromal scores as well as immune scores. ****$P < 0.0001$.

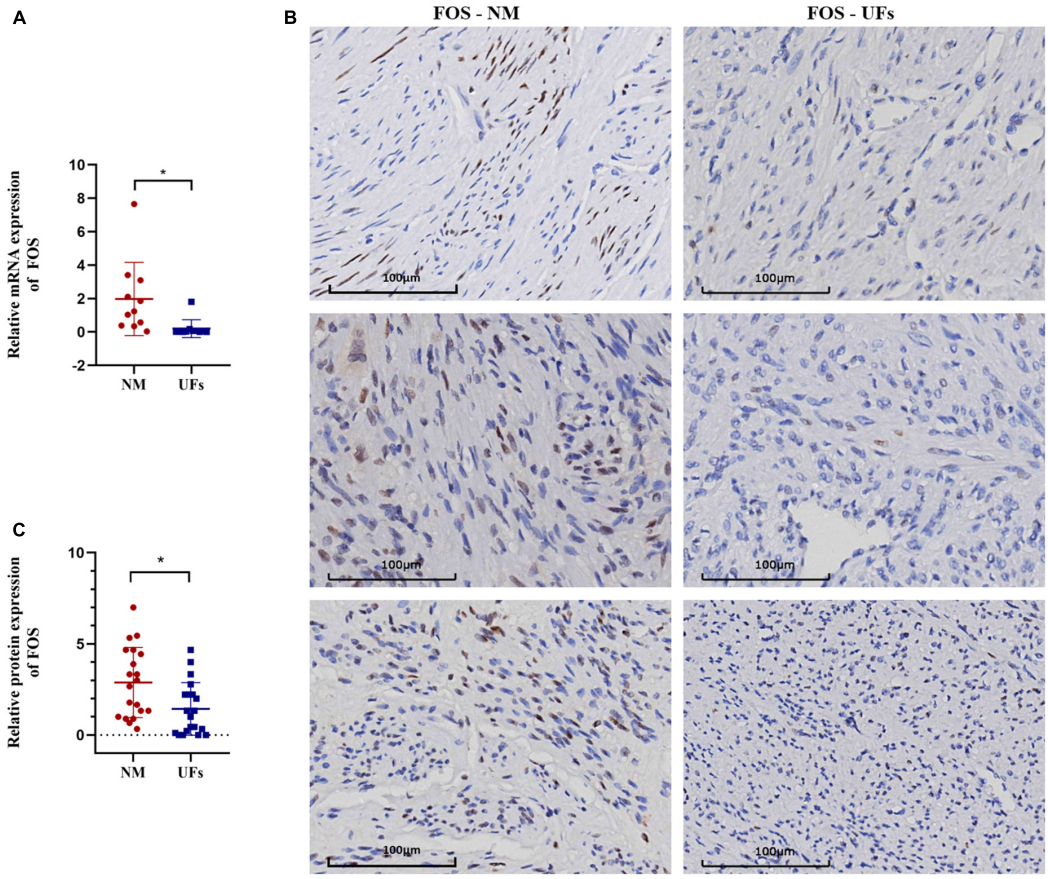

FIGURE 5
The expression of FOC in fibroid and normal myometrium tissue. **(A)** The relative expression of FOS in the mRNA level. **(B)** Immunohistochemical results of typical samples from two groups, all images were presented at 20-X. **(C)** IHC score. NM, normal myometrium, UFs, uterine fibroids. *$P < 0.05$.

hypermethylation state in the fibroid samples (Supplementary Table 5).

4. Discussion

Uterine fibroids (UFs) are regarded as the most common pelvic tumors in women of childbearing age and usually cause heavy menstrual bleeding, pain, and infertility. Although previous studies have demonstrated the potential biomarkers for the origin and development of UFs, the efficacies were still unclear. In this study, FOS was identified as a potential biomarker as well as a possible molecular mechanism underlying the development of UFs by comprehensively analyzing multiple databases and validating the down-regulated expression of FOS in UFs tissue by IHC and RT-PCR.

It has been widely recognized that aberrant DNA methylation is significantly associated with UFs. Several studies demonstrated that the aberrant DNA methylation of the key tumor suppressor and developmental genes may partly involve in the pathogenesis of UFs via genome-wide DNA methylation assays and *in vitro* experiments (24). Therefore, in the current study, we analyzed the overlapped DEGs and DMGs of 4 datasets, including GSE64763, GSE120854, GSE45188, and GSE45187. A total of 167 DEGs with aberrant DNA methylation were identified between UFs and normal myometrium tissue samples. According to further GO and KEGG analysis, the DEGs were mainly enriched in connective tissue development and collagen-containing extracellular matrix, as well as the Wnt signaling pathway and JAK-STAT signaling pathway. The GO enrichment results are in line with our common experiments since UFs are composed of smooth muscle cells and varying amounts of fibrous connective tissue (33). The wingless-type (Wnt) signaling is considered a growth and development-related factor of the UFs, the elevated expression of WNT11, WNT16, and WNT5b, etc., were widely reported (34, 35). Canonical Wnt signaling pathway inhibitors reduce the proliferation of the primary human UFs cells and especially in the MED12 mutations type UFs which could be found in 70% of the UFs (36–38). Dai and his colleagues found that the promotion of uterine fibroids cell proliferation was accompanied by an increase in STAT-3 protein expression (39). Those studies supported our analyzed results that Wnt and JAK-STAT signaling pathways were involved in the development of UFs.

Aautophagy is a key contributor to the pathogenesis of UFs. In the Andaloussi AE et al. study, dysregulated autophagy has been shown to promote the growth of UFs in humans (14). Potential biomarkers of UFs collaborative diagnosis may be explored from the aspect of DNA methylation and autophagy. Therefore, 2 hub genes (FOS, and TNFSF10) with autophagy involvement

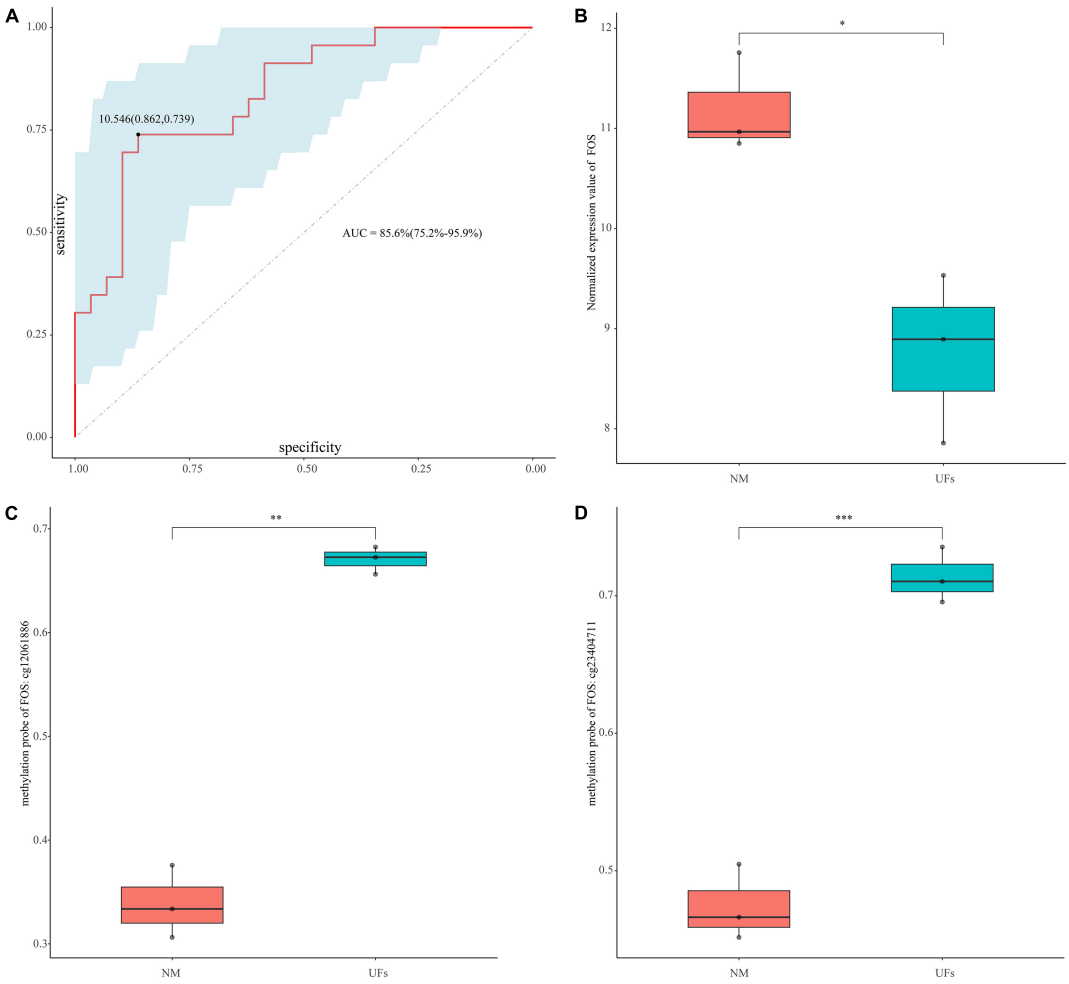

FIGURE 6
Diagnostic value of FOS. **(A)** ROC curve analysis and area under curve (AUC) of FOS. **(B)** GSE45188 supported the low expression of FOS in the fibroid samples. **(C,D)** The methylation level of the two differential methylation probes of FOS in GSE45188. $^{*}P < 0.05$, $^{**}P < 0.01$, and $^{***}P < 0.001$.

were discerned from the overlapping of 167 DEGs and the aberrantly autophagic genes extracted from the Human Autophagy Database. According to the PPI network with the more complicated interaction networks, FOS was speculated as a crucial gene in the molecular mechanism underlying the development of UFs.

The FOS gene encodes for a protein that contains a leucine zipper and dimerizes the activator protein 1 (AP1) complex which works as a transcription factor with the JUN family (40). The FOS protein has been widely reported in several cancers and inflammatory diseases as a regulator of cell proliferation, differentiation, and transformation (41). However, the relevant studies on the aspect of UFs were limited. The reduction of FOS in mRNA transcripts has been reported by Mark Payson et al. by RT-PCR in UFs compared with myometrium (42), and the decreasing of FOS has been reported to be impervious to the different menstrual cycle phases or GnRHa treatment (43). The reduction protein level of FOS was reported by Lessl M et al. which consists of our results (44). In the current study, we first extracted FOS as a potential biomarker of UFs by comprehensive analysis of autophagy and DNA methylation related genes, which inspired us to that the origin of UFs may consist of both impaired autophagy and DNA methylation with the down-regulation of FOS. We further validated the decreased expression of FOS in UFs tissue at both mRNA and protein levels by the tissue samples from Asian females.

Immune and inflammation play important roles in the pathophysiology of the UFs. The peripheral immune cell presented diverse conditions in the UFs patients, for instance, circulating CD4/CD8 T cells were increased while NK cells were decreased (45). Several studies highlighted the involvement and importance of the macrophages in the inflammation and consequent fibrosis which are typical features of UFs tissue (46). The study of indicated a higher level of macrophage infiltration in the myoma nodules and the autologous endometrium of the submucosal myomas (SMM) and intramural myomas (IMM) compared with women without UFs (47). In the present study, we estimated the immune scores of FOS in UFs patients, the positive correlation of the immune scores and the FOS expression indicated that autophagic-related mechanism was not the unique pathophysiologic prospect of the UFs, the FOS-related immune disorder may also involve in this process.

TABLE 2 Baseline characteristics of the study patients (n = 20).

Parameters		No. cases (%)
Age	<40	3 (15%)
	40–45	9 (45%)
	>45	7 (35%)
Location	Anterior	7 (35%)
	Posterior	6 (30%)
	Lateral	2 (10%)
	Fundal	2 (10%)
	others	3 (15%)
Maximum diameter	<5	8 (40%)
	5–8	9 (45%)
	>8	2 (10%)
Previous pregnancies	0	3 (15%)
	1–2	9 (45%)
	>2	7 (35%)
Previous myomectomy	Yes	2 (10%)
	No	18 (90%)

FOS is considered one of the diagnostic biomarkers of UFs which presented with decreased expression in UFs tissue. The diagnostic value of FOS was verified via AUC with a sensitivity of 86.2% and a specificity of 73.9%. However, the limitation is that the diagnostic value of FOS in UFs still based on invasive hysterectomy or myomectomy. The present study proposed the hypothesis of the FOS involved mechanisms of UFs development which is anomalous DNA methylation and autophagy condition, even the concomitant immune disorder.

5. Conclusion

In conclusion, we identified FOS as an autophagy-related biomarker for UFs by the comprehensive analysis of differential expression genes with aberrant DNA methylation and autophagy-related genes. And we validated the down-regulation of FOS in UFs tissue. These findings may reveal a potential diagnostic biomarker of uterine fibroids.

Data availability statement

The datasets presented in this study can be found in online repositories. The names of the repository/repositories and accession number(s) can be found in the article/**Supplementary material**.

Ethics statement

The studies involving human participants were reviewed and approved by the Ethics Committee of Tongji Medical College, Huazhong University of Science and Technology. The patients/participants provided their written informed consent to participate in this study.

Author contributions

HZ: study conception. LC: research design, UFs, and normal myometrium sample collection, manuscript preparation, conduction of the RT-PCR, and IHC experiments. JL: research design, data acquisition, and manuscript preparation. RL and JG: research design and manuscript preparation. ZL and BZ: check manuscript. All authors approved the final version to be published.

Funding

This work was supported by the Foundation of Tongji Hospital (No. 2020JZKT469).

Acknowledgments

We thank the Department of Pathology of Tongji Hospital for providing us with samples. LC appreciates Xiaoxu Liu for her encouragement since 2011.

Conflict of interest

The authors declare that the research was conducted in the absence of any commercial or financial relationships that could be construed as a potential conflict of interest.

The reviewer JT declared a shared parent affiliation with the author BZ to the handling editor at the time of review.

Publisher's note

Supplementary material

The Supplementary Material for this article can be found online at: https://www.frontiersin.org/articles/10.3389/fmed.2023.1153537/full#supplementary-material

References

1. Stewart EA, Cookson CL, Gandolfo RA, Schulze-Rath R. Epidemiology of uterine fibroids: A systematic review. *Bjog.* (2017) 124:1501–12. doi: 10.1111/1471-0528.14640

2. Pavone D, Clemenza S, Sorbi F, Fambrini M, Petraglia F. Epidemiology and risk factors of uterine fibroids. *Best Pract Res Clin Obstet Gynaecol.* (2018) 46:3–11. doi: 10.1016/j.bpobgyn.2017.09.004

3. Elkafas H, Badary O, Elmorsy E, Kamel R, Yang Q, Al-Hendy A. Endocrine-disrupting chemicals and vitamin D deficiency in the pathogenesis of uterine fibroids. *J Adv Pharm Res.* (2021) 5:260–75. doi: 10.21608/aprh.2021.66748.1124

4. Salehi AM, Jenabi E, Farashi S, Aghababaei S, Salimi Z. The environmental risk factors related to uterine leiomyoma: An umbrella review. *J Gynecol Obstet Hum Reprod.* (2023) 52:102517. doi: 10.1016/j.jogoh.2022.102517

5. Committee on Practice Bulletins—Gynecology. Practice bulletin no. 128: diagnosis of abnormal uterine bleeding in reproductive-aged women. *Obstet Gynecol.* (2012) 120:197–206. doi: 10.1097/AOG.0b013e318262e320

6. Marsh EE, Al-Hendy A, Kappus D, Galitsky A, Stewart EA, Kerolous M. Burden, Prevalence, and Treatment of Uterine Fibroids: A Survey of U.S. Women. *J Womens Health (Larchmt).* (2018) 27:1359–67. doi: 10.1089/jwh.2018.7076

7. Giuliani E, As-Sanie S, Marsh EE. Epidemiology and management of uterine fibroids. *Int J Gynaecol Obstet.* (2020) 149:3–9. doi: 10.1002/ijgo.13102

8. Cardozo ER, Clark AD, Banks NK, Henne MB, Stegmann BJ, Segars JH. The estimated annual cost of uterine leiomyomata in the United States. *Am J Obstet Gynecol.* (2012) 206:211.e1–9. doi: 10.1016/j.ajog.2011.12.002

9. Levens ED, Wesley R, Premkumar A, Blocker W, Nieman LK. Magnetic resonance imaging and transvaginal ultrasound for determining fibroid burden: implications for research and clinical care. *Am J Obstet Gynecol.* (2009) 200:537.e1–7. doi: 10.1016/j.ajog.2008.12.037

10. Machado-Lopez A, Simón C, Mas A. Molecular and Cellular Insights into the Development of Uterine Fibroids. *Int J Mol Sci.* (2021) 22:8483. doi: 10.3390/ijms22168483

11. Anderson GL, McIntosh M, Wu L, Barnett M, Goodman G, Thorpe JD, et al. Assessing lead time of selected ovarian cancer biomarkers: a nested case-control study. *J Natl Cancer Inst.* (2010) 102:26–38. doi: 10.1093/jnci/djp438

12. Mizushima N, Levine B. Autophagy in human diseases. *N Engl J Med.* (2020) 383:1564–76. doi: 10.1056/NEJMra2022774

13. Levine B, Kroemer G. Biological functions of autophagy genes: A disease perspective. *Cell.* (2019) 176:11–42. doi: 10.1016/j.cell.2018.09.048

14. Andaloussi AE, Habib S, Soylemes G, Laknaur A, Elhusseini H, Al-Hendy A, et al. Defective expression of ATG4D abrogates autophagy and promotes growth in human uterine fibroids. *Cell Death Discov.* (2017) 3:17041. doi: 10.1038/cddiscovery.2017.41

15. Del Bello B, Marcolongo P, Ciarmela P, Sorbi F, Petraglia F, Luisi S, et al. Autophagy up-regulation by ulipristal acetate as a novel target mechanism in the treatment of uterine leiomyoma: an in vitro study. *Fertil Steril.* (2019) 112:1150–9. doi: 10.1016/j.fertnstert.2019.08.007

16. Lin PH, Kung HL, Chen HY, Huang KC, Hsia SM. Isoliquiritigenin suppresses E2-induced uterine leiomyoma growth through the modulation of cell death program and the repression of ECM accumulation. *Cancers (Basel).* (2019) 11:1131. doi: 10.3390/cancers11081131

17. Liu B, Chen G, He Q, Liu M, Gao K, Cai B, et al. An HMGA2-p62-ERα axis regulates uterine leiomyomas proliferation. *Faseb J.* (2020) 34:10966–83. doi: 10.1096/fj.202000520R

18. Hu LF. Epigenetic regulation of autophagy. *Adv Exp Med Biol.* (2019) 1206:221–36. doi: 10.1007/978-981-15-0602-4_11

19. D'Urso A, Brickner JH. Mechanisms of epigenetic memory. *Trends Genet.* (2014) 30:230–6. doi: 10.1016/j.tig.2014.04.004

20. Baek SH, Kim KI. Epigenetic control of autophagy: Nuclear events gain more attention. *Mol Cell.* (2017) 65:781–5. doi: 10.1016/j.molcel.2016.12.027

21. Reik W, Dean W, Walter J. Epigenetic reprogramming in mammalian development. *Science.* (2001) 293:1089–93. doi: 10.1126/science.1063443

22. Schübeler D. Function and information content of DNA methylation. *Nature.* (2015) 517:321–6. doi: 10.1038/nature14192

23. Li S, Chiang TC, Richard-Davis G, Barrett JC, McLachlan JA. DNA hypomethylation and imbalanced expression of DNA methyltransferases (DNMT1, 3A, and 3B) in human uterine leiomyoma. *Gynecol Oncol.* (2003) 90:123–30. doi: 10.1016/s0090-8258(03)00194-x

24. Mlodawska OW, Saini P, Parker JB, Wei JJ, Bulun SE, Simon MA, et al. Epigenomic and enhancer dysregulation in uterine leiomyomas. *Hum Reprod Update.* (2022) 28:518–47. doi: 10.1093/humupd/dmac008

25. Carbajo-García MC, Corachán A, Juárez-Barber E, Monleón J, Payá V, Trelis A, et al. Integrative analysis of the DNA methylome and transcriptome in uterine leiomyoma shows altered regulation of genes involved in metabolism, proliferation, extracellular matrix, and vesicles. *J Pathol.* (2022) 257:663–73. doi: 10.1002/path.5920

26. George JW, Fan H, Johnson B, Carpenter TJ, Foy KK, Chatterjee A, et al. Integrated epigenome, exome, and transcriptome analyses reveal molecular subtypes and homeotic transformation in uterine fibroids. *Cell Rep.* (2019) 29:4069–85.e6. doi: 10.1016/j.celrep.2019.11.077

27. Yamagata Y, Maekawa R, Asada H, Taketani T, Tamura I, Tamura H, et al. Aberrant DNA methylation status in human uterine leiomyoma. *Mol Hum Reprod.* (2009) 15:259–67. doi: 10.1093/molehr/gap010

28. Tian Y, Morris TJ, Webster AP, Yang Z, Beck S, Feber A, et al. ChAMP: updated methylation analysis pipeline for Illumina BeadChips. *Bioinformatics (Oxford, England).* (2017) 33:3982–4. doi: 10.1093/bioinformatics/btx513

29. Morris TJ, Butcher LM, Feber A, Teschendorff AE, Chakravarthy AR, Wojdacz TK, et al. ChAMP: 450k chip analysis methylation pipeline. *Bioinformatics (Oxford, England).* (2014) 30:428–30. doi: 10.1093/bioinformatics/btt684

30. Ritchie ME, Phipson B, Wu D, Hu Y, Law CW, Shi W, et al. limma powers differential expression analyses for RNA-sequencing and microarray studies. *Nucleic Acids Res.* (2015) 43:e47. doi: 10.1093/nar/gkv007

31. Yu G, Wang L-G, Han Y, He Q-Y. clusterProfiler: An R package for comparing biological themes among gene clusters. *Omics.* (2012) 16:284–7. doi: 10.1089/omi.2011.0118

32. Cai L, Liao Z, Li S, Wu R, Li J, Ren F, et al. PLP1 may serve as a potential diagnostic biomarker of uterine fibroids. *Front Genet.* (2022) 13:1045395. doi: 10.3389/fgene.2022.1045395

33. Russo C, Camilli S, Martire FG, Di Giovanni A, Lazzeri L, Malzoni M, et al. Highly vascularized uterine myomas (uterine smooth muscle tumors) on ultrasound and correlation to histopathology. *Ultrasound Obstet Gynecol.* (2022) 60:269–76. doi: 10.1002/uog.24855

34. Ono M, Yin P, Navarro A, Moravek MB, Coon J. S. t, Druschitz SA, et al. Paracrine activation of WNT/β-catenin pathway in uterine leiomyoma stem cells promotes tumor growth. *Proc Natl Acad Sci USA.* (2013) 110:17053–8. doi: 10.1073/pnas.1313650110

35. Mangioni S, Viganò P, Lattuada D, Abbiati A, Vignali M, Blasio A. M. Di. Overexpression of the Wnt5b gene in leiomyoma cells: implications for a role of the Wnt signaling pathway in the uterine benign tumor. *J Clin Endocrinol Metab.* (2005) 90:5349–55. doi: 10.1210/jc.2005-0272

36. Ono M, Yin P, Navarro A, Moravek MB, Coon VJ, Druschitz SA, et al. Inhibition of canonical WNT signaling attenuates human leiomyoma cell growth. *Fertil Steril.* (2014) 101:1441–9. doi: 10.1016/j.fertnstert.2014.01.017

37. Corachán A, Ferrero H, Aguilar A, Garcia N, Monleon J, Faus A, et al. Inhibition of tumor cell proliferation in human uterine leiomyomas by vitamin D via Wnt/β-catenin pathway. *Fertil Steril.* (2019) 111:397–407. doi: 10.1016/j.fertnstert.2018.10.008

38. Corachán A, Trejo MG, Carbajo-García MC, Monleón J, Escrig J, Faus A, et al. Vitamin D as an effective treatment in human uterine leiomyomas independent of mediator complex subunit 12 mutation. *Fertil Steril.* (2021) 115:512–21. doi: 10.1016/j.fertnstert.2020.07.049

39. Huang D, Xue H, Shao W, Wang X, Liao H, Ye Y. Inhibiting effect of miR-29 on proliferation and migration of uterine leiomyoma via the STAT3 signaling pathway. *Aging (Albany NY).* (2022) 14:1307–20. doi: 10.18632/aging.203873

40. Wagner EF. Bone development and inflammatory disease is regulated by AP-1 (Fos/Jun). *Ann Rheum Dis.* (2010) 69(Suppl. 1):i86–8. doi: 10.1136/ard.2009.119396

41. Alfonso-Gonzalez C, Riesgo-Escovar JR. Fos metamorphoses: lessons from mutants in model organisms. *Mech Dev.* (2018) 154:73–81. doi: 10.1016/j.mod.2018.05.006

42. Payson M, Malik M, Siti-Nur Morris S, Segars JH, Chason R, Catherino WH. Activating transcription factor 3 gene expression suggests that tissue stress plays a role in leiomyoma development. *Fertil Steril.* (2009) 92:748–55. doi: 10.1016/j.fertnstert.2008.06.030

43. Gustavsson I, Englund K, Faxén M, Sjöblom P, Lindblom B, Blanck A. Tissue differences but limited sex steroid responsiveness of c-fos and c-jun in human fibroids and myometrium. *Mol Hum Reprod.* (2000) 6:55–9. doi: 10.1093/molehr/6.1.55

44. Lessl M, Klotzbuecher M, Schoen S, Reles A, Stöckemann K, Fuhrmann U. Comparative messenger ribonucleic acid analysis of immediate early genes and sex steroid receptors in human leiomyoma and healthy myometrium. *J Clin Endocrinol Metab.* (1997) 82:2596–600. doi: 10.1210/jcem.82.8.4141

45. Liu ZQ, Lu MY, Sun RL, Yin ZN, Liu B, Wu YZ. Characteristics of peripheral immune function in reproductive females with uterine leiomyoma. *J Oncol.* (2019) 2019:5935640. doi: 10.1155/2019/5935640

46. Zannotti A, Greco S, Pellegrino P, Giantomassi F, Delli Carpini G, Goteri G, et al. Macrophages and immune responses in uterine fibroids. *Cells.* (2021) 10:982. doi: 10.3390/cells10050982

47. Miura S, Khan KN, Kitajima M, Hiraki K, Moriyama S, Masuzaki H, et al. Differential infiltration of macrophages and prostaglandin production by different uterine leiomyomas. *Hum Reprod.* (2006) 21:2545–54. doi: 10.1093/humrep/del205

frontiers | Frontiers in Medicine

TYPE Systematic Review
PUBLISHED 31 May 2023
DOI 10.3389/fmed.2023.1211070

OPEN ACCESS

EDITED BY
Yujiao Deng,
The Second Affiliated Hospital of Xi'an Jiaotong University, China

REVIEWED BY
Shengnan Yu,
First Affiliated Hospital of Chongqing Medical University, China
Ping Li,
Novo Nordisk, China
Xiaodi Huang,
Peking Union Medical College Hospital (CAMS), China

*CORRESPONDENCE
Liang Wang
✉ 2196042@zju.edu.cn

†These authors have contributed equally to this work

RECEIVED 24 April 2023
ACCEPTED 12 May 2023
PUBLISHED 31 May 2023

CITATION
Wang X, Li T, Bai X, Zhu Y, Zhang M and Wang L (2023) Therapeutic prospect on umbilical cord mesenchymal stem cells in animal model with primary ovarian insufficiency: a meta-analysis. *Front. Med.* 10:1211070. doi: 10.3389/fmed.2023.1211070

Therapeutic prospect on umbilical cord mesenchymal stem cells in animal model with primary ovarian insufficiency: a meta-analysis

Xinrun Wang[1†], Tianye Li[1†], Xuechai Bai[2], Yun Zhu[3], Meiliang Zhang[4] and Liang Wang[1*]

[1]Department of Gynecology, The Second Affiliated Hospital, Zhejiang University School of Medicine, Hangzhou, Zhejiang, China, [2]Center for Reproductive Medicine, Department of Gynecology, Zhejiang Provincial People's Hospital (Affiliated People's Hospital, Hangzhou Medical College), Hangzhou, Zhejiang, China, [3]Center for Clinical Big Data and Analytics, The Second Affiliated Hospital Zhejiang University School of Medicine, Hangzhou, Zhejiang, China, [4]Department of Obstetrics and Gynecology, Yiwu Maternity and Children Hosptial, Yiwu Branch of Children's Hospital Zhejiang University School of Medicine, Yiwu, Zhejiang, China

Background: Primary ovarian insufficiency (POI) leads to not only infertile but several adverse health events to women. Traditional treatment methods have their own set of limitations and drawbacks that vary in degree. Application of human umbilical cord mesenchymal stem cell (hUCMSC) is a promising strategy for POI. However, there is a lack of literatures on application of hUCMSC in human. Animal experimental model, however, can reflect the potential effectiveness of this employment. This study aimed to evaluate the curative effect of hUCMSC on animals with POI on a larger scale.

Methods: To gather data, Pubmed, Embase, and Cochrane Library were searched for studies published up to April 2022. Various indices, including the animals' estrous cycle, serum sex hormone levels, and follicle number in the ovary, were compared between the experimental group and those with Premature Ovarian Insufficiency (POI).

Results: The administration of human umbilical cord-derived mesenchymal stem cells (hUCMSC) has been shown to significantly improve the estrous cycle (RR: 3.32, 95% CI: [1.80, 6.12], $I^2 = 0\%$, $P = 0.0001$), but robustly decrease its length (SMD: −1.97, 95% CI: [−2.58, −1.36], $I^2 = 0\%$, $P < 0.00001$). It can also strikingly increase levels of serum estradiol (SMD: 5.34, 95% CI: [3.11, 7.57], $I^2 = 93\%$, $P < 0.00001$) and anti-müllerian hormone (SMD: 1.92, 95% CI: [0.60, 3.25], $I^2 = 68\%$, $P = 0.004$). Besides, it lowers levels of serum follicle-stimulating hormone (SMD: −3.02, 95% CI: [−4.88, −1.16], $I^2 = 93\%$, $P = 0.001$) and luteinising hormone (SMD: −2.22, 95% CI: [−3.67, −0.76], $I^2 = 78\%$, $P = 0.003$), and thus collectively promotes folliculogenesis (SMD: 4.90, 95% CI: [3.92, 5.88], $I^2 = 0\%$, $P < 0.00001$).

Conclusions: Based on the presented findings, it is concluded that the administration of hUCMSC in animal models with POI can result in significant improvements in several key indicators, including estrous cycle recovery, hormone level modulation, and promotion of folliculogenesis. These positive outcomes suggest that hUCMSC may have potential as a treatment for POI in humans.

However, further research is needed to establish the safety and efficacy of hUCMSC in humans before their clinical application.

Systematic review registration: https://inplasy.com/inplasy-2023-5-0075/, identifier: INPLASY202350075.

KEYWORDS

primary ovarian insufficiency, human umbilical cord mesenchymal stem cells, animal model, meta-analysis, estrous cycle, hormone level, folliculogenesis

1. Introductions

Primary ovarian insufficiency (POI), also known as premature ovarian failure (POF), is a syndrome characterized by reduced or absent ovarian function (hypogonadism) and elevated levels of gonadotropins, specifically luteinising hormone (LH) and follicle-stimulating hormone (FSH) (hypergonadotropic) (1, 2). This occurs due to the lack of negative sex-steroid and inhibin feedback. Therefore, POI is also referred to as hypergonadotropic hypogonadism. The condition is diagnosed when oocytes and the surrounding support cells are lost before the age of 40 years, along with serum FSH levels above the threshold range of 30–40 mIU/mL twice (at least 1 month apart). POI is a systemic disease that can lead to various effects. Recent research has summarized the long-term health consequences of POI, including an increased risk of cardiovascular disease (CVD), decreased bone mineral density, significantly reduced fertility, psychological distress, vulvovaginal atrophy, neurological effects, and overall reduced life expectancy (3). While the incidence of POI is not peculiar, the underlying causes of this condition remain largely unknown (4). Despite extensive research, the etiology of POI is still not fully elucidated, and it is considered a complex and multifactorial condition. Genetic disorders, such as chromosomal abnormalities, are among the most prevalent causes of POI (5). These disorders can lead to early ovarian failure and an increased risk of POI. However, other factors like autoimmune diseases, iatrogenic injuries, and infectious diseases can also contribute to the onset of POI (6–8). In some cases, autoimmune disorders like systemic lupus erythematosus or Hashimoto's thyroiditis can trigger the body's immune system to attack ovarian tissue, leading to POI (9). Additionally, with the increasement of gynaecologic cancer, medical treatments like chemotherapy, radiation therapy, or surgical removal of the ovaries can also cause damage to the ovarian tissue, leading to POI (10). Infections, such as mumps, tuberculosis, or sexually transmitted diseases like gonorrhea, can also contribute to POI by damaging the ovaries or disrupting their function (11). Given the complex and multifactorial nature of POI, early detection and timely intervention are crucial to help manage the condition and improve the quality of life of affected individuals. Therefore, a better understanding of the factors contributing to POI and advancements in diagnostic methods can aid in developing effective treatments and management strategies for this condition (12). Currently, traditional therapy for POI is limited. To patients without desire for pregnancy, hormone replacement therapy (HRT) is appropriate. HRT can significantly relieve POI symptoms and decrease bone fracture and CVD risks. It can even help fertility for those females who still have ovarian follicle reserve (13). Infertility treatment is another therapeutic aspect for POI. Oocyte donation is a traditional but useful way to help delivery, but is limited in many countries and regions. A way to preserve fertility is the cryopreservation of oocytes, embryos and ovarian tissues. For those who undergo radiotherapy, GnRH analog can help protect fertility, but some data are conflicting. Furthermore, a new method called *in vitro* activation (IVA) of dormant follicles can help patients with POI conceive as well (14). However, all of these therapies can be conducive to helping a small proportion of patients with POI. Human umbilical cord mesenchymal stem cell (hUCMSC) is mesenchymal stem cells derived from Wharton's jelly of a fetal umbilical cord. These cells have multiple differentiation potentials. They can generate cell types such as adipocytes, osteocytes and cartilage. In addition, neurons, astrocytes, glial cells, liver and islet cells are the potential lineage of hUCMSC (15). Stem cell therapy has been proposed for a long time. Some clinical trials have tried to understand the therapeutic effect of hUCMSC in POI. Evidence revealed follicular activated, estradiol (E_2) increased and FSH decreased after hUCMSC transplantation in patients with POI (16, 17). Collagen scaffold with hUCMSC is another stem cell delivery approach that has shown a therapeutic effect. In an *in vivo* study, hUCMSC activated primordial follicles by phosphorylating FOXO3a and FOXO1 (17). Apart from clinical trials, many studies tested the therapeutic effect of hUCMSC on the ovary of animals. For instance, hUCMSC introduction led to an atretic follicle decrease and a healthy antral follicle increase in mice. Granulosa cell (GC) apoptosis induced by POI was inhibited. Based on molecular analysis, the expression of SOD2, CAT and Bcl2 mRNA increased, whereas *Bax* mRNA expression declined (18). Given that these genes are associated with oxidation and apoptosis, hUCMSC infusion may influence the antioxidative and antiapoptotic procedures of the ovary. Furthermore, *in vivo* cell culture found that hUCMSC can secrete VEGF, IGF-1 and HGF (19). Through Sirius red and Masson trichrome staining of the ovary tissue, researchers found that fibrosis developed in POI rats, but after hUCMSC treatment, the fibrosis area was significantly

Abbreviations: AMH, anti-mullerian hormone; ART, assisted reproductive technology; CI, confidence interval; CVD, cardiovascular disease; E_2, estradiol; FSH, follicle stimulating hormone; GC, granulosa cell; GSC, germline stem cell; GnRH, gonadotropin-releasing hormone; HRT, hormone replacement therapy; hUCMSC, human umbilical cord mesenchymal stem cell; IVA, *in vitro* activation; IVF-ET, *in vitro* fertilization and embryo transfer; LH, luteinizing hormone; MeSH, medical subject heading; POF, premature ovarian failure; POI, primary ovarian insufficiency; PRISMA, preferred reporting items for meta-analysis and systematic review; RCT, randomized clinical trail; RR, risk ratio; SMD, standardized mean difference; TC, theca cell.

reduced. The TGF-β_1 signaling pathway is a crucial immune regulative factors (20), also reportedly involved in hUCMSC regulation. The hUCMSC can inhibit the expression of TGF-β_1 and p-smad3 in the ovary, thereby depressing the differentiation of stromal cells into inner theca cells (TCs) and consequently inhibiting fibrosis in POI rats (21). However, only few integrated analyses have been found. Thus, this study aimed to summarize the results of animal studies investigating on hUCMSC and POI, form more valid evidence and confirm the therapeutic effect of hUCMSC on experimental animals compared with the POI model by analyzing the estrous cycle, serum sex hormone and ovarian follicles in the two groups.

2. Methods

This systematic meta-analysis appraises the association between employment of hUCMSC and the indices of ovarian reserve function in experimental animal models. We followed the preferred reporting items for meta-analysis and systematic review (PRISMA) 2020 guidelines and putting forward the research question using the PECOS format. We have registered at International Platform of Registered Systematic Review and Meta-analysis Protocols (INPLASY). Registration number is INPLASY202350075.

2.1. Search strategy

We searched the Pubmed, Embase and Cochrane Library databases. Specific search strategy is "((Primary Ovarian Insufficiency) OR (Premature Ovarian Failure) OR (Gonadotropin-Resistant Ovary Syndrome) OR (Hypergonadotropic Ovarian Failure)) AND ((Stem cell) OR (Progenitor Cell))". To conclude, we used MeSH terms and their typical synonyms and combined them with "OR." Then, we combined the results of "primary ovarian insufficiency" and "stem cell" with "AND." All results from the date of database establishment to 1 April 2022 were included.

2.2. Inclusion and exclusion criteria

Initially, we excluded all duplicated studies. Subsequently, we collected studies that met the following criteria: female animals; hUCMSC; successful POF model establishment; and serum hormone, follicle count and estrous cycle as the outcome. Furthermore, the following five study types were excluded: reviews and meta-analysis, studies that are not associated with stem cell or POI, non-animal studies, case reports and animal studies without hUCMSC application. After selecting studies related to hUCMSC and POI, we thoroughly read the full text and further excluded

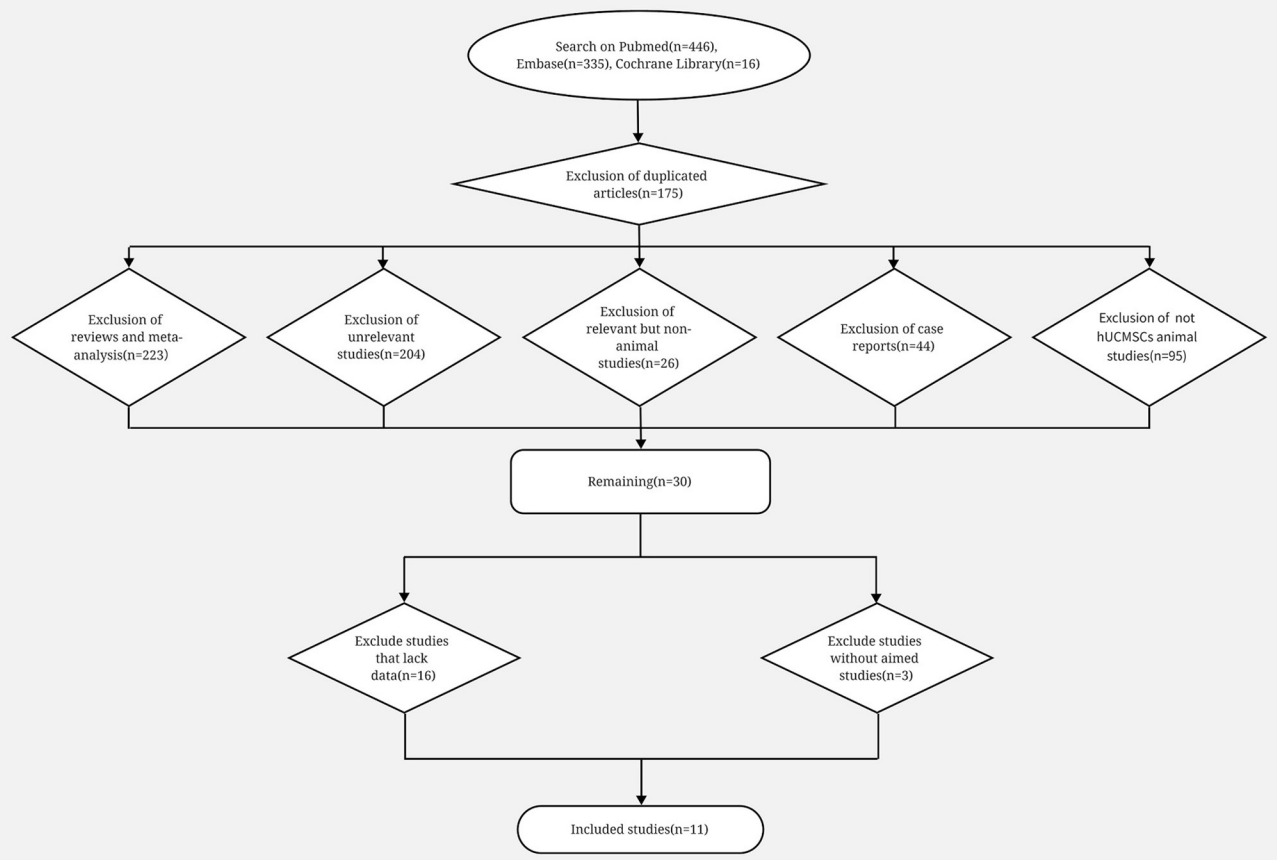

FIGURE 1
Flow diagram on search procedure of Pubmed, Embase and Cochrane Library and the exclusion criteria.

TABLE 1 Characteristics of the included studies.

First author	Country	Publication year	Experiment animal	Total animal numbers	Animal age	Model establishment	Establishment time	Transplantation time	Transplantation route	Available outcome*	Web link
Jian Shen	China	2020	BALB/c mice	110	7–8 weeks old	Cyclophosphamide	14 d	60 d	tail vein	Estrous cycle; Follicle number; E_2; FSH	https://www.wjgnet.com/1948-0210/full/v12/i4/277.htm
He Jie	China	2021	BALB/C female mice	30	7 to 8 weeks	Cyclophosphamide + baixioan	1 d	15 d	tail vein	E_2; FSH; AMH; LH; Follicle number	https://cellmolbiol.org/index.php/CMB/article/view/4071
Amr K. Elfayomy	Saudi Arabia	2016	albino Wistar rats	95	-	Paclitaxel	1 d	6 wk	*in situ*	Follicle number; E_2; FSH	https://www.sciencedirect.com/science/article/pii/S0040816616300246?via%3Dihub
Xunyi Zhang	China	2020	SD rats	80	6–8 weeks	pZP3 suspension	1 d	20 d	*in situ*	Estrous cycle; E_2; FSH; LH; Follicle number	https://www.tandfonline.com/doi/full/10.1080/09513590.2021.1878133
Ladan Jalalie	Iran	2021	C57BL/6 mice	30	6–8-week-old	Cyclophosphamide	15 d	1 wk	tail vein	Follicle number; FSH; E_2	https://www.sciencedirect.com/science/article/abs/pii/S0065128120301574?via%3Dihub
Taoran Deng	China	2021	C57BL/6 mice	27	6–7 weeks old	Cyclophosphamide and busulfan	1 d	2 wk	tail vein	Estrous cycle; Follicle number; E_2; FSH	https://link.springer.com/article/10.1007/s43032-021-00499-1
Dan Song	China	2016	Wistar rats	40	8 weeks old	Cyclophosphamide	1 d	6 wk	tail vein+*in situ*	E_2; FSH; AMH; Follicle number	https://www.hindawi.com/journals/bmri/2016/2517514/
Zhe Wang	China	2020	SD rats	120	8 weeks old	Ovarian antigen	30 d	2 wk	tail vein	Estrous cycle; Follicle number	https://www.hindawi.com/journals/sci/2020/3249495/

(Continued)

10.3389/fmed.2023.1211070

TABLE 1 (Continued)

First author	Country	Publication year	Experiment animal	Total animal numbers	Animal age	Model establishment	Establishment time	Transplantation time	Transplantation route	Available outcome*	Web link
Shufang Wang	China	2013	CD1 (ICR) mice	45	-	Cyclophosphamide	15 d	1 wk	tail vein	Follicle number	https://www.hindawi.com/journals/bmri/2013/690491/
Yanjun Yang	China	2019	C57BL/6 mice	24	6 weeks old	Cyclophosphamide	15 d	4 wk	*in situ*	Estrous cycle; E_2; FSH; AMH; Follicle number	https://link.springer.com/article/10.1007/s11626-019-00337-4
Qun Zheng	China	2019	SD rats	40	12 weeks old	Cyclophosphamide	15 d	2 wk	tail vein	Estrous cycle; AMH; E_2; FSH; Follicle number	https://www.hindawi.com/journals/bmri/2019/6539294/

*Wang et al. (30), Wang et al. (31), and Zheng et al. (33) lack exact data of serum sex hormone.

TABLE 2 Quality assessment of the included studies.

Study	①	②	③	④	⑤	⑥	⑦	⑧	⑨	⑩
Shen et al. (23)	No	Yes	Unknown	Unknown	Unknown	Unknown	Yes	Yes	Yes	Yes
Jie et al. (24)	Unknown	Yes	Unknown	Unknown	Unknown	Unknown	Yes	Yes	Yes	Yes
Elfayomy et al. (25)	Unknown	Yes	Unknown	Unknown	Unknown	Unknown	Yes	Yes	Yes	Yes
Zhang et al. (26)	Unknown	Yes	Unknown	Unknown	Unknown	Unknown	Yes	Yes	Yes	Yes
Jalalie. et al. (27)	Unknown	Yes	Unknown	Unknown	Unknown	Unknown	Yes	Yes	Yes	Yes
Deng. et al. (23)	Unknown	Yes	Unknown	Unknown	Unknown	Unknown	Yes	Yes	Yes	Yes
Song et al. (28)	Unknown	Yes	Unknown	Unknown	Unknown	Unknown	Yes	Yes	Yes	Yes
Wang et al. (29)	Unknown	Yes	Unknown	Unknown	Unknown	Unknown	Yes	Yes	Yes	Yes
Wang et al. (30)	Unknown	Yes	Unknown	Unknown	Unknown	Unknown	Yes	Yes	Yes	Yes
Yang et al. (31)	Unknown	Yes	Unknown	Unknown	Unknown	Unknown	Yes	Yes	Yes	Yes
Zheng et al. (32)	Unknown	Yes	Unknown	Unknown	Unknown	Unknown	Yes	Unknown	Yes	Yes

SYRCLE animal experiment bias risk assessment form:① Distribution sequence production is sufficient ② Baselines of groups are the same ③ Distribution concealing is sufficient ④ Experiment animals are randomly fed ⑤ Blinding to researcher ⑥ Randomly select animals to assess result ⑦ Blinding to result evaluator ⑧ No incomplete data ⑨ No selective result report ⑩ No other biases.

10.3389/fmed.2023.1211070

studies that we failed to collect the exact data and studies with no outcomes that we aimed.

2.3. Data extraction and statistical analysis

Data were extracted and qualifiedly assessed by using "SYRCLE animal experiment bias risk assessment form." We used risk ratios (RRs) with 95% confidence intervals (CI) for categorical data, and standardized mean difference (SMD) for numerical data to combine studies. If the heterogeneity test showed $I^2 >$ 50%, we used random effects model. Otherwise, we used fixed effects model. All statistical data were analyzed on RevMan 5.4 (22). The extracted data from each study included the first author, country or region, publishing year, experiment animal, POI model establishing method, hUCMSC intervention situation, group situation and outcome data. During the analysis, we firstly tested the heterogeneity of the studies and selected the effects model, as mentioned before. Then, we divided the studies according to unit, injection location, hUCMSC concentration, transplantation time and follicle type for the subgroup analyses. Sensitivity was assessed by eliminating studies one by one. We also used funnel plot to determine the publication bias. All statistical significances were defined at $P < 0.05$.

3. Results

3.1. Description of search results

We identified 446, 335 and 16 studies from Pubmed, Embase and Cochrane Library, respectively. Among them, 175 duplicate studies, 223 reviews or meta-analyses, 204 studies that are not associated with stem cell or POI, 26 animal studies, 44 case reports and 95 animal studies without hUCMSC used were excluded. Conclusively, 30 animal studies remained, and they were all correlated to hUCMSC and POI. After full text reading, we further excluded 16 studies because we failed to obtain the exact data, and three studies because they lack our aimed outcome. Ultimately, 11 studies were analyzed (Figure 1) (23–33).

3.2. Basic characteristics and quality assessment

We extracted the data on the first author, country, publication year, experiment animal number and situation, model establishment situation, group situation, some outcomes and web link. We included nine studies from China (23, 24, 26, 28–33), one from Saudi Arabia (25) and one from Iran (27). A total of 158 stem cell–treated animals and 155 POI model animals were included. Eight studies infused hUCMSC by tail vein (23, 24, 27–31, 33), whereas four injected hUCMSC directly into the ovary (25, 26, 29, 32); in addition, one study compared the effects of these two methods (29). Stem cell concentrations varied, ranging from 1×10^5 to 5×10^6. However, the concentration units in some studies were unclear; thus, we only conducted a subgroup analysis by stem cell concentration in hormone analyses. Transplantation time also varied. Some studies set a series of observation time to better show the effect of hUCMSC. To simplify our analysis, we only chose the data at the end of the study for our meta-analysis (Tables 1, 2). In order to identify the effect of different transplantation time, we conducted a subgroup analysis as well.

3.3. Analysis of outcomes

3.3.1. Estrous cycle

Five studies reported estrous cycle situation (23, 26, 28, 30, 32). Two outcomes were used to divide them into two analyses. Of the five studies, two (23, 30) calculated the proportion of animals with normal estrous cycle. Based on different cell concentrations, four groups were included in one analysis. The three other studies (26, 28, 32) measured the length of the estrous cycle in animals. Results showed that hUCMSC significantly improved the proportion of animals with normal estrous cycle (RR: 3.32, 95% CI: [1.80, 6.12], $I^2 = 0\%$, $P = 0.0001$; Figure 2A) and shortened the estrous cycle length (SMD: −1.97, 95% CI: [−2.58, −1.36], $I^2 = 0\%$, $P < 0.00001$; Figure 2B). Based on the location of stem cell injection, the subgroup analysis showed that estrous cycle improvement is independent of the injection site (Table 3).

3.3.2. E_2

Eight studies reported serum E_2 levels (23–29, 32). Based on the injection location, nine groups were included in the analysis. Serum E_2 significantly increased in the hUCMSC group compared with that in the POI model group (SMD: 5.34, 95% CI: [3.11, 7.57], $I^2 = 93\%$, $P < 0.00001$; Figure 3A). We conducted a subgroup analysis according to the statistical units, stem cell injection location and stem cell concentration. Besides, as some included studies compared several transplantation time, we also conducted a subgroup analysis based on it. The elevation of serum E_2 level was not significant when calculated by ng/mL or when the stem cell concentration was 2 × 10e6. However, the effect of hUCMSC on the serum E_2 level of animals was independent of the injection location. Significance was observed in all intervention time subgroup, indicating hUCMSC can increase serum E_2 level at the beginning of 2 weeks (Table 3).

3.3.3. AMH

Three studies reported serum AMH (24, 29, 32). Based on the injection location, four groups were included in the analysis. Serum AMH significantly increased in the hUCMSC group compared with that in the POI model group (SMD: 1.92, 95% CI: [0.60, 3.25], $I^2 = 68\%$, $P = 0.004$; Figure 3B). The subgroup analysis revealed that serum AMH was independent of the statistical units and injection location. However, when the stem cell concentration was 2 × 10e5 and 2 × 10e6, no significant change was observed between the model and hUCMSC groups (Table 3).

3.3.4. FSH

Eight studies reported serum FSH levels (23–29, 32). Based on the injection location, nine groups were included in the analysis.

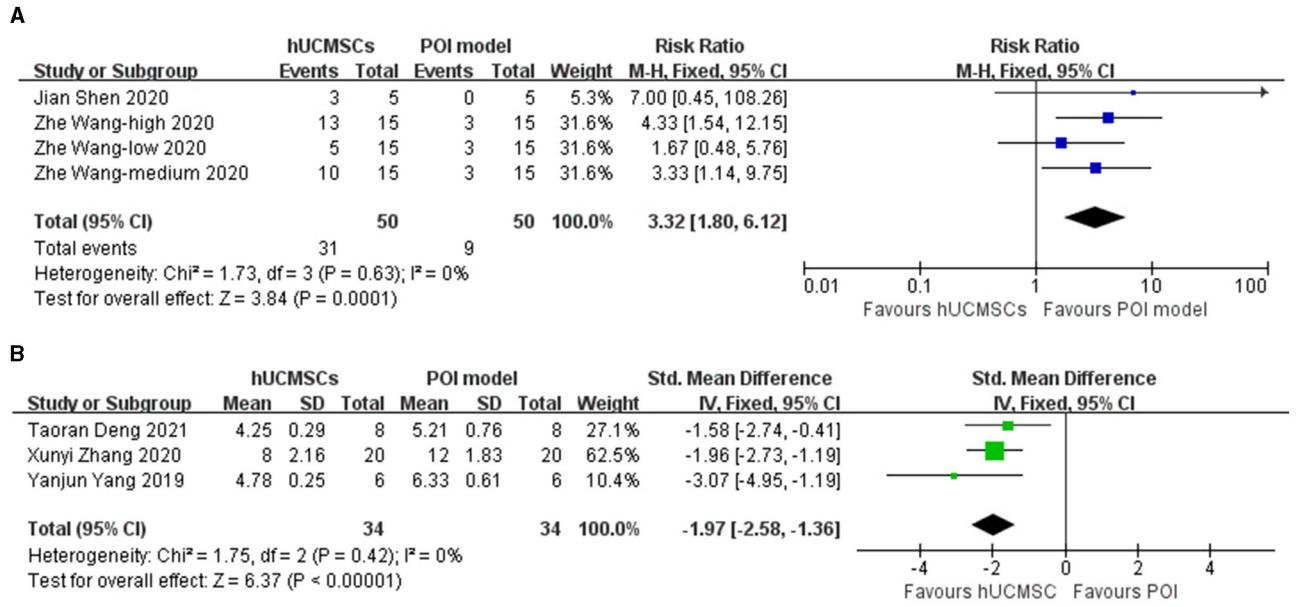

FIGURE 2
Forest plot of animals' estrous cycle situation in the hUCMSC group versus the POI model group. **(A)** Numerous animals in the hUCMSC group recovered normal estrous cycle compared with those in the POI model group (RR: 3.32, 95% CI: [1.80, 6.12], $I^2 = 0\%$, $P = 0.0001$). **(B)** The cycle length significantly decreased in the hUCMSC group compared with that in the POI model group (SMD: −1.97, 95% CI: [−2.58, −1.36], $I^2 = 0\%$, $P < 0.00001$).

Compared with the POI model group, the hUCMSC group showed a significant reduction in serum FSH (SMD: −3.02, 95% CI: [−4.88, −1.16], $I^2 = 93\%$, $P = 0.001$; Figure 3C). According to the statistical units, stem cell injection location, stem cell concentration and transplantation time, the subgroup analysis showed that no significant change was observed when hUCMSC was injected *in situ* and when the stem cell concentration was 2 × 10e6. However, in most cases, the FSH level decreased significantly after hUCMSC injection. Meanwhile, FSH decreases significantly 2 weeks after hUCMSC injection, indicating the effect of hUCMSC works at the beginning of 2 weeks (Table 3).

3.3.5. LH

Two studies reported serum LH (24, 26). Given that they used different calculation units, injection location and stem cell concentration, we conducted a subgroup analysis. Compared with the POI model group, the hUCMSC group showed a significant decrease in serum LH (SMD: −2.22, 95% CI: [−3.67, −0.76], $I^2 = 78\%$, $P = 0.003$; Figure 3D). Subgroup analysis results showed that the treatment effect on LH concentration was independent of the calculation unit, injection location and stem cell concentration (Table 3).

3.3.6. Follicle number

Ten studies determined the follicle count in animals (24–33). However, considering the various follicle types, we only conducted a subgroup analysis based on the follicle types (Figure 3E). All subgroups, except the atresia follicles ($P = 0.08$) and corpus luteum ($P = 0.45$), showed significant differences. After hUCMSC injection, the antral follicles (SMD: 4.64, 95% CI: [2.89, 6.39], $I^2 = 87\%$, $P < 0.00001$), secondary follicles (SMD: 2.14, 95% CI: [1.07, 3.21], $I^2 = 84\%$, $P < 0.0001$), primordial follicles (SMD: 1.68, 95% CI: [0.26, 3.09], $I^2 = 89\%$, $P = 0.02$), pre-antral follicles (SMD: 1.73, 95% CI: [0.37, 3.10], $I^2 = 70\%$, $P = 0.01$), primary follicles (SMD: 2.23, 95% CI: [1.10, 3.35], $I^2 = 85\%$, $P = 0.0001$) and all follicles (SMD: 4.90, 95% CI: [3.92, 5.88], $I^2 = 0\%$, $P < 0.00001$) significantly increased compared with those in the POI model group.

3.4. Sensitivity analysis

By picking out studies one by one, we conducted a sensitivity analysis on five outcomes of the estrous cycle, E_2, FSH, AMH and LH. Results of the estrous cycle, E_2, FSH and LH were stable, but after picking out Jie et al. (24) or Yang et al. (32), the heterogeneity of the AMH outcome reduced significantly (Jie et al.: $I^2 = 0\%$, $P = 0.53$; Yang et al.: $I^2 = 43\%$, $P = 0.17$). The data unit, transplantation time and study animals may explain the heterogeneity; larger data are needed to determine the origin (Table 4).

3.5. Publication bias

Funnel plots of the normal estrous cycle proportion, E_2, FSH and follicle number are asymmetric, whereas those of the estrous cycle length, AMH and LH are symmetric. Publication bias likely existed, especially in the results of the estrous cycle, E_2, FSH and follicle number (Figure 4).

TABLE 3 Subgroup analysis results of animals' estrous cycle and serum hormone level.

Comparison	Result					
Estrous cycle length	Subgroup name	Study number	Included study	SMD [95%CI]	I^2	*P*
	Injection location					
	Tail vein	1	Deng et al. (28)	−1.58 [−2.74, −0.41]	Not applicable	0.008
	In situ	2	Zhang et al. (26); Yang et al. (34)	−2.12 [−2.83, −1.41]	13%	<0.00001
E_2	Subgroup name	Study number	Included study	SMD [95%CI]	I^2	P
	Calculate unit					
	unknown	1	Shen et al. (23)	9.68 [4.09, 15.27]	Not applicable	0.0007
	pg/mL, ng/L	6	Elfayomy et al. (25); Song et al.–*in situ* (29); Dan Song et al.–tail vein (29); Jie et al. (24); Jalalie et al. (27); Zhang et al. (26)	6.07 [2.84, 9.31]	94%	0.0002
	ng/mL	1	Deng et al. (28)	0.25 [−0.73, 1.24]	Not applicable	0.62
	pmol/L	1	Yang et al. (32)	6.41 [3.86, 8.95]	Not applicable	<0.00001
	Injection location					
	Tail vein	5	Song et al.–tail vein (29); Jie et al. (24); Jalalie et al. (27); Shen et al. (23); Deng et al. (28)	5.32 [1.86, 8.79]	92%	0.003
	In situ	4	Elfayomy et al. (25); Song–*in situ* et al. (29); Zhang et al. (26); Yang et al. (32)	6.25 [1.67, 10.82]	95%	0.007
	Stem cell concentration					
	1 × 10E5	1	Zhang et al. (26)	0.69 [0.05, 1.33]	Not applicable	0.03
	2 × 10E5	1	Yang et al. (32)	6.41 [3.86, 8.95]	Not applicable	<0.00001
	1 × 10E6	5	Song–tail vein et al. (29); Jie et al. (24); Jalalie et al. (27); Shen et al. (23); Deng et al. (28)	5.32 [1.86, 8.79]	92%	0.03
	2 × 10E6	2	Elfayomy et al. (25); Song et al.–*in situ* (29)	10.44 [−6.37, 27.24]	97%	0.22
	Transplantation time					
	2 weeks or 15 days	5	Elfayomy et al. (25); Song et al.–*in situ* (29); Song et al.–tail vein (29); Shen et al. (23); Deng et al. (28)	2.26 [1.11, 3.42]	61%	0.0001
	4 weeks or 30 days	5	Elfayomy et al. (25); Song et al.–*in situ* (29); Song et al.–tail vein (29); Shen et al. (23); Deng et al. (28)	3.91 [0.96, 6.86]	92%	0.009
	6 weeks or 45 days	4	Elfayomy et al. (25); Song et al.–*in situ* (29); Song et al.–tail vein (29); Shen et al. (23)	7.33 [1.87, 12.78]	93%	0.008
	60 days	1	Shen et al. (23)	9.68 [4.09, 15.27]	Not applicable	0.0007
AMH	Subgroup name	Study number	Included study	SMD [95%CI]	I^2	P
	Calculate unit					
	ng/mL	1	Jie et al. (24)	3.64 [2.11, 5.17]	Not applicable	<0.00001

(Continued)

TABLE 3 (Continued)

Comparison	Result					
	Subgroup name	Study number	Included study	SMD [95%CI]	I^2	*P*
	pg/mL	3	Song et al.–*in situ* (29); Song et al.–tail vein (29); Yang et al. (32)	1.14 [0.37, 1.92]	0%	0.004
	Injection location					
	Tail vein	2	Song et al.–tail vein (29); Jie et al. (24)	2.84 [1.11, 4.57]	51%	0.001
	In situ	2	Song et al.–*in situ* (29); Yang et al. (32)	1.00 [0.15, 1.85]	0%	0.02
	Stem cell concentration					
	2 × 10E5	1	Yang et al. (32)	0.81 [−0.16, 1.78]	Not applicable	0.1
	1 × 10E6	2	Song et al.–tail vein (29); Jie et al. (24)	2.84 [1.11, 4.57]	51%	0.001
	2 × 10E6	1	Song et al.–*in situ* (29)	1.62 [−0.16, 3.40]	Not applicable	0.07
FSH	Subgroup name	Study number	Included study	SMD [95%CI]	I^2	P
	Calculate unit					
	unknown	1	Shen et al. (23)	−7.28 [−11.56, −3.00]	Not applicable	0.0009
	mIU/mL, U/L, IU/L	7	Elfayomy et al. (25); Song et al.–*in situ* (29); Song et al.–tail vein (29); Jie et al. (24); Jalali et al. (27); Deng et al. (28); Yang et al. (32)	−2.26 [−4.11, −0.41]	92%	0.02
	pg/mL	1	Zhang et al. (26)	−5.27 [−6.64, −3.91]	Not applicable	<0.00001
	Injection location					
	Tail vein	5	Song et al.–tail vein (29); Jie et al. (24); Shen et al. (23); Jalali et al. (27); Deng et al. (28)	−2.51 [−4.19, −0.84]	82%	0.003
	In situ	4	Elfayomy et al. (25); Song et al.–*in situ* (29); Zhang et al. (26); Yang et al. (32)	−3.40 [−7.44, 0.65]	96%	0.1
	Stem cell concentration					
	1 × 10E5	1	Zhang et al. (26)	−5.27 [−6.64, −3.91]	Not applicable	<0.00001
	2 × 10E5	1	Yang et al. (32)	1.49 [0.41, 2.56]	Not applicable	0.007
	1 × 10E6	5	Song et al.–tail vein (29); Jie et al. (24); Shen et al. (23); Jalali et al. (27); Deng et al. (28)	−2.51 [−4.19, −0.84]	82%	0.003
	2 × 10E6	2	Elfayomy et al. (25); Song et al.–*in situ* (29)	−4.96 [−11.50, 1.59]	95%	0.14
	Transplantation time					
	2 weeks or 15 days	5	Elfayomy et al. (25); Song et al.–*in situ* (29); Song et al.–tail vein (29); Shen et al. (23); Deng et al. (28)	−2.10 [−3.71, −0.50]	79%	0.01
	4 weeks or 30 days	5	Elfayomy et al. (25); Song et al.–*in situ* (29); Song et al.–tail vein (29); Shen et al. (23); Deng et al. (28)	−3.28 [−5.54, −1.01]	86%	0.005

(Continued)

TABLE 3 (Continued)

Comparison	Result					
	Subgroup name	Study number	Included study	SMD [95%CI]	I^2	*P*
	6 weeks or 45 days	4	Elfayomy et al. (25); Song et al.–*in situ* (29); Song et al.–tail vein (29); Shen et al. (23)	−4.03 [−7.09, −0.97]	87%	0.01
	60 days	1	Shen et al. (23)	−7.28 [−11.56, −3.00]	Not applicable	0.0009
LH	Subgroup name	Study number	Included study	SMD [95%CI]	I^2	P
	Calculate unit					
	mIU/mL	1	Jie et al. (24)	−1.46 [−2.47, −0.45]	Not applicable	0.005
	pg/mL	1	Zhang et al. (26)	−2.94 [−3.86, −2.02]	Not applicable	<0.00001
	Injection location					
	Tail vein	1	Jie et al. (24)	−1.46 [−2.47, −0.45]	Not applicable	0.005
	In situ	1	Zhang et al. (26)	−2.94 [−3.86, −2.02]	Not applicable	<0.00001
	Stem cell concentration					
	1 × 10E5	1	Zhang et al. (26)	−2.94 [−3.86, −2.02]	Not applicable	<0.00001
	1 × 10E6	1	Jie et al. (24)	−1.46 [−2.47, −0.45]	Not applicable	0.005

4. Discussions

In the year 1942, POI was initially described as a mysterious ailment that perplexed medical practitioners. As the medical community's focus began to shift toward unraveling its elusive nature, POI gradually gained notoriety and its prevalence surged to an alarming 1% (35). Chemical injury is a common method to establish POI model and a main cause of POI clinically apart from genetic disorders (12, 36). But the pathophysiological change of POI is similar regardless of etiology. According to our results, the reduced ovarian function and elevated gonadotropins is reversed by hUCMSC therapy. Follicles are stimulated as well. Therefore, we think the therapeutic effect of hUCMSC is adaptable to all causes. The traditional treatment for POI is HRT, but it only relieves symptoms. The ovarian function remains poor and bring many clinical adverse events about in many patients. In a retrospective cohort study, only 3 of 20 patients achieved pregnancy by assisted reproductive technology (ART) (37). Besides, patients with HRT are more likely to develop sleep problems (38). Given these limitations, stem cell therapy has gained considerable attention recently. Currently, hUCMSC has two other different forms to apply, that is, the microvesicles (34) and extracellular vesicles (39) derived from such cells. Stem cells in the umbilical cord are easy to acquire and do not cause extra donor injury compared with the other stem cell types. Considering their proliferative ability, multidifferentiation and safety, hUCMSC has been researched in the treatment of respiratory (40), cardiovascular (41), liver (42), central nervous system (43, 44) and autoimmune (45) diseases as well as diabetes (46). AMH is crucial in POI diagnosis. In our search on POI, AMH research has gained a large proportion. Physiologically, AMH is secreted by primary ovarian follicles and can negatively regulate the progression of earlier resting follicles into active and progressive ones (47). Considering that AMH secretion slightly varies in menstrual cycle and only healthy follicles secrete it, AMH is considered as a stable marker of ovarian reserve and POI. Our results showed a significant increase of AMH in the hUCMSC group, possibly because of the cytokine secreted by hUCMSC. However, the follicle number increased after stem cell transplantation; the proliferation of healthy follicles may be the cause of the AMH increase. Further research is needed to elucidate the underlying mechanism.

Many factors contribute to the development of infertility. And the gene expressions of different cases are various according to the diseases as a bioinformatic analysis showed (48). As a result, there are only some general treatments of infertility like IVF-ET and artificial insemination. Etiology based therapy of infertility is rare. Infertility therapies are mainly ART, aiming at gaining embryo directly (49). Our meta-analysis confirms folliculogenesis of hUCMSC in animal models, providing an etiology-specific therapy of POI. Apart from efficacy, safety is another important factors under evaluation. Although our result does not cover safety concerns, several phase 1/2 trials have been conducted for hUCMSC in other diseases. General outcomes for safety consideration include immediate infusion related adverse events, blood test like hepatic and renal function and blood cell count, inflammatory cytokine level, hypersensitive, infection, tumorigenesis (50–52). No adverse event is observed in these studies.

Although many studies tried to determine the mechanism of hUCMSC, the specific target remains unclear. Apoptosis regulation was often observed in many animal studies. This result may be derived from some signaling pathways. In a previous study, the expression of CK 8/18, TGF-ß and PCNA increased, while that of CASP-3 decreased (25). Other candidate molecular signals include Bcl-2 (53) and PI3K-Akt (54). Some researchers also hypothesized that angiogenesis can explain the anti-apopotic effect of hUCMSC (32). Further studies should be conducted to determine the exact mechanism and guide the clinical application of hUCMSC. However, hUCMSC can definitely promote ovarian function. Not only AMH but also E_2, FSH and LH showed

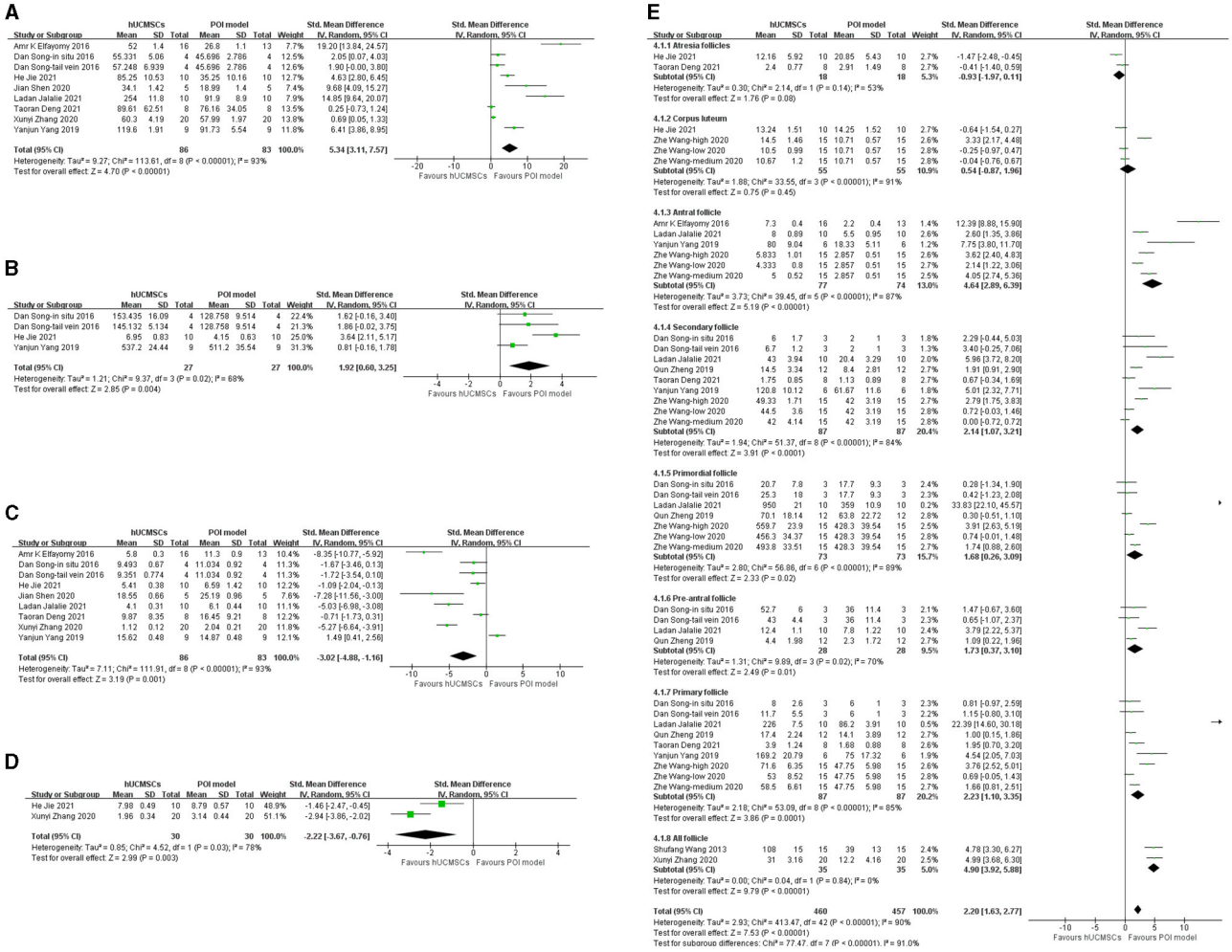

FIGURE 3
Forest plot of animals' serum hormone level and follicle number in the hUCMSC group vs. the POI model group. **(A)** Serum E_2 concentrations significantly increased in the hUCMSC group compared with those in the POI model group (SMD: 5.34, 95% CI: [3.11, 7.57], $I^2 = 93\%$, $P < 0.00001$). **(B)** Serum AMH concentrations significantly increased in the hUCMSC group compared with those in the POI model group (SMD: 1.92, 95% CI: [0.60, 3.25], $I^2 = 68\%$, $P = 0.004$). **(C)** Serum FSH concentrations significantly decreased in the hUCMSC group compared with those in the POI model group (SMD: −3.02, 95% CI: [−4.88, −1.16], $I2 = 93\%$, $P = 0.001$). **(D)** Serum LH concentrations significantly decreased in the hUCMSC group compared with those in the POI model group (SMD: −2.22, 95% CI: [−3.67, −0.76], $I^2 = 78\%$, $P = 0.003$). **(E)** Ovarian follicle count comparison between the hUCMSC group versus the POI model group. Antral follicles (SMD: 4.64, 95% CI: [2.89, 6.39], $I^2 = 87\%$, $P < 0.00001$), pre-antral follicles (SMD: 1.73, 95% CI: [0.37, 3.10], $I^2 = 70\%$, $P = 0.01$), secondary follicles (SMD: 2.14, 95% CI: [1.07, 3.21], $I^2 = 84\%$, $P < 0.0001$), primary follicle (SMD: 2.23, 95% CI: [1.10, 3.35], $I^2 = 85\%$, $P = 0.0001$), primordial follicle (SMD: 1.68, 95% CI: [0.26, 3.09], $I^2 = 89\%$, $P = 0.02$) and all follicles (SMD: 4.90, 95% CI: [3.92, 5.88], $I^2 = 0\%$, $P < 0.00001$) increased significantly in the hUCMSC group compared with those in the POI model group.

significant changes. Estrogen is mainly produced in the ovarian follicle, and LH and FSH play a crucial role. In addition, GCs and their aromatase convert androgen into estrogen (55). Our results proved the therapeutic effect of hUCMSC on E_2, FSH and LH. We also found some pioneering clinical trials, and their results are optimistic. They investigate antral follicle number and sex hormone of patients to evaluate their ovary function. After UCMSC transplantation, patients showed significant recovery of sex hormone, with decreased level of FSH and increased number of antral follicle (16, 17). Further pregnancy follow up showed that UCMSC transplantation does not affect genetic source of fetus (16). Ovarian volume increases after hUCMSC transplantation with significance, but no significance was observed in collagen scaffold group (17). Nevertheless, compared with animal studies, number of high-quality randomized controlled trials (RCTs) is little. Considering the differences between animals and humans, our meta-analysis result cannot fully support stem cell therapy in POI in human, but can provide a preclinical evidence. However, given that hUCMSC is proven to be effective in POI animals, researchers may pay more attention to RCTs. With abundant and valid RCT evidence, further application of stem cells can be discussed in the future. According to quality assessment table (Table 2), major problems are insufficient randomization and blinding. Thus, it is necessary for researchers to exactly illustrate their randomization settings and blinding measures to prove the function of hUCMSC especially in clinical stage. Traditionally, ovarian follicle number is thought to be fixed and decreases by age (56). So folliculogenesis is traditionally thought as an

TABLE 4 Sensitivity analysis of the results.

Outcome	Excluded study	Number of observation	I^2	SMD/RR [95%CI]	P value of overall effect
Normal estrous cycle proportion	–	4	0%	3.32 [1.80, 6.12]	0.0001
	Shen et al. (23)	3	0%	3.11 [1.66, 5.82]	0.0004
	Wang–High et al. (30)	3	0%	2.85 [1.32, 6.13]	0.008
	Wang–Low et al. (30)	3	0%	4.08 [1.99, 8.37]	0.0001
	Wang–Medium et al. (30)	3	0%	3.31 [1.57, 6.97]	0.002
Duration of estrous cycle	–	3	0%	−1.97 [−2.58, −1.36]	<0.00001
	Zhang et al. (18)	2	43%	−1.99 [−2.98, −1.00]	<0.0001
	Yang et al. (32)	2	0%	−1.84 [−2.48, −1.20]	<0.00001
	Deng et al. (28)	2	13%	−2.12 [−2.83, −1.41]	<0.00001
E_2	–	9	93%	5.34 [3.11, 7.57]	<0.00001
	Shen et al. (23)	8	93%	4.95 [2.69, 7.20]	<0.0001
	Elfayomy et al. (25)	8	90%	3.89 [2.00, 5.79]	<0.0001
	Song–*in situ* et al. (29)	8	94%	5.93 [3.42, 8.44]	<0.00001
	Song–tail vein et al. (29)	8	94%	5.96 [3.44, 8.48]	<0.00001
	Jie et al. (24)	8	93%	5.47 [3.06, 7.89]	<0.00001
	Jalalie et al. (27)	8	92%	4.35 [2.26, 6.44]	<0.0001
	Zhang et al. (26)	8	93%	6.51 [3.48, 9.54]	<0.0001
	Deng et al. (28)	8	93%	6.49 [3.60, 9.38]	<0.0001
	Yang et al. (32)	8	93%	5.13 [2.83, 7.43]	<0.0001
FSH	–	9	93%	−3.02 [−4.88, −1.16]	0.001
	Shen et al. (23)	8	93%	−2.67 [−4.57, −0.77]	0.006
	Elfayomy et al. (25)	8	91%	−2.35 [−4.09, −0.62]	0.008
	Song–*in situ* et al. (29)	8	94%	−3.22 [−5.29, −1.15]	0.002
	Song–tail vein et al. (29)	8	94%	−3.21 [−5.27, −1.15]	0.002
	Jie et al. (24)	8	94%	−3.35 [−5.61, −1.09]	0.004
	Jalalie et al. (27)	8	93%	−2.76 [−4.71, −0.82]	0.005
	Deng et al. (28)	8	93%	−3.39 [−5.60, −1.18]	0.003
	Yang et al. (32)	8	90%	−3.60 [−5.39, −1.81]	<0.0001
	Zhang et al. (26)	8	91%	−2.68 [−4.51, −0.84]	0.004
AMH	–	4	68%	1.92 [0.60, 3.25]	0.004
	Jie et al. (24)	3	0%	1.14 [0.37, 1.92]	0.004
	Song–*in situ* et al. (29)	3	79%	2.04 [0.25, 3.84]	0.03
	Song–tail vein et al. (29)	3	79%	1.97 [0.21, 3.72]	0.03
	Yang et al. (32)	3	43%	2.46 [1.14, 3.78]	0.0003

irreversible procedure. Besides, traditional therapy such as HRT can only relieve symptoms. Fertility preservation is indeed hard to achieve. But recently, the discovery of stem cell in ovary gives a new hope for ovarian regeneration. Germline stem cell (GSC) is identified and isolated from human ovarian cortex. The property of isolated stem cell is proved to be stable after cell culture. *DDX4, OCT4. IFITM3* and *BLIMP-1* are confirmed to be expressed by the GSC (57). Moreover, it can promote ovarian function recovery in sterile animals and achieve pregnancy (58). As our result shows a recovery of ovarian follicle after hUCMSC transplantation. Given the genetic origin of offspring is not from hUCMSC donor as clinical trial proves (16), new experiments can pay some attentions to the effect of hUCMSC on ovarian GSC to explore the mechanism. Many genes can regulate folliculogenesis. Genes, cells or molecules such as *SP1, mTOR, Ube2i, YAP1, C1QTNF3, GPR173*, ovarian fat pad factors, *α-SNAP*, $CD11c^+$ cells,

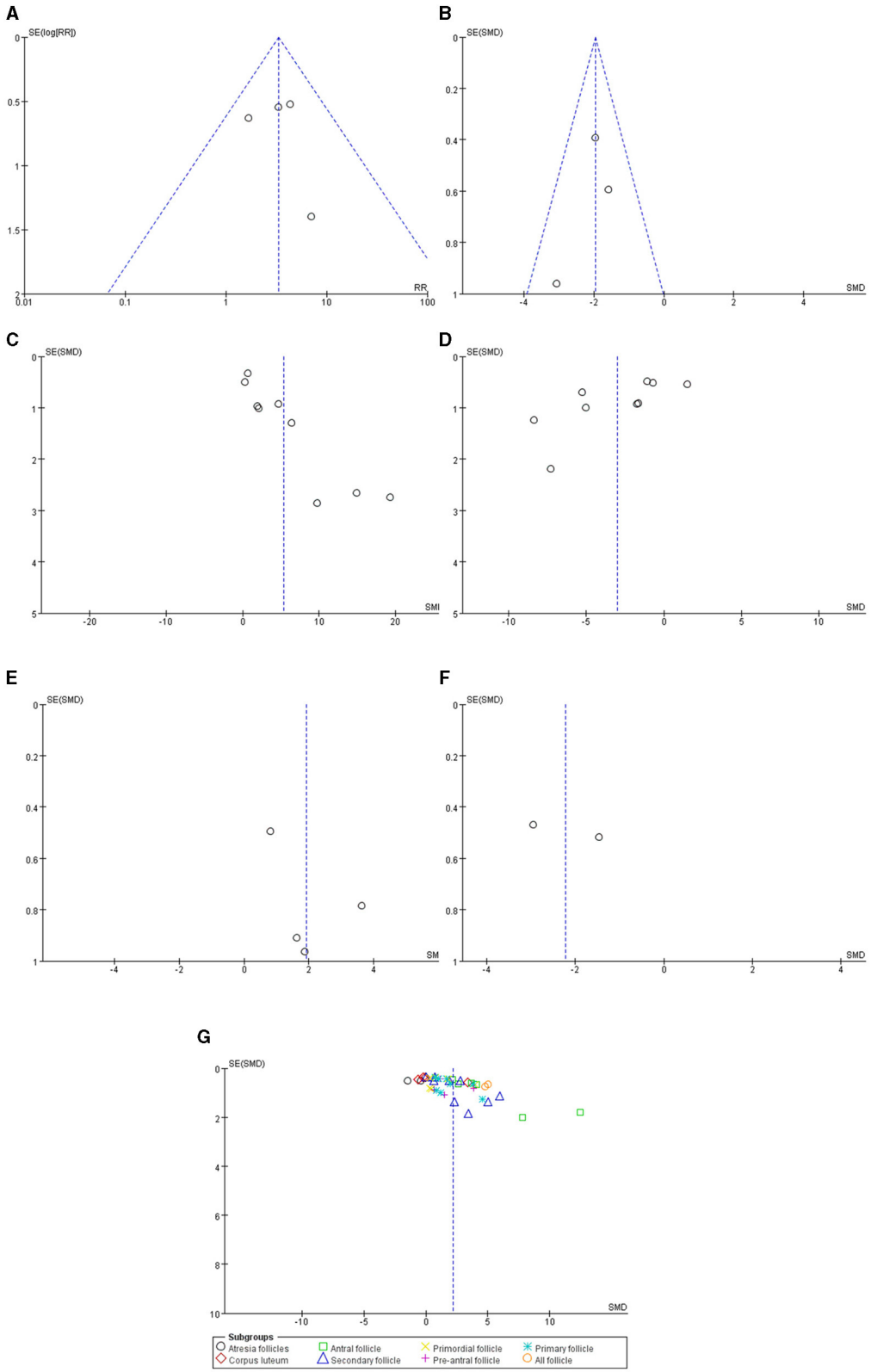

FIGURE 4
Funnel plots of the **(A)** normal estrous cycle, **(B)** estrous cycle length, **(C)** serum E_2, **(D)** serum FSH, **(E)** serum AMH, **(F)** serum LH and **(G)** follicle count.

M1 MΦs and DCs all play a role in folliculogenesis (59). Some studies have tried to find the association between these genes and the hUCMSC treatment effect. For example, Lu Xueyan et al. found that hUCMSC can inhibit the autophagy of theca-interstitial cells

via the AMPK/mTOR signaling pathway (60). Depending on our results, folliculogenesis is a promising direction. Considering that folliculogenesis is tightly connected to anti-apoptosis in GCs (61), some cytokines that can affect GCs may be the target of future mechanism research.

Finally, this study has some limitations that should not be ignored. Clinical study of hUCMSC is rare, and this is also one reason for us to conduct this meta-analysis. Preclinical study is an important part of scientific experiment. Because of limited number of clinical data, it is not the optimal time to conduct a clinical meta-analysis. The meta-analysis of preclinical animal study can promote the development of clinical trails. The relatively insufficient included study, medium quality, high diversity and heterogeneity restrict the application of conclusion. Though random effects model was applied in the analysis, the impact cannot be fully eliminated. All included studies are of medium-quality studies, and higher-quality studies are needed in future research. Due to the limited number of studies, publication bias likely exists in this meta-analysis. However, according to current results, hUCMSC is able to recover ovarian function of POI animals. The result is not affected by limitation. The mentioned limitation should be considered when our conclusion serves as an evidence for clinical study. Thus, we hold a conservative but optimistic view and think more studies are needed in the future to further support the results. Considering the characteristic table, we can observe that a standard animal study procedure has not been formed yet. Future research may focus on a suitable stem cell concentration and transplantation time to eliminate heterogeneity.

5. Conclusions

The transplantation of hUCMSC has the potential to restore the estrous cycle, increase E_2 and AMH levels, decrease FSH and LH levels, and promote folliculogenesis in female rodent models. The results strongly support the use of this therapeutic strategy with a promising outlook. It is important to evaluate the safety and effectiveness of hUCMSC in clinical trials. Randomized controlled trials should also be approached with caution, and safety and adverse effects of hUCMSC should be thoroughly examined in future studies.

Data availability statement

The original contributions presented in the study are included in the article/supplementary material, further inquiries can be directed to the corresponding authors.

Author contributions

XW and TL conducted study collection, indentification, data extraction, and statistical disposal. XW drafted the manuscript. TL polished the manuscript. XB, YZ, and MZ collected the relevant references and participated in the discussion. LW designed this meta-analysis and revised the manuscript. All authors contributed to this manuscript. All authors read and approved the final manuscript.

Funding

This work was supported by Department of Science and Technology of Zhejiang Province, Lingyan Project (2022C03097).

Conflict of interest

The authors declare that the research was conducted in the absence of any commercial or financial relationships that could be construed as a potential conflict of interest.

Publisher's note

References

1. Han Q, Chen ZJ, Du Y. Dietary supplementation for female infertility: recent advances in the nutritional therapy for premature ovarian insufficiency. *Front Microbiol.* (2022) 13:1001209. doi: 10.3389/fmicb.2022.1001209

2. Liu M, Zhang D, Li W, Xu B, Feng HL. Editorial. Ovarian aging and reproduction. *Front Endocrinol.* (2022) 13:1081348. doi: 10.3389/fendo.2022.1081348

3. Tsiligiannis S, Panay N, Stevenson JC. Premature ovarian insufficiency and long-term health consequences. *Curr Vasc Pharmacol.* (2019) 17:604–9. doi: 10.2174/1570161117666190122101611

4. Li M, Zhu Y, Wei J, Chen L, Chen S, Lai D. The global prevalence of premature ovarian insufficiency: a systematic review and meta-analysis. *Climacteric.* (2023) 26:95–102. doi: 10.1080/13697137.2022.2153033

5. Ruth KS, Day FR, Hussain J, Martínez-Marchal A, Aiken CE, Azad A, et al. Genetic insights into biological mechanisms governing human ovarian ageing. *Nature.* (2021) 596:393–7. doi: 10.1038/s41586-021-03779-7

6. Domniz N, Meirow D. Premature ovarian insufficiency and autoimmune diseases. *Best Pract Res Clin Obstet Gynaecol.* (2019) 60:42–55. doi: 10.1016/j.bpobgyn.2019.07.008

7. Cattoni A, Parissone F, Porcari I, Molinari S, Masera N, Franchi M, et al. Hormonal replacement therapy in adolescents and young women with chemo- or radio-induced premature ovarian insufficiency. Practical recommendations. *Blood Rev.* (2021) 45:100730. doi: 10.1016/j.blre.2020.100730

8. Wilkins J, Al-Inizi S. Premature ovarian insufficiency secondary to COVID-19 infection. An original case report. *Int J Gynaecol Obstet.* (2021) 154:179–80. doi: 10.1002/ijgo.13719

9. Bakalov VK, Gutin L, Cheng CM, Zhou J, Sheth P, Shah K, et al. Autoimmune disorders in women with turner syndrome and women with karyotypically normal primary ovarian insufficiency. *J Autoimmun.* (2012) 38:315–21. doi: 10.1016/j.jaut.2012.01.015

10. Yi M, Li T, Niu M, Luo S, Chu Q, Wu K. Epidemiological trends of women's cancers from 1990 to 2019 at the global, regional, and national levels: a population-based study. *Biomark Res.* (2021) 9:55. doi: 10.1186/s40364-021-00310-y

11. Jin M, Yu Y, Huang H. An update on primary ovarian insufficiency. *Sci China Life Sci.* (2012) 55:677–86. doi: 10.1007/s11427-012-4355-2

12. Ishizuka B. Current understanding of the etiology, symptomatology, and treatment options in premature ovarian insufficiency (POI). *Front Endocrinol.* (2021) 12:626924. doi: 10.3389/fendo.2021.626924

13. Sullivan SD, Sarrel PM, Nelson LM. Hormone replacement therapy in young women with primary ovarian insufficiency and early menopause. *Fertil Steril.* (2016) 106:1588–99. doi: 10.1016/j.fertnstert.2016.09.046

14. Meczekalski B, Maciejewska-Jeske M, Podfigurna A. Reproduction in premature ovarian insufficiency patients—From latest studies to therapeutic approach. *Prz Menopauzalny.* (2018) 17:117–9. doi: 10.5114/pm.2018.78554

15. Ding DC, Chang YH, Shyu WC, Lin SZ. Human umbilical cord mesenchymal stem cells: a new era for stem cell therapy. *Cell Transplant.* (2015) 24:339–47. doi: 10.3727/096368915X686841

16. Yan L, Wu Y, Li L, Wu J, Zhao F, Gao Z, et al. Clinical analysis of human umbilical cord mesenchymal stem cell allotransplantation in patients with premature ovarian insufficiency. *Cell Prolif.* (2020) 53:e12938. doi: 10.1111/cpr.12938

17. Ding L, Yan G, Wang B, Xu L, Gu Y, Ru T, et al. Transplantation of UC-MSCs on collagen scaffold activates follicles in dormant ovaries of POF patients with long history of infertility. *Sci China Life Sci.* (2018) 61:1554–65. doi: 10.1007/s11427-017-9272-2

18. Zhang J, Xiong J, Fang L, Lu Z, Wu M, Shi L, et al. The protective effects of human umbilical cord mesenchymal stem cells on damaged ovarian function. A comparative study. *Biosci Trends.* (2016) 10:265–76. doi: 10.5582/bst.2016.01125

19. Zhu SF, Hu HB, Xu HY, Fu XF, Peng DX, et al. Human umbilical cord mesenchymal stem cell transplantation restores damaged ovaries. *J Cell Mol Med.* (2015) 19:2108–17. doi: 10.1111/jcmm.12571

20. Yi M, Wu Y, Niu M, Zhu S, Zhang J, Yan Y, et al. Anti-TGF-β/PD-L1 bispecific antibody promotes T cell infiltration and exhibits enhanced antitumor activity in triple-negative breast cancer. *J Immunother Cancer.* (2022) 10:5543. doi: 10.1136/jitc-2022-005543

21. Cui L, Bao H, Liu Z, Man X, Liu H, Hou Y, et al. hUMSCs regulate the differentiation of ovarian stromal cells via TGF-beta1/Smad3 signaling pathway to inhibit ovarian fibrosis to repair ovarian function in POI rats. *Stem Cell Res Ther.* (2020) 11:386. doi: 10.1186/s13287-020-01904-3

22. Collaboration TC. Review Manager (RevMan) [Computer program]. *Version 541 In.* (2020).

23. Shen J, Cao D, Sun JL. Ability of human umbilical cord mesenchymal stem cells to repair chemotherapy-induced premature ovarian failure. *World J Stem Cells.* (2020). doi: 10.4252/wjsc.v12.i4.277

24. Jie H, Jinxiang W, Ye L, Jing Z, Xiangqing Z, Jinxiu H, et al. Effects of umbilical cord mesenchymal stem cells on expression of CYR61, FSH and AMH in mice with premature ovarian failure. *Cell Mol Biol.* (2022) 67:358–66. doi: 10.14715/cmb/2021.67.5.41

25. Elfayomy AK, Almasry SM, El-Tarhouny SA, Eldomiaty MA. Human umbilical cord blood-mesenchymal stem cells transplantation renovates the ovarian surface epithelium in a rat model of premature ovarian failure. Possible direct and indirect effects. *Tissue Cell.* (2016) 48:370–82. doi: 10.1016/j.tice.2016.05.001

26. Zhang X, Zhang L, Li Y, Yin Z, Feng Y, Ji Y. Human umbilical cord mesenchymal stem cells (hUCMSCs) promotes the recovery of ovarian function in a rat model of premature ovarian failure (POF). *Gynecol Endocrinol.* (2021) 37:353–7. doi: 10.1080/09513590.2021.1878133

27. Jalalie L, Rezaee MA, Rezaie MJ, Jalili A, Raoofi A, Rustamzade A. Human umbilical cord mesenchymal stem cells improve morphometric and histopathologic changes of cyclophosphamide-injured ovarian follicles in mouse model of premature ovarian failure. *Acta Histochem.* (2021) 123:151658. doi: 10.1016/j.acthis.2020.151658

28. Deng T, He J, Yao Q, Wu L, Xue L, Wu M, et al. Human umbilical cord mesenchymal Stem cells improve ovarian function in chemotherapy-induced premature ovarian failure mice through inhibiting apoptosis and inflammation via a paracrine mechanism. *Reprod Sci.* (2021) 28:1718–32. doi: 10.1007/s43032-021-00499-1

29. Song D, Zhong Y, Qian C, Zou Q, Ou J, Shi Y, et al. Human umbilical cord mesenchymal stem cells therapy in cyclophosphamide-induced premature ovarian failure rat model. *Biomed Res Int.* (2016) 2016:2517514. doi: 10.1155/2016/2517514

30. Wang Z, Wei Q, Wang H, Han L, Dai H, Qian X, et al. Mesenchymal stem cell therapy using human umbilical cord in a rat model of autoimmune-induced premature ovarian failure. *Stem Cells Int.* (2020) 2020:3249495. doi: 10.1155/2020/3249495

31. Wang S, Yu L, Sun M, Mu S, Wang C, Wang D, et al. The therapeutic potential of umbilical cord mesenchymal stem cells in mice premature ovarian failure. *Biomed Res Int.* (2013) 2013:690491. doi: 10.1155/2013/690491

32. Yang Y, Lei L, Wang S, Sheng X, Yan G, Xu L, et al. Transplantation of umbilical cord-derived mesenchymal stem cells on a collagen scaffold improves ovarian function in a premature ovarian failure model of mice. *In Vitro Cell Dev Biol Anim.* (2019) 55:302–11. doi: 10.1007/s11626-019-00337-4

33. Zheng Q, Fu X, Jiang J, Zhang N, Zou L, Wang W, et al. umbilical cord mesenchymal stem cell transplantation prevents chemotherapy-induced ovarian failure via the NGF/TrkA pathway in rats. *Biomed Res Int.* (2019) 2019:6539294. doi: 10.1155/2019/6539294

34. Yang Z, Du X, Wang C, Zhang J, Liu C, Li Y, et al. Therapeutic effects of human umbilical cord mesenchymal stem cell-derived microvesicles on premature ovarian insufficiency in mice. *Stem Cell Res Ther.* (2019) 10:250. doi: 10.1186/s13287-019-1327-5

35. European Society for Human R, Embryology Guideline Group on POI, Webber L, Davies M, Anderson R, Bartlett J, et al. ESHRE guideline: management of women with premature ovarian insufficiency. *Hum Reprod.* (2016) 31:926–37. doi: 10.1093/humrep/dew027

36. McGlacken-Byrne SM, Conway GS. Premature ovarian insufficiency. *Best Pract Res Clin Obstet Gynaecol.* (2022) 81:98–110. doi: 10.1016/j.bpobgyn.2021.09.011

37. Sato T, Kusuhara A, Kasahara Y, Haino T, Kishi H, Okamoto A. Follicular development during hormone replacement therapy in patients with premature ovarian insufficiency. *Reprod Med Biol.* (2021) 20:234–40. doi: 10.1002/rmb2.12375

38. Benetti-Pinto CL, Menezes C, Yela DA, Cardoso TM. Sleep quality and fatigue in women with premature ovarian insufficiency receiving hormone therapy: a comparative study .*Menopause.* (2019) 26:1141–5. doi: 10.1097/GME.0000000000001379

39. Liu C, Yin H, Jiang H, Du X, Wang C, Liu Y, et al. Extracellular vesicles derived from mesenchymal stem cells recover fertility of premature ovarian insufficiency mice and the effects on their offspring. *Cell Transplant.* (2020) 29:963689720923575. doi: 10.1177/0963689720923575

40. Hao Y, Ran Y, Lu B, Li J, Zhang J, Feng C, et al. Therapeutic effects of human umbilical cord-derived mesenchymal stem cells on canine radiation-induced lung injury. *Int J Radiat Oncol Biol Phys.* (2018) 102:407–16. doi: 10.1016/j.ijrobp.2018.05.068

41. Fang Z, Yin X, Wang J, Tian N, Ao Q, Gu Y, et al. Functional characterization of human umbilical cord-derived mesenchymal stem cells for treatment of systolic heart failure. *Exp Ther Med.* (2016) 12:3328–32. doi: 10.3892/etm.2016.3748

42. Zhang GZ, Sun HC, Zheng LB, Guo JB, Zhang XL. In vivo hepatic differentiation potential of human umbilical cord-derived mesenchymal stem cells. Therapeutic effect on liver fibrosis/cirrhosis. *World J Gastroenterol.* (2017) 23:8152–68. doi: 10.3748/wjg.v23.i46.8152

43. Tian DZ, Deng D, Qiang JL, Zhu Q, Li QC, Yi ZG. Repair of spinal cord injury in rats by umbilical cord mesenchymal stem cells through P38MAPK signaling pathway. *Eur Rev Med Pharmacol Sci.* (2019) 23:47–53. doi: 10.26355/eurrev_201908_18627

44. Wang S, Cheng H, Dai G, Wang X, Hua R, Liu X, et al. Umbilical cord mesenchymal stem cell transplantation significantly improves neurological function in patients with sequelae of traumatic brain injury. *Brain Res.* (2013) 1532:76–84. doi: 10.1016/j.brainres.2013.08.001

45. Wang D, Niu L, Feng X, Yuan X, Zhao S, Zhang H, et al. Long-term safety of umbilical cord mesenchymal stem cells transplantation for systemic lupus erythematosus. A 6-year follow-up study. *Clin Exp Med.* (2017) 17:333–40. doi: 10.1007/s10238-016-0427-0

46. Kong D, Zhuang X, Wang D, Qu H, Jiang Y, Li X, et al. Umbilical cord mesenchymal stem cell transfusion ameliorated hyperglycemia in patients with type 2 diabetes mellitus. *Clin Lab.* (2014) 60:1969–76. doi: 10.7754/Clin.Lab.2014.140305

47. Lew R. Natural history of ovarian function including assessment of ovarian reserve and premature ovarian failure. *Best Pract Res Clin Obstet Gynaecol.* (2019) 55:2–13. doi: 10.1016/j.bpobgyn.2018.05.005

48. Huang X, Yu Q. Bioinformatic analysis confirms differences in circular RNA expression profiles of cumulus cells between patients with ovarian and peritoneal endometriosis-associated infertility. *Front Endocrinol.* (2023) 14:1137235. doi: 10.3389/fendo.2023.1137235

49. Carson SA, Kallen AN. Diagnosis and management of infertility. A review. *Jama.* (2021) 326:65–76. doi: 10.1001/jama.2021.4788

50. Wang L, Huang S, Li S, Li M, Shi J, Bai W, et al. Efficacy and safety of umbilical cord mesenchymal stem cell therapy for rheumatoid arthritis patients. a prospective phase I/II study. *Drug Des Devel Ther.* (2019) 13:4331–40. doi: 10.2147/DDDT.S225613

51. Zang L, Li Y, Hao H, Liu J, Cheng Y, Li B, et al. Efficacy and safety of umbilical cord-derived mesenchymal stem cells in Chinese adults with type 2 diabetes. A single-center, double-blinded, randomized, placebo-controlled phase II trial. *Stem Cell Res Ther.* (2022) 13:180. doi: 10.1186/s13287-022-02848-6

52. Lanzoni G, Linetsky E, Correa D, Messinger Cayetano S, Alvarez RA, Kouroupis D, et al. Umbilical cord mesenchymal stem cells for COVID-19 acute respiratory distress syndrome. A double-blind, phase 1/2a, randomized controlled trial. *Stem Cells Transl Med.* (2021) 10:660–73. doi: 10.1002/sctm.20-0472

53. Nassauw LV, Tao L, Harrisson F. Distribution of apoptosis-related proteins in thequail ovary during folliculogenesis. BCL-2, BAX, and CPP32. *Acta Histochemica*. (1999) 101:103–12. doi: 10.1016/S0065-1281(99)80010-5

54. Zhao Y, Ma J, Yi P, Wu J, Zhao F, Tu W, et al. Human umbilical cord mesenchymal stem cells restore the ovarian metabolome and rescue premature ovarian insufficiency in mice. *Stem Cell Res Ther*. (2020) 11:466. doi: 10.1186/s13287-020-01972-5

55. Findlay JK BK, Kerr JB, O'Donnell L, Jones ME, Drummond AE, Simpson ER. The road to ovulation the role of oestrogens. *Reprod Fertil Dev*. (2001) 3:71. doi: 10.1071/RD01071

56. Woods DC, Tilly JL. An evolutionary perspective on adult female germline stem cell function from flies to humans. *Semin Reprod Med*. (2013) 31:24–32. doi: 10.1055/s-0032-1331794

57. Ding X, Liu G, Xu B, Wu C, Hui N, Ni X, et al. Human GV oocytes generated by mitotically active germ cells obtained from follicular aspirates. *Sci Rep*. (2016) 6:28218. doi: 10.1038/srep 28218

58. Zhang C, Wu J. Production of offspring from a germline stem cell line derived from prepubertal ovaries of germline reporter mice. *Mol Hum Reprod*. (2016) 22:457–64. doi: 10.1093/molehr/gaw030

59. Gershon E, Dekel N. Newly Identified Regulators of Ovarian Folliculogenesis and Ovulation. *Int J Mol Sci*. (2020) 21:4565. doi: 10.3390/ijms21124565

60. Lu X, Bao H, Cui L, Zhu W, Zhang L, Xu Z, et al. hUMSC transplantation restores ovarian function in POI rats by inhibiting autophagy of theca-interstitial cells via the AMPK/mTOR signaling pathway. *Stem Cell Res Ther*. (2020) 11:268. doi: 10.1186/s13287-020-01784-7

61. Matsuda F, Inoue N, Manabe N, Ohkura S. Follicular growth and atresia in mammalian ovaries: regulation by survival and death of granulosa cells. *J Reprod Dev*. (2012) 58:44–50. doi: 10.1262/jrd.2011-012

frontiers | Frontiers in Oncology

TYPE Case Report
PUBLISHED 21 July 2023
DOI 10.3389/fonc.2023.1207991

OPEN ACCESS

EDITED BY
Yujiao Deng,
The Second Affiliated Hospital of Xi'an Jiaotong University, China

REVIEWED BY
Sheng Yu,
Second Hospital of Anhui Medical University, China
Shengnan Yu,
First Affiliated Hospital of Chongqing Medical University, China

*CORRESPONDENCE
Zhili Li
lizhili@ibms.pumc.edu.cn
Qiang Sun
sunqiangpumch@sina.com

†These authors have contributed equally to this work and share first authorship

RECEIVED 27 April 2023
ACCEPTED 26 June 2023
PUBLISHED 21 July 2023

CITATION
Chen C, Xu Y, Lai Z, Li Z and Sun Q (2023) Case Report: Exploration of changes in serum immunoinflammation-related protein complexes of patients with metastatic breast cancer.
Front. Oncol. 13:1207991.
doi: 10.3389/fonc.2023.1207991

Case Report: Exploration of changes in serum immunoinflammation-related protein complexes of patients with metastatic breast cancer

Chang Chen[1†], Yali Xu[1†], Zhizhen Lai[2], Zhili Li[2*] and Qiang Sun[1*]

[1]Department of Breast Surgery, Peking Union Medical College Hospital, Chinese Academy of Medical Sciences and Peking Union Medical College, Beijing, China, [2]Department of Biophysics and Structural Biology, Institute of Basic Medical Sciences, Chinese Academy of Medical Sciences and School of Basic Medicine, Peking Union Medical College, Beijing, China

Patients with advanced breast cancer are difficult to treat and have poor prognosis. At present, the commonly used methods to monitor the disease progression of breast cancer are imaging examinations such as breast ultrasound, mammography and peripheral blood tumor markers such as carcinoembryonic antigen (CEA) and carbohydrate antigen 15-3 (CA15-3). However, none of them can detect tumor progression at an early stage. Serum immunoinflammation-related protein complexes (IIRPCs) showed potential to indicate cancer progression. Therefore, we attempted to monitor the level of IIRPCs in peripheral blood of patients with metastatic breast cancer and compare it with patients' treatment and disease progression, and here we performed case reports of two of them.

KEYWORDS

immunoinflammation-related protein complexes, breast cancer, serum, biomarker, disease surveillance

Introduction

In recent years, the breast cancer has become the second leading cause of cancer death among women after lung cancer in the United States (1). It is also the most common cancer and the sixth leading cause of cancer death in Chinese women (2). Recurrent and metastatic breast cancer is currently the most difficult part to diagnosis and treatment. The sensitivity of imaging tests (such as ultrasound, mammography, MRI, and PET/CT) and peripheral blood tumor markers currently used in clinical practice is not high enough (3–5). Early detection of disease progression is also a hot topic of current research. Blood components such as free DNA and RNA, proteins, peptides, circulating tumor cells, and metabolites, are indicators of health status as well as disease status (6). And protein complexes assembled by non-covalent bond interactions have already showed potentials in

differentiation of disease in different status (7–9). Disease-specific immune response-related protein complexes in the blood are associated with disease conditions, especially for cancer (10). Previous study has revealed that inflammation regulated by immunoglobulin and immune complexes might be a functionally significant factor in cancer progression (11). Serum immunoinflammation-related protein complexes (IIRPCs) were found significantly different between cancer patients and healthy control, which including immune-related proteins, inflammation-related proteins, and complement-related proteins (12). The levels of IIRPCs in non-small cell lung cancer patients had been found to vary with cancer progression (13). And monitoring IIRPCs may help guide therapeutic management (13). We therefore attempted to monitor IIRPCs in patients with metastatic breast cancer to explore whether it could reflect disease changes.

Case description

Case 1

The first case was a 54-year-old woman who underwent a modified radical mastectomy for left breast cancer in May 2018 with a postoperative pathology of invasive ductal carcinoma (IDC). The maximum diameter of her tumor was 4 cm and the axillary lymph node had metastasis (2/18). Immunohistochemical results were ER negative, PR negative, HER-2 positive and ki67 40%. Postoperatively, the patient did not undergo further radiotherapy, chemotherapy or targeted therapy for personal reasons. The patient had no significant abnormalities on postoperative review until January 2020, when the imaging revealed left chest wall recurrence and multiple lymph node metastases in the left supraclavicular area, left axilla, and left internal mammary artery. She came to our hospital in April of the same year. At the time of the patient's visit, we retained a specimen of her peripheral blood for monitoring of IIRPCs, and blood samples were retained at each subsequent visit for blood testing. Serum protein complexes were isolated using native polyacrylamide gel electrophoresis (PAGE), which was described in detail in our previous article (12). The quality control (QC) sample was a mixture of serum from 5 random patients. An UMAX PowerLook 2100XL scanner (Techville, Inc., USA) was used to scan the stained gel for quantification based on optical density. The gray value of each band was calculated using Quantity One software (version 4.6.3, Bio-Rad). The levels of bands in each gel were exported into Microsoft Excel after the gel background had been subtracted. Previous research had shown that the transferrin-related protein complex (TRPC) had no statistical differences in patients with different sex, age, patterns of the IIRPCs, or health status (12), so the TRPC can be as an internal reference for quantifying the IIRPCs. We quantified the gray value of TRPC in each sample relative to the TRPC of the QC sample to ensure consistency, and then normalized it to 100. After that the amounts of serum IIRPCs relative to serum TRPC in each gel were quantified and calculated. We recommended chemotherapy in combination with targeted therapy to her. And she began treatment in June 2020 after careful consideration. Figure 1A

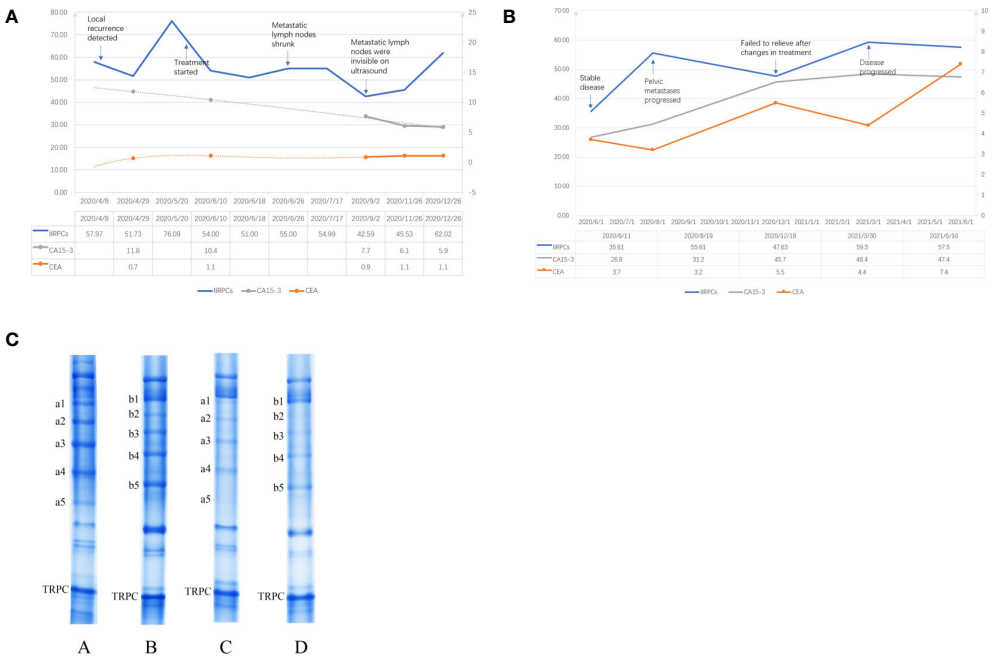

FIGURE 1
(A) Change trends in the levels of the IIRPCs, CEA, and CA15-3 during follow-up of case 1. The left vertical coordinate applied to the values of IIRPCs, the right vertical coordinate applied to the values of CEA (ng/ml) and CA15-3 (U/ml). **(B)** Change trends in the levels of the IIRPCs, CEA, and CA15-3 during follow-up of case 2. The left vertical coordinate applied to the values of IIRPCs and CA15-3 (U/ml), the right vertical coordinate applied to the values of CEA (ng/ml). **(C)** Examples of serum IIRPCs with or without tumor metastasis. The amount of serum IIRPCs relative to serum TRPC in each gel was quantified. The gray value of IIRPCs in metastasis patients (A and B) is substantially higher than in disease-free patients (C and D).

demonstrates the changes in IIRPCs levels at each monitoring visit and the changes in peripheral blood tumor markers over the corresponding time period. The level of IIRPCs rose to peak before treatment and then dramatically fell. The patient's condition significantly relieved after treatment. Subsequent ultrasound review revealed that the metastatic lymph nodes were significantly reduced and almost invisible. Both carcinoembryonic antigen (CEA) and carbohydrate antigen 15-3 (CA15-3) were at normal levels during the same period and did not change with disease.

Case 2

The second case was a 48-year-old woman who underwent a modified radical mastectomy for right breast cancer in 2014. The postoperative pathology was invasive micropapillary carcinoma (5*3.5*2.5cm) with axillary lymph node metastasis (7/36). Immunohistochemistry results were ER negative, PR negative, HER2 positive and ki67 40%. The patient underwent 6 courses adjuvant chemotherapy (docetaxel + cyclophosphamide + pirarubicin) and one year targeted (Herceptin) therapy after surgery. Chemotherapy was followed by adjuvant radiotherapy. By 2018, the patient's review revealed chest wall recurrence, multiple lymph node metastases (bilateral supraclavicular, bilateral axillary, neck), and pericardial metastasis. After therapy with docetaxel + pyrotinib, the patient's condition stabilized. At her visit to our hospital in June 2020 we retained her peripheral blood sample for IIRPCs testing and dynamic monitoring. However, the patient's pelvic metastases progressed two months later and failed to relieve even after changes in treatment regimen. The detection method for IIRPCs and the quantification method were the same as in case 1. Figure 1B demonstrated the dynamic changes of IIRPCs as well as tumor markers of this patient. The quantitative detection of IIRPCs found its level was elevated in response to disease progression. The patient's condition alleviated unsatisfactorily in the subsequent treatment and the level of IIRPCs did not decrease to the baseline(the level at the first sampling, shown in Figure 1B). In this case, her CEA and CA15-3 levels also increased significantly with disease progression.

Discussion

Serum IIRPCs protein complexes are composed of variable inflammation and immunity related protein molecules through non-covalent interactions, mainly including complement factor H, complement C3, C4, C7 components, haptoglobin, immunoglobulin α, γ, and κ components, apolipoprotein A-I and so on (12). It has been shown that peripheral blood complement and immunoglobulins are associated with the development and progression of cancer (10, 14–16). And previous studies have found significant differences in the levels of IIRPCs between tumor patients and healthy individuals (12). In patients with advanced non-small cell lung cancer, changes in the levels of IIRPCs were associated with patient response to treatment and changes in disease status (13). We selected some breast cancer patients to initially explore whether the IIRPCs levels and patterns were associated with breast cancer disease progression.

The results of our pre-experiment found that the IIRPCs bands patterns of all breast cancer patients were classified into seven major patterns (from a to g), which were consistent with previous studies (12, 13, 17). And no new banding pattern was identified. The patients in our cases had no severe infection, other primary tumor, pregnancy, lactation, other serious medical conditions, or other diseases known to be significantly associated with IIRPCs. The patterns of IIRPCs in our assay did not correlate significantly with patient age, tumor stage, grade, and whether metastasis was present. Therefore we mainly want to monitor the changes in the levels of IIRPCs dynamically. We initially found higher concentrations of IIRPCs protein bands in patients with metastatic breast cancer than in patients without metastasis (as shown in Figure 1C). As mentioned above, IIRPCs contains many immune-inflammatory related proteins including haptoglobin, complements. It has been found that higher level of haptoglobin was related to pooler survival of breast cancer (18). And haptoglobin could regulated cell cycle progression and apoptosis in breast cancer cells (19). Lisa J had reported the level of apolipoprotein A-I might be positively correlated with the risk of breast cancer (20). Complement C3 also had been researched as a predictive biomarker in breast cancer (21).

In the first patient, IIRPCs levels decreased after treatment, consistent with the patient's remission. In contrast, the second patient responded poorly to treatment, failed to achieve disease remission, and IIRPCs remained at high levels. However, tumor markers represented by CEA and CA15-3 were consistently elevated with disease progression only in the second patient. We think it may be because the second patient had more metastatic lesions and the first patient had only local recurrence and regional lymph node metastasis. The sensitivity of CEA and CA15-3 for detecting disease progression in breast cancer is not high (22, 23). So personalized IIRPCs could be a potential indicator that reflects the tumor burden in breast cancer patients, which might have good sensitivity. We will continue to collect samples for IIRPCs assays and will follow up with statistical analysis to further explore the role of IIRPCs

Data availability statement

The raw data supporting the conclusions of this article will be made available by the authors, without undue reservation.

Ethics statement

Written informed consent was obtained from the individual(s) for the publication of any potentially identifiable images or data included in this article.

Author contributions

CC performed the result analysis and wrote the draft manuscript. YX and ZLL designed the study. CC and ZZL performed the experiments and the data analysis. QS edited the draft. All authors contributed to the article and approved the submitted version.

Funding

CAMS Innovation Fund for Medical Sciences (CIFMS) 2021-I2M-1-014.

Conflict of interest

The authors declare that the research was conducted in the absence of any commercial or financial relationships that could be construed as a potential conflict of interest.

Publisher's note

References

1. Akram M, Iqbal M, Daniyal M, Khan AU. Awareness and current knowledge of breast cancer. *Biol Res* (2017) 50(1):33. doi: 10.1186/s40659-017-0140-9

2. Fan L, Strasser-Weippl K, Li JJ, St Louis J, Finkelstein DM, Yu KD, et al. Breast cancer in China. *Lancet Oncol* (2014) 15(7):e279–89. doi: 10.1016/S1470-2045(13)70567-9

3. Coombes RC, Page K, Salari R, Hastings RK, Armstrong A, Ahmed S, et al. Personalized detection of circulating tumor DNA antedates breast cancer metastatic recurrence. *Clin Cancer Res* (2019) 25(14):4255–63. doi: 10.1158/1078-0432.CCR-18-3663

4. Eichler C, Abrar S, Puppe J, Arndt M, Ohlinger R, Hahn M, et al. Detection of ductal carcinoma *In situ* by ultrasound and mammography: size-dependent inaccuracy. *Anticancer Res* (2017) 37(9):5065–70. doi: 10.21873/anticanres.11923

5. Fenton JJ, Taplin SH, Carney PA, Abraham L, Sickles EA, D'Orsi C, et al. Influence of computer-aided detection on performance of screening mammography. *New Engl J Med* (2007) 356(14):1399–409. doi: 10.1056/NEJMoa066099

6. Hanash SM, Pitteri SJ, Faca VM. Mining the plasma proteome for cancer biomarkers. *Nature* (2008) 452(7187):571–9. doi: 10.1038/nature06916

7. Hedström J, Haglund C, Haapiainen R, Stenman UH. Serum trypsinogen-2 and trypsin-2-alpha(1)-antitrypsin complex in malignant and benign digestive-tract diseases. preferential elevation in patients with cholangiocarcinomas. *Int J cancer* (1996) 66(3):326–31. doi: 10.1002/(SICI)1097-0215(19960503)66:3<326::AID-IJC10>3.0.CO;2-9

8. Hedström J, Sainio V, Kemppainen E, Haapiainen R, Kivilaakso E, Schröder T, et al. Serum complex of trypsin 2 and alpha 1 antitrypsin as diagnostic and prognostic marker of acute pancreatitis: clinical study in consecutive patients. *BMJ (Clinical Res ed)* (1996) 313(7053):333–7. doi: 10.1136/bmj.313.7053.333

9. Hedström J, Kemppainen E, Andersén J, Jokela H, Puolakkainen P, Stenman UH. A comparison of serum trypsinogen-2 and trypsin-2-alpha1-antitrypsin complex with lipase and amylase in the diagnosis and assessment of severity in the early phase of acute pancreatitis. *Am J Gastroenterol* (2001) 96(2):424–30. doi: 10.1111/j.1572-0241.2001.03457.x

10. Singh R, Mishra MK, Aggarwal H. Inflammation, immunity, and cancer. *Med Inflamm* (2017) 2017:6027305. doi: 10.1155/2017/6027305

11. Tan TT, Coussens LM. Humoral immunity, inflammation and cancer. *Curr Opin Immunol* (2007) 19(2):209–16. doi: 10.1016/j.coi.2007.01.001

12. Wang Y, Song G, Wang Y, Qiu L, Qin X, Liu H, et al. Elevated serum levels of circulating immunoinflammation-related protein complexes are associated with cancer. *J Proteome Res* (2014) 13(2):710–9. doi: 10.1021/pr4008255

13. Song G, Liu Y, Wang Y, Ren G, Guo S, Ren J, et al. Personalized biomarkers to monitor disease progression in advanced non-small-cell lung cancer patients treated with icotinib. *Clinica Chimica Acta; Int J Clin Chem* (2015) 440:44–8. doi: 10.1016/j.cca.2014.11.010

14. Mantovani A, Allavena P, Sica A, Balkwill F. Cancer-related inflammation. *Nature* (2008) 454(7203):436–44. doi: 10.1038/nature07205

15. Schreiber H, Rowley DA. Cancer. awakening immunity. *Sci (New York NY)* (2010) 330(6005):761–2. doi: 10.1126/science.1198345

16. Cuzick J, Otto F, Baron JA, Brown PH, Burn J, Greenwald P, et al. Aspirin and non-steroidal anti-inflammatory drugs for cancer prevention: an international consensus statement. *Lancet Oncol* (2009) 10(5):501–7. doi: 10.1016/S1470-2045(09)70035-X

17. Sun YH, Li J, Shu HJ, Li ZL, Qian JM. Serum immunoinflammation-related protein complexes discriminate between inflammatory bowel disease and colorectal cancer. *Clin Trans Oncol* (2019) 21(12):1680–6. doi: 10.1007/s12094-019-02100-3

18. Wulaningsih W, Holmberg L, Garmo H, Malmstrom H, Lambe M, Hammar N, et al. Prediagnostic serum inflammatory markers in relation to breast cancer risk, severity at diagnosis and survival in breast cancer patients. *Carcinogenesis* (2015) 36(10):1121–8. doi: 10.1093/carcin/bgv096

19. Chen J, Cheuk IW, Siu MT, Yang W, Cheng AS, Shin VY, et al. Human haptoglobin contributes to breast cancer oncogenesis through glycolytic activity modulation. *Am J Cancer Res* (2020) 10(9):2865–77.

20. Martin LJ, Melnichouk O, Huszti E, Connelly PW, Greenberg CV, Minkin S, et al. Serum lipids, lipoproteins, and risk of breast cancer: a nested case-control study using multiple time points. *J Natl Cancer Inst* (2015) 107(5):djv032. doi: 10.1093/jnci/djv032

21. Michlmayr A, Bachleitner-Hofmann T, Baumann S, Marchetti-Deschmann M, Rech-Weichselbraun I, Burghuber C, et al. Modulation of plasma complement by the initial dose of epirubicin/docetaxel therapy in breast cancer and its predictive value. *Br J Cancer* (2010) 103(8):1201–8. doi: 10.1038/sj.bjc.6605909

22. Li H, Wang S, Li X, Cheng C, Shen X, Wang T. Dual-channel detection of breast cancer biomarkers CA15-3 and CEA in human serum using dialysis-silicon nanowire field effect transistor. *Int J Nanomed* (2022) 17:6289–99. doi: 10.2147/IJN.S391234

23. Fu Y, Li H. Assessing clinical significance of serum CA15-3 and carcinoembryonic antigen (CEA) levels in breast cancer patients: a meta-analysis. *Med Sci Monit* (2016) 22:3154–62. doi: 10.12659/MSM.896563

Frontiers in Oncology

Advances knowledge of carcinogenesis and tumor progression for better treatment and management

The third most-cited oncology journal, which highlights research in carcinogenesis and tumor progression, bridging the gap between basic research and applications to imrpove diagnosis, therapeutics and management strategies.

Discover the latest Research Topics

See more →

Frontiers

Avenue du Tribunal-Fédéral 34
1005 Lausanne, Switzerland
frontiersin.org

Contact us

+41 (0)21 510 17 00
frontiersin.org/about/contact